3-2004

An Evaluation of Formate as an Electron Donor to Facilitate Palladium (PD) - Catalyzed Destruction of Chlorinated Aliphatic Hydrocarbons

Matthew D. Welling

AN EVALUATION OF FORMATE AS AN ELECTRON DONOR TO FACILITATE PALLADIUM (PD) - CATALYZED DESTRUCTION OF CHLORINATED ALIPHATIC HYDROCARBONS

Matthew D. Welling, Capt, USAF

AFIT/GEM/ENV/04M-21

DEPARTMENT OF THE AIR FORCE
AIR UNIVERSITY

AIR FORCE INSTITUTE OF TECHNOLOGY

Wright-Patterson Air Force Base, Ohio

AFIT/GEM/ENV/04M-21

AN EVALUATION OF FORMATE AS AN ELECTRON DONOR TO FACILITATE PALLADIUM (PD) - CATALYZED DESTRUCTION OF CHLORINATED ALIPHATIC HYDROCARBONS

THESIS

Presented to the Faculty

Department of Systems and Engineering Management

Graduate School of Engineering and Management

Air Force Institute of Technology

Air University

Air Education and Training Command

In Partial Fulfillment of the Requirements for the

Degree of Master of Science in Engineering Management

Matthew D. Welling, BS

Captain, USAF

March 2004

AFIT/GEM/ENV/04M-21

AN EVALUATION OF FORMATE AS AN ELECTRON DONOR TO FACILITATE PALLADIUM (PD) - CATALYZED DESTRUCTION OF CHLORINATED ALIPHATIC HYDROCARBONS

Matthew D. Welling, BS
Captain, USAF

Approved:

//Signed//	5 Mar 04
Dr. Mark N. Goltz, (Co-Chairman)	date
//Signed//	26 Feb 04
Dr. Abinash Agrawal, (Co-Chairman)	date
//Signed//	1 Mar 04
Dr. Alfred E. Thal Jr. (Member)	date

Abstract

Chlorinated aliphatic hydrocarbons (CAHs) such as trichloroethylene (TCE), tetrachloroethylene (PCE), and trichloroethane (TCA) are probable human carcinogens that have been used widely within the DoD, primarily as solvents for cleaning and metal degreasing. These compounds are frequently found to be groundwater contaminants. In fact, TCE and PCE are the first and third most commonly detected groundwater contaminants nationwide.

The focus of this study was to determine the effectiveness of using a palladium (Pd) catalyst with formate as a reductant to treat CAH-contaminated groundwater. TCE was used as a model CAH. Other investigators have focused on hydrogen gas (H_2) as a reductant to treat CAH-contaminated groundwater. However, when using H_2 as a reductant, catalyst deactivation is observed due to the production of hydrochloric acid. In this study, formic acid was used as the reductant, resulting in no observed catalyst deactivation even at high contaminant concentrations. Reaction rates achieved when using 100% H_2 as a reductant could be matched by using 4 mM (184 mg/L) formic acid. At increased formic acid concentrations, system performance exceeded performance achievable when using H_2. It is also noted that while hydrogen is an explosive, low solubility gas, formic acid can easily and safely be added to contaminated water. The aforementioned work has shown that this method for treating CAH-contaminated groundwater by using formic acid and a Pd-catalyst is more efficient, safe, and less costly than using hydrogen gas as a reductant.

Acknowledgments

I would like to recognize a number of individuals who have helped me complete this thesis. I would like specifically thank my two advisors, Dr. Mark Goltz and Dr. Abinash Agrawal for their dedication to this research effort. Dr. Goltz championed for the required funding to make this research possible, and provided timely feedback and comments throughout the writing process. Dr. Agrawal's expertise and guidance were instrumental in construction of the experimental setup and data analysis. He taught me a new definition of patience and a better understanding of how everything can go wrong when doing lab work. I would also like to thank my third committee member Lt Col Alfred Thal for his review and comment of my document.

I would also like to thank my wife for her continued support and gracious understanding of the long nights and longer weekends frequently spent in the lab. In addition to my wife, I would also like to thank my in-laws for supporting my family while I was conducting research. Finally, I'd like to thank the other students working in Dr. Agrawal's laboratory, their presence provided entertainment and a constant source of ideas.

Table of Contents

Page

Table of Figures

Page

Page

Page

Page

Page

Page

Page

List of Tables

Page

Page

Page

AN EVALUATION OF FORMATE AS AN ELECTRON DONOR TO FACILITATE PALLADIUM (PD) - CATALYZED DESTRUCTION OF CHLORINATED ALIPHATIC HYDROCARBONS

1.0 INTRODUCTION

1.1 Motivation

Chlorinated aliphatic hydrocarbons (CAHs) such as trichloroethylene (TCE), tetrachloroethylene (PCE), and trichloroethane (TCA) have been used widely within the United States and the Department of Defense (DoD), primarily as solvents for cleaning and metal degreasing. CAHs are among the most commonly encountered groundwater pollutants in the United States (Masters, 1998) and the DoD (DENIX, 2003). According to the Agency for Toxic Substances and Disease Registry, TCE and PCE, respectively, are the first and third most commonly detected contaminants at the approximately 330,000 hazardous waste sites across the United States (National Research Council, 1994). This national problem of CAH-contaminated groundwater also affects the United States Air Force, which is responsible for managing roughly 5,000 active hazardous waste sites (Defense Environmental Restoration Program (DERP), 2002). According to the Air Force Center for Environmental Excellence (AFCEE, 2003) there are currently over 860 TCE-contaminated sites within the Air Force. With the United States projected to produce or import 228 million pounds of TCE in 2003 (DENIX, 2002), CAHs will undoubtedly continue to be a source of groundwater contamination.

TCE and PCE, as well as the chlorinated ethane TCA are probable human carcinogens (Masters, 1998). In addition, the daughter product of biodegradation of PCE

and TCE under anaerobic conditions is vinyl chloride, which is a known human carcinogen. Based on the ubiquity of CAH groundwater contaminants and their adverse health effects, there is a need for an effective means of remediating CAH-contaminated groundwater.

Currently there are three commonly used methods for remediation of CAH-contaminated groundwater. These are pump-and-treat systems, permeable reactive barriers, and natural attenuation. Unfortunately, all three of these methods have shortcomings which, in some cases, limit or preclude their use for remediating CAH-contaminated groundwater.

In 1997, pump-and-treat systems were in operation at nearly three quarters of all ground water remediation projects (Masters, 1998). A pump-and-treat system is primarily used to contain and prevent the migration of contaminated plumes towards human and environmental receptors. This method of remediation involves pumping contaminated water from aquifers to aboveground treatment facilities. Often the aboveground treatment technology merely relies on transferring the chlorinated contaminants to other media such as volatilizing them into the air or sorbing them onto granulated activated carbon (GAC). The contaminated air or GAC must still be properly managed, often at substantial cost. Another disadvantage of pump-and-treat systems is the costs associated with pumping contaminated water from the aquifer. Furthermore, the need to bring contaminated water to the surface for treatment also increases the risk of exposure to humans and adds further regulatory constraints.

The potential to destroy chlorinated compounds without having to remove the contaminants from below ground (also called *in situ* treatment) has prompted the

development of systems such as permeable reactive barriers. Reactive barriers are zones emplaced within the subsurface through which contaminated groundwater flows. As the groundwater flows through the barrier, the dissolved CAH is chemically or biologically degraded or mineralized (Domenico and Schwartz, 1998). Reactive barriers consisting of zero-valent iron have commonly been used to successfully dehalogenate chlorinated ethenes (McMahon *et al*., 1999). However, permeable reactive barriers have a number of problems and limitations. One potential problem is due to precipitation or biological growth on the reactive barrier media (Domenico and Schwartz, 1998). These processes may result in loss of permeability of the media over time, causing the contaminant plume to bypass the barrier. The oxidation of Fe^0 to Fe^{2+} also causes a loss in the available redox active sites (Furukawa *et al*., 2002) which could lead to reduced reactivity and permeability of the reactive medium (Gavaskar, 1999). The depth to which reactive barriers can be emplaced is also limited to approximately forty to fifty feet under standard installation procedures (Gavaskar, 1999). Also, as a passive technology, changes in regional groundwater flow may result in the contaminant plume bypassing the barrier.

Another possible strategy, under proper conditions, is to use natural attenuation to remediate CAH-contaminated groundwater. The Environmental Protection Agency (EPA) defines natural attenuation as:

> A carefully controlled and monitored clean-up approach to achieve specific remediation objectives that implements a variety of physical, chemical, or biological processes that act without human intervention to reduce the mass, toxicity, mobility, volume, or concentration of contaminants in soil and groundwater. (U.S. EPA, 1997)

A potential shortcoming of this management strategy is that the biodegradation process typically takes a long time. Under certain conditions the time required to degrade

these compounds via natural attenuation may be excessive, resulting in un-met remediation objectives. In some cases the hydrogeologic and geochemical conditions that favor significant degradation of these chlorinated compounds may not be present (NRC, 1993). Under these conditions, natural attenuation would be deemed ineffective. The EPA has estimated that natural attenuation will be effective as the sole remediation strategy at only about 20% of all chlorinated solvent sites (ITRC, 1999) and that it may serve as a portion of the remedy at an additional 50% of all chlorinated solvent sites (Ellis *et al.*, 1996).

Due to the limitations of conventional remedial strategies noted above, there is a need for innovative technologies to more effectively remediate CAH-contaminated groundwater. An innovative approach that has recently been proposed (Stoppel and Goltz, 2003; Lowry and Reinhard, 2000) is to use palladium (Pd) as a catalyst to chemically destroy the CAH contaminants *in situ* using hydrogen (H_2) gas as an electron donor. One advantage of Pd catalysis is that it results in rapid conversion of chlorinated compounds, which is imperative for *in situ* applications where residence times are typically short. In a trilogy of papers, Lowry and Reinhard (1999; 2000; 2001) studied the Pd-catalyzed destruction of halogenated organics, specifically focusing on TCE. The investigators used H_2 as an electron donor and found that the pH of the system directly affected the rate at which the chlorinated compound was destroyed. They noted that as pH increased from 4.3 to 11 the TCE conversion increased by 30% (Lowry and Reinhard, 2000).

Recent research into Pd-catalyzed reduction of nitroaromatic compounds has found an inverse relationship between conversion efficiency and pH. Phillips (2003)

found that optimal degradation of nitroaromatic compounds (NACs) was achieved at a pH of around 4; and that formate worked well as an electron donor. Provided in the form of formic acid, it served to keep the pH low, thereby improving the destruction kinetics for NACs.

Due to the rapid rate of Pd-catalyzed CAH destruction, a palladium catalyst has been successfully used in-well as a component of an *in situ* treatment system for degradation of CAHs (McNab *et al.*, 2000). One implementation of an in-well system that has been proposed for *in situ* CAH destruction is to install a Pd reactor as a component of a horizontal flow treatment well (HFTW) system (Stoppel and Goltz, 2003). Figure 1.1 shows how an HFTW system can be applied to contain and treat a contaminant plume. In an HFTW system, multiple dual-screened wells pump water in opposite directions, so that one well pumps water in an upflow direction while the adjacent well pumps water downward. The bi-directional flow established in this system results in recirculation of groundwater between the wells and leads to an improvement in the removal efficiency because the contaminated water makes multiple passes through the reactors that are installed in each of the two treatment wells (Stoppel and Goltz, 2003). Currently, the effectiveness of an HFTW system with an in-well Pd catalytic reactor using H_2 gas as an electron donor to manage CAH-contaminated groundwater is being evaluated (Munakata *et al*., 2002).

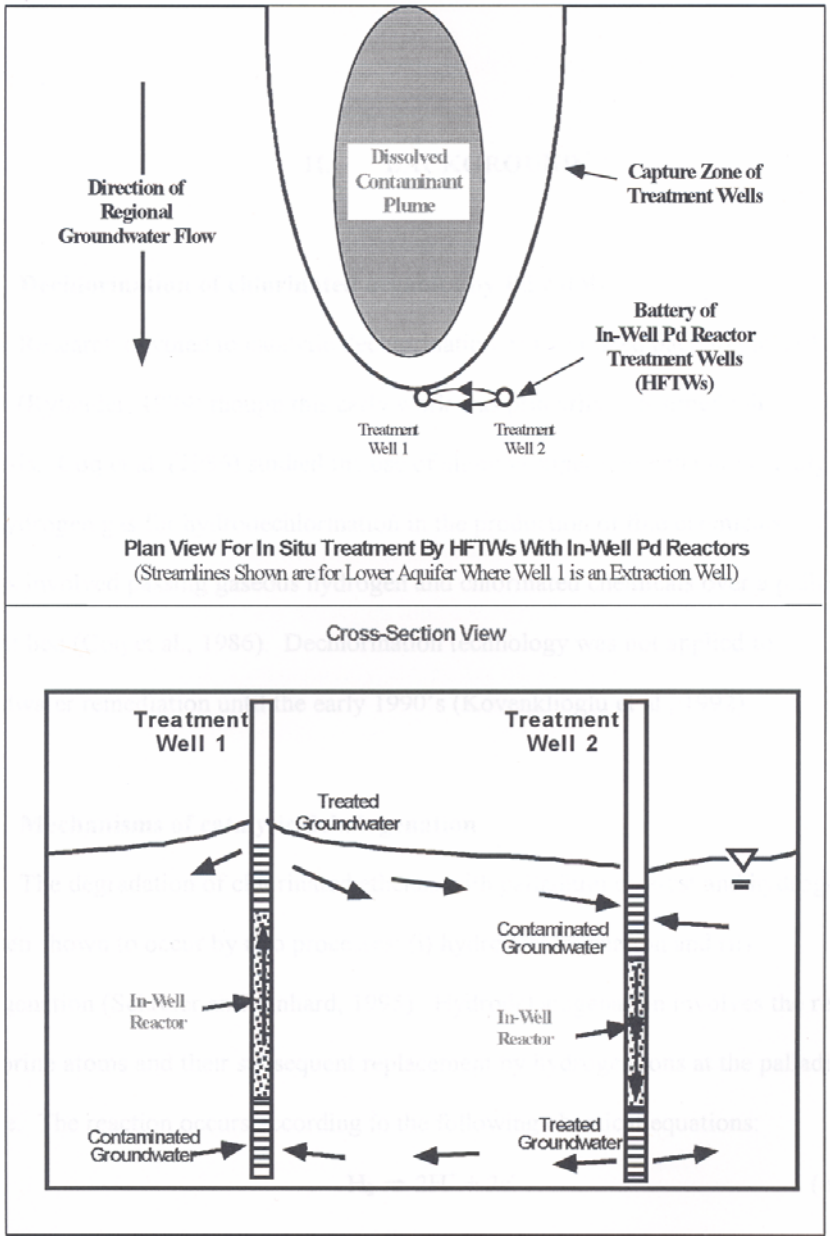

Figure 1.1 Horizontal flow treatment well system (from Stoppel, 2001)

This research study will focus on evaluating the potential of using formate as an electron donor for the Pd-catalyzed destruction of CAHs. A benefit of formate is that it could potentially be provided in the form of formic acid along with a strong base such as sodium hydroxide to adjust the system pH and improve CAH reduction. Other benefits

of using formate as an electron donor are that it can be supplied in high concentrations and diluted as required. In addition, formic acid is much less expensive and safer to use than H_2. Based on the promising results obtained using formate to reduce NACs (Phillips, 2003), it is hypothesized that formate may have the potential to serve as an electron donor to facilitate the Pd-catalyzed reduction of CAHs.

1.2 Research Objectives

The focus of this study will be to determine the effectiveness of formate as an electron donor to reduce TCE and other CAHs in the presence of a Pd catalyst. The research will focus on answering the following questions:

1. How can the kinetics of Pd-catalyzed transformation of CAHs using formate as an electron donor be modeled? What are the values of the kinetic parameters?

2. What products and transformation byproducts result from Pd-catalyzed reduction of CAHs? Are any of these products or byproducts potentially harmful?

3. What factors (*e.g.* reactant concentration, pH, dissolved oxygen, temperature) influence the extent of CAH reduction and the distribution of transformation products?

4. How do formate and hydrogen gas compare as reductants for Pd-catalyzed destruction of CAHs?

5. How might Pd catalysis using formate as an electron donor be used in-well to effect *in situ* destruction of CAHs in groundwater?

1.3 Research Approach

1. Conduct a literature review with a specific emphasis on the work that has been done regarding the Pd-catalyzed reduction of TCE (*e.g.* Lowry and Reinhard, 1999; 2000; 2001) and other CAHs using hydrogen gas as an electron donor, as well as a review of other electron donor/catalyst reaction studies for the destruction of CAHs.
2. Construct a flow-through laboratory column containing a Pd catalyst bed (Niekamp, 2001) to study the rate, extent, and transformation products of CAH destruction in water flowing through the column, under various conditions, using formate as an electron donor.
3. Compare the rate of CAH destruction using formate as an electron donor with the rates achieved using other electron donors. Rates achievable using other donors may be determined from the literature or by conducting additional column studies.
4. Use experimentally determined rate parameters to evaluate how the technology might be used to treat CAH-contaminated water as an in-well component of an HFTW system.

1.4 Study Scope and Limitations

1. This study will be focused on groundwater contamination, not on CAH-contaminated soil.
2. TCE will be used as a model compound.

2.0 LITERATURE REVIEW

2.1 Introduction

This chapter reviews the literature pertinent to the destruction of chlorinated aliphatic hydrocarbons (CAH) by heterogeneous metal catalysts. The early sections of this chapter provide details on how CAHs are mobilized in the environment, health effects associated with CAHs, and some of the basic chemistry associated with CAHs. Later sections of this chapter specifically review the research conducted with respect to palladium (Pd)-catalyzed hydrodehalogenation and hydrogenation of CAHs to achieve groundwater remediation.

2.2 Groundwater Contamination by Chlorinated Aliphatic Hydrocarbons (CAHs)

As mentioned in Section 1.1, chlorinated aliphatic hydrocarbons like TCE, PCE, and TCA have been used widely within the DoD, primarily as solvents for cleaning and metal degreasing. CAHs are among the most commonly encountered groundwater pollutants in the United States (Masters, 1998) and the DoD (DENIX, 2003).

DNAPLs (dense non-aqueous phase liquids), including chlorinated solvents such as TCE, have been a major source of contamination in ground water aquifers since World War II (Pankow and Cherry, 1996). Production of TCE and PCE began in 1923 and the use of both solvents grew in the U.S. in the 1970s along with the economic growth of the country (Pankow and Cherry, 1996). In the mid 1970s widespread testing of drinking water revealed the presence of volatile organic compounds in many of the country's most

important aquifers. Safety and health concerns were quickly raised and production of these compounds was reduced. Unfortunately, the damage was already done; ubiquitous contamination of chlorinated solvents was already a problem. In fact, a survey of 1,070 wells in New Jersey in 1981 showed 58% of the wells contained TCE, 65% contained carbon tetrachloride, and 43% contained PCE (Page, 1981).

Chlorinated solvents can enter the subsurface in various ways. Pankow and Cherry (1996) describe six possible contamination sources for DNAPLs: (1) leaking underground or above ground storage tanks, (2) leaking drum storage areas, (3) leaking buried chemical distribution pipelines, (4) spillage at chemical handling facilities, (5) spillage during highway accidents and train derailments, and (6) intentional disposal into the subsurface in various ways. Intentional disposal of chlorinated solvents include: (a) release from domestic septic tile fields (from using solvent-containing septic tank cleaning fluid), (b) municipal landfills, (c) chemical waste disposal landfills, (d) settling ponds and lagoons, (e) landfarming of contaminated sludge and solids, and (f) injection well disposal of either used liquid solvent, or contaminated liquids.

Many of the sources of contamination listed by Pankow and Cherry (1996) are also applicable to DoD and USAF installations. Due to the widespread use of chlorinated solvents within the DoD and the USAF, primarily for cleaning and metal degreasing, groundwater contamination by CAHs is quite common. In fact, according to the Agency for Toxic Substances and Disease Registry, TCE and PCE, respectively, are the first and third most commonly detected contaminants at the approximately 330,000 hazardous waste sites across the United States (National Research Council, 1994). In addition there are currently over 860 TCE-contaminated sites within the Air Force (AFCEE, 2003).

Other factors that greatly contributed to widespread groundwater contamination by these compounds are their physical and chemical characteristics (see Table 2.1). Since these compounds are relatively volatile, past disposal practices may have relied on the supposition that these compounds would simply evaporate if left exposed to the atmosphere (Pankow and Cherry, 1996). Unfortunately, this proved to be untrue, and many CAHs that were dumped on the dry ground, placed into storage ponds, or discharged into drainage ditches have become the ground water contamination problems we face today.

Compound	Boiling Point (°C)	Vapor pressure (mmHg) (at 25°C)	Density (g/cm^3) (at 25°C)	Solubility (mg/L) (at 25°C)	Henry's Law constant ($atm*m^3/mole$) (at 25°C)
Tetrachloroethylene (C_2Cl_4)	121.07	18.6	1.623	150	0.0177
Trichloroethylene (C_2HCl_3)	86.7	69.0	1.463	1,100	0.00985
1,1-Dichloroethylene ($C_2H_2Cl_2$)	31.56	600	1.213	2,250	0.0261
c-1,2-Dichloroethylene ($C_2H_2Cl_2$)	60.2	201	1.284	3,500	0.00408
t-1,2-Dichloroethylene ($C_2H_2Cl_2$)	47.7	331	1.257	6,300	0.00938
1,1-Dichloroethane ($C_2H_4Cl_2$)	57.3	227	1.175	5,060	0.00562
1,1,1-Trichloroethane ($C_2H_3Cl_3$)	74.08	124	1.338	1,500	0.0172

Table 2.1 Properties of common chlorinated aliphatic hydrocarbons (Sellers, 1999)

DNAPLs have a density greater than water (see Table 2.1), and therefore are likely to sink below the water table after passing through the vadose zone, when released in sufficient quantity. As the DNAPL moves through the vadose and saturated zones it fingers downward, as well as spreading laterally on capillary barriers. The compound may also pool atop impermeable layers (Wiedemeier *et al*., 1999). In this situation, the CAH source area consists of two regions: (1) pools of separate phase contamination resting upon impermeable layers which slowly dissolve as groundwater flows over them; and (2) areas of residual DNAPL saturation within the vadose and saturated zones,

created after the flowing DNAPL passes through, leaving behind separate phase residual NAPL. This "residual zone" consists of NAPL droplets which are held by capillary forces in the pore space between soil grains. As groundwater flows through this zone of residual contamination, the contaminant slowly dissolves into the water. Because of the relatively low solubility of most DNAPLs (see Table 2.1), these source areas can continue to contaminate the aquifer for many years following the compounds' original release.

Although relatively insoluble, most chlorinated aliphatic hydrocarbons are potentially harmful to human health at concentrations well below their solubilities. That is, the maximum contaminant levels (MCLs) for most of these compounds are orders of magnitude below their solubilities, where the MCL is the safe level of contaminant permitted in drinking water, as established by the U.S. Environmental Protection Agency (U.S. EPA) in compliance with the Safe Drinking Water Act (Sellers, 1999). As an example, while the solubility of TCE is 1,100 mg/L, its MCL is only 0.005 mg/L (Sellers, 1999).

2.3 Health Effects of CAHs

Solvents in the environment may be inhaled, ingested, or brought into contact with the skin. Generally, exposure to these compounds results in some degree of central nervous system depression, skin irritation, and potential liver or kidney damage (Hathaway *et al*., 1996). The risk for exposure to groundwater contaminated with a CAH

is either through ingestion and adsorption into the gastrointestinal track, or through inhalation of volatilized CAHs from daily residential water usage.

Klaassen (2001) states the majority of the toxicities associated with TCE are thought to be caused by metabolites rather than by the parent compound. Klaassen (2001) also reported that two studies have provided some evidence of a link between kidney cancer and TCE, although the link may be applicable only under extreme exposure conditions. TCE can be readily adsorbed into the circulatory system via oral or inhalation routes.

Williams *et al*. (1985) reported that the capability for central nervous system depression and liver or kidney injury increases with degree of chlorination. According to Klaassen (2001) there are two potential pathways that may result from ingestion of a CAH; an oxidative pathway and a glutathione (GSH) pathway. The majority of the TCE ingested is oxidized, with only a small proportion being conjugated with the GSH pathway (Klaassen, 2001). Both metabolic pathways are implicated in the carcinogenicity of TCE: reactive metabolites of the GSH pathway have resulted in kidney tumors in rats, and oxidative metabolites have caused liver and lung tumors in mice, though it appears that direct extrapolation from rodent data would overstate human TCE cancer risk (Klaassen, 2001). Both TCE's and PCE's potential for causing cancer in humans continues to be a subject of controversy.

Unlike the more highly chlorinated ethylenes like PCE and TCE, which have the controversial potential to be cancer causing agents (Klaassen, 2001); vinyl chloride is considered a known human carcinogen. Experimental evidence links vinyl chloride to tumor induction in a variety of organs, including the liver, lung, brain, and kidney.

Evidence also suggests a relationship between vinyl chloride and nonmalignant alterations, such as fibrosis and connective tissue deterioration (Williams *et al.,* 1985). In addition to its carcinogenic properties, vinyl chloride is also a demonstrated mutagen and an agent toxic to the male reproductive system.

Prior to 1974, when the U.S. EPA banned many uses of this substance, vinyl chloride was used as a refrigerant, an extraction solvent for heat sensitive materials, an aerosol propellant, an ingredient of drug and cosmetic products, and a compound used in the synthesis of other organic compounds (U.S. EPA, 2003). Today vinyl chloride is primarily used in the production of polyvinyl resins (PVCs). Unlike vinyl chloride, PVC is considered non toxic; therefore, natural degradation of PVCs would not be considered a significant source of environmental vinyl chloride contamination. Currently, the major source of vinyl chloride release to the environment (atmosphere and groundwater) is believed to be from the emissions and effluent streams of plastics industries (U.S. EPA, 2003). Since DoD installations do not produce plastics, vinyl chloride contamination on these installations is probably a result of natural reductive dehalogenation of solvents like PCE and TCE in anaerobic groundwater (Wiedemeier *et al*., 1999).

2.4 Mechanisms for Noble Metal Catalyzed Reduction of CAHs

Due to the potential adverse health effects detailed in Section 2.3, and the fact that there is potential of human exposure to CAHs through contaminated groundwater, an emphasis has been placed on finding ways to remediate CAH-contaminated groundwater. An innovative technology uses palladium catalysis with molecular hydrogen to effect *in*

situ destruction of CAHs (McNab *et al*., 2000; Munakata *et al*., 2002). There are four possible processes by which chlorinated ethylenes may degrade in the presence of a noble metal catalyst, such as palladium, and an electron donor like hydrogen gas or formic acid: (1) hydrodehalogenation, (2) hydrogenation (Schreier and Reinhard, 1995), and possibly by (3) reductive β-elimination or (4) formation of free radical species at the surface of the catalyst.

Hydrodehalogenation is the process by which chlorine atoms are removed and replaced by hydrogen ions at the surface of the palladium. The reaction is believed to proceed according to the following equations:

$$H_2 \rightarrow 2H^+ + 2e^- \qquad \text{(Eqn 2.1)}$$

$$X\text{-}Cl + 2H^+ + 2e^- \rightarrow X\text{-}H + H^+ + Cl^- \qquad \text{(Eqn 2.2)}$$

This process produces a lesser-chlorinated ethylene, hydrogen ions, and chloride ions. An electron donor, such as hydrogen, is required for the reaction to proceed. In this case molecular hydrogen is oxidized and the contaminant is reduced.

Hydrogenation involves breaking the contaminant carbon-carbon double bond and the subsequent addition of two hydrogen ions at the surface of the metal catalyst (Schreier and Reinhard, 1995). This process takes a double-bonded molecule like an ethylene and converts it to a single-bonded molecule like an ethane. This process can be explained by the following equations:

$$H_2 \rightarrow 2H^+ + 2e^- \qquad \text{(Eqn 2.1)}$$

$$H_2C{=}CH_2 + 2H^+ \rightarrow H_3C\text{-}CH_3 \qquad \text{(Eqn 2.3)}$$

As with hydrodehalogenation, hydrogen ions are required for this reaction to occur. Rylander (1985) suggested that hydrogenation was a multi-step process in which

two hydrogen ions are sequentially transferred to the species on the surface of the catalyst. Lowry and Reinhard (2001) showed that under hydrogen-poor conditions, coupling and isomerization reactions may occur as a result of transfer limitations to produce C-4 and C-6 radicals. Boggs (2000) and Niekamp (2001) also noted the formation of four and six carbon hydrocarbons while studying the Pd/H_2 system. These byproducts appeared to form as a result of the coupling and polymerization of free radical species (Niekamp, 2001). There are two possible explanations for the formation of longer chain hydrocarbons in this system. One explanation involves the hydrogenation process as shown in Equations 2.1 and 2.3. Hydrogenation is believed to be a two-step process involving the sequential transfer of two hydrogen atoms. When the concentration of molecular hydrogen on the Pd surface is low compared to the number of reactive species, the hydrogen limitation may result in an incomplete transfer of hydrogen and hence formation of a free radical species (Niekamp, 2001). These free radical species, being highly unstable, may combine with each other or with unsaturated hydrocarbons in the system to form these long chain hydrocarbons (Niekamp, 2001). The second explanation for the production of these longer chain hydrocarbons is the possibility that the system can follow the β-elimination pathway for reduction of these chlorinated solvents, as described below.

Reductive β-elimination is most notably associated with the reduction of chlorinated ethylenes on the surface of zero-valent iron (Roberts *et al.*, 1996). However, this pathway may also be relevant for the reduction of CAHs on the surface of a noble metal catalyst such as palladium. The mechanism of reductive β-elimination is differentiated from hydrodehalogenation because two halide ions are released in a single

step instead of one (Roberts *et al.*, 1996). In the presence of zero-valent metals, particularly zero-valent iron, reductive β-elimination appears to be the major pathway for degradation of chlorinated ethylenes (Roberts *et al.*, 1996). Reductive β-elimination is shown for the reduction of TCE to chloroacetylene in Equation 2.4 and for reduction of the DCE isomers to acetylene in Equation 2.5:

$$ClHC{=}CCl_2 + 2e^- \rightarrow HC{\equiv}CCl + 2Cl^- \qquad \text{(Eqn 2.4)}$$

$$ClHC{=}CHCl + 2e^- \rightarrow HC{\equiv}CH + 2Cl^- \qquad \text{(Eqn 2.5)}$$

Niekamp (2001) suggested that since the zero-valent iron and Pd/H_2 systems are very similar, it might be possible for TCE to degrade in the Pd/H_2 system by the β-elimination pathway. Experimental evidence obtained while studying acetylene degradation in the Pd/H_2 system revealed the same four carbon chain and six carbon chain byproducts that were produced from TCE degradation in the Pd/H_2 system (Niekamp, 2001). The presence of chloroacetylene and acetylene has not been reported in the literature when degrading CAHs using a Pd/H_2 system (Lowry and Reinhard, 2001; Boggs, 2000; Niekamp, 2001); probably due to the extremely unstable nature of these two compounds. These compounds may have been present, but may have degraded prior to analysis of the samples. During degradation, production of four and six carbon hydrocarbons may indicate that the production of free radical species is occurring on the surface of the catalyst and/or that reduction via the β-elimination pathway is occurring. Figure 2.1 shows the potential sequence of degradation for hydrodehalogenation and reductive β-elimination pathways.

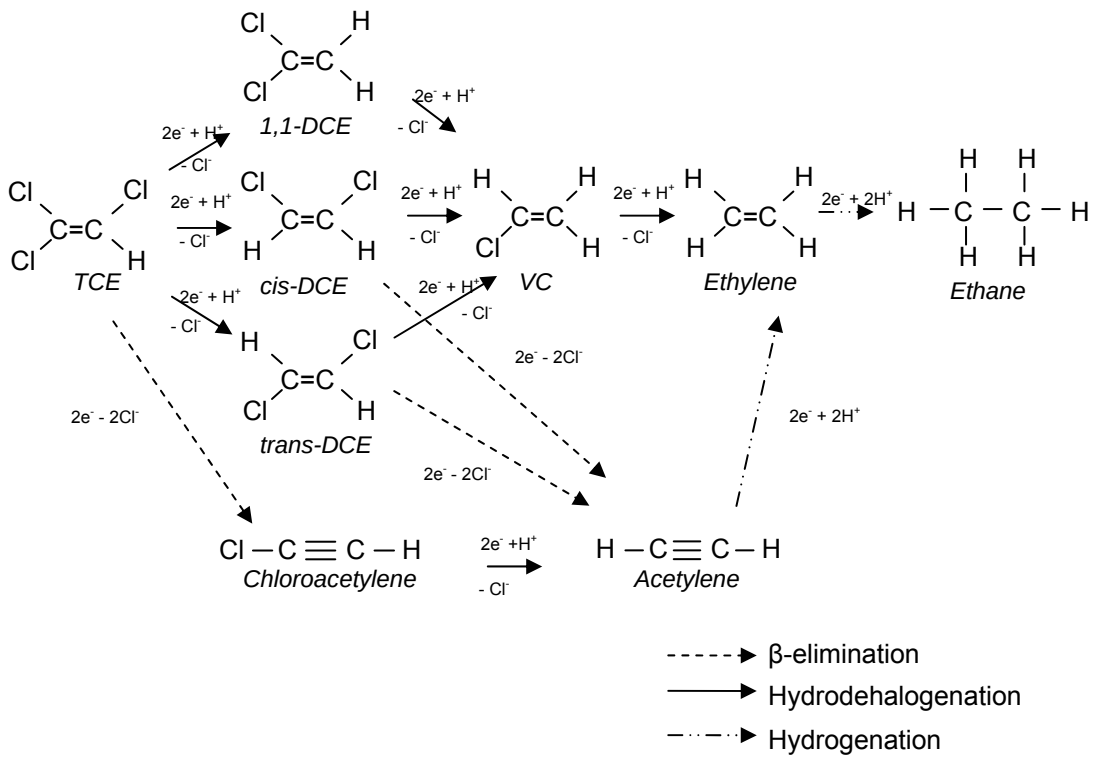

Figure 2.1 Hydrodehalogenation and reductive β-elimination pathways (Arnold and Roberts, 2000)

In all three of the reduction processes discussed above, an electron donor is required. Molecular hydrogen can be a source of electrons, as indicated in the following equations (Thomas, 1997):

$$H_2(gas) \leftrightarrow H_2(aq) \qquad \text{(Eqn 2.6)}$$

$$H_2(aq) \leftrightarrow H_2(Pd\ surface) \qquad \text{(Eqn 2.7)}$$

$$H_2(Pd\ surface) \leftrightarrow 2H^+(Pd\ surface) + 2e^-(Pd\ surface) \qquad \text{(Eqn 2.8)}$$

In Equation 2.6, molecular hydrogen dissolves into the aqueous phase, while Equations 2.7 and 2.8 show the dissociation of molecular hydrogen on the surface of the catalyst. The catalyst serves to reduce the required activation energy for the reaction(s)

to proceed. Without the presence of this heterogeneous catalyst the energy required to make the reaction proceed in the forward direction would be too great and reduction would not occur.

2.5 Experimental Application of Pd Catalysis using Molecular Hydrogen as an Electron Donor for CAH Reduction

Occasionally, the process of CAH reduction using Pd/H_2 is referred to as hydrodehalogenation in the literature (Perrone *et al*., 1998; Kopinke *et al*., 2003; Lowry and Reinhard, 1999). Hydrodehalogenation may in fact be the dominant pathway for the reduction of CAHs using a noble metal catalyst; however, this is not to say that it is the only pathway involved. Much research has shown TCE conversion with ethane as an end product (Lowry and Reinhard, 1999; Schreier and Reinhard, 1995; McNab *et al.*, 2000; Boggs, 2000; Niekamp, 2001). This is not feasible without hydrogenation. Another observation that supports multiple pathways is the production of C-4 and C-6 compounds in the Pd/H_2 system; as described in Section 2.4, production of these species indicates that the system is producing free radical species or the possibility for the system to follow the β-elimination pathway for reduction of chlorinated solvents. For the purpose of the following discussion, we will refer to the process of reducing CAHs using a noble metal catalyst and an electron donor as simply "dehalogenation", understanding that this term incorporates all the relevant processes described above.

The dehalogenation of organic compounds using a noble metal catalyst and hydrogen gas is a widely used process in the synthesis of various chemicals (Rylander,

1985). While this method for chemical synthesis can be traced as far back as the early 1950s, it wasn't until the early 1990s when it was first suggested as a treatment technology for use in groundwater remediation by Kovenklioglu *et al*. (1992). Investigators at Stanford University quickly followed with a series of research studies involving the use of palladium and hydrogen gas as an electron donor for the treatment of water contaminated with chlorinated ethylenes (Schreier and Reinhard, 1995; Lowry and Reinhard, 1999; 2000; 2001; McNab *et al*., 2000).

Schreier and Reinhard (1995) evaluated the use of 0.5% Pd on alumina and 0.1 atm of H_2 to treat chlorinated ethylenes in tap water. They found that in a batch system of various chlorinated ethylenes, including PCE and vinyl chloride, rapid and complete degradation would occur within 10 minutes with ethane and HCl as the final products of the reaction. In this system ethane accounted for as much as 85% of the mass balance and ethylene was a reactive intermediate whose maximum concentration accounted for less than 5% of the initial substrate (Schreier and Reinhard, 1995). The researchers also evaluated the use of palladium on granular carbon and found it also to be an effective catalyst, though ethane yield was somewhat lower (55%) than with the Pd on alumina catalyst (Schreier and Reinhard, 1995). The differences between the two ethane recovery yields are probably due to the sorption characteristics of the various catalyst support media. Other experimental results seemed to indicate that PCE could not be reduced efficiently with a palladium-on-carbon catalyst because PCE was irreversibly adsorbed to the carbon support (Schreier and Reinhard, 1995).

Similar research at the University of Arizona (Muftikian *et al*., 1995) found that a palladium-iron catalyst in batch experiments could be used to rapidly dechlorinate

chlorinated ethylenes to ethane with no intermediate reaction products. The researchers also evaluated dechlorination of various chloromethanes like carbon tetrachloride (CCl_4), chloroform ($CHCl_3$) and dichloromethane (CH_2Cl_2), on palladized iron. Muftikian *et al*. (1995) found that carbon tetrachloride dechlorinated completely to methane in a few minutes, while $CHCl_3$ and CH_2Cl_2 had somewhat slower degradation times; 1 hour and 4-5 hours, respectively.

McNab and Ruiz (1998) developed a two stage treatment column; the first stage consisted of an electrolyzer to produce hydrogen by passing DC current over graphite electrodes followed in series by a catalyst bed of Pd/Al_2O_3 pellets. This design was viewed as a practical solution to quickly saturate the aqueous phase influent with hydrogen. They found removal efficiencies greater than 95% with residence times on the order of 2 minutes for PCE, TCE, 1,1-DCE and carbon tetrachloride. Their results also indicated that dissolved oxygen does not completely inhibit reduction of the chlorinated hydrocarbons on the catalyst (McNab and Ruiz, 1998).

Perrone *et al.* (1998) studied the hydrodechlorination of TCE using a palladium-on-carbon catalyst with H_2 gas. Their experiments highlighted one of the major limitations of this process – catalyst deactivation. Catalyst deactivation occurred even at a concentration of a few ppm of HCl. They found that the catalyst was only effective when a base such as NaOH or NH_3 was present (Perrone *et al.*, 1998). The base served to neutralize the HCl produced by the dechlorination of TCE. The researchers also tested the capacity of palladium-on-carbon to adsorb TCE from saturated air and found that this catalyst had a high capacity to adsorb TCE vapors.

In a trilogy of papers, Lowry and Reinhard (1999; 2000; 2001) studied the dehalogenation of TCE and other CAHs on a palladium catalyst in the presence of hydrogen gas. Initial results indicated that TCE could be transformed quantitatively (97%) to ethane without the formation of any detectable chlorinated intermediates (Lowry and Reinhard, 1999). This implies a direct conversion of TCE to ethane is possible on the surface of the Pd catalyst. Table 2.2 summarizes the kinetic parameters obtained for some of the various CAHs studied. Additional experiments showed a direct relation between pH and TCE removal efficiency; TCE conversion increased 30% upon increasing the pH from 4.3 to 11 (Lowry and Reinhard, 2000). The researchers also found that the transformation rate of TCE was affected by the amount of H_2 gas present in the system. The investigators used a reactor filled with DI water and sparged with pure H_2 gas (P/Po = 1) or a H_2/N_2 gas mixture to remove dissolved oxygen and provide a specific $[H_2](aq)$. Table 2.3 summarizes the effects of H_2 gas concentration on the observed TCE reaction rate (k_{obs}) and half-lifetimes ($t_{1/2}$) (Lowry and Reinhard, 2001). In Table 2.3 P represents the pressure of H_2 gas and P_0 is the total pressure of gas in the system; when $P/P_0 = 1$ then no N_2 gas is present. As expected when the concentration of the electron donor is decreased the observed TCE reaction rate decreases. The investigators also noted that the concentration of the dissolved H_2 gas had little effect on the distribution of halogenated intermediates formed; cis-1,2-DCE and 1,1-DCE accounted for approximately 80% of the halogenated intermediates formed (Lowry and Reinhard, 2001). The investigators were unable to model the production of these chlorinated intermediates. This led them to believe that these intermediates were part of a transient process (Lowry and Reinhard, 2001). In addition to these chlorinated

intermediates the researchers also observed C4 and C6 radical coupling products which included: 1-butene, n-butane, cis-2-butene, trans-2-butene, and 2-hexane (Lowry and Reinhard, 2001). C4 and C6 radical coupling increased with decreasing $[H_2](aq)$ in the reactor and accounted for as much as 18% of the TCE converted at the lowest $[H_2](aq)$ (Lowry and Reinhard, 2001).

Compound	[CAH]o [μM]	k_{rxn} ($L*gcat^{-1}*min^{-1}$)	R^2	$t_{1/2}$ (min)
PCE	7.8	0.53	0.976	5.9
TCE	22.8	0.64	0.993	4.9
1,1-DCE	23.7	0.7	0.997	4.5
cis-DCE	76.3	0.83	0.996	3.8
trans-DCE	75.3	0.78	0.997	4.0

Table 2.2 CAH transformation rate constants and half lives in zero-headspace batch reactor using a 0.22 g/L concentration of 1% Pd on Al_2O_3, estimated dissolved H_2 concentration of 800 μM (Lowry and Reinhard, 1999)

P/P_0	$[H_2](aq)$ (μM)	k_{obs} (min^{-1})	$t_{1/2}$ (min)
1.0	1000	0.034 ± 0.006	20
0.4	400	0.025 ± 0.004	28
0.104	100	0.015 ± 0.001	46
0.04	40	0.0037 ± 0.0005	187
0.01	10	0.0007 ± 0.0003	990

Table 2.3 H_2 partial pressures and corresponding $[H_2](aq)$ and observed TCE reaction rate constants (k_{obs}) and half-lifetimes ($t_{1/2}$) in headspace batch reactors (initial TCE concentration of 21 mg/L) (Lowry and Reinhard, 2001**)**

Niekamp (2001) conducted similar research to evaluate the effectiveness of the Pd/H_2 system for the remediation of chlorinated ethylenes. Using a Pd/Al_2O_3 catalyst in powder form (1.0% Pd by weight) for batch systems and granular 0.5% Pd on Alumina pellets for column experiments he evaluated the effects of pH, substrate loading, catalyst concentration, reductant concentration, and the effects of various solutes on catalyst

performance. The researcher noticed increasing TCE degradation rates with increasing concentrations of dissolved molecular hydrogen. TCE degradation also decreased with decreasing pH. The investigator used a batch system to evaluate the effects of substrate concentration on the performance of the system. Experimental results showed that increasing TCE concentrations led to increased production of various C-4 reaction products such as 1-butene, cis-2-butene, trans-2-butene, and butane (Niekamp, 2001). Tables 2.4 through 2.6 summarize the modeling parameters obtained from his experiments. A discussion of Michaelis-Menten kinetics is covered in Section 3.7 of this document.

[Pd] (mg/L)	V_{max} (μM/min)	$K_{1/2}$ (μM)	V_{max} standard error	$K_{1/2}$ standard error	Correlation of Parameters	k_1 (min^{-1})	R^2
25	0.763	48.306	0.375	88.222	0.998	--	--
70	2.224	50.397	0.240	11.656	0.988	--	--
150	4.452	47.096	0.682	17.480	0.992	--	--
250	10.762	140.628	1.258	23.008	0.996	--	--
300	--	--	--	--	--	0.067	0.999

Table 2.4 Effects of [Pd] on Michaelis-Menten model parameters in a batch system, $[TCE]_0$=216 μM (28.4 mg/L), $[H_2]$=0.2 atm (Niekamp, 2001)

[TCE]o (μM)	V_{max} (μM/min)	$K_{1/2}$ (μM)	V_{max} standard error	$K_{1/2}$ standard error	Correlation of Parameters
61.83	11.84	193.21	0.47	7.52	1.00
92.74	12.89	156.04	0.23	2.79	1.00
154.5	15.53	146.73	0.15	1.58	1.00

Table 2.5 Effects of $[TCE]_0$ on Michaelis-Menten model parameters in a batch system, [Pd] = 25 mg/L, $[H_2]$ = 0.2 atm, buffered to pH = 10.1 (Niekamp, 2001)

pH	V_{max} (μM/min)	$K_{1/2}$ (μM)	V_{max} standard error	$K_{1/2}$ standard error	Correlation of Parameters
8.2	2.449	35.84	0.201	4.064	0.989
9.2	8.403	100.299	0.012	0.151	0.999
9.9	7.422	64.901	0.021	0.205	0.998

Table 2.6 Effects of pH on Michaelis-Menten model parameters in a batch system, [Pd] = 25 mg/L, $[TCE]_0$ = 92.74 μM (12.2 mg/L), $[H_2]$ = 0.2 atm, buffered to desired pH (Niekamp, 2001)

Lowry and Reinhard (2000) also conducted column experiments to determine the effectiveness of this treatment technology for the conversion of TCE in natural and synthetic groundwater. The column used had an empty bed volume of 10.5 mL and was filled with 0.5 g of 1% Pd on Alumina; the remaining volume of the reactor was filled with inert glass beads. The researchers studied the effects of various influent TCE concentrations ranging from 0.5 to 20 mg/L (4-152 μM) with a hydraulic retention time of 4.3 minutes and found that the percent TCE conversion remained unchanged. Longer term studies using DI water as a baseline found that a rapid decline in TCE conversion (dropping from 44% to 33%) occurred within the first two to three days on stream. The researchers found a steady state TCE conversion of greater than 24% for a period of 60 days using 0.5 g of catalyst and a retention time of 4.3 min for influent TCE concentrations of about 3.5 mg/L (27 μM). Ethane and trace amounts of ethylene were the only reaction products observed. The researchers calculated a catalyst deactivation rate constant, k_d, of 5.6 x 10^{-3} day^{-1} (Lowry and Reinhard, 2000). The researchers compared this value for catalyst deactivation in DI water with the deactivation observed due to the presence of common groundwater solutes (Table 2.7). Deactivation of the catalyst was observed due to the presence of a number of common groundwater constituents; however catalyst activity was restored after flushing with a dilute sodium

hypochlorite solution. A more detailed discussion of catalyst deactivation is covered in Section 2.6 of this chapter. The researchers found that they could maintain TCE conversion rates during a 63-day experiment using natural groundwater by periodic (every 4-7 day) 90-min pulses of a dilute sodium hypochlorite solution (Lowry and Reinhard, 2000).

Solute	[Solute] (mg/L)	pH[1] (influent –effluent)	k_{rxn}[2] (mL (g of catalyst)$^{-1}$ min-^{1})	k_d (day^{-1} x 10^3)
None (DI)		6.4 – 4.9	0.77 – 0.56	5.6
H_2CO_3	580	4.4	0.64-0.51	2.8
HCO^{3-}	660	8.6	0.81 -0.59	5.0
CO_3^{2-}	659	10.9	0.80 – 0.69	2.1
SO_4^{2-}	690	6.1 – 5.0	0.78 – 0.59	7.6
SO_3^{2-}	87	6.2 – 4.6	0.55 – 0.12	>500
SO_3^{2-}	44		0.76 – 0.02	>900
HS^-	0.4	8.1	0.85 – 0.04	424
HS^-	0.8		0.55 – 0.04	>2000
Cl^-	1003	9.6	0.84 – 0.72	3.7

Table 2.7 Effects of various solutes on catalyst performance (Lowry and Reinhard, 2000)
[1] – pH ranges for unbuffered systems (±0.2)
[2] – Deactivation of the catalyst is a slow process. The k_{rxn} ranges shown represent the initial pseudo steady-state reaction rate constant for TCE – final pseudo steady-state TCE reaction rate constant

2.5.1 Pd Catalyst Inhibition/Deactivation.

One of the main problems with catalytic hydrodehalogenation of CAHs is catalyst deactivation due to the presence of various groundwater constituents. A number of researchers have evaluated the potential of catalyst inhibition and deactivation in the Pd/H_2 system due to the presence of common groundwater constituents. In this section,

we will review their findings in order to gain understanding of the reactions between naturally occurring groundwater constituents and this noble metal catalyst.

Dissolved oxygen (DO) is a constituent of most surface water and groundwater. The presence of DO can serve as a catalyst inhibitor. Palladium catalyzes the reaction between oxygen and hydrogen on the surface of the catalyst to form water (Equation 2.9) (Lowry and Reinhard, 2001).

$$2\ H_2 + O_2 \xrightarrow{Pd} 2\ H_2O \qquad \text{(Eqn 2.9)}$$

Schreier and Reinhard (1995) noted that the presence of oxygen lowered catalyst performance by competing with the contaminant for hydrogen; however, by increasing the amount of hydrogen in the system this effect was minimized. In column experiments with H_2 as the electron donor, Lowry and Reinhard (2001) found that the reaction rate for oxygen reduction is approximately 2 to 2.5 times higher than the rate for TCE reduction. Fortunately until DO exceeds approximately 370 μM (11.8 mg/L), it has little or no effect on the TCE transformation rate constant (Lowry and Reinhard, 2001). Considering the DO concentration for water in equilibrium with air is approximately 8.4 mg/L, it seems that a system for catalytically reducing CAHs using a palladium catalyst could be deployed in naturally aerobic aquifers without the need to remove dissolved O_2 from the influent prior to treatment (McNab *et al*., 2000).

Chloride is also a common ground constituent. Recall from Equation 2.2 that the chloride and hydrogen ions are created at the catalyst surface as byproducts of the dechlorination reaction of CAHs (Lowry and Reinhard, 2000). Lowry and Reinhard

(2000) found that the presence of aqueous phase chloride ions did not negatively affect the conversion rate of TCE (see Table 2.7). On the other hand, molecular chlorine (Cl_2), as reported by Chang *et al*. (1999), acts as a catalyst poison as a result of the strong affinity of chlorine to adsorb to the catalyst surface.

Lowry and Reinhard (2000) also evaluated the effects of hydrogen sulfide (HS^-), sulfite (SO_3^{2-}), and sulfate (SO_4^-) ions on the performance of a palladium based catalyst (see Table 2.7). The presence of SO_4^- did not have any negative effects on catalyst activity, and as reported by Lowry and Reinhard (2000), in some cases sulfate served to improve catalyst performance for the conversion of TCE. However, the presence of 87 mg/L of SO_3^- or 0.4 mg/L HS^- caused rapid catalyst deactivation, possibly due to chemisorption of these ions to active sites on the catalyst (Lowry and Reinhard, 2000). It was also noted that the TCE conversion rate stabilized at 3-5%, indicating that some residual catalyst activity remains even in the presence of high concentration of SO_3^{2-}. This residual activity may suggest that SO_3^{2-} may compete for active sites and/or H_2 (Lowry and Reinhard, 2000), or that some catalytic sites may be resistant to deactivation due to mass transfer limitations (Schüth *et al*., 2000). Lab work indicates that dilute sodium hypochlorite solutions are effective for regenerating catalysts deactivated by HS^- and SO_3^{2-} (Lowry and Reinhard, 2000), indicating that field implementation of a palladium reactor can be accomplished in the presence of HS^- and SO_3^{2-} if the rector is flushed with a periodic pulse of dilute sodium hypochlorite to restore catalyst activity.

Other common groundwater constituents include nitrate (NO_3^-) and nitrite (NO_2^-). Lowry and Reinhard (2001) found that influent NO_3^- concentration had no effect on TCE conversion in column experiments. Nitrate and TCE did not appear to compete for

catalyst active sites because high concentrations of nitrate did not affect TCE conversion even though significant adsorption of nitrate to the catalyst surface would be expected as reported by Pintar (1996). Horold *et al*. (1993) and Daub *et al*. (1999) demonstrated that NO_2^- reacts with H_2 on the surface of the catalyst to produce N_2, H_2O and OH^-. Lowry and Reinhard (2001) showed that the presence of nitrite does decrease the TCE conversion rate, but the effects were minor when considering the influent nitrite concentrations were over 2 orders of magnitude greater than the influent TCE concentration. TCE was observed to be more reactive that nitrite in the Pd/H_2 system (percent nitrite converted 10-25%, percent of TCE converted 43%) (Lowry and Reinhard, 2001). Since the reactivity of nitrite is lower than the reactivity of TCE, and the fact that nitrite concentrations in groundwater are typically very low, these results would seem to indicate that nitrite will not lead to H_2 depletion in a Pd reactor even though small amounts of H_2 are utilized for the transformation of NO_2^- to N_2. Table 2.8 summarizes the researchers findings involving competing nitrate/nitrite solutes in the system.

Solute	[solute]in (μM)	[TCE]in (μM)	TCE conv (%)	k_{tce}^1 (min-1)	Solute conv (%)	k_{solute}^1 (min-1)
None	0	26.6	48.2	0.147	0	0
Nitrate	371	30.1	48.0	0.146	2	0.005
Nitrate	1290	31.0	47.4	0.143	0	0
Nitrite	1565	23.1	44.0	0.129	23	0.058
Nitrite	2609	30.3	43.3	0.127	10	0.024

Table 2.8 TCE and Nitrate/Nitrite conversion through column reactor
1 – observed first order rate constants for the respective species
(HRT=4.4 min, 1 g 1% Pd on Alumina)
(Lowry and Reinhard, 2001)

The carbonate system is one of the most prevalent in natural waters. For this reason it is important to understand the effects that the various carbonate species have on a Pd catalyst. Lowry and Reinhard (2000) introduced carbonate (CO_3^{2-}) and carbonic acid (H_2CO_3) at an order of magnitude greater than the TCE concentration and found that they had no impact on the TCE conversion rate (see Table 2.7). The researchers also tested bicarbonate (HCO_3^-) as a possible catalyst inhibitor. HCO_3^- was suspected as a potential catalyst inhibitor based on aqueous phase experimental results from McNab and Ruiz (1998) as well as results from Kramer *et al.* (1995). Bicarbonate may act as a catalyst poison due to the conversion of HCO_3^- to formate ($HCOO^-$) on the catalyst surface as shown by the following reaction (Lowry and Reinhard, 2000):

$$HCO_3^- + H_2 \xrightarrow{Pd} HCO_2^- + H_2O \qquad \text{(Eqn 2.10)}$$

Formate was reported as a catalyst inhibitor due to its strong affinity to bind to the Pd and its conversion to carbon monoxide at the surface of the Pd catalyst (Kramer *et al.*, 1995). Lowry and Reinhard (2000) conducted column experiments and monitored the effluent from all three of the carbonate species to check for the presence of formate. They detected small amounts of formate in the effluent of all three columns (1.2% conversion from HCO_3^- to $HCOO^-$, and 0.1% conversion of H_2CO_3 and CO_3^{2-} to $HCOO^-$). Even though formate was produced in the experiment it did not impact the TCE degradation rate constant which was almost identical to that of the rate constant measured in DI column experiments (Lowry and Reinhard, 2000). Since the concentrations of

formate produced were so low, the production of formate from the above reactions does not appear to inhibit the catalyst activity of Pd (Lowry and Reinhard, 2000).

One of the products of the catalytic reduction of CAHs is hydrochloric acid (HCl). Perrone *et al*. (1998) found that concentrations of even a few parts per million of HCl caused catalyst deactivation for 0.5% Pd on carbon pellets. As mentioned in earlier sections, this is the reason that catalyst performance is maximized at a higher pH for the Pd/H_2 system. When the substrate is mixed with water at a higher pH, the HCl produced by the reaction at the catalyst surface is neutralized by the elevated concentration of hydroxide ions associated with this higher pH. This high pH helps maintain a reduced state at the catalyst surface and enhances catalyst performance. Table 2.9 summarizes the known effects of potential groundwater constituents on catalyst activity in a Pd/H_2 system (Stoppel, 2001).

Groundwater Constituent	Effect on catalyst activity (Product(s) from rxn w/H_2)	Source(s)
Oxygen (O_2)	Catalyst inhibitor - competes for H_2. Effects can be minimized by increasing H_2 concentration. (water)	Schreier and Reinhard, 1995 McNab *et al*., 2000 Lowry and Reinhard, 2001 Siantar *et al*., 1996
Dissolved carbon dioxide (H_2CO_3)	No adverse effect on catalyst activity, relative to established baseline in DI water	Lowry and Reinhard, 2000
Carbonate (CO_3^{2-})	No adverse effect on catalyst activity, relative to established baseline in DI water	Lowry and Reinhard, 2000
Bicarbonate (HCO_3^-)	No adverse effect on catalyst activity, relative to established baseline in DI water	Lowry and Reinhard, 2000
Sulfate (SO_4^{2-})	No adverse effect on catalyst activity	Lowry and Reinhard, 2000 Siantar *et al*., 1996[1] Schreier and Reinhard, 1995[2]
Sulfite (SO_3^{2-})	Strong catalyst deactivation	Lowry and Reinhard, 2000 Siantar *et al*., 1996
Hydrogen sulfide (HS^-)	Strong catalyst deactivation	Lowry and Reinhard, 2000
Nitrate (NO_3^-)	No adverse effect on catalyst activity	Lowry and Reinhard, 2001 Siantar *et al*., 1996[1] Schreier and Reinhard, 1995[2]
Nitrite (NO_2^-)	Catalyst inhibitor (N_2, water, OH^-)	Lowry and Reinhard, 2001 Siantar *et al*., 1996 Schreier and Reinhard, 1995
Chloride (Cl^-)	No adverse effect on catalyst activity	Lowry and Reinhard, 2000 Schreier and Reinhard, 1995 Siantar *et al*., 1996[1] Chang *et al*. 1999[3]
Phosphate (PO_4^{3-})	Minor Catalyst deactivation observed	Munakata *et al*., 1998
Bisulfide	Strong catalyst deactivation	Schreier and Reinhard, 1995
Carbon Monoxide (CO)	Catalyst inhibitor formed from the conversion of formate on the catalyst surface	Kramer *et al*., 1995 Lowry and Reinhard, 2000

[1] - Siantar *et al*., 1996 reported only slightly inhibited transformation rates by H_2/Pd-alumina

[2] - Schreier and Reinhard, 1995 noted that (nitrate and sulfate) impacted PCE conversion at when [NO_3^-] was an order of magnitude larger than [PCE] and 200 times [Pd]

[3] - Chang *et al*. 1999 found that gas phase chloride acts as a catalyst poison as a result of the strong affinity of chloride to adsorb to the catalyst surface

Table 2.9 Common groundwater constituents and their effect on catalyst activity (Modified from Stoppel, 2001)

2.6 Experimental Application of Pd Catalysis using Reductants Other than Molecular Hydrogen

Section 2.5 reviews the literature pertinent to the reduction of CAHs using a palladium catalyst and dissolved H_2 gas as an electron donor. This section will review the research involving the reduction of various compounds using a palladium catalyst and other reductants, particularly formic acid. A review of the available literature indicates that H_2 is the only electron donor studied for the reductions of chlorinated aliphatic compounds via a Pd catalyst. However, formic acid has been used successfully with a Pd catalyst for the reduction of nitrates and nitroaromatic compounds (Prüsse *et al.,* 2000; Phillips, 2003). Cost comparison data as developed by Phillips (2003) has also shown that formic acid is approximately four times cheaper than hydrogen gas as a reductant for the conversion of nitroaromatic compounds.

Prüsse and Volrop (2001) studied the use of various bimetallic noble metal catalysts, including palladium and platinum, for the reduction of dissolved nitrate. The researchers found a drop in the activity of both catalysts at high pH values. Prüsse and Volrop (2001) hypothesized that this reduced activity was a result of active sites on the surface of the catalyst being blocked by strongly adsorbed hydroxide ions. The researchers suggested that with higher pH, the hydroxide ion concentration would increase and increasingly adsorb and cover the surface of the catalyst, ultimately blocking the nitrate adsorption sites and leading to the observed decrease in activity (Prüsse *et al.,* 2000).

Formic acid has been demonstrated to decompose at the surface of a metal catalyst, according to Equation 2.11, forming hydrogen and carbon dioxide as products

(Mars *et al.*, 1963). Theoretically, this hydrogen could act as the electron donor for the reduction of the contaminant at the surface of the catalyst and the carbon dioxide formed could serve as a buffer for the hydroxide ion according to Equation 2.12.

$$5HCOOH \xrightarrow{Pd} 5H_2 + 5CO_2 \qquad \text{(Eqn 2.11)}$$

$$2CO_2 + 2OH^- \longrightarrow 2HCO_3^- \qquad \text{(Eqn 2.12)}$$

Even though the above reaction provides a reductant (molecular hydrogen) from the degradation of formic acid, Prüsse *et al.* (2000) postulated that it was much more likely that formic acid itself, which is present as formate in solution and at the catalyst surface, was acting as the electron donor for the reduction of adsorbed nitrate by transfer hydrogenation. The researchers conducted experiments and found that in general catalyst activity was slightly higher when using formic acid as the reductant instead of hydrogen. Recent research by Phillips (2003) showed similar results for the reduction of nitroaromatic compounds.

2.7 Field Applications

The Pd/H_2 system has been successfully implemented in a demonstration at Lawrence Livermore National Laboratory (LLNL) in California with sustained performance of almost one year (McNab *et al.*, 2000). A Pd/H_2 reactor was used *in situ* as a result of unique site specific conditions that prevented the use of other more popular

remediation technologies. During the initial operation period the Pd/H_2 system ran for 4 hour/day and the system quantitatively (more than 99%) reduced PCE, TCE, 1,1-DCE and carbon tetrachloride with no observable chlorinated intermediates in the effluent (McNab *et al*., 2000). After the first 20 days of initial testing, treatment times were increased to 8 hours/day. With the increase in operating time, system behavior quickly changed: removal efficiencies began to decline, and vinyl chloride began to be produced in the column as an intermediate (McNab *et al*., 2000). The investigators were able to reverse this behavior by shutting down the system for a couple of days and then reducing the daily operation back to 4 hours/day. It was later shown that the system could operate at 5-6 hours/day for 5 days a week with removal efficiencies equivalent to operating everyday at 4 hours/day (McNab *et al*., 2000).

Researchers from the Naval Facilities Engineering Service Center and Stanford University have recently begun treatment of a TCE-contaminated plume at Edwards Air Force Base, California using 2% palladium on alumina spheres and hydrogen gas inside an HFTW. The reactor's design is modeled on the successful Pd reactors installed at LLNL (McNab *et al*., 2000), but has been altered to accommodate site specific conditions. The design calls for two reactors in series. Each reactor has a 6 inch diameter (constrained by the well diameter) and a 54 inch length for an empty bed volume of 6.5 gal (25 L) (Munakata *et al*., 2002).

A preliminary run demonstrated higher than 95% TCE removal with only a single pass of groundwater through the reactor (SERDP, 2003). The reactors are scheduled to operate *ex situ* for the first 4 months of the demonstration. Following this demonstration

period (which will be completed by August 2004) and once all maintenance and operation issues have been identified the reactors will be used *in situ*.

3.0 EXPERIMENTAL MATERIALS AND METHODS

3.1 Chemicals

High purity chemicals and gases were obtained and used without further purification. These included tetrachloroethylene (Aldrich, 99%), trichloroethylene (Acros, 99.5%), cis-1,2-dichloroethylene (97%), trans-1,2-dichloroethylene (Acros, 99.7%), 1,1-dichloroethylene (Aldrich, 99%), ethane (Air Products, technical grade, purity 99.99%), ethylene (Air products, technical grade, purity 99.99%), vinyl chloride (Air Products, 0.243% in N_2), and hydrogen gas (Air Products, ultra high purity, grade zero). In addition, for the preparation of analytical standards, high purity gaseous chemicals were obtained in canisters (from Scott Specialty Gases, PA) in N_2 in the following molar proportions: butane (1%), iso-butane (1.01%), n-butane (1%), 1-butene (1,002 ppm), trans-2-butene (1.01%), cis-2-butene (1%), iso-butylene (1%), acetylene (1.01%), n-hexane (411 ppm), propane (1%), propylene (1%), and n-pentane (996 ppm). Due to its higher solubility and ubiquity as a groundwater contaminant, TCE was selected as a model CAH. Other chemicals used in this research included formic acid (88%, Fischer Scientific), TAPS organic buffer (N-tris[Hydroxymethyl]methyl-3-aminopropanesulfonic acid sodium salt provided by Sigma Chemical Co.), Hydrochloric acid (Fisher Scientific), and sodium hydroxide (Fischer Scientific). High purity gases were supplied by Air Products (Allentown, PA).

3.2 Palladium Catalysts

Palladium catalysts were supplied by Sigma-Aldrich Chemical Company as 0.5% weight on alumina (Al_2O_3) 3.2 mm diameter pellets. The pellets were used as obtained from the manufacturer and were the sole media placed in the catalytic column reactor. The pellets were added to the column without special precautions to avoid exposure to air. A small layer of pesticide grade glass wool was used at each end of the column to prevent the media from clogging the inlet/outlet ports and any tubing.

3.3 Column

The column and end caps were purchased from Mainline Supply, Dayton, OH, a local plumbing supply store. The column is a 4 cm diameter, 316 gauge steel tube. End caps of the same material were also acquired for construction of the reactor. The column is 13 cm long and threaded on both ends. Teflon tape was applied to the threads of the column prior to wrench tightening the end caps. A single, threaded hole of ¼" diameter was drilled into each end cap for installation of inlet and outlet ports. Each end cap was packed with a thin layer of pesticide grade glass wool obtained from Sigma-Aldrich Chemical Co. to ensure even flow across the column and prevent the media from clogging the ports. The internal empty volume of the column was measured to be 176 mL. The column was packed with 154.14 g of Pd/Al_2O_3 pellets. During the packing process the column was tapped repeatedly to settle the pellets and minimize unintentional voids. Once the end caps were applied and tightened, the column was not opened again, nor was it rotated from its original vertical orientation. The column remained vertical

throughout the duration of all experiments, with the influent entering from the bottom of the column and the effluent exiting the top of the column. The pore volume, which was subsequently used to calculate hydraulic residence times (HRT), was 68.6 mL, the average of four measurements with a standard deviation of 1.1 mL.

3.4 Experimental Design

The column reactor described in Section 3.3 was positioned vertically for all experiments with the influent entering from the bottom and the effluent exiting the top. Ports were located as shown in Figure 3.1 to sample the column influent and effluent. A 20L glass vessel containing de-ionized water (18MΩ-cm_NANOpure) was amended with the desired concentration of formic acid or hydrogen gas, the sole electron donor, and mixed using a magnetic stir plate. The pH of the influent water was set at the desired level by manual titration using NaOH. A peristaltic digital drive pump (Masterflex® L/S Digital Standard Drive, model # 7523-70 with Barnant Company high capacity PTFE Diaphragm pump head, 800 mL/min at 0 PSI continuous duty, model # 7090-42) was used to pump the formate amended water into the 1L (actual volume 1146 mL) mixing chamber (Figure 3.1 and Figure 3.2). Flow rates were selected to obtain approximately integral (1, 2, 3 min) hydraulic retention times (HRTs) in the column. The mixing chamber stood on top of a stir plate (Fisher Scientific, catalog # 11-700-49S) to keep the mixture uniform. Another tube ran from the mixing chamber through the pump and into the column reactor. Effluent water passed through a series of drains allowing pH and conductivity measurements to be taken prior to discharge into a waste drum.

Prior to the start of an experiment, water amended with formic acid (or H_2 gas) was pumped through the reactor and the effluent stream's pH and conductivity values were allowed to stabilize. After stabilization, TCE was quickly added to the mixing chamber to achieve the desired initial concentration.

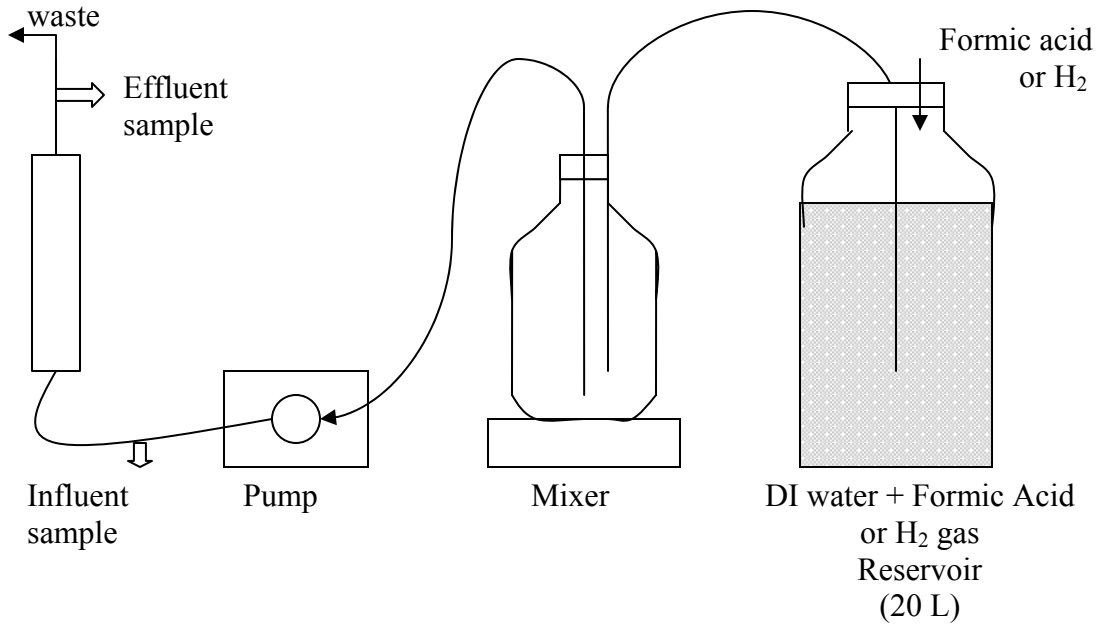

Figure 3.1 Experimental design

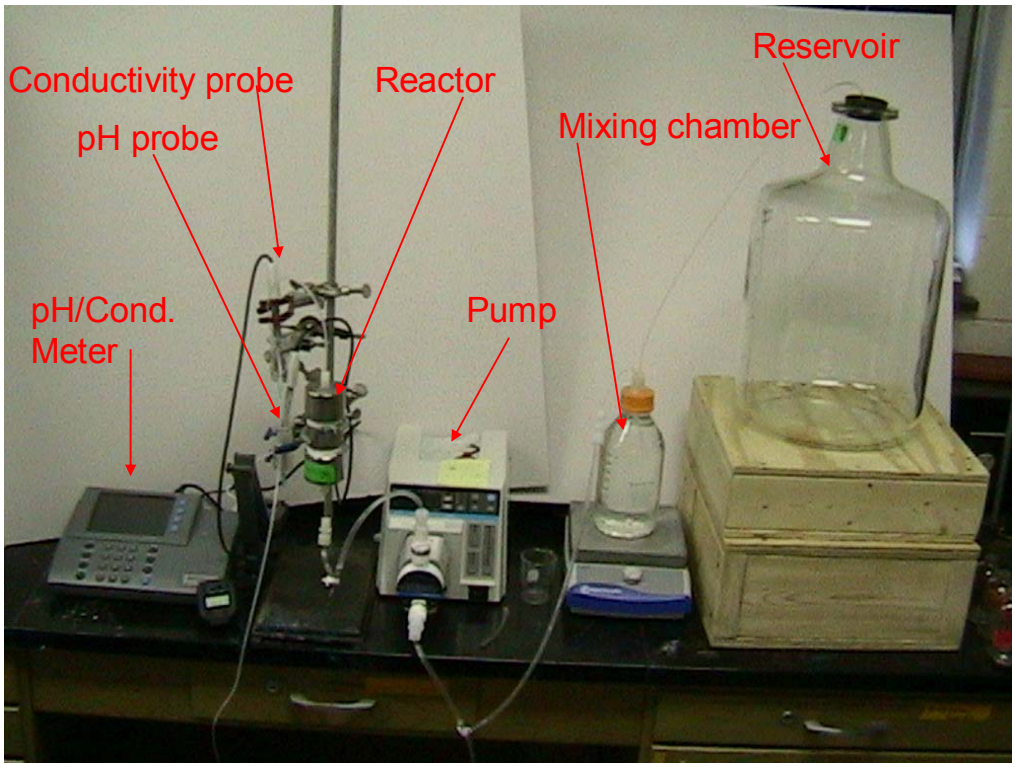

Figure 3.2 Experimental setup

As a result of the experimental configuration, substrate concentrations entering the reactor were diluted over time. Figure 3.3 illustrates the typical dilution curve for influent concentrations over time. An exponential curve can be fitted to approximate the dilution curve and was used to estimate influent concentrations when the length of time between two samples did not provide sufficient time to manually sample both the influent and effluent streams.

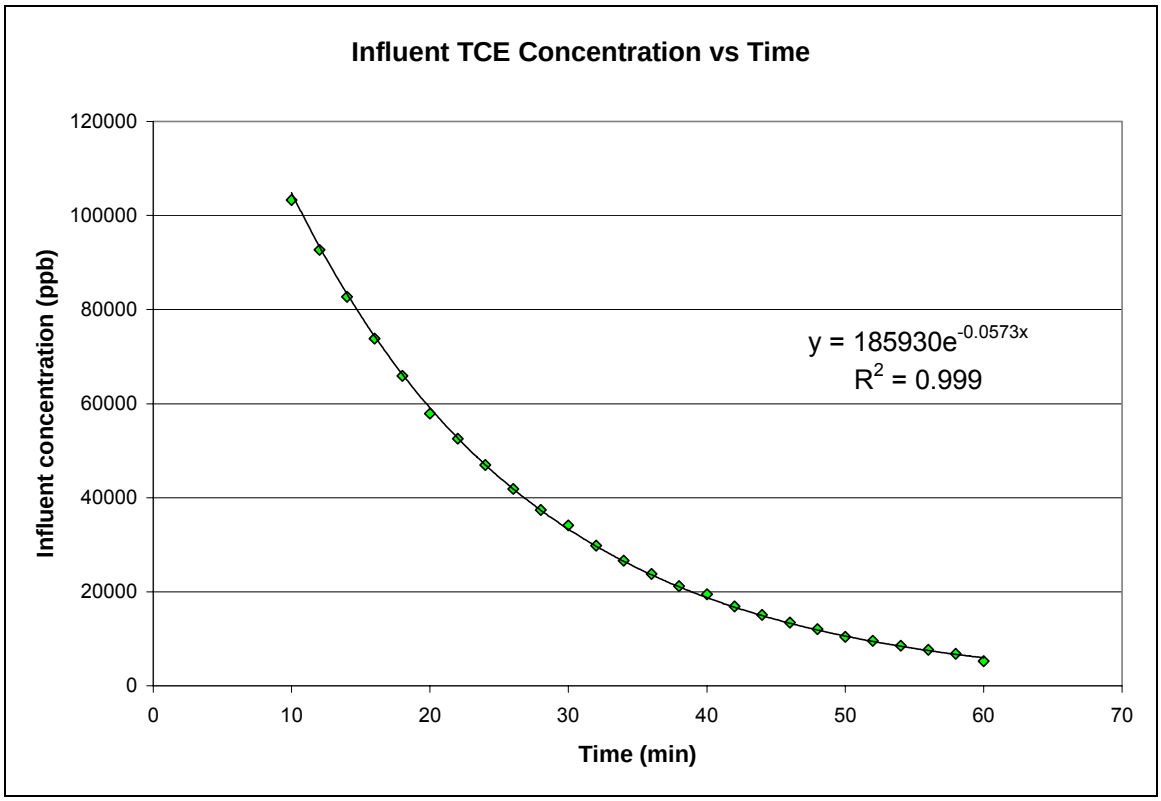

Figure 3.3 Typical dilution curve

During an experimental run, aqueous samples were periodically withdrawn from both the influent and effluent sampling ports into 14.7 mL glass serum vials, and sealed with a Teflon faced grey butyl stopper and an aluminum crimp. Headspace was created in each sample by extracting 6.3 mL of liquid sample. After headspace was created the samples were inverted so that the Teflon faced septa was in contact with only the liquid portion of the remaining sample, to prevent unnecessary loss of mass from the gas phase. Headspace samples were then withdrawn with a gas-tight syringe (Hamilton Co, Reno, NV) from the vials and injected into a Gas Chromatograph (Hewlett Packard®, HP 6890 Series GC System) for analysis. Calibration curves prepared from standards were used to determine concentrations of TCE in both effluent and influent samples. In addition to TCE, calibration curves for ethane, ethylene, vinyl chloride, the three DCE isomers, and

n-hexane were developed for evaluation of effluent sample concentrations for these various byproducts. All calibration curve data are listed in Appendix A.

Temperature was not controlled, however laboratory temperatures marginally fluctuated (a shift of less than 4 ºC) during the course of all experimental runs due to seasonal changes in the outside ambient air temperature.

3.5 Gas Chromatograph (GC)

Chemical constituents, daughter products, and concentrations were determined using a Gas Chromatograph detection system. The GC system consists of two detectors: a flame ionization detector (FID) and an electron capture detector (ECD). Each detector has its own inlet and high resolution gas chromatography column. The gas chromatograph used during this experiment was a Hewlett Packard®, HP 6890 Series GC System. The GC column was a GS-Gaspro, 15 meter, 0.32 mm I.D. J&W Scientific High resolution gas chromatography column obtained from Agilent Technologies. The columns were used with ultra high grade compressed helium (Zero Grade), nitrogen (Grade 5.0), hydrogen (Zero Grade), and compressed air (Zero Grade). All tanks of compressed gases were obtained from Air Products or AirGas Specialty Gases.

3.6 Stock Solutions and Standards

Saturated stock solutions of TCE and other chlorinated and non-chlorinated liquid hydrocarbons were prepared in 72 mL and 160 mL glass serum bottles. A known volume of free-phase (neat) chemical was added to these bottles in contact with de-ionized water

(without headspace). Concentrations were calculated for these stock solutions based on the volume of free-phase chemical added and the density of the chemical. Stock solution bottles were capped with Teflon-faced grey butyl rubber septa and sealed with an aluminum crimp. All stock solution bottles were placed on a rotary shaker and allowed to dissolve. Standards were made using multiple dilutions of this known concentration stock for each chemical used in the column. Retention times for each chemical were determined by GC analysis. Known concentrations were plotted against the peak area response resulting in a linear relation between peak area response from the GC and chemical concentration. Linear regression of the response plots of the dilution standards gave R^2 values greater than 0.98 for all chemicals. All calibration curve data is presented in Appendix A.

Gas phase hydrocarbon standards were also made; 72 mL glass serum vials were crimped and sealed with Teflon-faced grey butyl rubber septa and aluminum crimps. Gas was then injected into the vial through a needle in the septum. The original contents of the serum vial were vented by the use of a second "vent" needle. Serum vials were purged in this manner by tanks of the desired hydrocarbon for 2 hours. A known volume of the gas was then extracted for creation of standards. Assuming an ideal gas, the molar mass of a given volume of stock (n/V) was calculated using the ideal gas law ($n/V = P/RT$). Ambient atmospheric pressure (P) of 0.98 atmospheres, temperature (T) of 295 K, and the universal gas constant ($R = 0.0821$ L atm mol^{-1} K^{-1}) were assumed.

3.7 Michaelis-Menten Modeling

In many of the experiments, a simple first-order rate equation, $\frac{dC}{dt} = -k_1 C$, can be used to model degradation of the substrate (*i.e.* TCE). This apparent first-order behavior is expected if substrate concentrations (C) were low relative to both the capacity of the catalyst present in the column and the concentration of the electron donor. In experiments where transitional behavior from zero order to first order kinetics was not observed, this first-order model was used to describe degradation kinetics. First-order behavior, which means that the rate of substrate degradation is proportional only to the substrate concentration, may occur when all other factors (*e.g.* electron donor, catalyst) are not limiting. However, as the concentration of the substrate increases, it has often been found that the degradation kinetics transition from a first-order to a zero-order process, possibly due to the limited number of sites on the surface of the catalyst, insufficient electron donor available, or the presence of catalyst inhibitors. In a zero-order process, the degradation rate is constant. Michaelis-Menten kinetics uses the following equation to model this transition from first-order to zero-order kinetics with increasing substrate concentration:

$$\frac{dC}{dt} = -\frac{(V_{max})(C)}{(K_{1/2} + C)} \qquad \text{(Eqn 3.1)}$$

Where: dC/dt = reaction rate [μM T^{-1}]

V_{max} = maximum reaction rate [μM T^{-1}]

$K_{1/2}$ = half-velocity constant [μM]

C = substrate concentration [μM]

We see that at low substrate concentrations, where $K_{1/2} >> C$, the denominator of Equation 3.1 is approximately $K_{1/2}$ and the reaction can be approximated by first-order kinetics, with a first-order rate constant of $V_{max}/K_{1/2}$. As the substrate concentration is increased until $K_{1/2} << C$, the reaction rate (dC/dt) becomes constant, V_{max} (Figure 3.4). $K_{1/2}$ is often referred to as the affinity constant and, as shown in Figure 3.4, represents the substrate concentration at which the rate of substrate degradation is half of V_{max}.

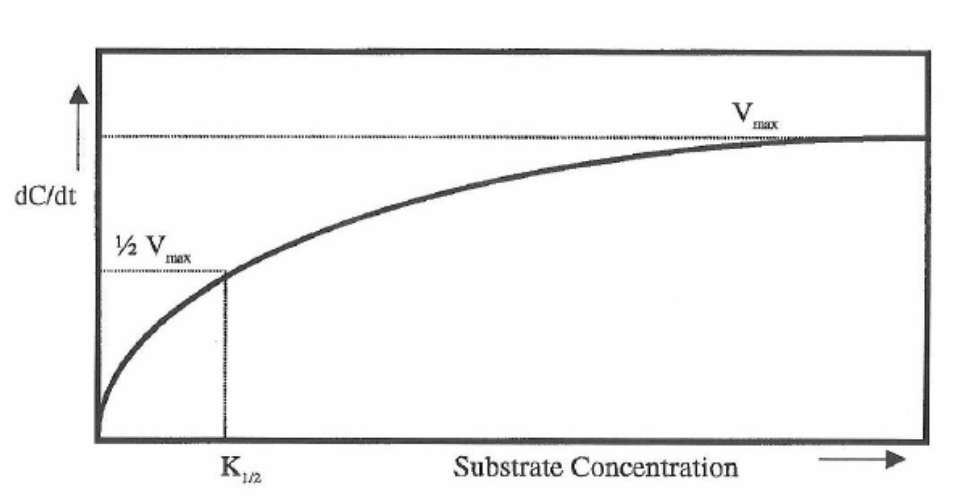

Figure 3.4 Typical Michaelis-Menten curve (from Boggs, 2000)

A plot of dC/dt versus C for the TCE column experiments was constructed using a method similar to that used by Phillips (2003). In this method, concentration in the column (C) was approximated as the log-mean concentration, C_{lm}:

$$C_{lm} = \frac{C_{in} - C_{out}}{\ln(C_{in} / C_{out})} \qquad \text{(Eqn 3.2)}$$

Where C_{in} and C_{out} are the influent and effluent TCE concentrations, respectively. The

rate of TCE degradation was estimated as:

$$\frac{dC}{dt} = \frac{(C_{in} - C_{out})}{\theta} \qquad \text{(Eqn 3.3)}$$

Where θ = hydraulic retention time in the column (min)

dC/dt vs. C_{lm} was graphed using Microsoft Excel 2000 spreadsheets and kinetic parameters (V_{max} and $K_{1/2}$) were estimated using a mathematical software package (Axum 7.0, Insightful Corporation, Seattle, WA). The package selected values of V_{max} and $K_{1/2}$ that minimized the sum of squares difference between measured and modeled values of dC/dt vs. C_{lm}, where modeled values were determined using Equation 3.1. In addition, the ratio of $V_{max}/K_{1/2}$ was used to approximate the pseudo first-order reaction rate, k_1. In cases where the dC/dt vs. C_{lm} plots were linear, the slope of a linear regression line was used to approximate k_1 ($V_{max}/K_{1/2}$).

Throughout the following chapters parameter values and rates are normalized with respect to the concentration of the palladium catalyst in the reactor ($g_{cat}\ L^{-1}$). The term $Rate_{norm}$ is used to refer to the normalized rate of reaction, dC/dt, and has units of ($\mu M\ L\ g_{cat}^{-1}\ min^{-1}$). In addition, parameter values are reported normalized to the concentration of catalyst in the reactor ($g_{cat}\ L^{-1}$) and are represented as $V_{maxNorm}$ and k_{1Norm} with units ($\mu M\ L\ g_{cat}^{-1}\ min^{-1}$) and ($L\ g_{cat}^{-1}\ min^{-1}$), respectively.

3.8 Effects of Formate Concentration

The experimental setup to determine the effects of formate concentration on the degradation of TCE followed the procedures outlined in Section 3.4. In this set of

experiments (see Table 3.1: Experiments 17-19; 22-26), formic acid was used at various concentrations (0.24 mM, 0.5 mM, 1 mM, 4 mM, and 10 mM). For each experiment, the appropriate amount of formate was added via injection of formic acid (88%, Fischer Scientific) into the DI water reservoir and pH was adjusted using sodium hydroxide before pumping began. The formic acid was thoroughly mixed with the DI water and the initial pH was verified. Approximately 1 L of the 20 L reservoir was then transferred into the mixing chamber. After the solution was transferred, various concentrations of TCE were added to the mixing chamber before pumping was started. After pumping began, sampling and analysis procedures followed those outlined in Section 3.4. Reaction rate coefficients were obtained by fitting first-order or Michaelis-Menten models to the data as described in Section 3.7.

3.9 Effects of pH on TCE Degradation

Experiments were conducted to determine the effects of pH on TCE degradation and byproduct formation in the column reactor (see Table 3.1: Experiments 11-16, 19-21). The pH of the dilution water was adjusted to a determined level for each experiment. After a set molar amount of formic acid was added to 20 L of DI water, the pH was adjusted by using NaOH to titrate the mixture to the desired pH (4.0, 5.0, 6.0, etc.). The DI reservoir was placed on a stir plate to ensure complete mixing while pH adjustments were being made. For each experiment, effluent pH was measured. No additional influent pH measurements were taken once the experiment began. After pumping began, sampling and analysis procedures followed those outlined in Section 3.4.

Reaction rate coefficients were obtained by fitting first-order and Michaelis-Menten models to the data as described in Section 3.7.

3.10 Effects of Initial Substrate Concentration

Experiments were conducted using the same experimental parameters (pH, reductant concentration, HRT, etc.) while changing the initial TCE concentration (see Table 3.1: Experiments 5, 18, 22, and 26; 11, 24, and 25; 19 and 23). The experiments were conducted following procedures outlined in Section 3.4 to determine if high concentrations produced elevated amounts of intermediates, or if catalyst deactivation resulted from these elevated substrate concentrations. A series of different initial concentrations of the contaminant were used in the mixing chamber. For each experiment, the concentration of formic acid as well as the pH of the dilution water was maintained throughout the duration of the experiment. After pumping began, sampling and analysis procedures followed those outlined in Section 3.4. Reaction rate coefficients were obtained by fitting first-order and Michaelis-Menten models to the data as described in Section 3.7.

3.11 Evaluation of H_2 as an Electron Donor in the Pd/Al_2O_3 System

Experiments were conducted using the same flow through column previously described in Section 3.3 to determine the effectiveness of molecular hydrogen as an electron donor for the Pd/Al_2O_3 system. Experiments were conducted at pH values of 8.5 and 10.5 (see Table 3.1: Experiments 27 and 28). DI water was saturated with 100%

hydrogen (Ultra high purity, grade zero) and TAPS sodium salt was added, concentration of 10 mM, to help buffer the pH of the system. For Experiment 28 approximately 70 mL of 1 molar hydrochloric acid was used to bring the pH of the system down from 10.5 to 8.5. Before each experiment, the mixing chamber and reservoir were purged with hydrogen gas. This eliminated oxygen in the system and the hydrogen served as an electron donor for the reaction. A hydraulic retention time of 1 minute was used for both experiments. After pumping was resumed, sampling and analysis procedures followed those outlined in Section 3.4. Reaction rate coefficients were obtained by fitting Michaelis-Menten models to the data as described in Section 3.7.

Experiment	Initial TCE Concentration	Influent pH	Formate Concentration	Other Parameters
1	5 mg/L	11	0.24 mM	
2	5 mg/L	11	1 mM	
3	5 mg/L	7.75	1 mM	HRT = 4 min
4	5 mg/L	4	1 mM	HRT = 4 min
5	5 mg/L	4	1 mM	
6	25 mg/L	4	2 mM	
7	25 mg/L	4	1 mM	
8	25 mg/L	5	1 mM	
9	25 mg/L	4	0.24 mM	
10	25 mg/L	6	1 mM	
11	25 mg/L	4	4 mM	
12	25 mg/L	5	4 mM	
13	25 mg/L	6	4 mM	
14	25 mg/L	7.5	4 mM	
15	25 mg/L	8	4 mM	
16	25 mg/L	11	4 mM	
17	45 mg/L	4	0.5 mM	
18	45 mg/L	4	1 mM	
19	45 mg/L	4	10 mM	
20	45 mg/L	5	10 mM	
21	45 mg/L	6	10 mM	
22	91.4 mg/L	4	1 mM	
23	91.4 mg/L	4	10 mM	
24	91.4 mg/L	4	4 mM	
25	182.9 mg/L	4	4 mM	
26	170 mg/L	4	1 mM	
27	45 mg/L	10.5	Purged with 100% H_2	10mM TAPS buffer used
28	45 mg/L	8.52	Purged with 100% H_2	10mM TAPS buffer used ~70mL 1N HCl used

Table 3.1 Experimental schedule
(HRT = 1 min unless otherwise noted)

4.0 RESULTS AND DISCUSSION

4.1 Introduction

This chapter presents and reviews the data collected from the experiments listed in Table 3.1. In most cases comparison charts and graphs are used to present trends in system behavior and catalyst performance. All other experimental data can be viewed in Appendix B. Throughout this chapter many terms and abbreviations are used; they are defined and presented below. Units used in figures and tables are as presented below unless noted otherwise.

The change in concentration with respect to time, dC/dt, is reported normalized to the concentration of the palladium catalyst in the reactor ($g_{cat}\ L^{-1}$) and is referred to as $Rate_{norm}$ with units of ($\mu M\ L\ g_{cat}^{-1}\ min^{-1}$). As discussed in Section 3.7, the substrate concentration in the column was approximated as a log-mean-concentration, C_{lm}, with units of μM. Values reported for V_{max} and k_1 are in units of $\mu M\ min^{-1}$ and min^{-1}, respectively. Additional parameter values are reported normalized to the concentration of catalyst in the reactor ($g_{cat}\ L^{-1}$) and are represented as $V_{maxNorm}$ and k_{1Norm} with units ($\mu M\ L\ g_{cat}^{-1}\ min^{-1}$) and ($L\ g_{cat}^{-1}\ min^{-1}$), respectively. Consistent with Section 3.7, the half velocity constant, $K_{1/2}$, is in units of μM.

When added to water, a monoprotic organic acid like formic acid will disassociate and two species (formic acid and formate ion) will exist in equilibrium, defined by the equilibrium constant or pK_a. The concentration of each species is dependent on the pH of the system and the pK_a of the acid (formic acid's pK_a = 3.75). In this discussion the two species will be differentiated by both name and chemical formula. The formic acid

species will be expressed as HCOOH and the formate ion species will be expressed as $HCOO^-$. During this discussion, when referring to both species, the term formate will be used and represented as HCOOH*.

4.2 Reaction Kinetics

In order to determine the reaction kinetics of TCE degradation in the Pd-HCOOH* system, experiments were conducted using a flow through column configuration. Michaelis-Menten (M-M) and first-order models were fit to the degradation data in order to obtain kinetic parameters. Results from the early experiments were difficult to fit using M-M curves because the initial concentrations of TCE were insufficient to see the zero-order portion of the curve. In these cases, only a pseudo-first-order rate constant, k_1 ($V_{max}/K_{1/2}$), was determined with linear regression. Table 4.1 summarizes the first-order kinetic parameters obtained from these experiments.

As discussed in Section 3.7, M-M kinetics were used in conjunction with a fitting program to determine the model parameters, V_{max} and $K_{1/2}$, for the experimental data. Table 4.2 summarizes the M-M kinetic parameters obtained; Appendix C shows the fits of M-M model to data for all experiments where M-M kinetics (transition from zero- to first-order behavior) were observed.

Exp #	TCE Initial Conc. (ppm)	TCE Initial Conc. (μM)	HCOOH* Conc. (mM)	Influent pH	k_1 (min^{-1})	k_{1Norm} ($L\ g_{cat}^{-1}\ min^{-1}$)	R^2
5	5	38	1	4	1.7423	0.0020	0.9915
6	25	190.1	2	4	2.1276	0.0024	0.9967
11	25	190.1	4	4	2.6475	0.003	0.9757
13	25	190.1	4	6	1.95	0.0022	0.9961
19	44.7	339.9	10	4	2.42	0.0028	0.997
20	44.7	339.9	10	5	2.1582	0.0025	0.9929
21	44.7	339.9	10	6	1.3889	0.0016	0.9835

Table 4.1 Observed first-order rate constants for TCE degradation at various conditions

Exp #	TCE Initial Conc. (ppm)	TCE Initial Conc. (μM)	HCOOH* Conc. (mM)	Inf pH	V_{max} ($\mu M\ min^{-1}$)	$V_{maxNorm}$ ($\mu M\ L\ g_{cat}^{-1}\ min^{-1}$)	$K_{1/2}$ (μM)
14	25	190.1	4	7.5	79.01	0.0902102	38.3
16	25	190.1	4	11	38.97	0.0445012	42.5
17	44.7	339.9	0.5	4	61.45	0.07016	86.2
18	44.7	339.9	1	4	105.99	0.121023	52.5
22	91.4	695.1	1	4	100.32	0.114545	38.88
24	91.4	695.1	4	4	544.39	0.621591	286.3
23	91.4	695.1	10	4	800.17	0.913654	350.8
26	170	1292.8	1	4	203.32	0.23215	87.3
25	182.9	1390.9	4	4	892.17	1.0187	478.7

Table 4.2 Michaelis-Menten kinetic parameter values for TCE at various conditions

4.3 pH Effects

Experiments were conducted to determine the effect of pH on the reactor's performance. Figures 4.1 and 4.2 show how pH affects the rate of TCE degradation in the column reactor for reductant concentrations of 4 mM and 10 mM, respectively. In both sets of experiments, pH varied while all other experimental parameters (reductant concentration, substrate concentration, and flow rate) were held constant. We observe

that as pH increased, the rate of TCE degradation decreased for both reductant concentrations. For lower values of pH the system kinetics appear to be pseudo-first-order; however, as pH increases the system kinetics transitioned to zero-order for the range of conditions studied. Values for the kinetic parameters fit to these data are shown in Tables 4.1 and 4.2.

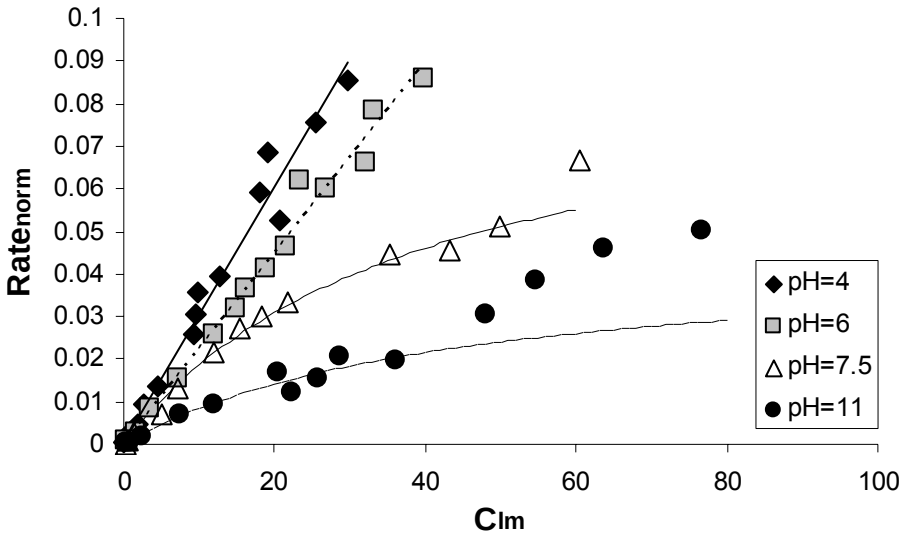

Figure 4.1 Effects of pH on $Rate_{norm}$ vs. C_{lm}, [HCOOH*] = 4 mM, $[TCE]_0$ = 25 ppm;
Experiment #11: pH = 4, Experiment #13: pH = 6,
Experiment #14: pH = 7.5, Experiment #16: pH = 11.

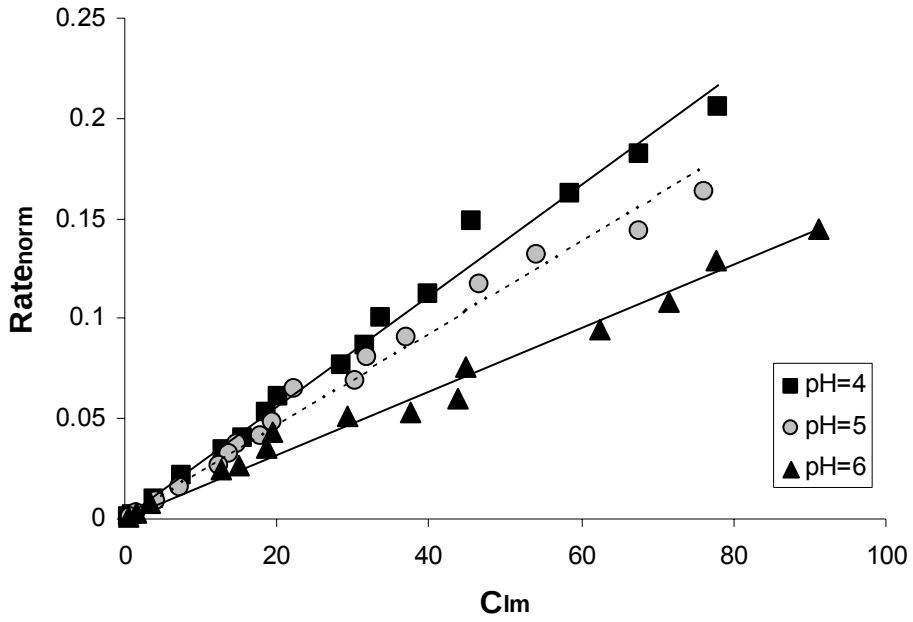

Figure 4.2 Effects of pH on $Rate_{norm}$ vs. C_{lm}, [HCOOH*] = 10 mM, $[TCE]_0$ = 44.7 ppm; Experiment #19: pH = 4, Experiment #20: pH = 5, Experiment #21: pH = 6.

Figure 4.1 also highlights an important phenomenon. Early experiments conducted at relatively low formate concentration, 1 mM, showed no apparent degradation at values of pH between 7.75 and 11 (see Figures B.1 and B.2 of Appendix B) even at hydraulic retention times of 4 minutes. Figure 4.1 shows that at a higher reductant concentration ([HCOOH*] = 4 mM) degradation of TCE can be achieved at a relatively high pH. The most likely explanation can be associated with the positive charge of the catalyst surface and the negative ions in solution. For reduction to take place the surface of the catalyst must be protonated; this positively charged surface will attract negatively charged ions. At high pH values the negatively charged ions in solution will consist of the hydroxide ion (OH^-), the formate ion ($HCOO^-$), the carbonate ion (CO_3^{2-}), and the bicarbonate ion (HCO_3^-). Of these, carbonate and hydroxide are known to interfere with the active sites of the catalyst. These large ions effectively block

active sites and prevent adsorption of the reductant to the surface of the catalyst. As reductant concentrations are increased the limitations associated with adsorption of the reductant can be overcome and degradation is observed.

A plot of fraction of contaminant removed versus log mean contaminant concentration (Figure 4.3) also shows that there are higher removals at lower pH levels. As high as 95% removal was observed at a pH of 4.0 at low TCE concentrations (20 μM), while only 74% and 51% was removed at pH values of 7.5 and 11.0, respectively.

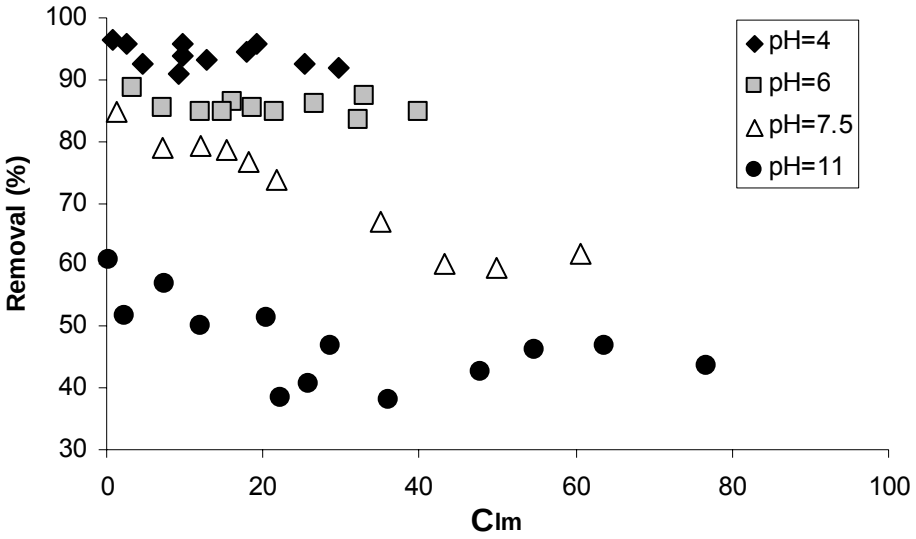

Figure 4.3 Fraction of TCE removed vs. C_{lm} at $[TCE]_0$ = 25 ppm, [HCOOH*] = 4 mM;
Experiment #11: pH = 4, Experiment #13: pH = 6,
Experiment #14: pH = 7.5, Experiment #16: pH = 11.

Increasing the pH also dramatically affected the distribution of byproducts in the effluent stream. As shown in Figures 4.4 and 4.5, at a formate concentration of 4 mM (184 mg L^{-1}) and an initial concentration of TCE of 25 mg L^{-1} (190 μmoles L^{-1}), at pH = 11, vinyl chloride accounted for as much as 27% of the total byproducts produced, with ethane making up the majority of the remaining byproducts. Production of vinyl chloride

was dramatically reduced, accounting for approximately 1% of the total byproducts produced at its maximum, by decreasing the pH of the system to 4. Ethylene appeared to be a transient species whose molar mass consistently accounted for approximately 0.4% of the total byproducts produced for the range of pH values studied (data not shown here, see Appendix B). Concentrations of the other chlorinated and non-chlorinated ethylenes accounted for less than 1% of the byproducts produced for all experiments at these conditions (data not shown here, see Appendix B). Many other chemical species were identified in these TCE degradation experiments. These species included butane, 1-butene, cis-2-butene, trans-2-butene, iso-butane, isobutylene, propane, propylene, and n-hexane and a couple of unidentified heavier chemical species. Production of these higher weight hydrocarbons probably indicates that radical coupling and polymerization was occurring. Generally production of these higher weight hydrocarbons increased with increasing pH. Although these species were observed, they represented an insignificant proportion of the total byproduct mass.

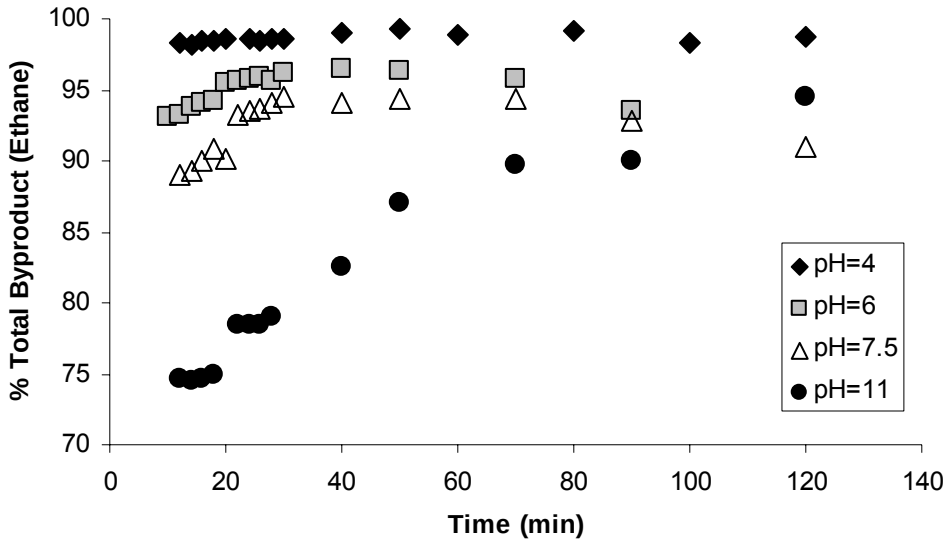

Figure 4.4 Effects of pH on ethane's percent of total byproducts produced vs. time, [HCOOH*] = 4 mM, $[TCE]_0$ = 25 ppm;
Experiment #11: pH = 4, Experiment #13: pH = 6,
Experiment #14: pH = 7.5, Experiment #16: pH = 11.

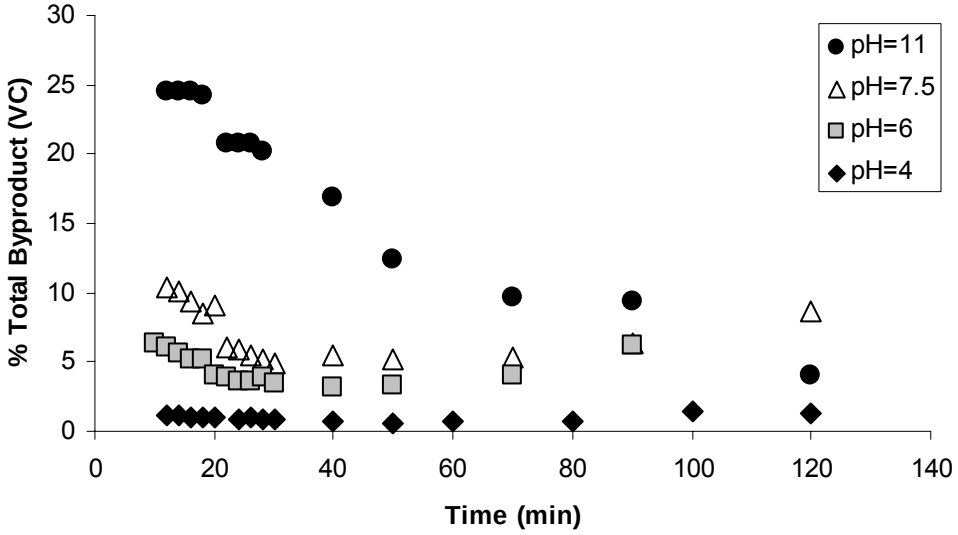

Figure 4.5 Effects of pH on vinyl chloride's percent of total byproducts produced vs. time, [HCOOH*] = 4 mM, $[TCE]_0$ = 25 ppm;
Experiment #11: pH = 4, Experiment #13: pH = 6,
Experiment #14: pH = 7.5, Experiment #16: pH = 11.

An increase in the production of chlorinated intermediates would be expected if reductant concentrations were limited. Figures 4.4 and 4.5 demonstrate an increased production of vinyl chloride as values of pH are increased from 4 to 11. If the hydroxide and/or carbonate species were interfering with the adsorption of the reductant to the catalyst surface the result would be an incomplete reduction of TCE. This incomplete reduction could be indicated by elevated concentrations of vinyl chloride and decreased concentrations of ethane in the effluent, as presented in Figures 4.4 and 4.5.

4.4 Reductant Concentration Effects

Experiments were designed to determine the effects of reductant concentration on TCE degradation in the system. A pH value of 4 was selected based on the experimental results obtained in Section 4.3. Reductant concentrations were varied from 0.5 to 10 mM as the other experimental parameters such as pH, substrate concentration, and flow rate were held constant. Results are shown in Figures 4.6 and 4.7. As can be seen in the figures, as formate concentrations increased, so did the rate of TCE degradation. The percent of TCE removed also increased with increasing reductant concentration as shown in Figure 4.8.

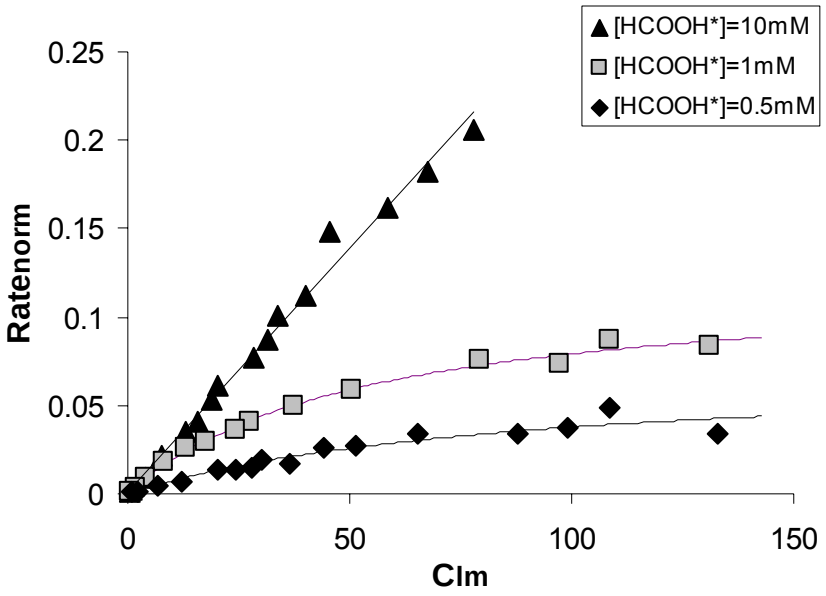

Figure 4.6 Effects of reductant conc. on $Rate_{norm}$ vs. C_{lm}, pH = 4, $[TCE]_0$ = 44.7 ppm; Experiment # 17: [HCOOH*] = 0.5 mM, Experiment #18: [HCOOH*] = 1 mM, Experiment #19: [HCOOH*] = 10 mM.

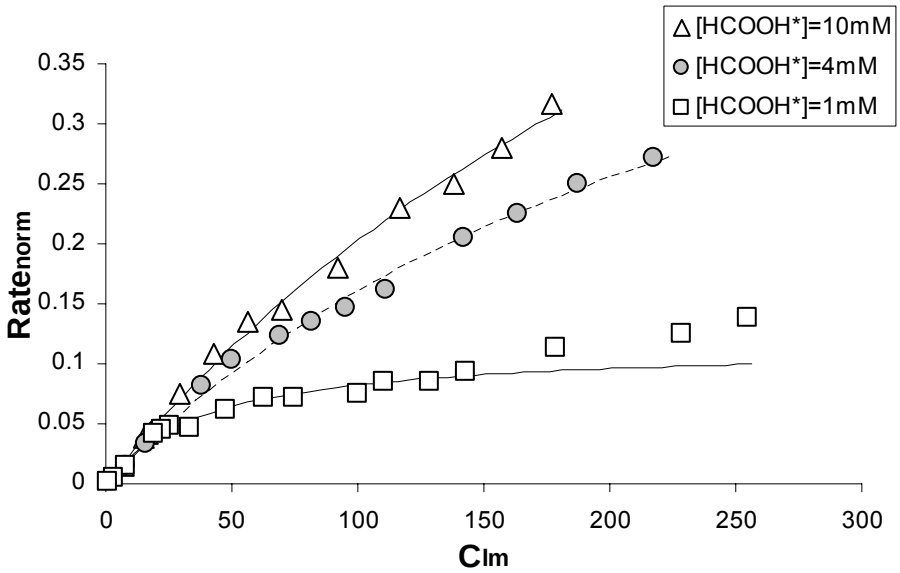

Figure 4.7 Effects of reductant conc. on $Rate_{norm}$ vs. C_{lm}, pH =4, $[TCE]_0$ = 91.4 ppm; Experiment # 22: [HCOOH*] = 1 mM, Experiment #23: [HCOOH*] = 4 mM, Experiment #24: [HCOOH*] = 10 mM.

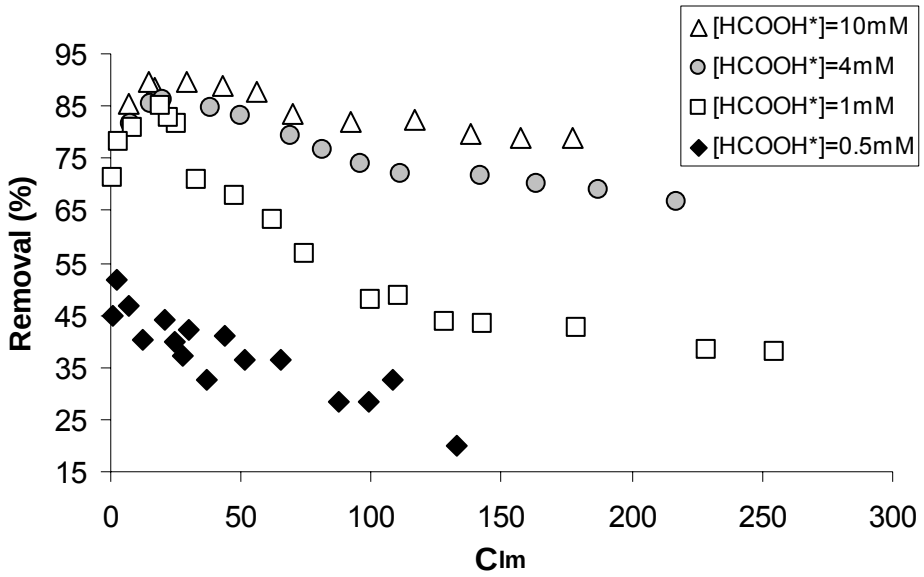

Figure 4.8 Effects of [HCOOH*] on TCE percent removal;
Experiment # 17: [HCOOH*] = 0.5 mM, pH = 4, $[TCE]_0$ = 44.7 ppm,
Experiment # 22: [HCOOH*] = 1 mM, pH = 4, $[TCE]_0$ = 91.4 ppm,
Experiment #23: [HCOOH*] = 4 mM, pH = 4, $[TCE]_0$ = 91.4 ppm,
Experiment #24: [HCOOH*] = 10 mM, pH = 4, $[TCE]_0$ = 91.4 ppm.

Figure 4.7 also illustrates that at high formate concentrations, TCE degradation rates continue to rise even at very high TCE concentrations (91.4 ppm). With an initial TCE concentration of 44.7 mg L^{-1} and a formate concentration of 1 mM (46 mg L^{-1}), the fitted $V_{maxNorm}$ is nearly two times the $V_{maxNorm}$ fitted at 0.5 mM (23 mg L^{-1}) formate (0.121 μM L g_{cat}^{-1} min^{-1} versus 0.0702 μM L g_{cat}^{-1} min^{-1}). The fitted $V_{maxNorm}$ of the 10 mM (460 mg L^{-1}) formate system was roughly 9 times greater than the 1mM formate system. Figure 4.9 presents a summary of the kinetic parameters fit to the data in Figures 4.6 and 4.7. The results shown in Figure 4.9 indicate that the maximum reaction rate, $V_{maxNorm}$, and the half-saturation constant, $K_{1/2}$, both generally increase with increasing [HCOOH*].

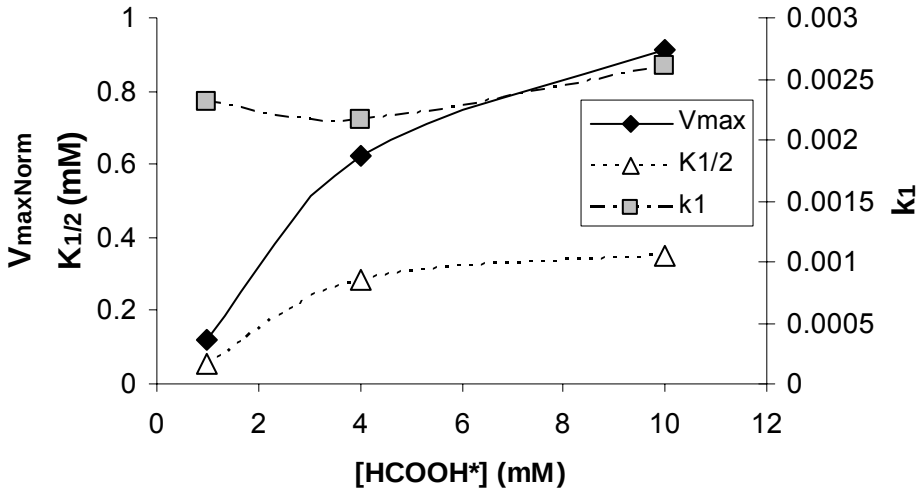

Figure 4.9 Effects of [HCOOH*] on Michaelis-Menten kinetic parameters; Experiment # 22: [HCOOH*] = 1 mM, pH = 4, $[TCE]_0$ = 91.4 ppm, Experiment #23: [HCOOH*] = 4 mM, pH = 4, $[TCE]_0$ = 91.4 ppm, Experiment #24: [HCOOH*] = 10 mM, pH = 4, $[TCE]_0$ = 91.4 ppm.

Recall from Section 2.6, formic acid, HCOOH, will degrade on the surface of the catalyst to produce molecular hydrogen and carbon dioxide (Prüsse *et al.*, 2000) as shown in Equation 4.1. The formate ion, $HCOO^-$, at high temperatures can decompose to carbon monoxide and is thought to also be degradable in the presence of Pd at ambient temperatures (Kramer, 1995).

$$5HCOOH \rightarrow 5H_2 + 5CO_2 \qquad \text{(Eqn 4.1)}$$

As discussed in Section 2.5.1, CO is a catalyst inhibitor that may lead to catalyst deactivation because it strongly sorbs to Pd; this may have also contributed to the decreased reactivity observed at higher values of pH. However, Lowry and Reinhard (2000) reported that the presence of the formate ion appeared to have no significant influence on catalyst activity in the Pd-H_2 system, suggesting that CO production at ambient temperatures is not significant. Investigations conducted in this effort showed

that increasing formate concentrations resulted in increased catalyst activity, further supporting the findings of Lowry and Reinhard (2000) that CO production at ambient temperatures is probably not significant.

Carbon dioxide produced from Equation 4.1 will dissolve into the water leaving the reactor. The following equations describe the effect that this dissolved carbon dioxide will have on the carbonate species present in solution (Snoeyink and Jenkins, 1980):

$$CO_2(g) \leftrightarrow CO_2(aq) \qquad \text{(Eqn 4.2)}$$

$$CO_2(aq) + H_2O \leftrightarrow H_2CO_3; \qquad \text{(Eqn 4.3)}$$

$$H_2CO_3 \leftrightarrow HCO_3^- + H^+; \qquad pK_a = 6.38 \qquad \text{(Eqn 4.4)}$$

$$HCO_3^- \leftrightarrow CO_3^{2-} + H^+; \qquad pK_a = 10.38 \qquad \text{(Eqn 4.5)}$$

The pK_a values for the equations listed above are for temperatures of 20°C.

Hydrodehalogenation of a chlorinated hydrocarbon will produce hydrogen ions and chloride ions, as mentioned in Section 2.4. This increased production of hydrogen ions will result in a decreased pH value for the effluent stream and is apparent from the data presented in Appendix B. However, the degree to which the HCl production affects the effluent pH is directly related to concentrations of the various carbonate species in the effluent, predominantly the carbonic acid species (H_2CO_3) at low pH values. The higher the concentration of the various carbonate species present in solution, as a result of the degradation of formic acid, the less of an effect the production of HCl will have on the effluent stream's pH. This buffering effect will prevent pH drift, which we define in this work as a change in pH measured in the effluent over the course of a single experiment. In Figure 4.10, we see pH drift manifested as a decrease in the change in pH with C_{lm}

(since influent pH is held constant) and note that drift increases as formate concentrations decrease. The carbonate buffering capacity of the system also helps mitigate the effects of catalyst deactivation from the production of HCl.

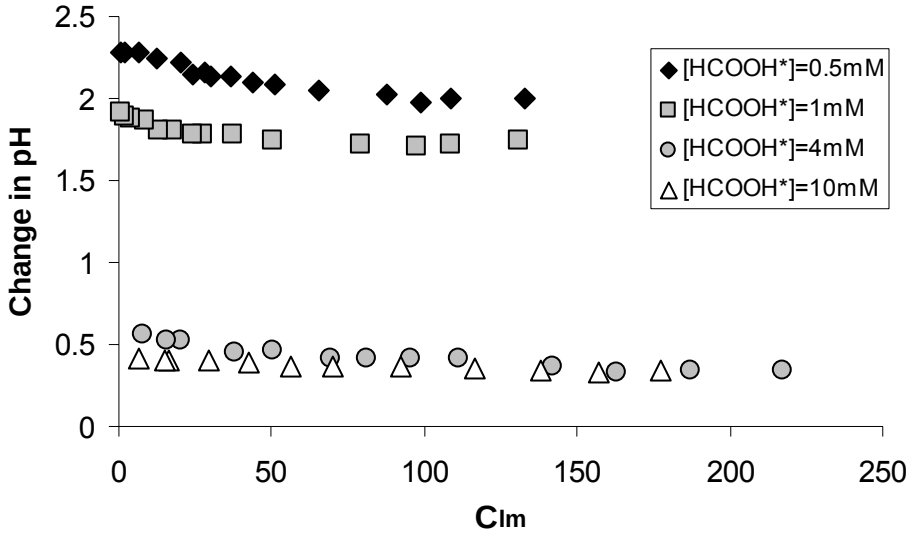

Figure 4.10 Change in pH (Effluent pH – Influent pH) vs. C_{lm} for experiments at pH = 4;
Experiment # 17: [HCOOH*] = 0.5 mM, pH = 4, $[TCE]_0$ = 44.7 ppm,
Experiment #18: [HCOOH*] = 1 mM, pH = 4, $[TCE]_0$ = 44.7 ppm,
Experiment #23: [HCOOH*] = 4 mM, pH = 4, $[TCE]_0$ = 91.4 ppm,
Experiment #24: [HCOOH*] = 10 mM, pH = 4, $[TCE]_0$ = 91.4 ppm.

It is also important to mention that as the reductant concentrations are increased the difference between the influent and effluent pH, defined as the pH shift, is decreased as shown in Figure 4.10. This is probably a result of the finite number of active sites upon which formic acid can degrade. At any given flow rate there is a maximum amount of formic acid that can degrade within the reactor. At particularly high concentrations of formic acid, for example 10 mM (460 mg L^{-1}), the amount of formic acid degraded to carbon dioxide and molecular hydrogen is probably small compared to total concentration of this acid in solution. If only a small portion of the formic acid species is

degraded only a small shift in pH would be expected between the influent and effluent as presented in Figure 4.10.

Like the effects of varying the influent pH, the effects of varying the formate concentration also played a role in the distribution of the byproducts. The increased production of CO_2 from the degradation of formic acid on the surface of the catalyst led to difficulties in obtaining good mass balance for the system at high reductant concentrations. At formate concentrations of 10 mM and a pH of 4, noticeable off gassing was observed in the effluent stream, and only 55 – 75% of the carbon mass balance was achieved (data not shown here, see Appendix B). It is likely that off gassing may have effectively stripped many of the byproducts from solution, thus resulting in a poor mass balance. Typically, carbon mass balance in the experiments ranged from 80% to greater than 95% (data not shown here, see Appendix B).

Figures 4.11 and 4.12 show the same relationship between ethane and vinyl chloride as presented earlier for experiments with varying pH. When the system appeared to be formate-limited, production of vinyl chloride increased, with a corresponding decrease in the production of ethane.

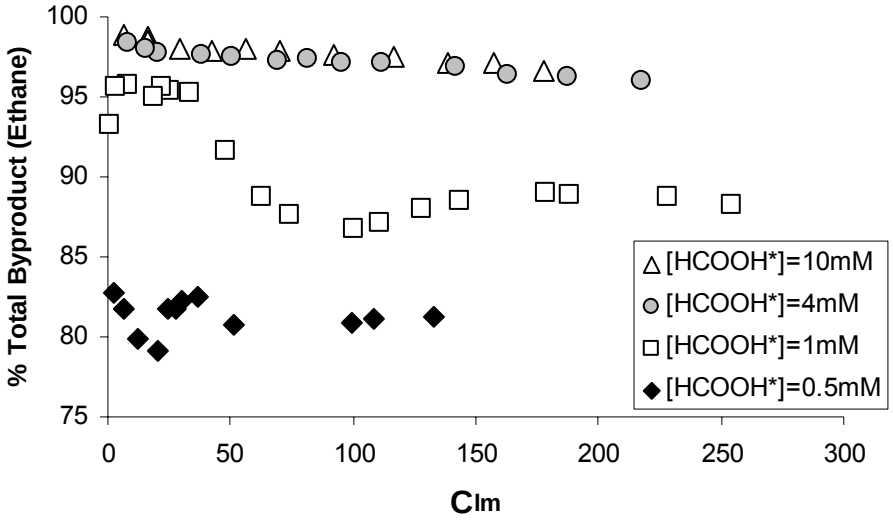

Figure 4.11 Effects of reductant conc. on ethane's percent of total byproducts produced;
Experiment # 17: [HCOOH*] = 0.5 mM, pH = 4, $[TCE]_0$ = 44.7 ppm,
Experiment # 22: [HCOOH*] = 1 mM, pH = 4, $[TCE]_0$ = 91.4 ppm,
Experiment #23: [HCOOH*] = 4 mM, pH = 4, $[TCE]_0$ = 91.4 ppm,
Experiment #24: [HCOOH*] = 10 mM, pH = 4, $[TCE]_0$ = 91.4 ppm.

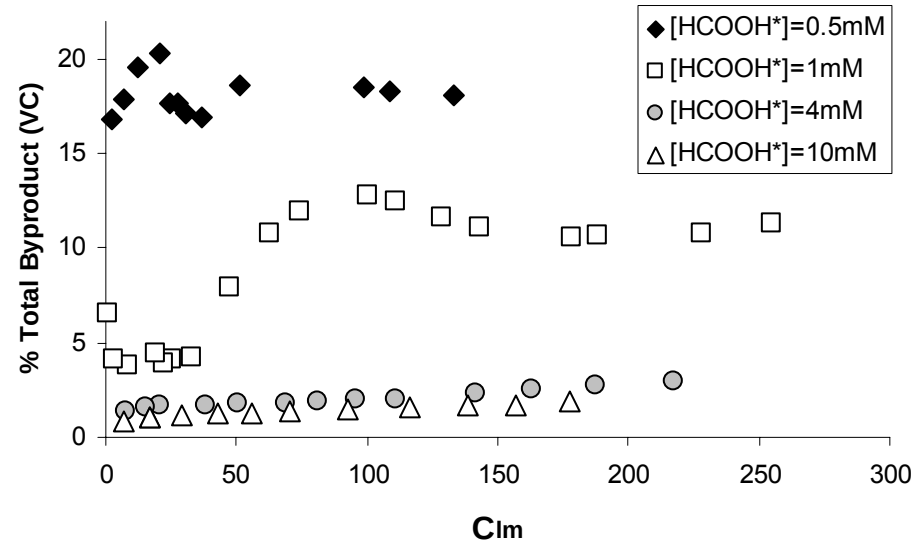

Figure 4.12 Effects of reductant conc. on vinyl chloride's % total byproducts produced;
Experiment # 17: [HCOOH*] = 0.5 mM, pH = 4, $[TCE]_0$ = 44.7 ppm,
Experiment # 22: [HCOOH*] = 1 mM, pH = 4, $[TCE]_0$ = 91.4 ppm,
Experiment #23: [HCOOH*] = 4 mM, pH = 4, $[TCE]_0$ = 91.4 ppm,
Experiment #24: [HCOOH*] = 10 mM, pH = 4, $[TCE]_0$ = 91.4 ppm.

Reductant limitations can also be observed by examining the byproducts produced. As shown in Figures 4.11 and 4.12 nonlinear increases in the percentage of vinyl chloride produced are evident for the experiments at formate concentrations of 0.5 and 1mM. During this same period the percentage of ethane produced dips; possibly a result of reductant limitations on the catalyst surface.

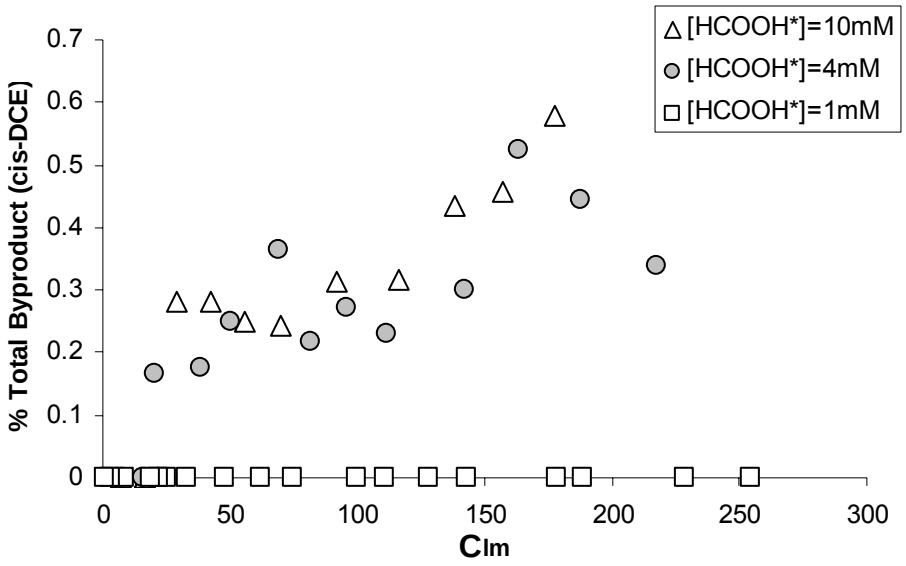

Figure 4.13 Effects of reductant conc. on cis-DCE's percent of total byproducts produced, pH = 4, $[TCE]_0$ = 91.4 ppm; Experiment # 22: [HCOOH*] = 1 mM, Experiment #23: [HCOOH*] = 4 mM, Experiment #24: [HCOOH*] = 10 mM

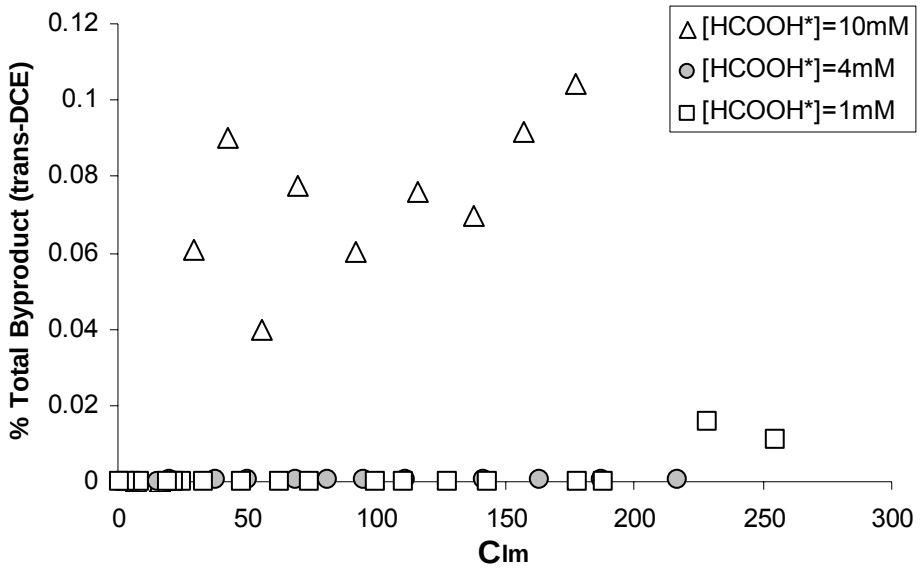

Figure 4.14 Effects of reductant conc. on trans-DCE's percent of total byproducts produced, pH = 4, $[TCE]_0$ = 91.4 ppm; Experiment # 22: [HCOOH*] = 1 mM, Experiment #23: [HCOOH*] = 4 mM, Experiment #24: [HCOOH*] = 10 mM.

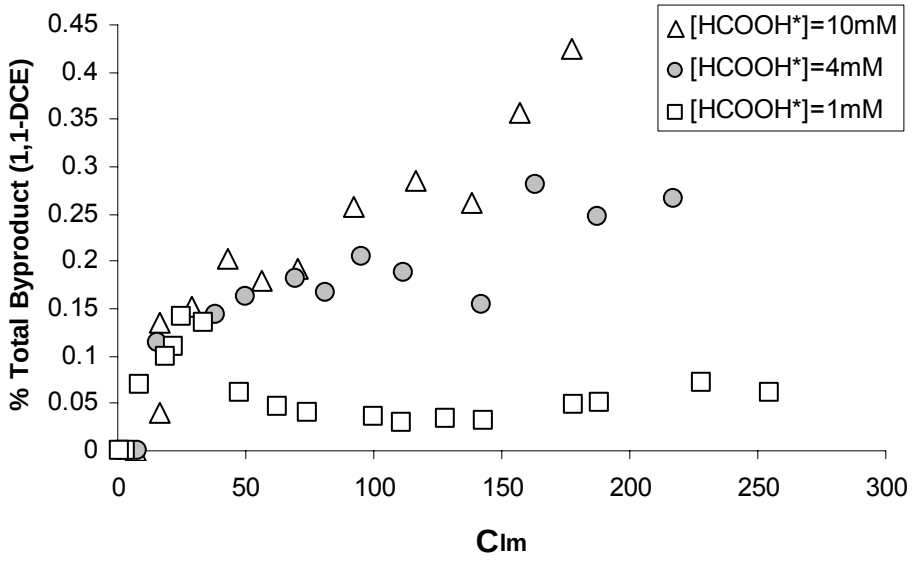

Figure 4.15 Effects of reductant conc. on 1,1-DCE's percent of total byproducts produced, pH = 4, $[TCE]_0$ = 91.4 ppm; Experiment # 22: [HCOOH*] = 1 mM, Experiment #23: [HCOOH*] = 4 mM, Experiment #24: [HCOOH*] = 10 mM.

Figures 4.13 through 4.15 highlight an interesting phenomenon; as reductant concentrations increased concentrations of the three DCE isomers measured in the

effluent also increased. Although the percentages shown are very small, this relative trend appeared evident from Figures 4.13 - 4.15. Since degradation of TCE also increased with increasing reductant concentration, the production of increased amounts of cis-, trans-, and 1,1-DCE could be the result of: (1) the reductant, formic acid, displacing these chlorinated intermediates from active catalyst sites so they could not further degrade, or (2) increased degradation of TCE occurred at higher reductant concentrations (that is, even though production of these chlorinated intermediates was occurring at lower formate concentrations, it was below the level of detection for the equipment used).

As mentioned in Section 4.3, ethylene appeared to be a transient species and accounted for approximately 0.3% of the total byproducts produced (data not shown here, see Appendix B). The presence of longer hydrocarbon chains was also observed for these sets of experiments. Production of these higher order hydrocarbons generally increased with decreasing reductant concentration. N-hexane was the most abundant of these species. N-hexane, a product of radical coupling, could be used as an indicator of radical coupling and polymerization activity in the system. Figure 4.16 illustrates that at low reductant concentrations, [HCOOH*] = 0.5 and 1 mM, n-hexane production is increased indicating increased free radical production and polymerization when insufficient reductant was present.

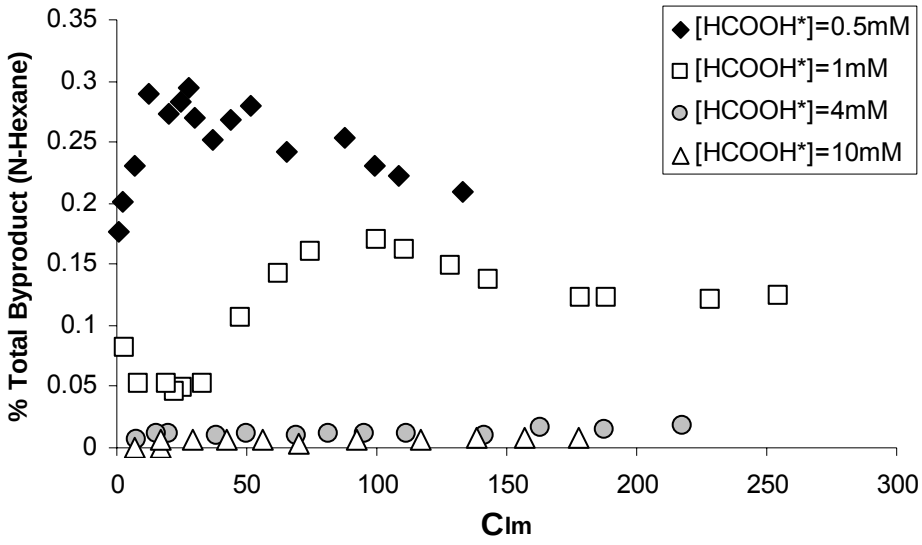

Figure 4.16 Effects of reductant conc. on n-hexane's % total byproducts produced;
Experiment # 17: [HCOOH*] = 0.5 mM, pH = 4, $[TCE]_0$ = 44.7 ppm,
Experiment # 22: [HCOOH*] = 1 mM, pH = 4, $[TCE]_0$ = 91.4 ppm,
Experiment #23: [HCOOH*] = 4 mM, pH = 4, $[TCE]_0$ = 91.4 ppm,
Experiment #24: [HCOOH*] = 10 mM, pH = 4, $[TCE]_0$ = 91.4 ppm.

4.5 Substrate Concentration Effects

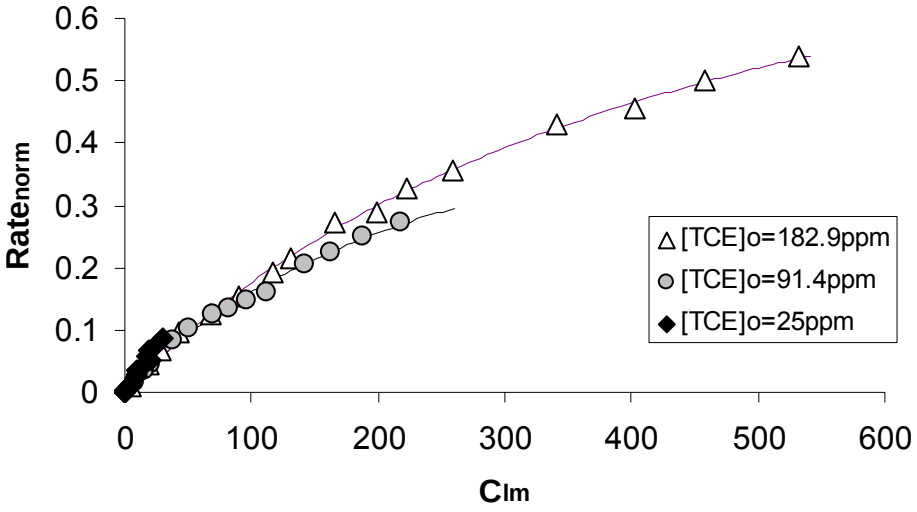

Figure 4.17 Effects of $[TCE]_0$ on $Rate_{norm}$ vs. C_{lm}, pH =4, [HCOOH*] =4 mM; Experiment #11: $[TCE]_0$ = 25 ppm, Experiment #24: $[TCE]_0$ = 91.4 ppm, Experiment # 25: $[TCE]_0$ = 182.9 ppm.

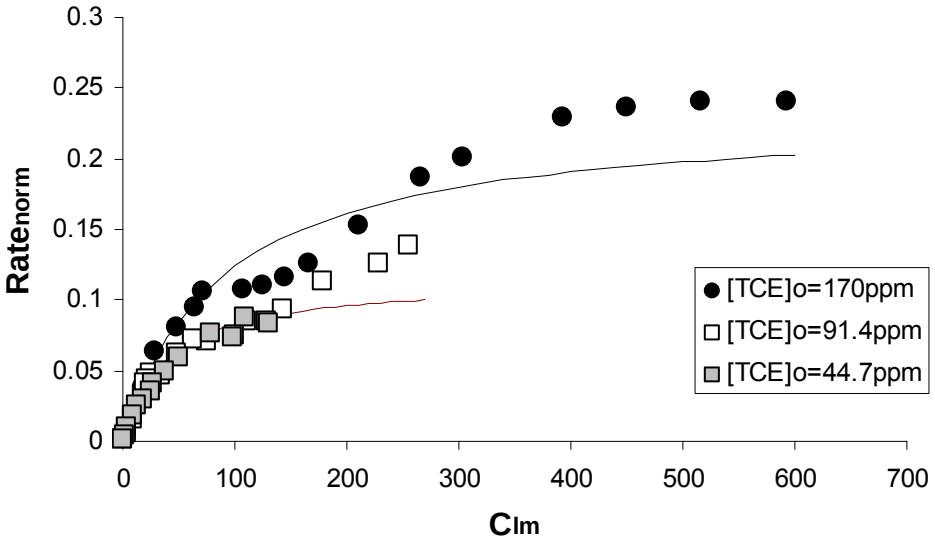

Figure 4.18 Effects of $[TCE]_0$ on $Rate_{norm}$ vs. C_{lm}, pH =4, [HCOOH*] =1 mM; Experiment #18: $[TCE]_0$ = 44.7 ppm, Experiment #22: $[TCE]_0$ = 91.4 ppm, Experiment #26: $[TCE]_0$ = 170 ppm.

A comparison of system performance at varying influent TCE concentrations is presented for reductant concentrations of 4 mM (Figure 4.17) and 1 mM (Figure 4.18). Experiments conducted at [HCOOH*] of 4 mM showed that $[TCE]_0$ had little effect on performance. However, the experiments carried out at lower reductant concentrations, [HCOOH*] = 1 mM, exhibited greater effects on catalyst performance for the range of influent initial TCE concentrations studied. Additionally, for both sets of experiments, TCE conversions at the highest influent C_0 were unexpectedly high. It appeared that the rates of removal, dC/dt, for the highest $[TCE]_0$ (170 ppm and 182.9 ppm for the 1 mM and 4mM, respectively) were higher than the rates at lower initial substrate concentrations. Both Figures 4.17 and 4.18 unexpectedly show that the rate of TCE reduction at higher $[TCE]_0$ is greater than the rate at lower substrate concentrations, and that the rate difference was greater for the lower reductant concentration.

An examination of Figure 4.19 and 4.20 shows that substrate loading had little effect on the conversion of TCE in either set of experiments.

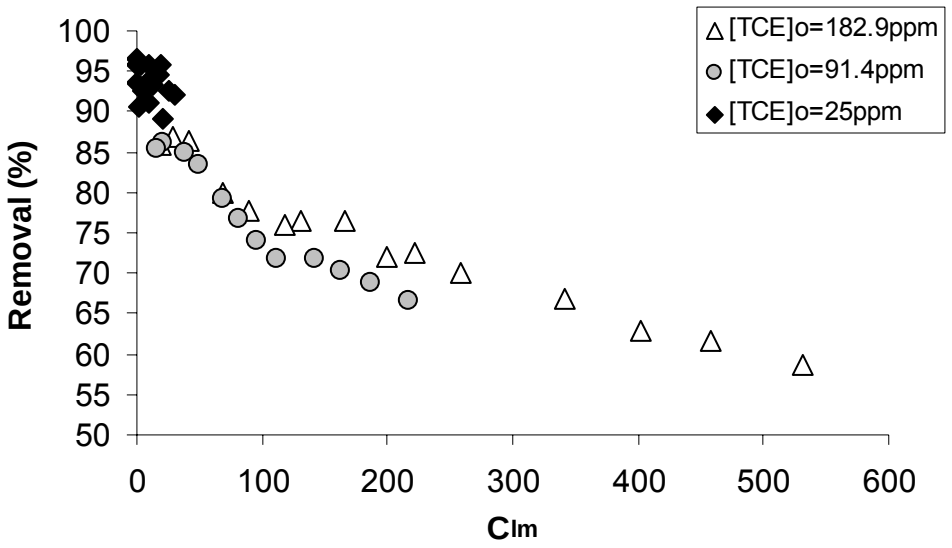

Figure 4.19 Effects of $[TCE]_0$ on TCE percent removal, pH = 4, [HCOOH*] = 4 mM; Experiment #11: $[TCE]_0$ = 25 ppm, Experiment #24: $[TCE]_0$ = 91.4 ppm, Experiment # 25: $[TCE]_0$ = 182.9 ppm.

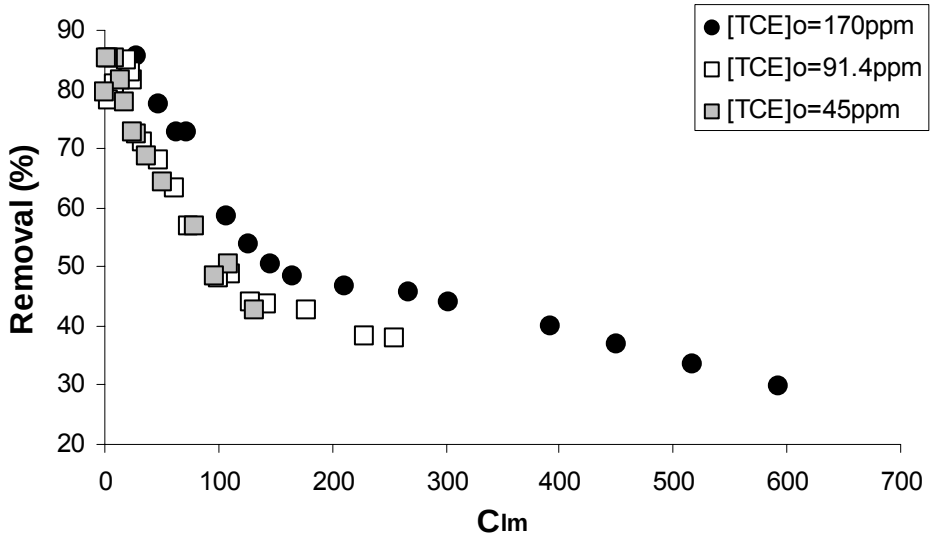

Figure 4.20 Effects of $[TCE]_0$ on TCE percent removal, pH = 4, [HCOOH*] = 1 mM; Experiment #18: $[TCE]_0$ = 44.7 ppm, Experiment #22: $[TCE]_0$ = 91.4 ppm, Experiment #26: $[TCE]_0$ = 170 ppm.

An effect of higher initial [TCE] is seen in Figure 4.20, where the change in pH of the system is plotted versus the log mean TCE concentration. The figure suggests greater HCl formation at influent C_0 = 91.4 and 170 mg L^{-1} TCE leading to lower effluent pH readings.

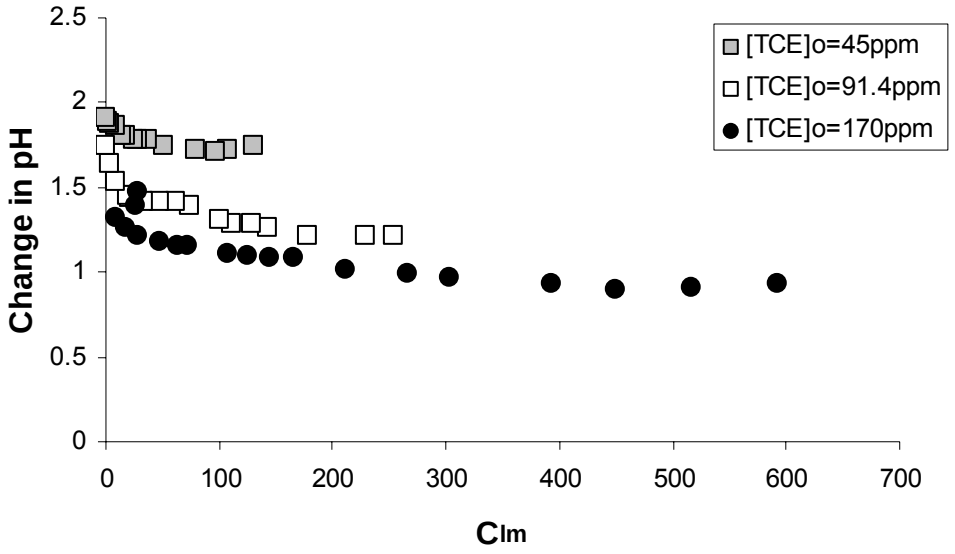

Figure 4.21 Effects of $[TCE]_0$ on Change in pH (effluent – Influent) vs. C_{lm}, [HCOOH*] = 1 mM; Experiment #18: $[TCE]_0$ = 44.7 ppm, Experiment #22: $[TCE]_0$ = 91.4 ppm, Experiment #26: $[TCE]_0$ = 170 ppm.

When sufficient reductant was present the effects of increased substrate concentration had little effect on the distribution of byproducts (Figures 4.23 and 4.24). At [HCOOH*] = 4 mM no apparent reductant limitations were observed for initial TCE concentrations up to 182.9 ppm. The percentage of the total byproduct in the form of ethane, measured in the effluent, steadily increased from 91% (accounting for roughly 55% of the carbon mass balance) to 97% (accounting for roughly 75% of the carbon mass balance), as the concentration of TCE in the reactor is decreased from 532 μM to 100

μM; while the percentage of total byproduct in the form of vinyl chloride steadily decreased, from 7% (accounting for roughly 4% of the carbon mass balance) to 2% (accounting for roughly 1.5% of the carbon mass balance) as the concentration of TCE in the reactor decreased over the same range. The three DCE isomers made up less than 1.4% of the total byproduct identified (accounting for less than 0.8% of the carbon mass balance) at their maximum concentrations under these experimental conditions (data not shown here, see Appendix B). As mentioned in Sections 4.3 and 4.4, ethylene appeared to be a transient species whose percentage of the total byproduct identified accounted for approximately 0.3% for all experiments under these conditions (data not shown here, see Appendix B). Production of higher weight hydrocarbons was also observed to generally increase with increasing substrate concentrations. Hexane appeared to be the most abundant of these species and generally increased as C_0 increased (as shown in Figure 4.22). This indicates that increased polymerization and radical coupling occurred at higher initial TCE concentrations.

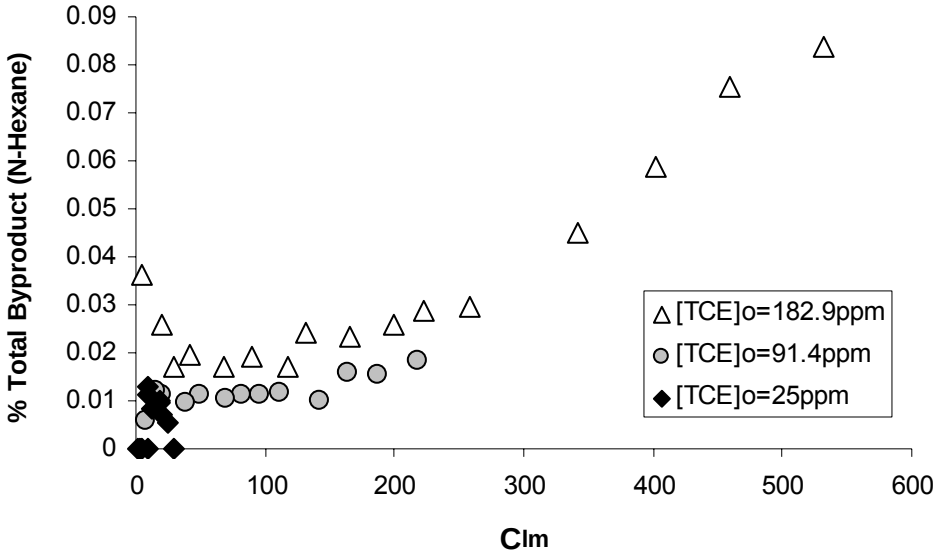

Figure 4.22 Effects of $[TCE]_0$ on n-hexane's percent of total byproducts produced, [HCOOH*] = 4 mM, pH = 4; Experiment #11: $[TCE]_0$ = 25 ppm, Experiment #24: $[TCE]_0$ = 91.4 ppm, Experiment # 25: $[TCE]_0$ = 182.9 ppm.

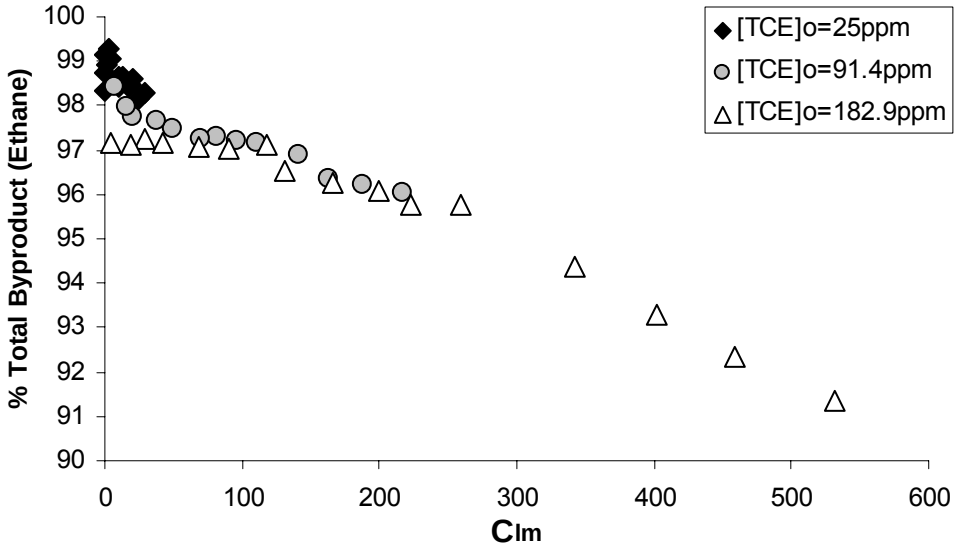

Figure 4.23 Effects of $[TCE]_0$ on ethane's percent of total byproducts produced, [HCOOH*] = 4 mM, pH = 4; Experiment #11: $[TCE]_0$ = 25 ppm, Experiment #24: $[TCE]_0$ = 91.4 ppm, Experiment # 25: $[TCE]_0$ = 182.9 ppm.

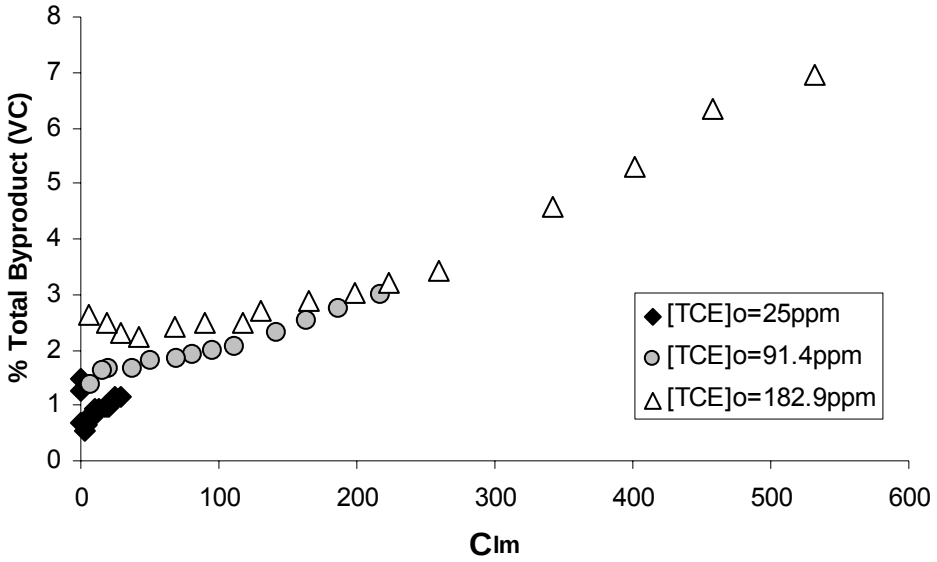

Figure 4.24 Effects of $[TCE]_0$ on vinyl chloride's percent of total byproducts produced, [HCOOH*] = 4 mM, pH = 4; Experiment #11: $[TCE]_0$ = 25 ppm, Experiment #24: $[TCE]_0$ = 91.4 ppm, Experiment # 25: $[TCE]_0$ = 182.9 ppm.

Further evidence of reduced performance was observed when low [HCOOH*] (1 mM) and high initial [TCE] were passed through the reactor (Figures 4.25 and 4.26). The effects of reductant limitation were evident at this lower formate concentration which led to elevated production of vinyl chloride and decreased production of ethane (as discussed in Section 4.4). This suggests that catalyst activity, with respect to byproduct production, was influenced by the ambient [TCE], C_{lm}, in the reactor for low [HCOOH*].

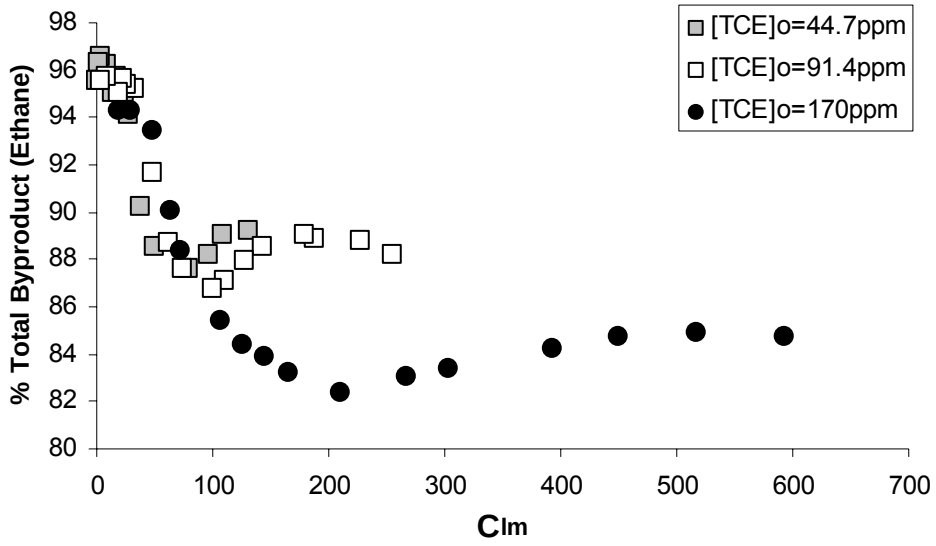

Figure 4.25 Effects of $[TCE]_0$ on ethane's percent of total byproducts produced, [HCOOH*] = 1 mM, pH = 4; Experiment #18: $[TCE]_0$ = 44.7 ppm, Experiment #22: $[TCE]_0$ = 91.4 ppm, Experiment #26: $[TCE]_0$ = 170 ppm.

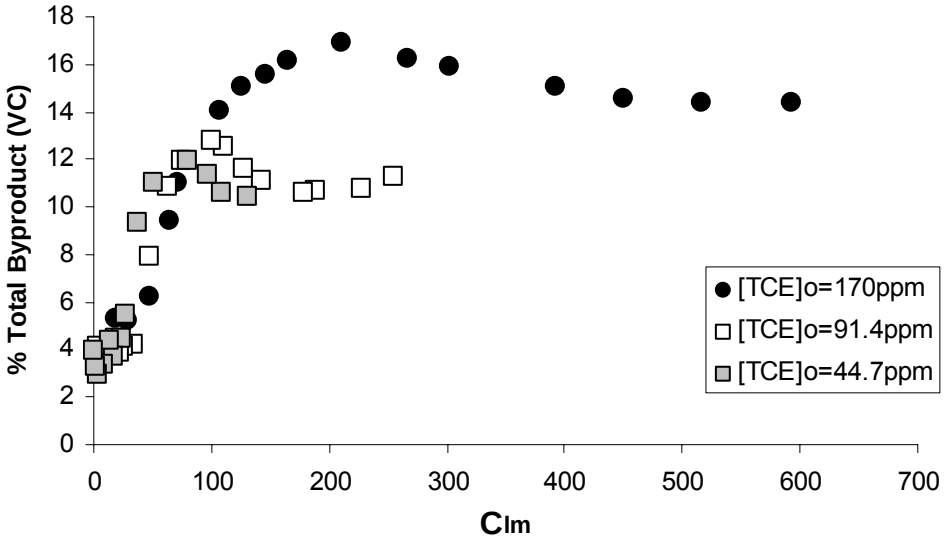

Figure 4.26 Effects of $[TCE]_0$ on vinyl chloride's percent of total byproducts produced, [HCOOH*] = 1 mM, pH = 4; Experiment #18: $[TCE]_0$ = 44.7 ppm, Experiment #22: $[TCE]_0$ = 91.4 ppm, Experiment #26: $[TCE]_0$ = 170 ppm.

The effects of radical coupling and polymerization were also more apparent when reductant concentrations were lower, [HCOOH*] = 1 mM. Figure 4.27 shows that n-

hexane production dramatically increased as the initial TCE influent concentration increased from 44.7 ppm to 170 ppm.

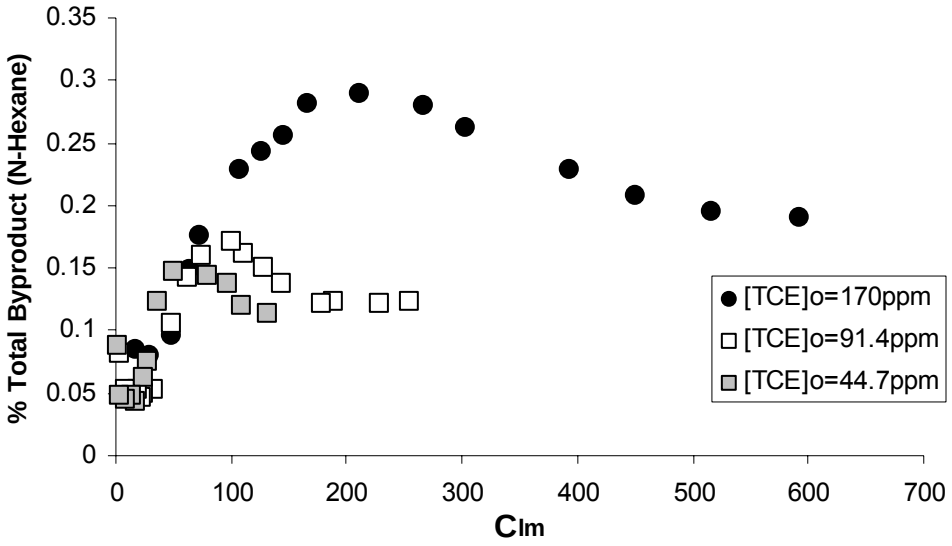

Figure 4.27 Effects of $[TCE]_0$ on n-hexane's percent of total byproducts produced, [HCOOH*] = 1 mM, pH = 4; Experiment #18: $[TCE]_0$ = 44.7 ppm, Experiment #22: $[TCE]_0$ = 91.4 ppm, Experiment #26: $[TCE]_0$ = 170 ppm.

The carbon mass balance of the system also decreased as the initial TCE influent concentrations were increased (data not shown here, see Appendix B). This loss of mass balance was probably a result of radical coupling and polymerization of various species in solution. These heavier hydrocarbons could not be identified.

As discussed earlier, Figures 4.17 and 4.18 showed an unexpected increase in the rate of TCE reduction as $[TCE]_0$ increased. This was observed when initial substrate concentrations were high and reductant concentrations low. One explanation for this unexpected behavior is that as $[TCE]_0$ was increased, radical coupling and polymerization, caused by reductant limitations on the catalyst surface, also increased. The formation of free radical species is a result of insufficient reductant in the system.

As reductant concentrations were increased, the effects of radical coupling on the TCE conversion rate was reduced. This may be seen by comparing Figures 4.17 and 4.18. Radical formation occurs when two chlorine atoms are simultaneously removed from a single carbon on the TCE molecule and the subsequent transfer of hydrogen atoms does not occur. The resulting radical species is highly reactive and attacks any carbon-carbon double bond it encounters. These free radical species could have reduced the TCE concentration in the reactor by coupling with TCE molecules and creating a long chain chlorinated hydrocarbon. Increased radical coupling can be supported by the increased production of n-hexane (shown in Figure 4.22 and 4.26), a product of radical coupling, and by the loss of carbon mass balance as substrate concentrations are increased.

4.6 TCE Reduction with Pd Catalyst: H_2 vs. HCOOH as an Electron Donor

Experiments were conducted with molecular hydrogen as the sole electron donor to aid in the comparison between different reductants. Two different pH values, 10.5 and 8.5, were selected to evaluate the effectiveness of H_2 gas as a reductant in the flow through column used in this research. As discussed in Section 2.5, previous studies have shown an increase in system performance as pH values were increased from 4.3 to 11 (Lowry and Reinhard, 2000).

Results from experiments conducted using H_2 gas are shown in Figure 4.28. As can be seen in the figure, both values of pH produced similar behavior. A comparison with formate shows a close resemblance in system performance to a previous experiment with parameters: [HCOOH*] = 4 mM, pH = 4, $[TCE]_0$ = 91.4 ppm and HRT of 1 minute.

Figure 4.28 clearly indicates that rates of removal with formate are comparable and in some cases, when formate concentrations are greater than 4mM, exceed the rates associated with the hydrogen system. Estimates for the kinetic parameters obtained for these experiments are presented in Table 4.3.

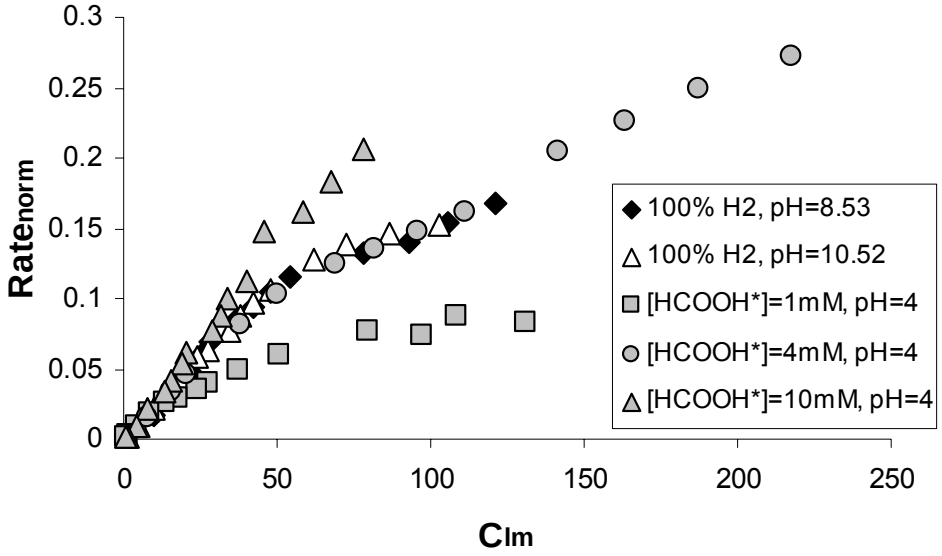

Figure 4.28 Comparison between H_2 and HCOOH* on $Rate_{norm}$ vs. C_{lm};
Experiment #19: [HCOOH*] = 10 mM, pH = 4, $[TCE]_0$ = 44.7 ppm,
Experiment #24: [HCOOH*] = 4 mM, pH = 4, $[TCE]_0$ = 91.4 ppm,
Experiment #18: [HCOOH*] = 1 mM, pH = 4, $[TCE]_0$ = 44.7 ppm,
Experiment #27: 100% H_2, pH = 10.5, $[TCE]_0$ = 44.7 ppm, [TAPS] = 10 mM,
Experiment #28: 100% H_2, pH = 8.53, $[TCE]_0$ = 44.7 ppm, [TAPS] = 10 mM.

Exp #	TCE Initial Conc. (ppm)	HCOOH* Conc. (mM)	Infl. pH	k_{1Norm} (L g_{cat}^{-1} min^{-1})	$V_{maxNorm}$ (μM L g_{cat}^{-1} min^{-1})	$K_{1/2}$ (μM)
18	44.7	1	4	---	0.121023	52.5
19	44.7	10	4	0.0028	---	---
24	91.4	4	4	---	0.621591	286.3
27	44.7	100% H_2	10.5	---	0.54515	205.7
28	44.7	100% H_2	8.53	---	0.297312	96.1

Table 4.3 Kinetic parameter comparison: H_2 vs. HCOOH

The greatest difference between the two systems, H_2 and HCOOH, was evident in a comparison of the byproducts produced. Although, generally the same intermediates were formed for the two systems, the distribution of these compounds was quite different. Figures 4.29 through 4.31 illustrate this point. Concentrations of vinyl chloride in the hydrogen system dramatically increased as the pH was increased from 8.5 to 10.5. Reductant limitations as a result of OH^- inhibition were probably the cause of these elevated vinyl chloride concentrations. Production of n-hexane, a product of radical coupling, was also observed to be higher for the experiment conducted at a pH of 10.5, further supporting the theory of reductant limitations in this experiment. It is also important to note that the carbon mass balance between experiments using H_2 was noticeably poorer for the pH value of 8.5 (data not shown here, see Appendix B).

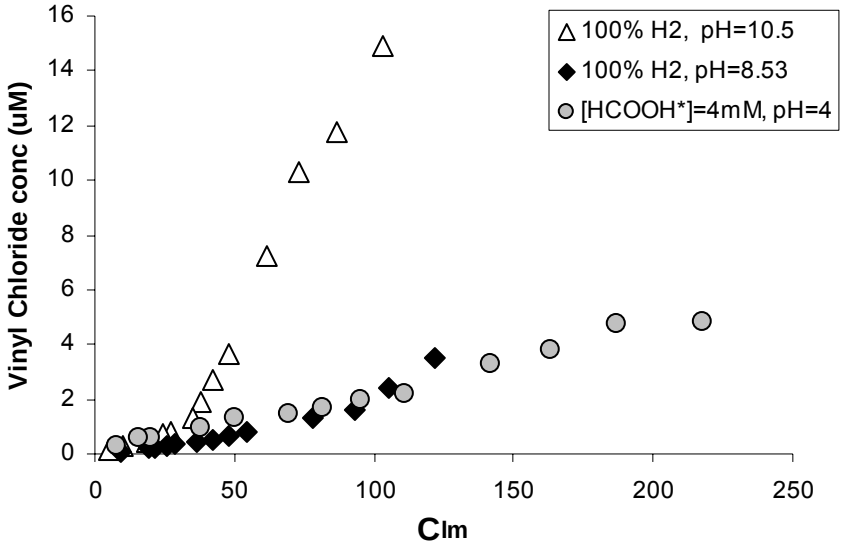

Figure 4.29 Vinyl chloride concentration vs. C_{lm}, formate vs. hydrogen;
Experiment #24: [HCOOH*] = 4 mM, pH = 4, $[TCE]_0$ = 91.4 ppm,
Experiment #27: 100% H_2, pH = 10.5, $[TCE]_0$ = 44.7 ppm, [TAPS] = 10 mM,
Experiment #28: 100% H_2, pH = 8.53, $[TCE]_0$ = 44.7 ppm, [TAPS] = 10 mM.

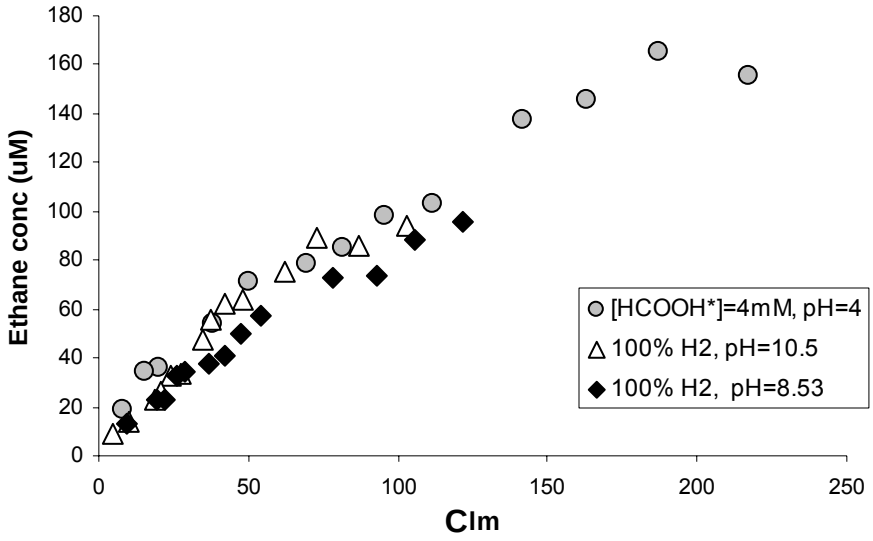

Figure 4.30 Ethane concentration vs. C_{lm}, formate vs. hydrogen;
Experiment #24: [HCOOH*] = 4 mM, pH = 4, $[TCE]_0$ = 91.4 ppm,
Experiment #27: 100% H_2, pH = 10.5, $[TCE]_0$ = 44.7 ppm, [TAPS] = 10 mM,
Experiment #28: 100% H_2, pH = 8.53, $[TCE]_0$ = 44.7 ppm, [TAPS] = 10 mM.

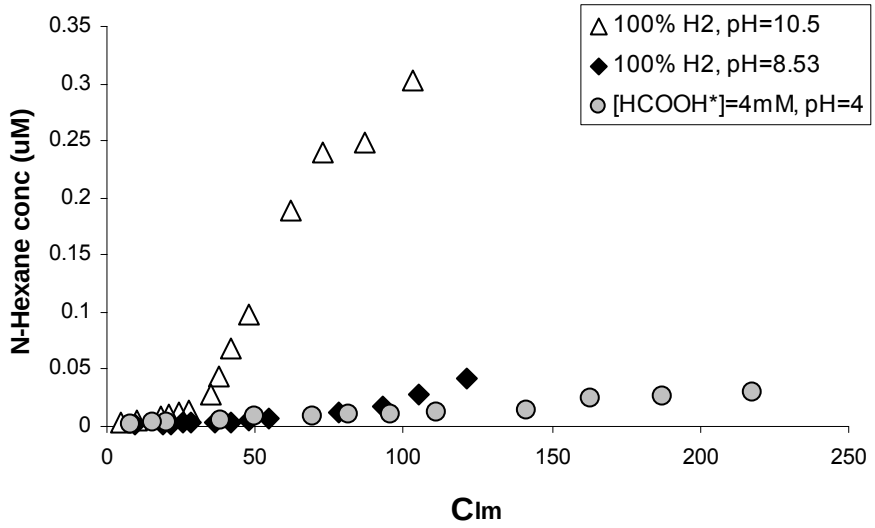

Figure 4.31 N-hexane concentration vs. C_{lm}, formate vs. hydrogen;
Experiment #24: [HCOOH*] = 4 mM, pH = 4, $[TCE]_0$ = 91.4 ppm,
Experiment #27: 100% H_2, pH = 10.5, $[TCE]_0$ = 44.7 ppm, [TAPS] = 10 mM,
Experiment #28: 100% H_2, pH = 8.53, $[TCE]_0$ = 44.7 ppm, [TAPS] = 10 mM.

5.0 CONCLUSIONS

5.1 Summary

The use of a palladium catalyst for the degradation of CAHs was investigated using a flow through column reactor. Trichloroethylene (TCE) was selected as the model CAH due to its high solubility and relative abundance as a groundwater contaminant. Studies were conducted to determine the effects of reductant concentration, pH, and initial substrate concentration on catalytic reduction of TCE by palladium. Results were modeled using Michaelis-Menten kinetics with a mathematical software package to obtain the kinetic parameters V_{max} and $K_{1/2.}$ For those experiments where data could not be fit using a Michaelis-Menten curve, simple linear regression was used to determine a first-order rate constant, k_1.

5.2 Conclusion

Conclusions are presented below for each of the five research objectives established in Section 1.2.

1) How can the kinetics of Pd-catalyzed transformation of CAHs using formate as an electron donor be modeled?

   - **Degradation kinetics could be simulated using a Michaelis-Menten model.** At low substrate concentrations, the Pd-HCOOH* system exhibited pseudo first-order kinetic behavior while at higher initial TCE concentrations degradation kinetics approached zeroth-order behavior.

2) What products and transformation byproducts result from Pd-catalyzed reduction of CAHs? Are any of these products or byproducts potentially harmful?

- **Ethane and vinyl chloride were the most abundant species observed in the effluent.** The distribution of byproducts was generally related to the pH of the system and the concentration of the reductant present. Ethane accounted for as much as 99% of the carbon mass balance under formate-rich conditions. At high pH values and at low reductant concentrations vinyl chloride concentrations measured in the effluent accounted for as much as 25% of the carbon mass balance with ethane making up the majority of the remaining 75% carbon mass balance.
- **Increased formate concentrations led to increased production of the three DCE isomers.** Although production was very low throughout all experiments, the general trend of increasing reductant concentrations resulted in increasing concentrations of the three DCE isomers measured in the effluent. It was unclear whether the increased concentrations observed were a result of interactions with the reductant at the catalyst surface or simply an artifact of increased TCE conversion.
- **Long chain hydrocarbons were detected under reductant-limited conditions.** In systems with limited reductant long chain hydrocarbons were detected, possibly the result of radical coupling and polymerization.

3) What factors influence the extent of CAH reduction and the distribution of transformation products?

- **TCE degradation rates are dependent on the influent pH.** TCE degradation rates decrease as pH values are increased when formic acid is used as a reductant.

At high pH (≥ 8) values and low formate concentrations (≤ 1 mM) no apparent degradation occurred.

- **TCE degradation rates are dependent on the concentration of the reductant.** Degradation rates were reduced dramatically when HCOOH* concentrations were decreased from 10 mM to 0.25 mM. This was noted across pH values. Off-gassing and loss of carbon mass balance were the only apparent disadvantages of increasing the formic acid concentration. Catalyst deactivation was minimal at higher reductant concentrations.
- **$[TCE]_0$ had little effect on the rate of reaction.** Initial substrate concentration had little observable effect on the rate of TCE degradation. At low reductant concentrations the effects of substrate loading produced a more dramatic increase in the production of chlorinated intermediates, such as vinyl chloride. Radical coupling possibly resulted in the apparent increase in TCE conversion as $[TCE]_0$ was increased (as discussed in Section 4.5). This effect was minimized by increasing reductant concentration.

4) How do formate and hydrogen gas compare as reductants for Pd-catalyzed destruction of CAHs?

- **Reaction rates, removal efficiencies, and byproduct distributions were comparable for the Pd-HCOOH* and Pd-H_2 systems.** The 100% H_2 system resulted in rates of removal that were similar to the rates of the formate system at a concentration of [HCOOH*] = 4 mM. The distribution of byproducts for the two systems was also similar when the pH of the Pd-H_2 system was 8.53. Production of

vinyl chloride dramatically increased as the pH of the Pd-H_2 system increased to 10.5. Reaction rates, removal efficiencies, and byproduct distributions for the Pd-HCOOH* system appeared to be superior to the Pd-H_2 system when the concentration of formate was increased above 4 mM.

- **Formate acted as a buffer.** The buffering capacity of the HCOOH* system enabled the effects of catalyst deactivation due to the production of HCl to be reduced. HCl production is a problem for the H_2 system. To deal with the problem, a buffer must be added to the influent in addition to the electron donor, hydrogen gas. The use of formate eliminates the need to add an additional compound to buffer the system.

5) How might Pd catalysis using formate as an electron donor be used in-well to effect *in situ* destruction of CAHs in groundwater?

- **Reaction rates and removal efficiencies of a palladium catalyst using formate as a reductant show potential for use in an HFTW.** The reaction rates and removal efficiencies for TCE achieved by formate show promise for in-well use as part of an HFTW system. Up to 90% of the TCE was removed with a single-pass of contaminated water ([TCE] = 25 ppm, [HCOOH*] = 10 mM) through a reactor with a residence time of only 1 minute. As HFTW systems have been designed to achieve down gradient concentration goals with only 85% single-pass removal efficiencies, this would seem to indicate that performance of a Pd/formate system is more than adequate for application in-well as a component of an HFTW system. Based on the experiments conducted in this study which compared hydrogen and formate, it is

apparent that a Pd/formate system could be installed in a reactor similar in size to those which are currently being evaluated in the field (McNab *et al*., 2000; Munakata *et al*., 2002). Cost comparison data as developed by Phillips (2003) have also shown that formic acid is approximately four times less expensive than hydrogen gas as a reductant. Additionally, formic acid does not require the use of another compound to buffer the system and has less safety concerns than hydrogen gas when storing, transporting, and injecting into the subsurface.

5.3 Future Work

- **Study the long term performance of the Pd-HCOOH system.** Long term studies could be conducted to evaluate the optimal conditions for sustained TCE degradation using a palladium catalyst. A certain degree of catalyst deactivation would be expected during long term use of the system. Characterization of this deactivation would be essential if field application of this technology is to be successful.
- **Study the effects of common groundwater constituents on catalyst performance.** As mentioned in Section 2.5.1, many common groundwater constituents are able to reduce catalyst performance in the Pd-H_2 system. The effect that these solutes have on the ability of the Pd-HCOOH* system to reduce TCE has not been determined.
- **Extend studies to examine other CAHs.** This research has investigated reduction of one of the most prevalent CAHs, TCE. Future work could be done

with the other chlorinated ethylenes and chlorinated ethanes. Contaminated sites often have a plethora of contaminants. Determining reaction rates and the associated system performance for different CAHs would be useful for field implementation.

- **Ascertain how the concentration of formate affects the degradation of the DCE isomer?** Experimental evidence suggested that increasing formate concentrations led to increased production of the three DCE isomers. Experiments could be conducted to further evaluate the effects of formate concentration on the degradation of these chlorinated compounds.
- **Determine if formic acid that would be added in-well as a component of an HFTW system could act as a carbon source for microbes that could stimulate biological growth and lead to biofouling?** *In situ* reactors are often susceptible to biofouling from increased microbial activity. Studies would be required to determine if formic acid acts as a source of carbon for subsurface microorganisms.
- **Incorporate results into an existing HFTW model.** The results of the bench scale kinetic studies completed in this research could be used to develop a sub-model of Pd catalyst performance for incorporation into an HFTW design model. The existing HFTW model (Stoppel, 2001) for in-well Pd catalytic reactors, which was based on hydrogen gas as a reductant, may be revised using the kinetic data from this research in order to evaluate the feasibility of this technology for field-scale TCE remediation.

APPENDIX A: CALIBRATION CURVE DATA

TCE Calibration Curves

	TCE	6-Oct-03
		5 µL
Standard #	y Expected Conc. (ppb)	x Peak Area (ECD)
1	19460	89587.2
2	15130	64632.4
3	10810	52662.7
4	5400	25301.7

Table A.1 Calibration curve data: 5 µL TCE injection, ECD splitless method

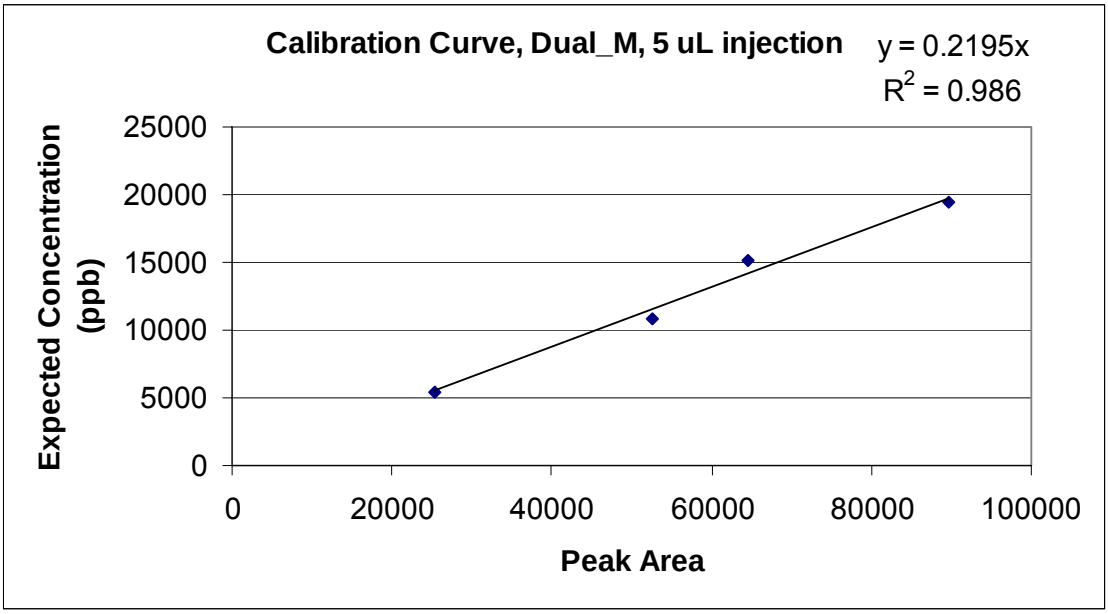

Figure A.1 Calibration curve: 5 µL TCE injection, ECD splitless method

	TCE	6-Oct-03
		25 µL
Standard #	y Expected Conc. (ppb)	x Peak Area (ECD)
1	4863.8	112055.5
2	1945.5	48438.2
3	972.8	24226.9
4	194.6	6139.1

Table A.2 Calibration curve data: 25 µL TCE injection, ECD splitless method

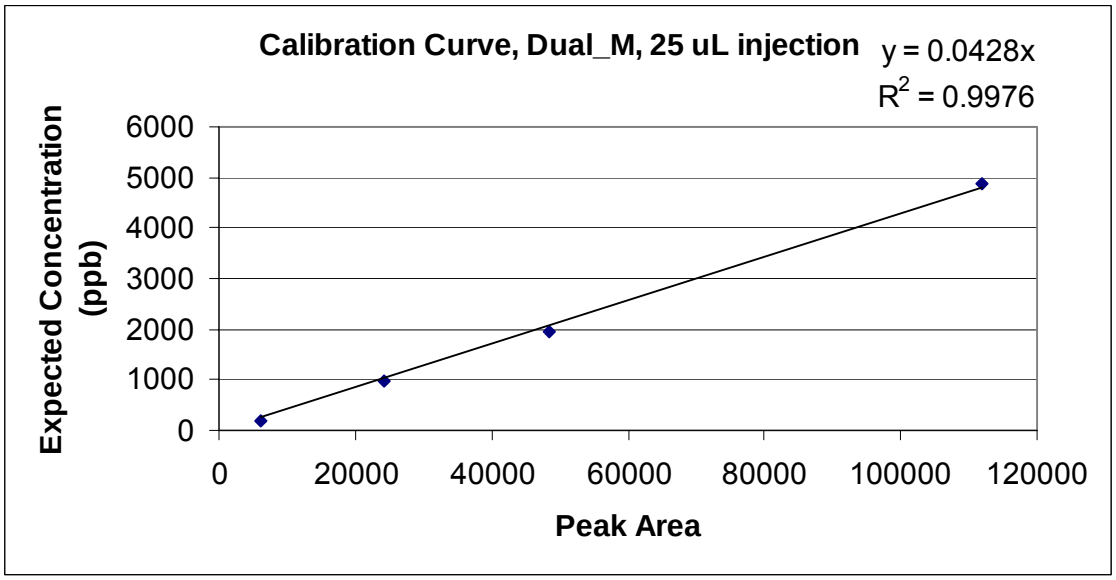

Figure A.2 Calibration curve: 25 µL TCE injection, ECD splitless method

Standard #	TCE y Expected Conc. (ppb)	3-Oct-03 250 µL x Peak Area (ECD)
1	4.86	733
2	43.75	5905.1
3	97.23	12069.5

Table A.3 Calibration curve data: 250 µL TCE injection, ECD splitless method

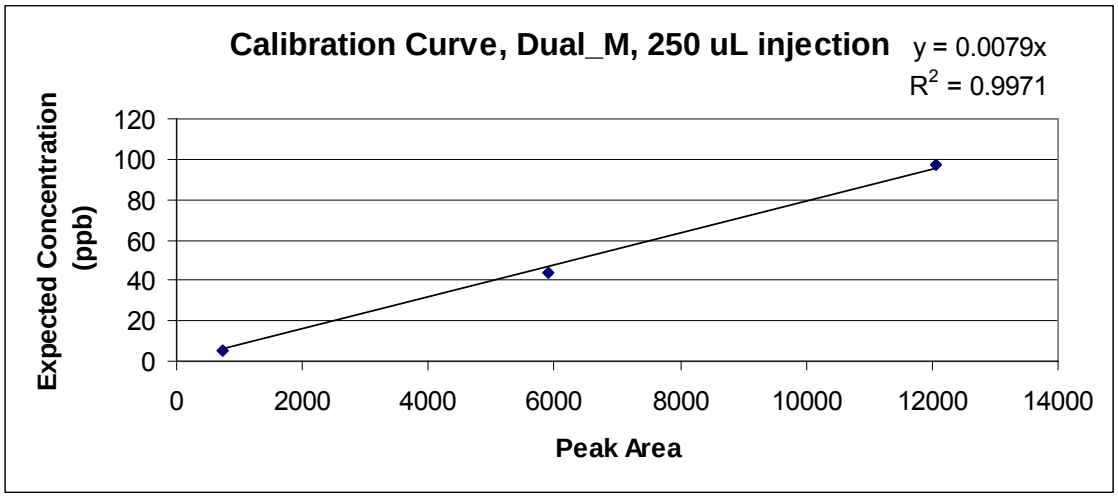

Figure A.3 Calibration curve: 250 µL TCE injection, ECD splitless method

DUAL_M2	TCE	12-Nov-03
		5 µL
Standard #	y Expected Conc. (ppb)	x Peak Area (ECD)
1	108090	13307.4
2	75660	10214.7
3	43230	6332.9
4	10810	1898.4
5	2160	345.2

Table A.4 Calibration curve data: 5 µL TCE injection, ECD split ratio 5.0:1 method

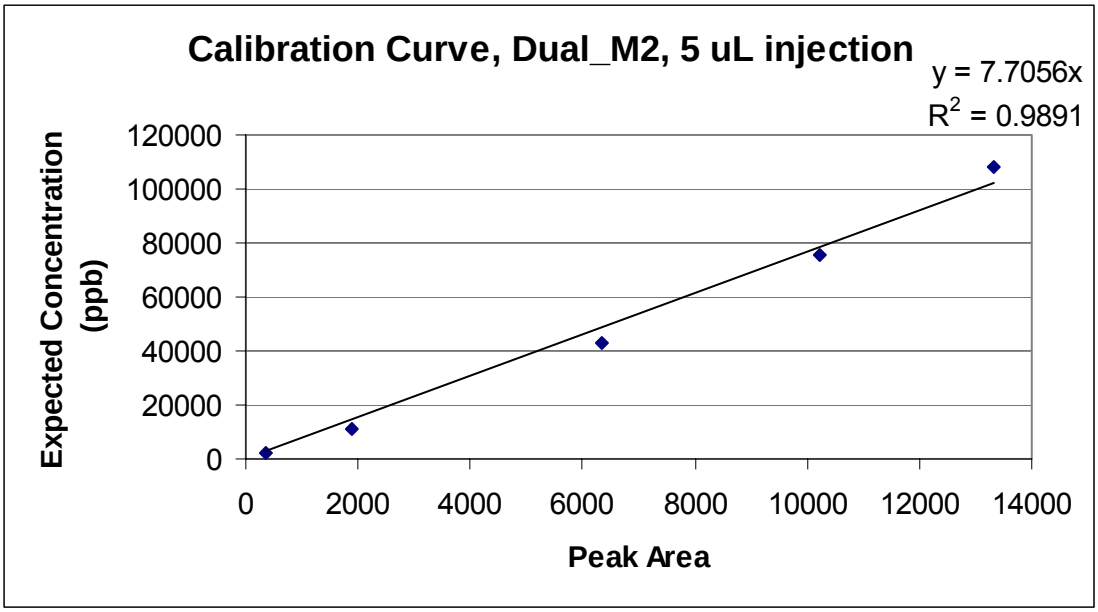

Figure A.4 Calibration curve: 5 µL TCE injection, ECD split ratio 5.0:1 method

Ethane Calibration Curve

		Ethane	7-Nov-03
		Injection Vol =	250 µL
Standard #	Volume injected into HS (µL)	y Expected Initial Conc. Aqueous Phase (µmole/L)	x Peak Area (FID)
1	80	353.96	8903.7
2	20	88.49	2417.2
3	10	44.24	1094.5
4	5	22.12	581.7
5	1	4.42	122.4

Table A.5 Calibration curve data: 250 µL ethane injection, FID method

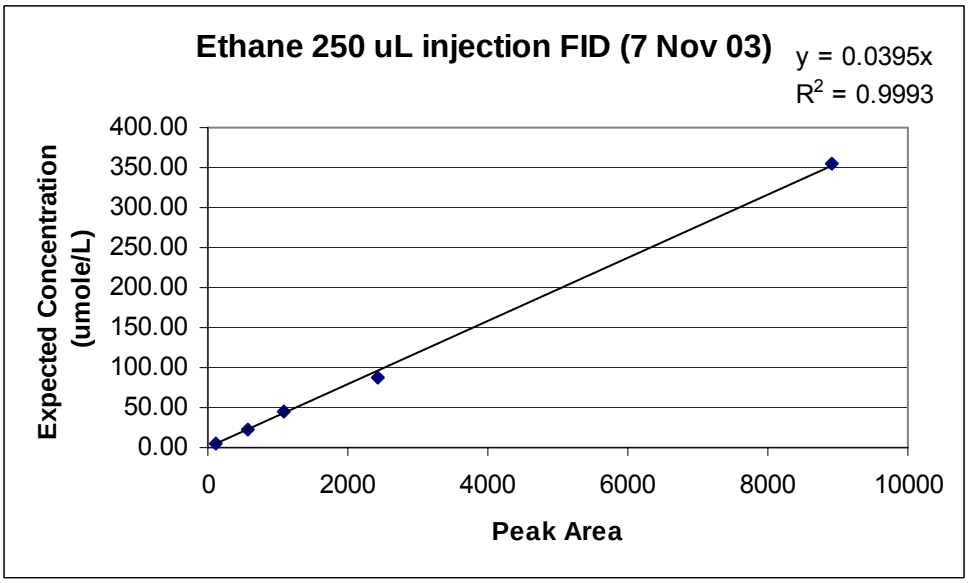

Figure A.5 Calibration curve: 250 µL ethane injection, FID method

Ethylene Calibration Curve

		Ethylene	8-Oct-03
		Injection Vol =	250 µL
Standard #	Volume injected into HS (µL)	y Expected Initial Conc. Aqueous Phase (µmole/L)	x Peak Area (FID)
1	500		
2	70	309.71	6732.1
3	20	88.49	2141.7
4	4	17.70	397.4

Table A.6 Calibration curve data: 250 µL ethylene injection, FID method

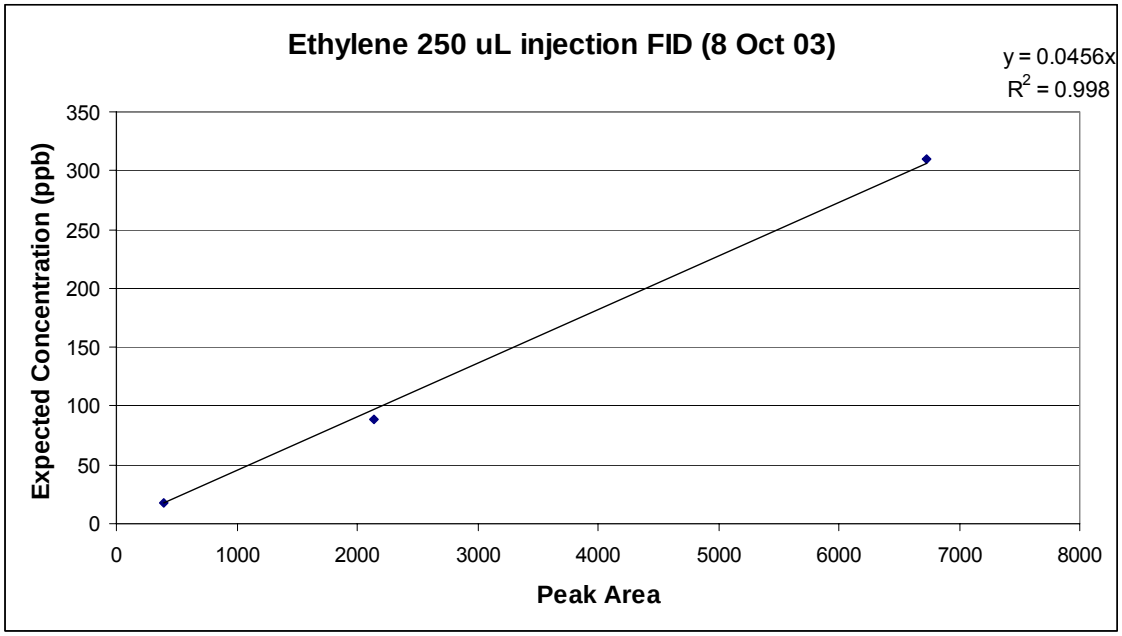

Figure A.6 Calibration curve: 250 µL ethylene injection, FID method

Vinyl Chloride Calibration Curve

		Ethane	7-Nov-03
		Injection Vol =	250 µL
Standard #	Volume injected into HS (µL)	y Expected Initial Conc. Aqueous Phase (µmole/L)	x Peak Area (FID)
1	400	4.30	35.9
2	100	1.08	10.1
3	40	0.43	4.5
4	20	0.22	2.1
5	10	0.11	1
6	5	0.0538	0.5

Table A.7 Calibration curve data: 250 µL vinyl chloride injection, FID method

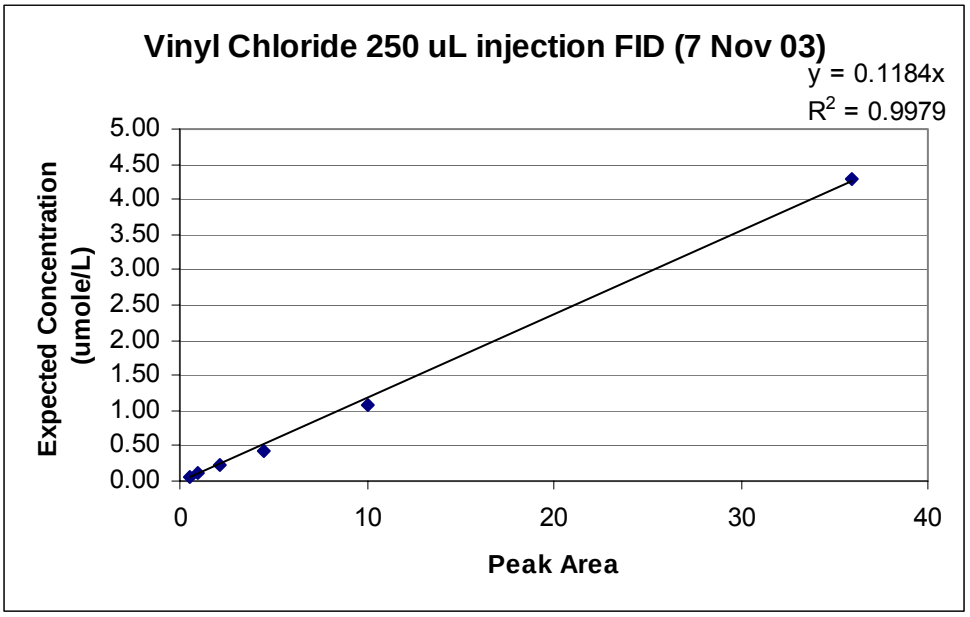

Figure A.7 Calibration curve: 250 µL vinyl chloride injection, FID method

cis-DCE Calibration Curve

	FID	cis-DCE	18-Dec-03
		Injection Vol =	250 µL
Standard #	Volume injected into HS (µL)	y Expected Initial Conc. Aqueous Phase (µmole/L)	x Peak Area (FID)
1	5	0.4887	0.9
2	15	1.4649	2.3
3	50	4.8825	8

Table A.8 Calibration curve data: 250 µL cis-DCE injection, FID method

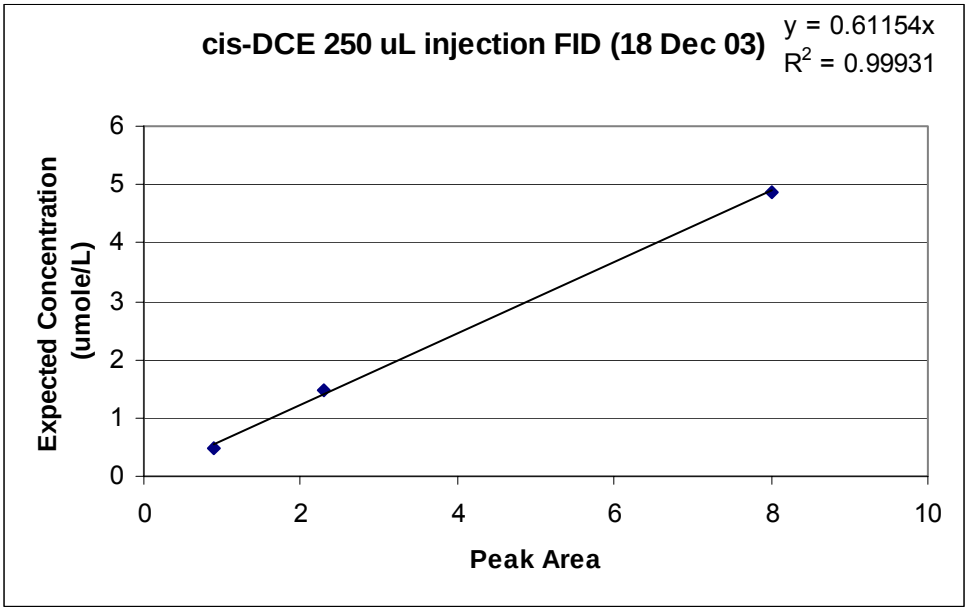

Figure A.8 Calibration curve: 250 µL cis-DCE injection, FID method

trans-DCE Calibration Curve

	FID	trans-DCE	18-Dec-03
		Injection Vol =	250 µL
Standard #	Volume injected into HS (µL)	y Expected Initial Conc. Aqueous Phase (µmole/L)	x Peak Area (FID)
1	5	0.4794	1.6
2	15	1.4392	5.2
3	50	4.7979	16.2

Table A.9 Calibration curve data: 250 µL trans-DCE injection, FID method

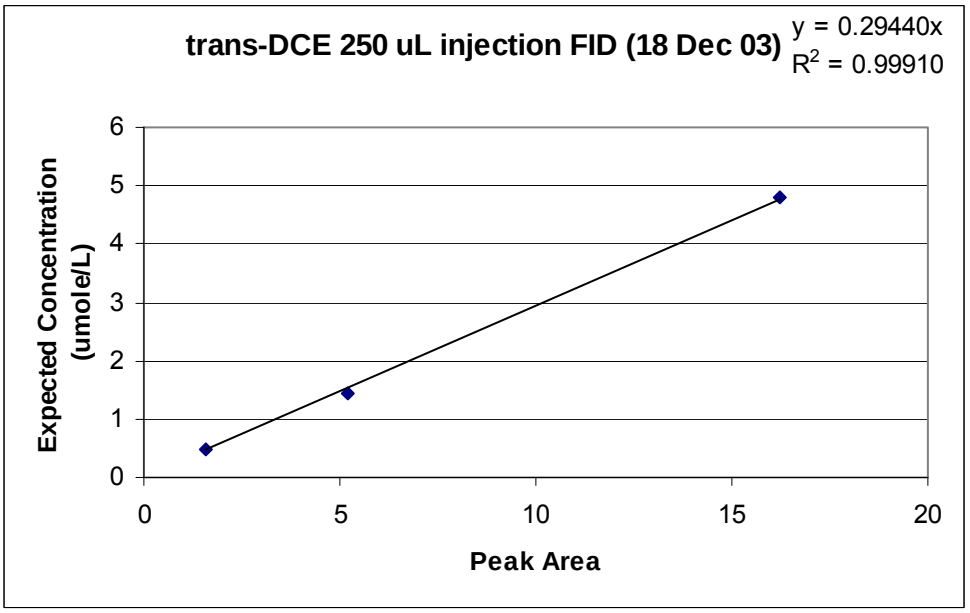

Figure A.9 Calibration curve: 250 µL trans-DCE injection, FID method

1,1-DCE Calibration Curve

	FID	1,1-DCE	18-Dec-03
		Injection Vol =	250 µL
		y	x
Standard #	Volume injected into HS (µL)	Expected Initial Conc. Aqueous Phase (µmole/L)	Peak Area (FID)
1	5	0.4619	3.7
2	15	1.3856	9.9
3	50	4.6196	34.9

Table A.10 Calibration curve data: 250 µL 1,1-DCE injection, FID method

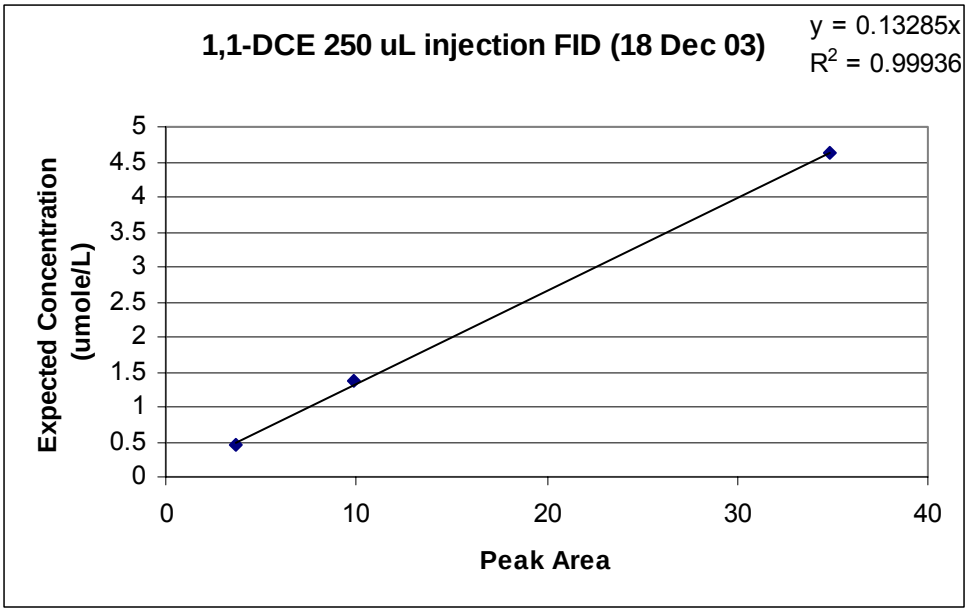

Figure A.10 Calibration curve: 250 µL 1,1-DCE injection, FID method

N-Hexane Calibration Curve

		N-Hexane	18-Dec-03
		Injection Vol =	250 µL
		y	x
Standard #	Volume injected into HS (µL)	Expected Initial Conc. Aqueous Phase (µmole/L)	Peak Area (FID)
1	4	0.007177713	0.36
2	10	0.017944284	1.06
3	25	0.044860709	2.86
4	50	0.089721419	5.52
5	100	0.179442837	12.8
6	400	0.717771349	50.9

Table A.11 Calibration curve data: 250 µL n-hexane injection, FID method

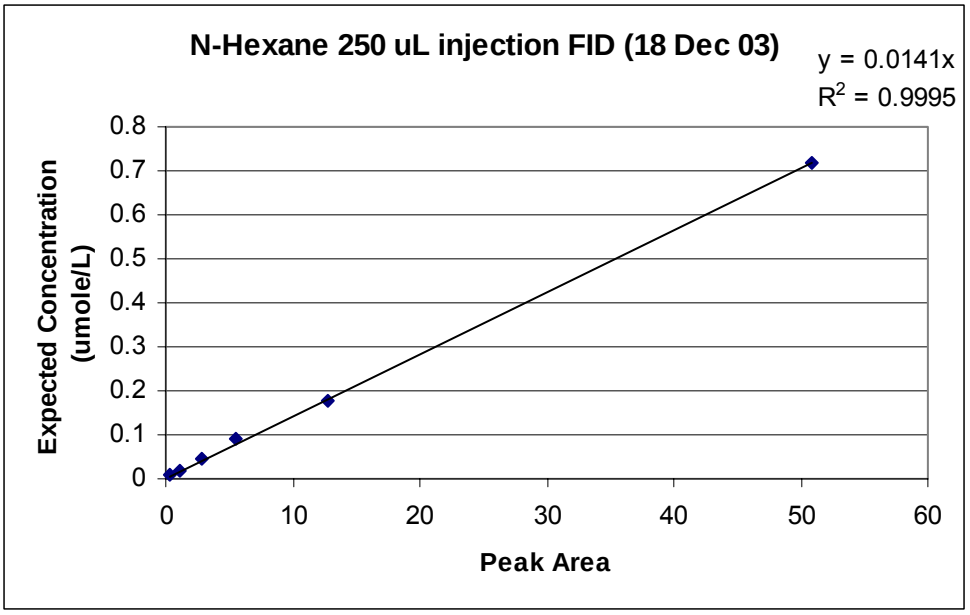

Figure A.11 Calibration curve: 250 µL n-hexane injection, FID method

APPENDIX B: COLUMN EXPERIMENT DATA

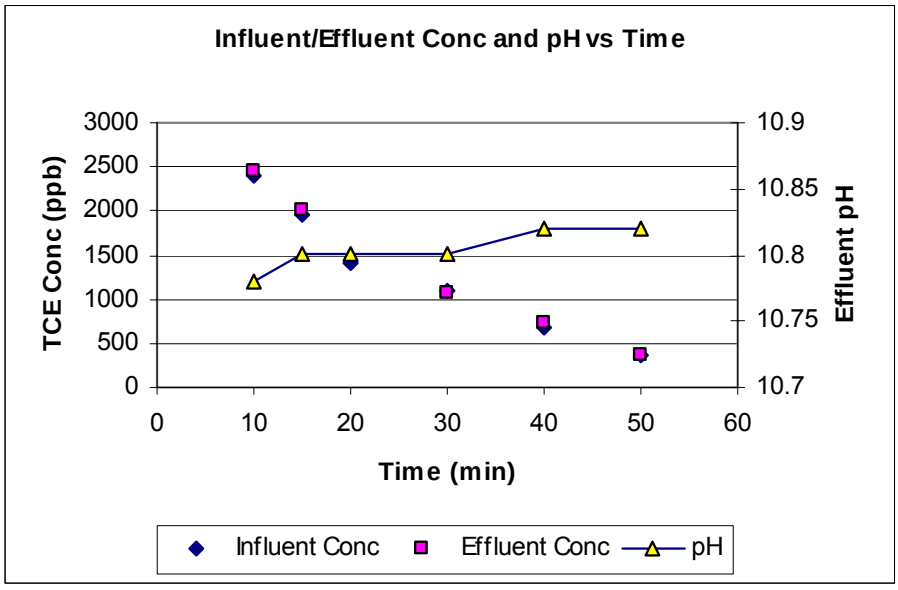

Figure B.1 Experiment #2 – pH = 10.95, [HCOOH*] = 1 mM, $[TCE]_0$ = 5 ppm, HRT = 1 min

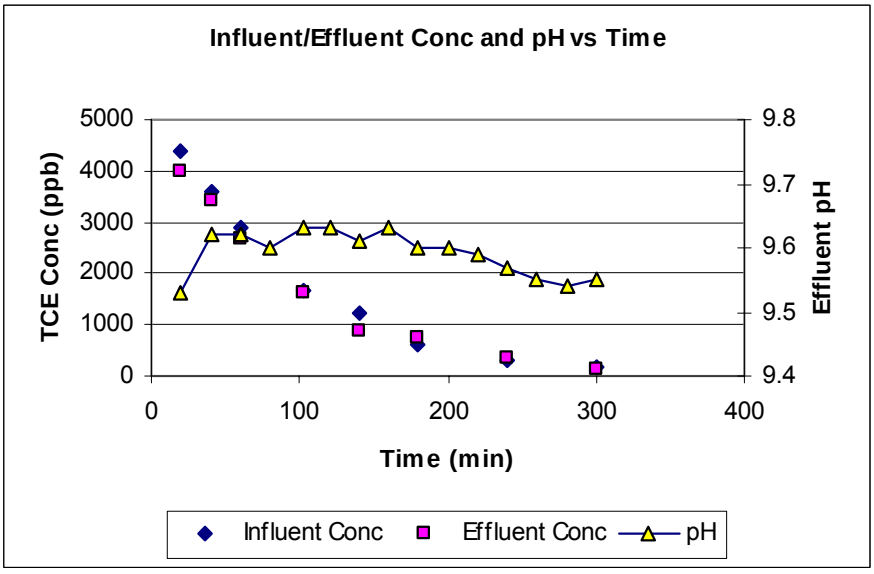

Figure B.2 Experiment #3 – pH = 7.75, [HCOOH*] = 1 mM, $[TCE]_0$ = 5 ppm, HRT = 4 min

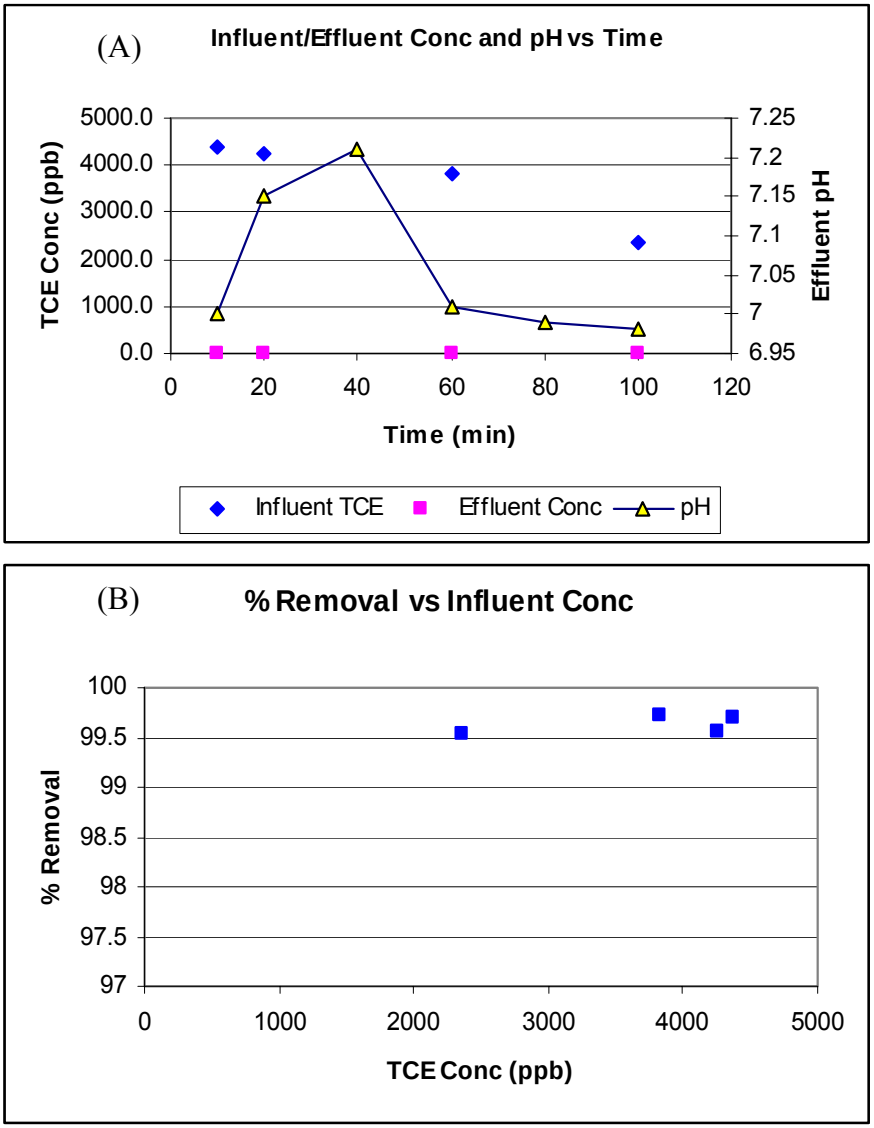

Figure B.3 Experiment #4 – pH = 4, [HCOOH*] = 1 mM, $[TCE]_0$ = 5 ppm, HRT = 4 min
(A) Influent/Effluent TCE conc. and pH vs. Time (B) % Removal vs. Influent conc.

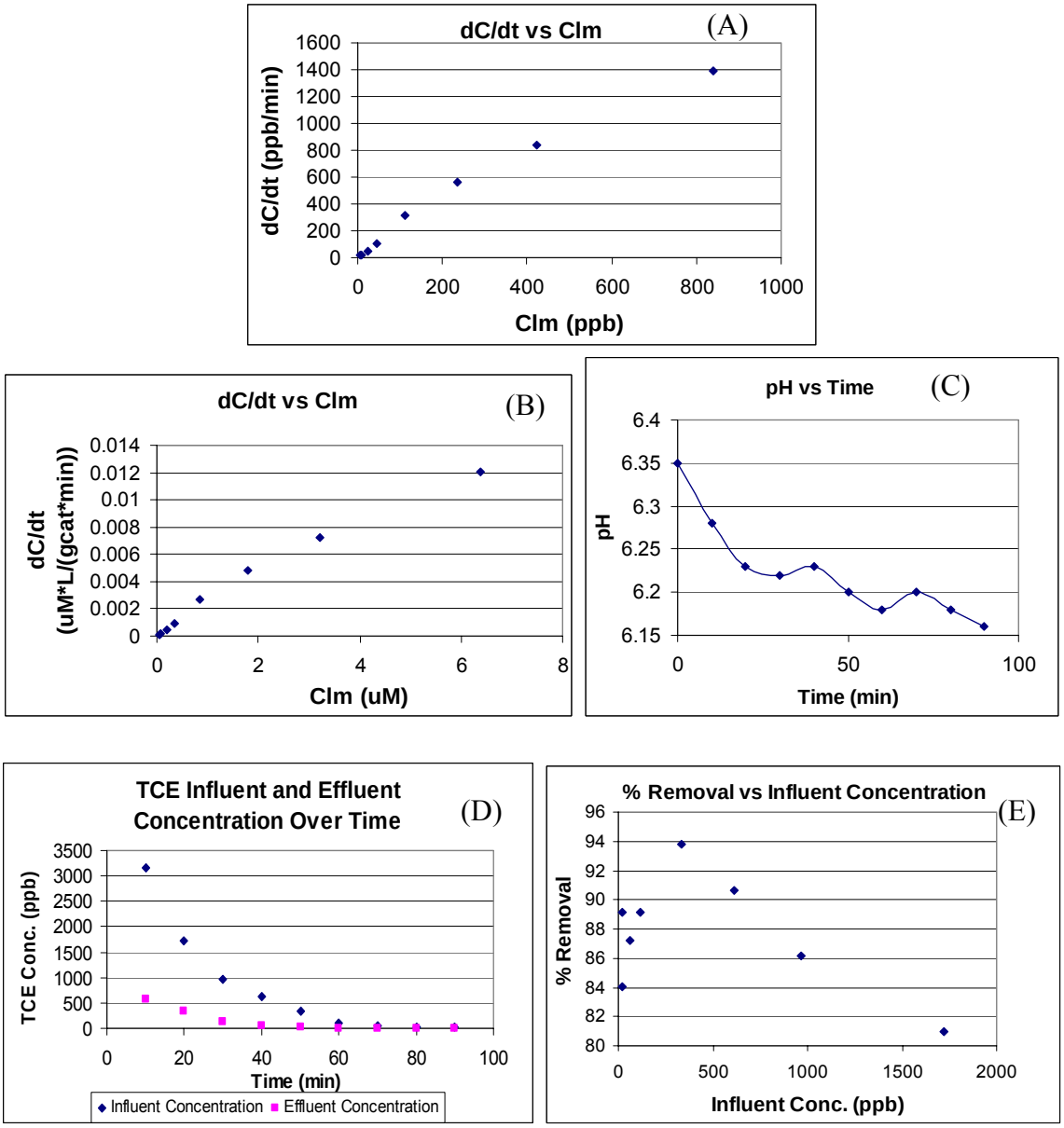

Figure B.4 Experiment #5 – pH = 4, [HCOOH*] = 1 mM, $[TCE]_0$ = 5 ppm
(A) Degradation Rate vs. Clm (B) Degradation Rate vs. Clm normalized
(C) pH vs. Time [measured at the effluent]
(D) Influent and Effluent TCE conc. vs. Time (E) % Removal vs. Influent conc.

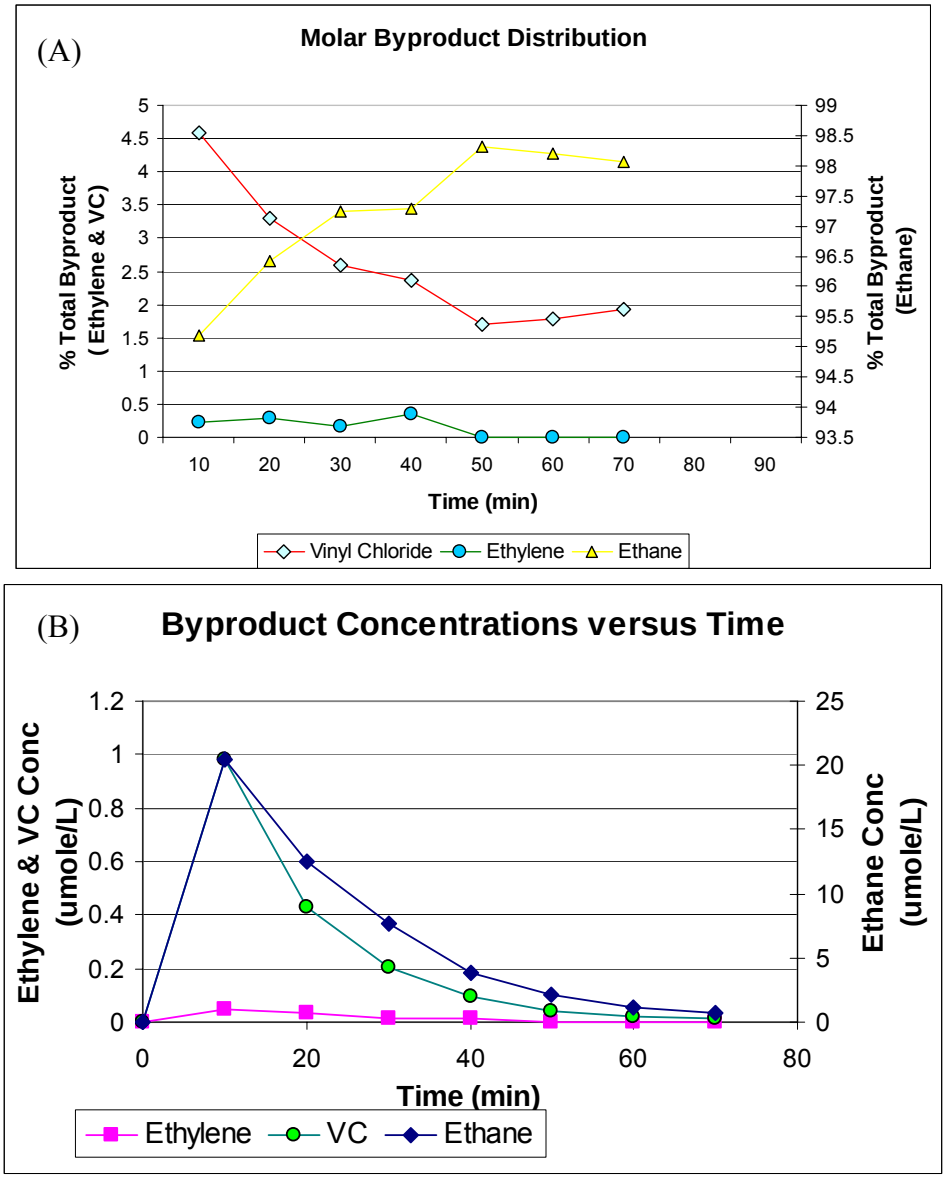

Figure B.5 Experiment #5 – pH = 4, [HCOOH*] = 1 mM, $[TCE]_0$ = 5 ppm cont.
(A) Molar Byproduct Distribution vs. Time [measured at the effluent]
(B) Ethane, Ethylene, VC Conc. vs. Time [measured at the effluent]

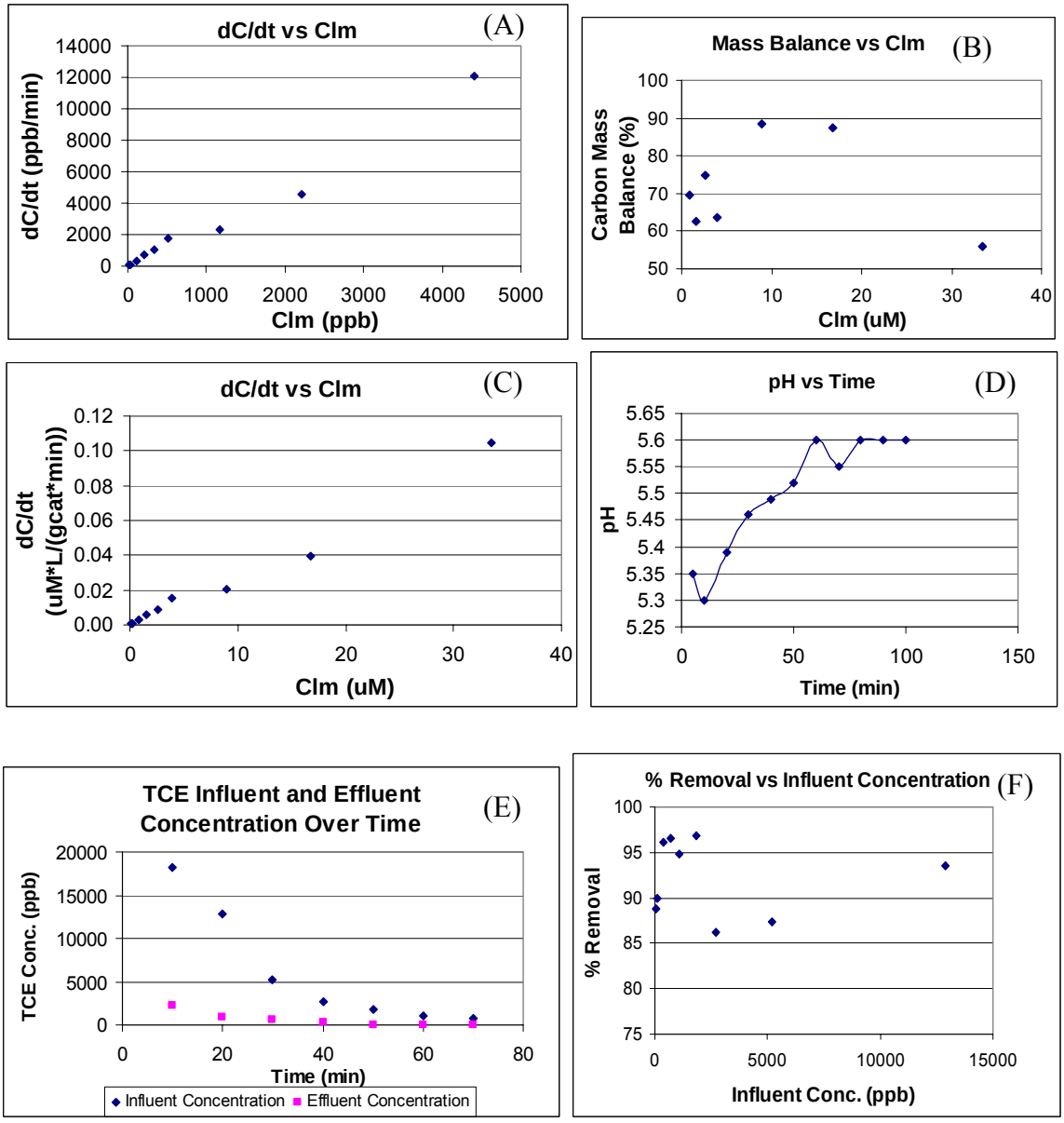

Figure B.6A Experiment #6 – pH = 4, [HCOOH*] = 2 mM, $[TCE]_0$ = 25 ppm
(A) Degradation Rate vs. Clm (B) Carbon Mass Balance vs. Clm
(C) Degradation Rate vs. Clm normalized (D) pH vs. Time [measured at the effluent]
(E) Influent and Effluent TCE conc. vs. Time
(F) % Removal vs. Influent conc.

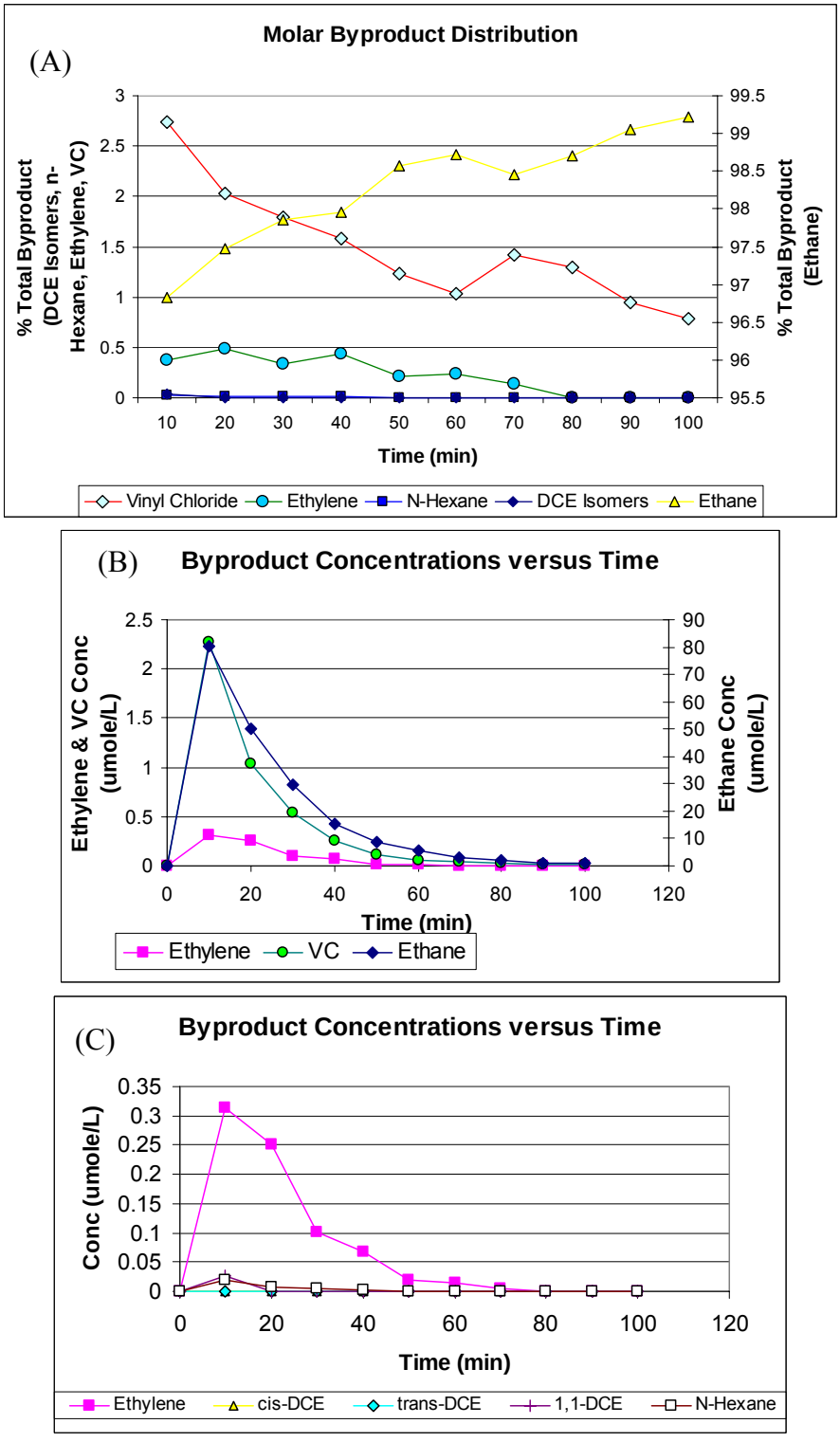

Figure B.6B Experiment #6 – pH = 4, [HCOOH*] = 2 mM, $[TCE]_0$ = 25 ppm cont.
(A) Molar Byproduct Distribution vs. Time [measured at the effluent]
(B) Ethane, Ethylene, VC Conc. vs. Time [measured at the effluent]
(C) Ethylene, DCE, Hexane Conc. vs. Time [measured at the effluent]

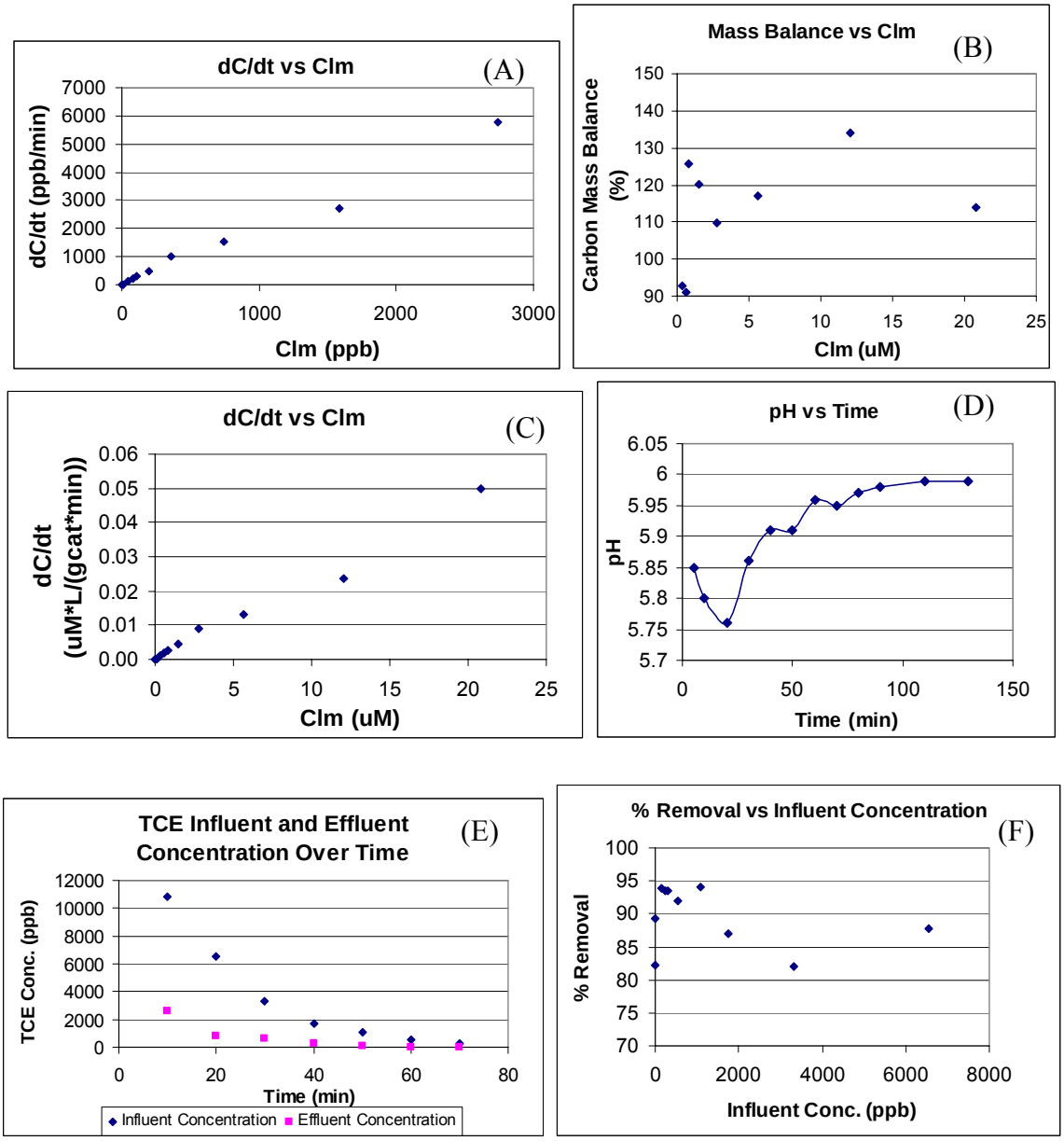

Figure B.7A Experiment #7 – pH = 4, [HCOOH*] = 1 mM, $[TCE]_0$ = 25 ppm
(A) Degradation Rate vs. Clm (B) Carbon Mass Balance vs. Clm
(C) Degradation Rate vs. Clm normalized (D) pH vs. Time [measured at the effluent]
(E) Influent and Effluent TCE conc. vs. Time
(F) % Removal vs. Influent conc.

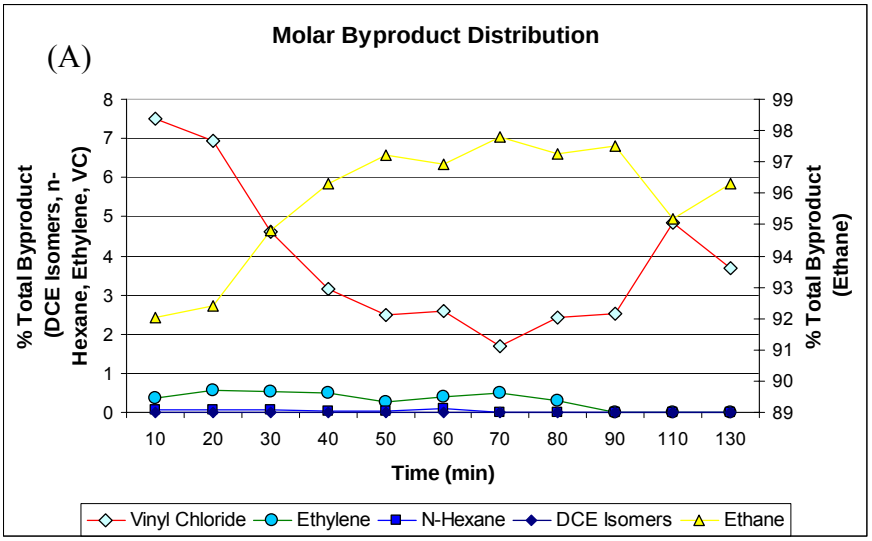

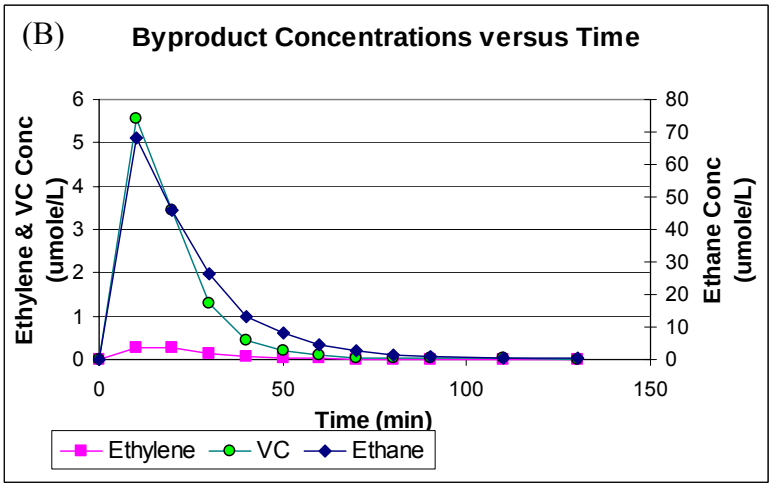

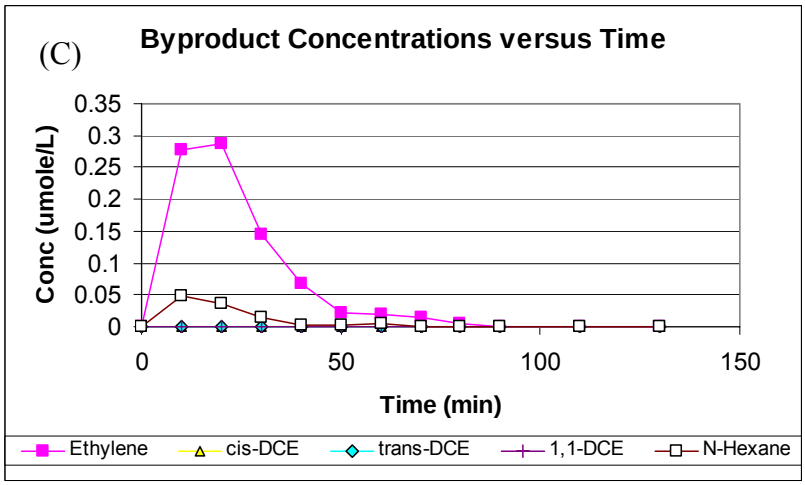

Figure B.7B Experiment #7 – pH = 4, [HCOOH*] = 1 mM, $[TCE]_0$ = 25 ppm cont.
(A) Molar Byproduct Distribution vs. Time [measured at the effluent]
(B) Ethane, Ethylene, VC Conc. vs. Time [measured at the effluent]
(C) Ethylene, DCE, Hexane Conc. vs. Time [measured at the effluent]

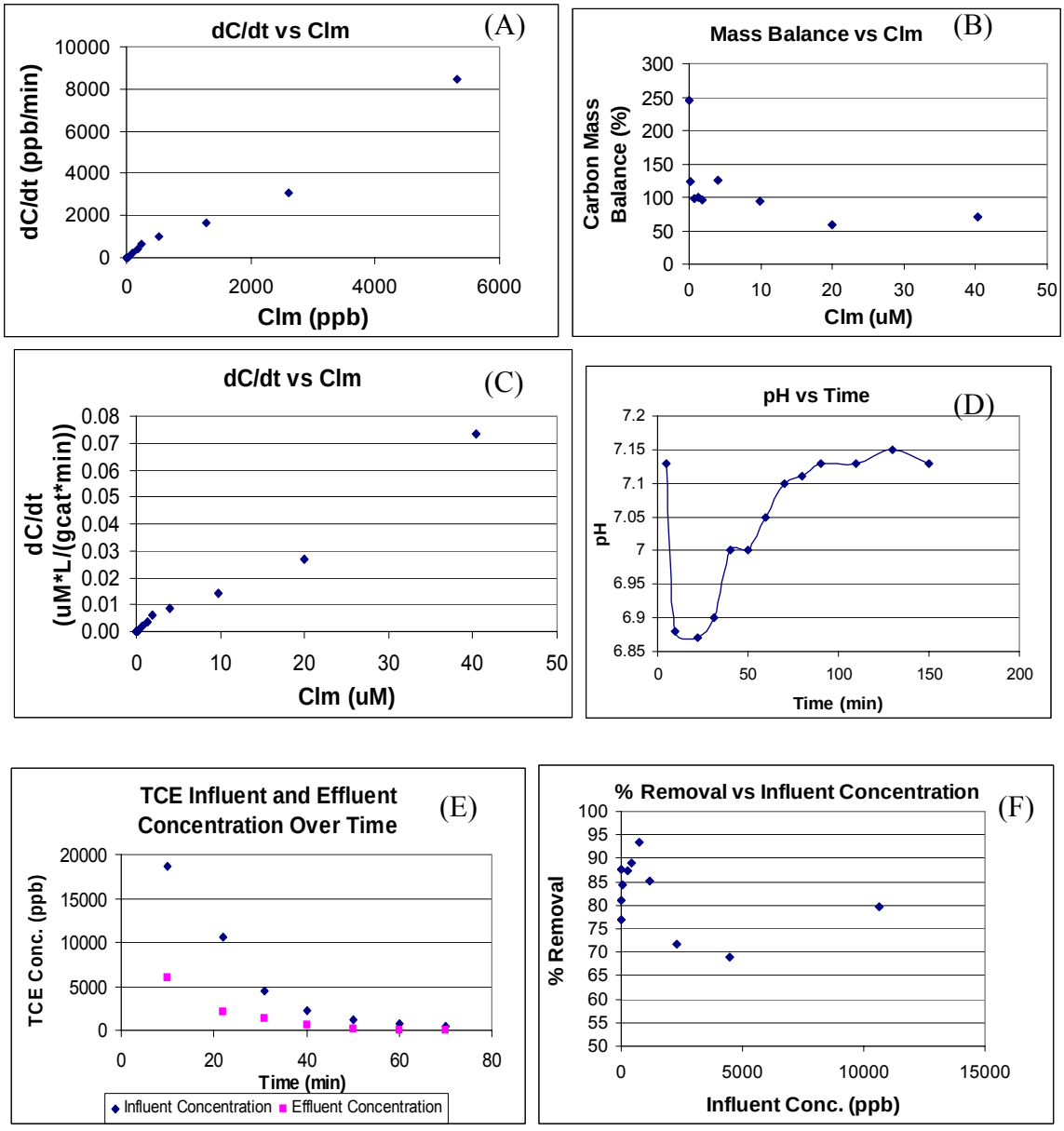

Figure B.8A Experiment #8 – pH = 5, [HCOOH*] = 1 mM, $[TCE]_0$ = 25 ppm
(A) Degradation Rate vs. Clm (B) Carbon Mass Balance vs. Clm
(C) Degradation Rate vs. Clm normalized (D) pH vs. Time [measured at the effluent]
(E) Influent and Effluent TCE conc. vs. Time
(F) % Removal vs. Influent conc.

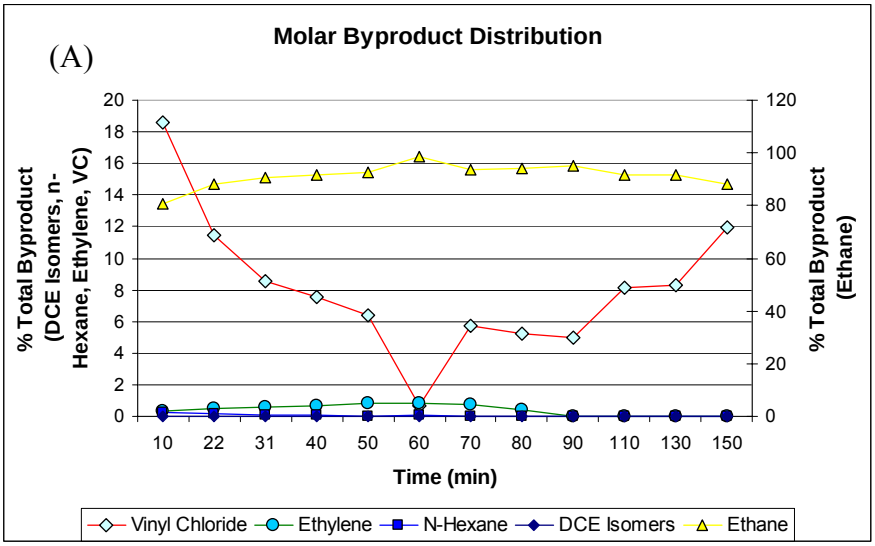

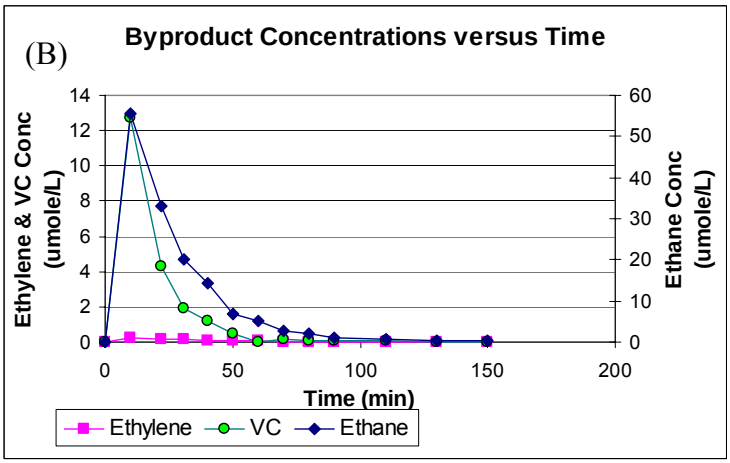

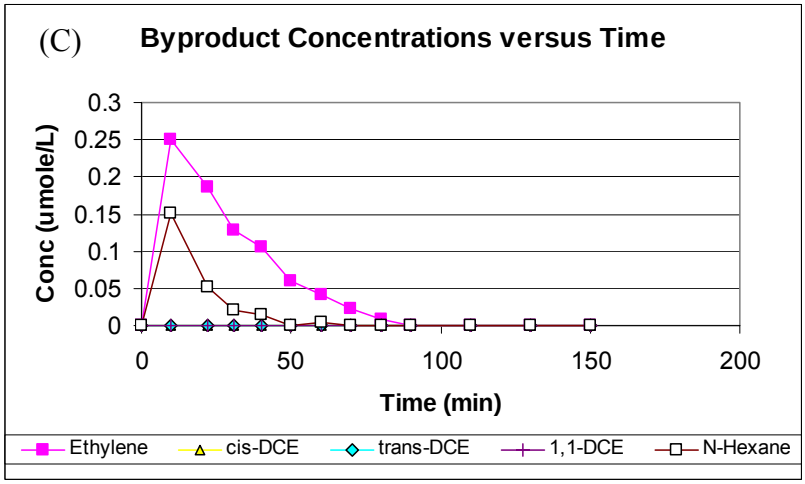

Figure B.8B Experiment #8 – pH = 5, [HCOOH*] = 1 mM, $[TCE]_0$ = 25 ppm cont.
(A) Molar Byproduct Distribution vs. Time [measured at the effluent]
(B) Ethane, Ethylene, VC Conc. vs. Time [measured at the effluent]
(C) Ethylene, DCE, Hexane Conc. vs. Time [measured at the effluent]

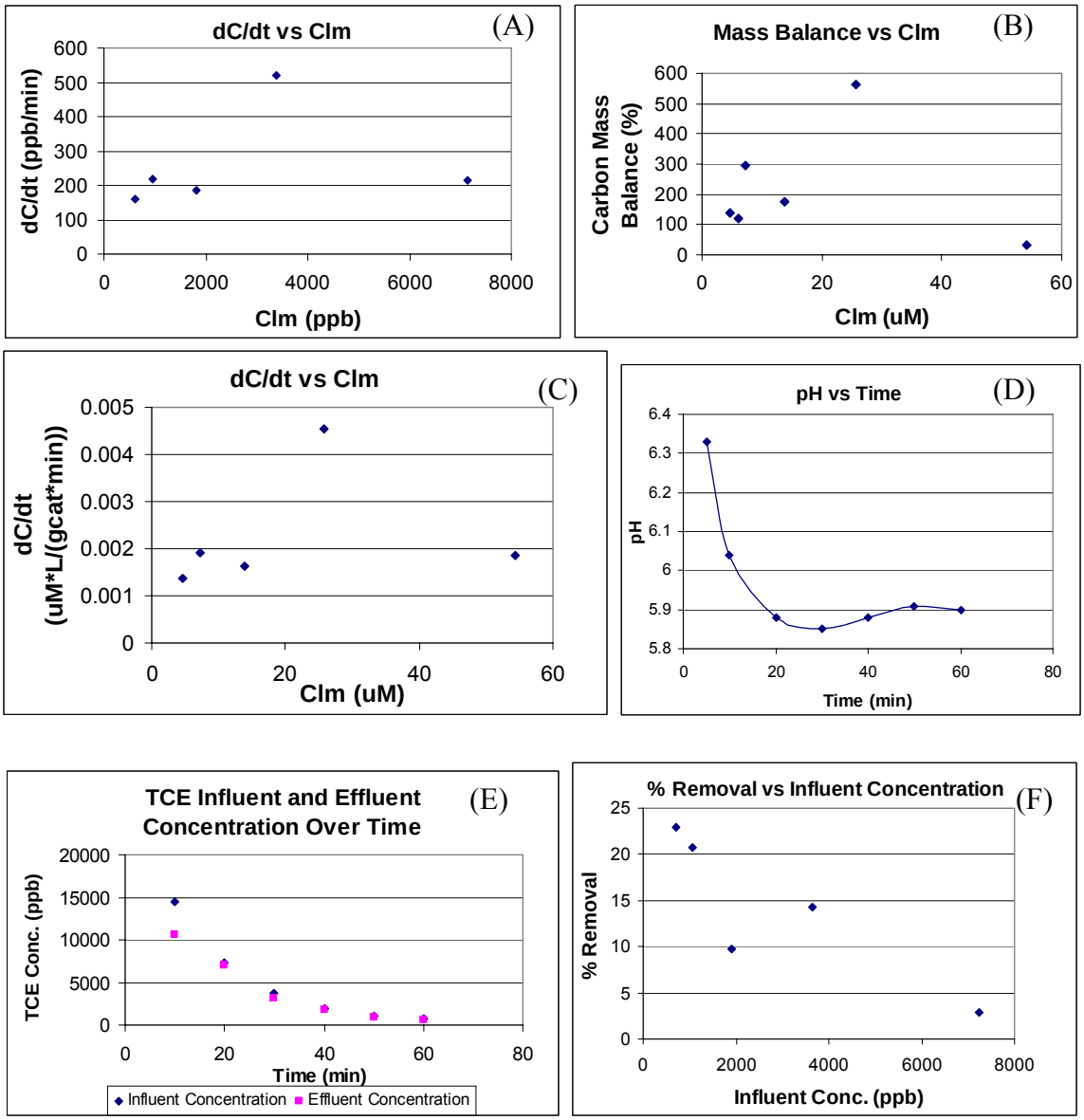

Figure B.9A Experiment #9 – pH = 4, [HCOOH*] = 0.24 mM, $[TCE]_0$ = 25 ppm
(A) Degradation Rate vs. Clm (B) Carbon Mass Balance vs. Clm
(C) Degradation Rate vs. Clm normalized (D) pH vs. Time [measured at the effluent]
(E) Influent and Effluent TCE conc. vs. Time
(F) % Removal vs. Influent conc.

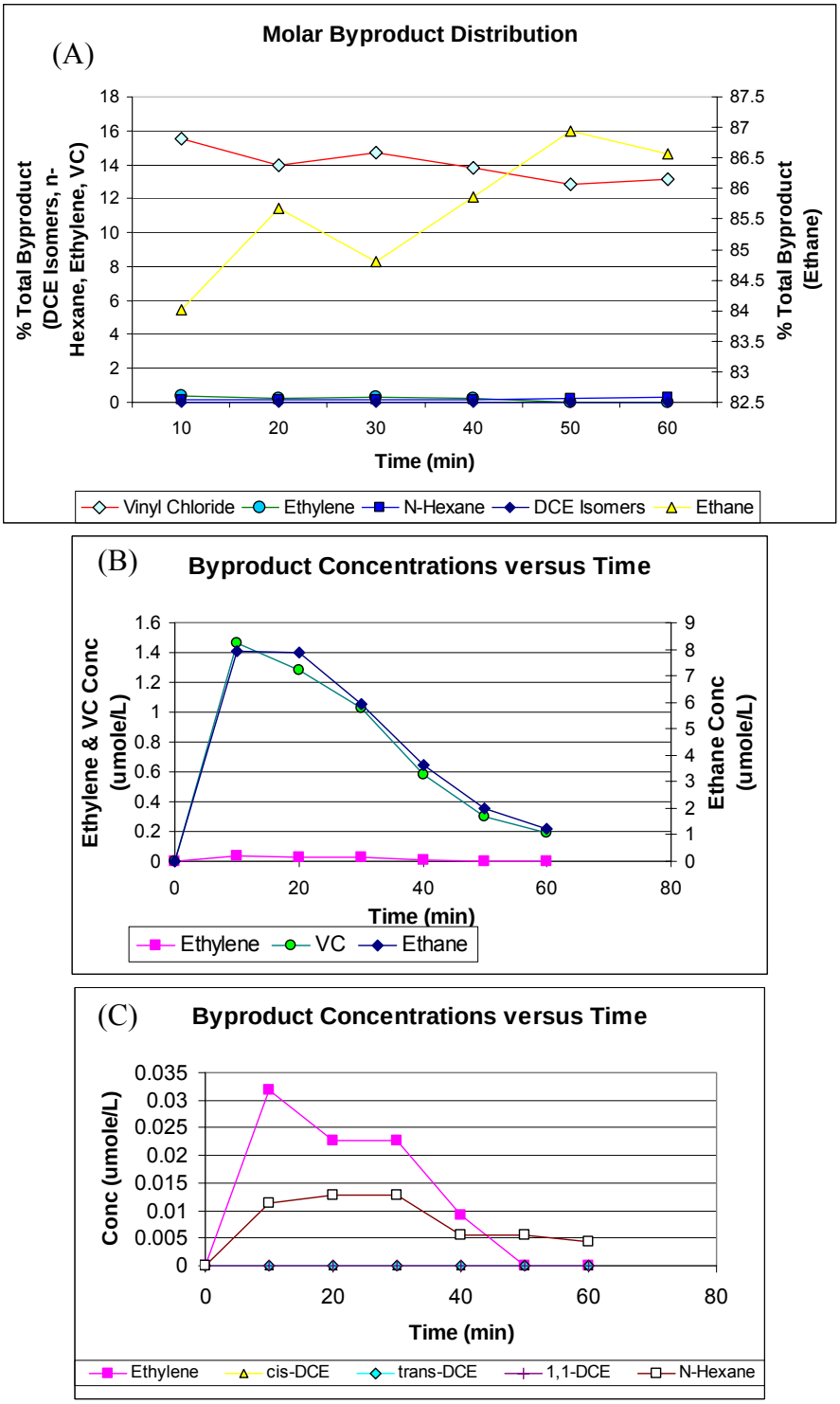

Figure B.9B Experiment #9 – pH = 4, [HCOOH*] = 0.24 mM, $[TCE]_0$ = 25 ppm cont.
(A) Molar Byproduct Distribution vs. Time [measured at the effluent]
(B) Ethane, Ethylene, VC Conc. vs. Time [measured at the effluent]
(C) Ethylene, DCE, Hexane Conc. vs. Time [measured at the effluent]

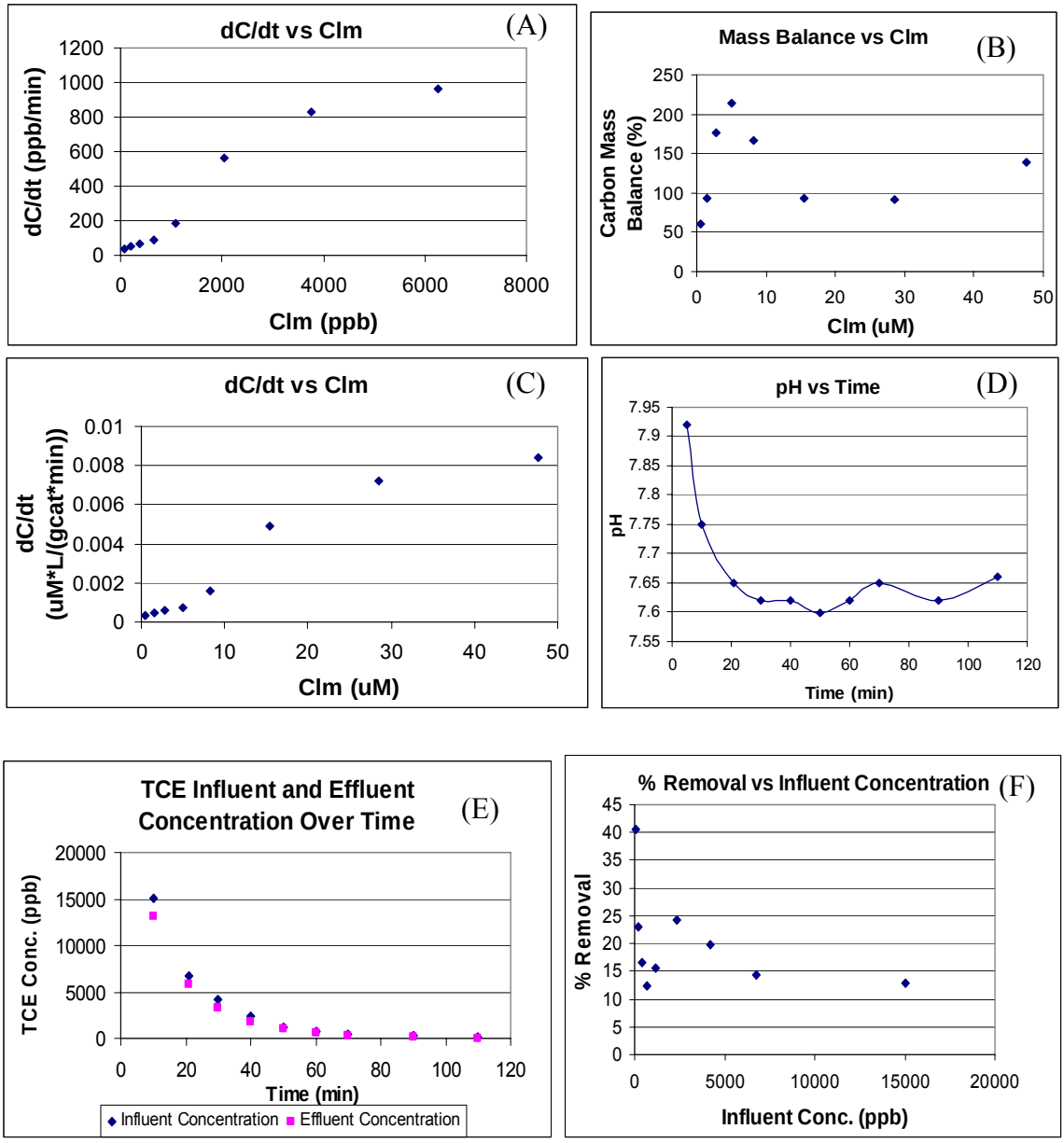

Figure B.10A Experiment #10 – pH = 6, [HCOOH*] = 1 mM, $[TCE]_0$ = 25 ppm
(A) Degradation Rate vs. Clm (B) Carbon Mass Balance vs. Clm
(C) Degradation Rate vs. Clm normalized (D) pH vs. Time [measured at the effluent]
(E) Influent and Effluent TCE conc. vs. Time
(F) % Removal vs. Influent conc.

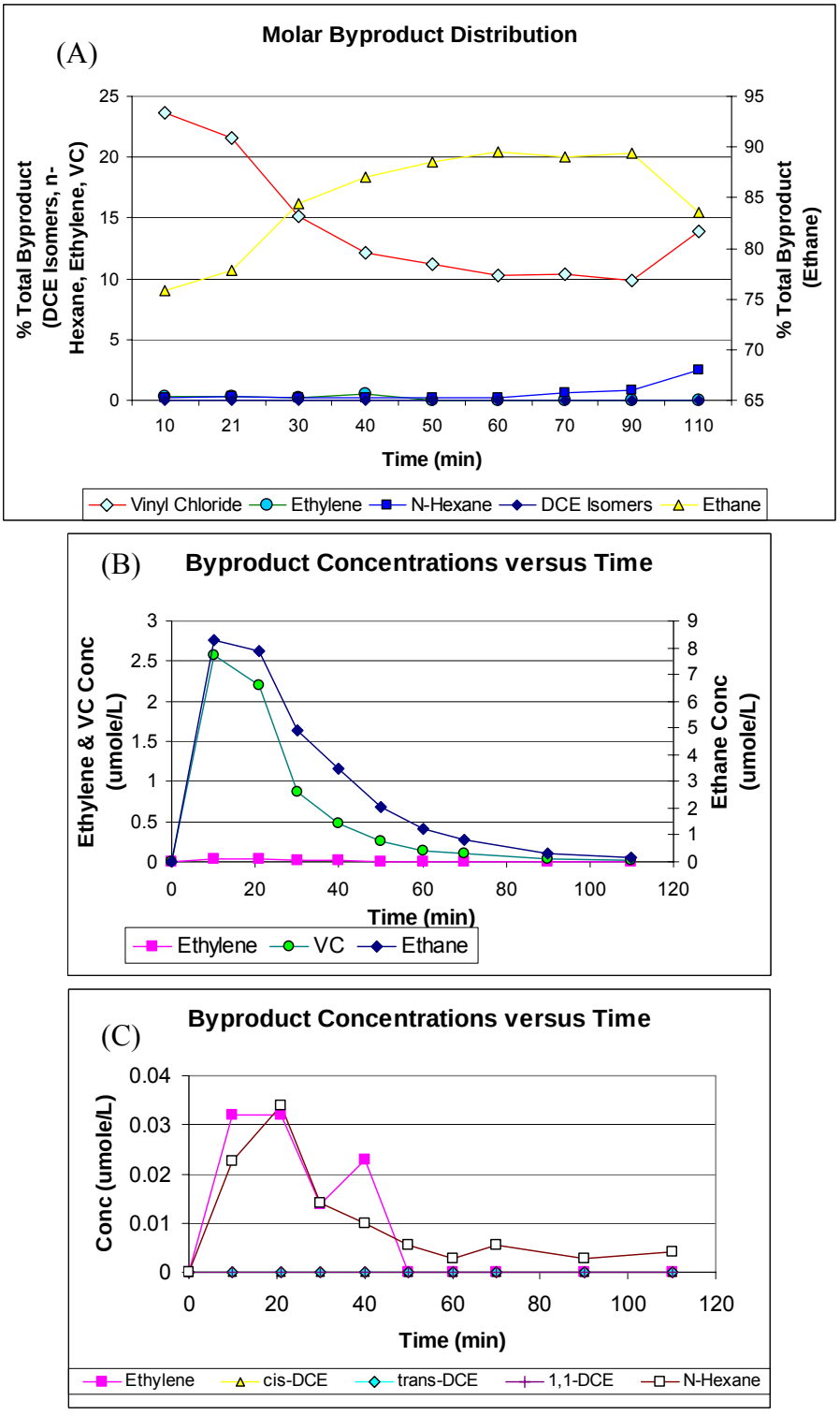

Figure B.10B Experiment #10 – pH = 6, [HCOOH*] = 1 mM, $[TCE]_0$ = 25 ppm cont.
(A) Molar Byproduct Distribution vs. Time [measured at the effluent]
(B) Ethane, Ethylene, VC Conc. vs. Time [measured at the effluent]
(C) Ethylene, DCE, Hexane Conc. vs. Time [measured at the effluent]

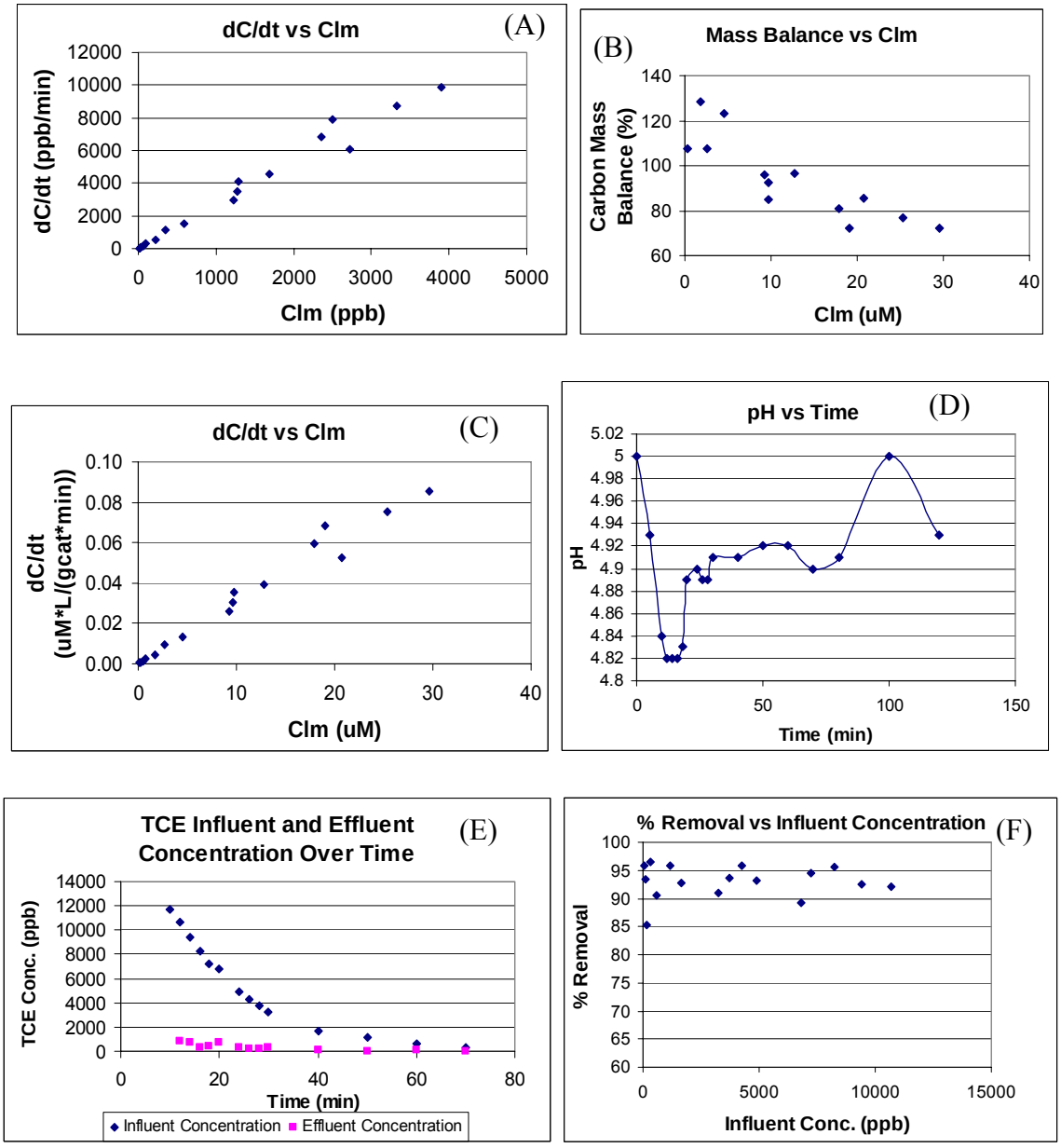

Figure B.11A Experiment #11 – pH = 4, [HCOOH*] = 4 mM, $[TCE]_0$ = 25 ppm
(A) Degradation Rate vs. Clm (B) Carbon Mass Balance vs. Clm
(C) Degradation Rate vs. Clm normalized (D) pH vs. Time [measured at the effluent]
(E) Influent and Effluent TCE conc. vs. Time
(F) % Removal vs. Influent conc.

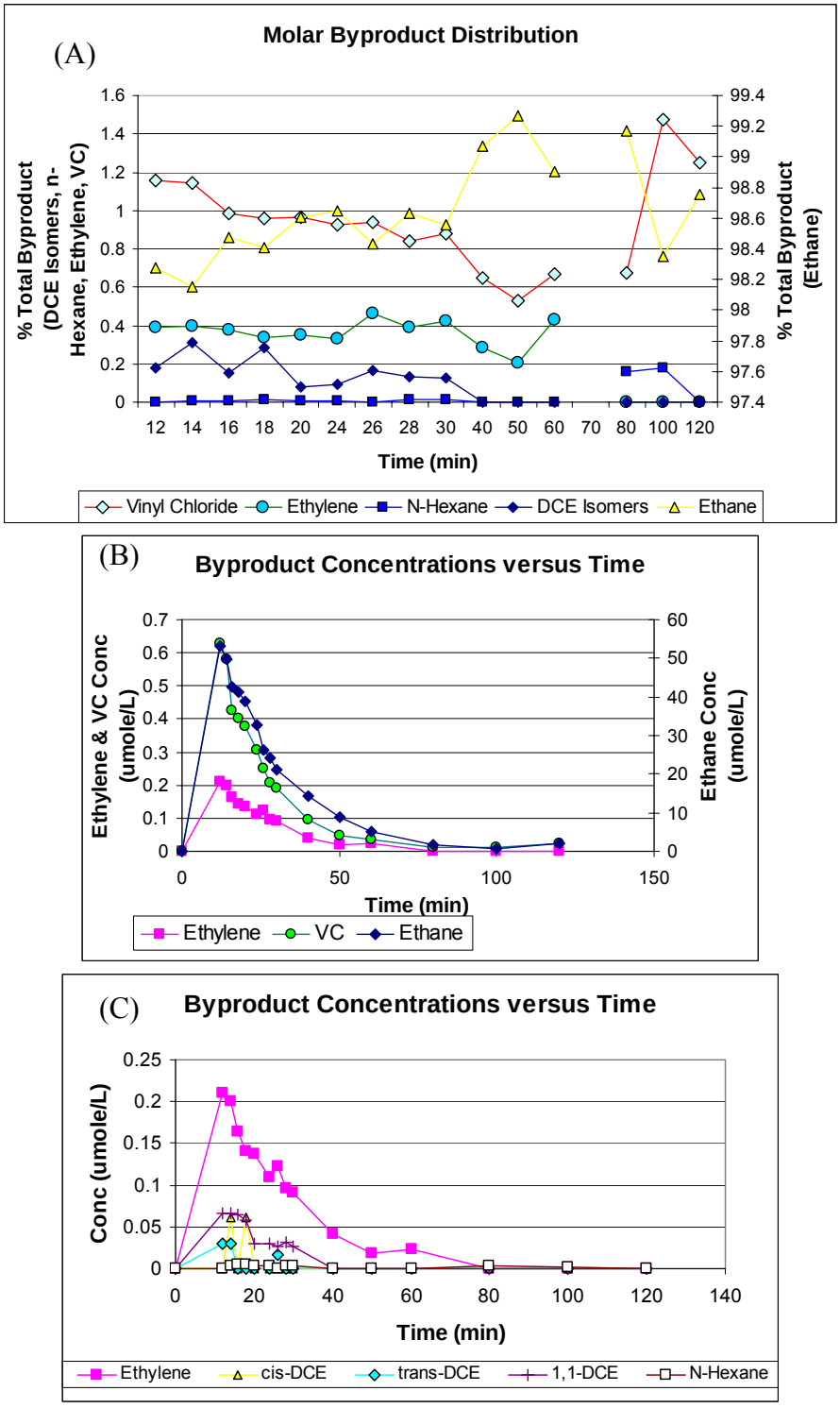

Figure B.11B Experiment #11 – pH = 4, [HCOOH*] = 4 mM, $[TCE]_0$ = 25 ppm cont.
(A) Molar Byproduct Distribution vs. Time [measured at the effluent]
(B) Ethane, Ethylene, VC Conc. vs. Time [measured at the effluent]
(C) Ethylene, DCE, Hexane Conc. vs. Time [measured at the effluent]

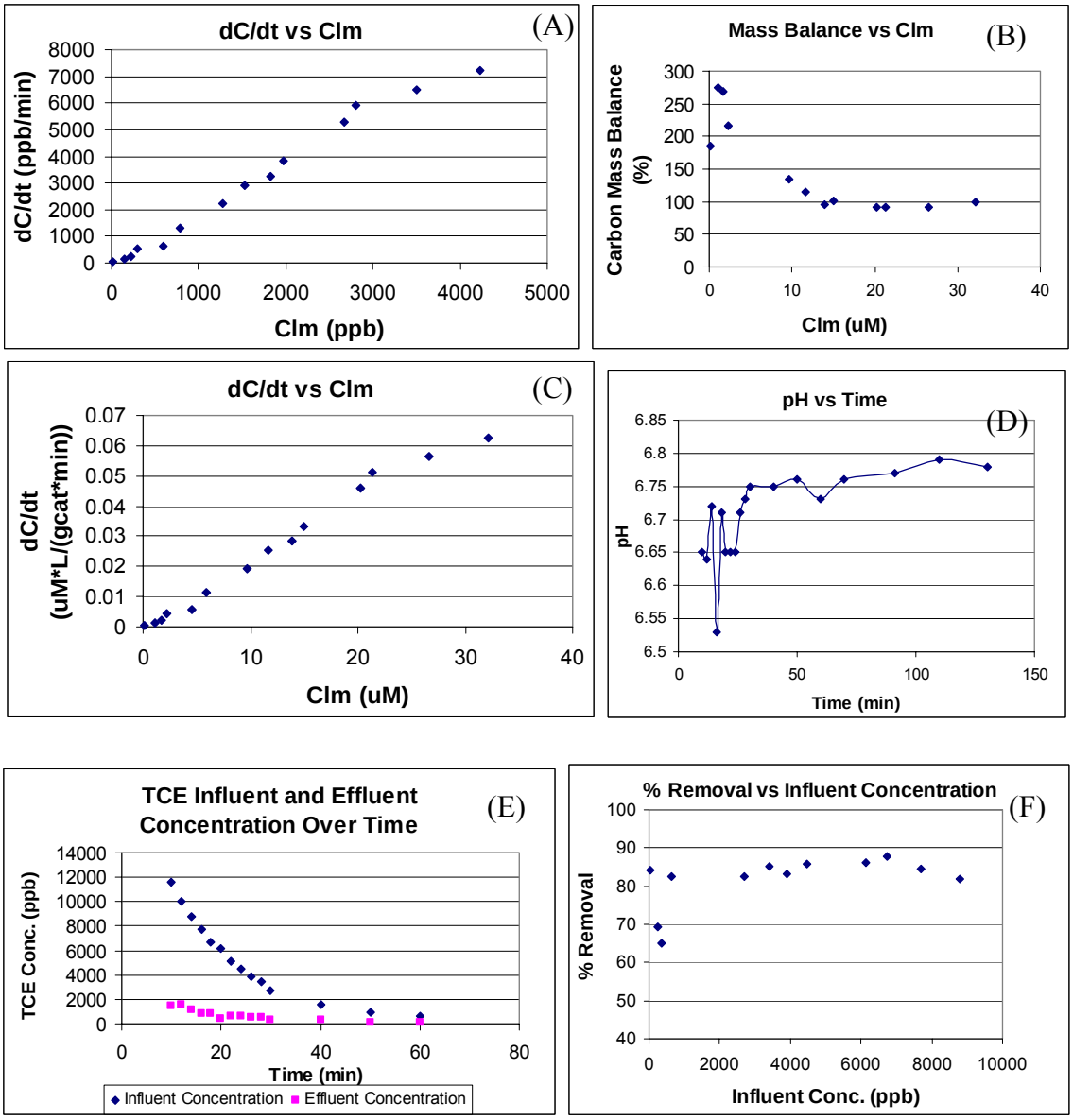

Figure B.12A Experiment #12 – pH = 5, [HCOOH*] = 4 mM, $[TCE]_0$ = 25 ppm
(A) Degradation Rate vs. Clm (B) Carbon Mass Balance vs. Clm
(C) Degradation Rate vs. Clm normalized (D) pH vs. Time [measured at the effluent]
(E) Influent and Effluent TCE conc. vs. Time
(F) % Removal vs. Influent conc.

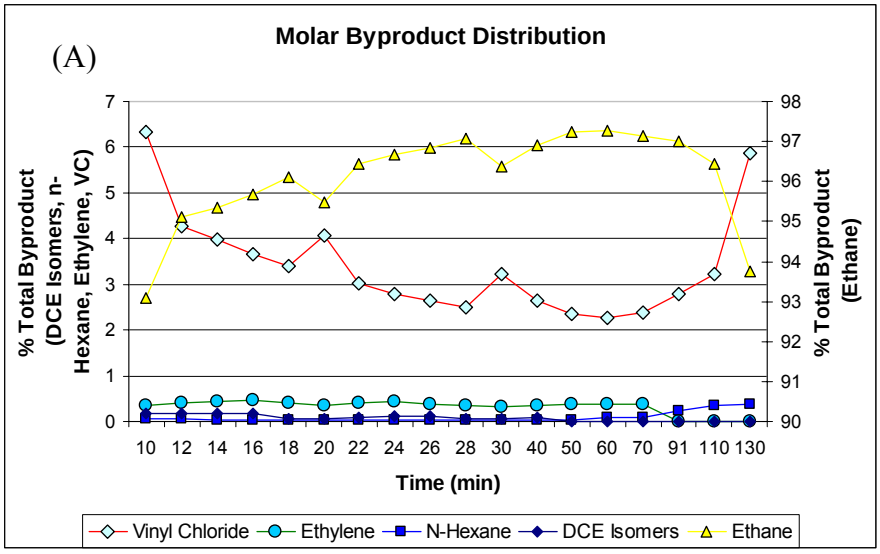

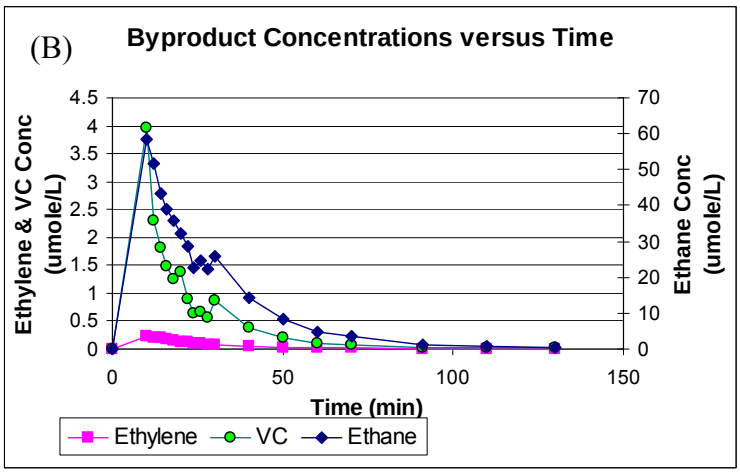

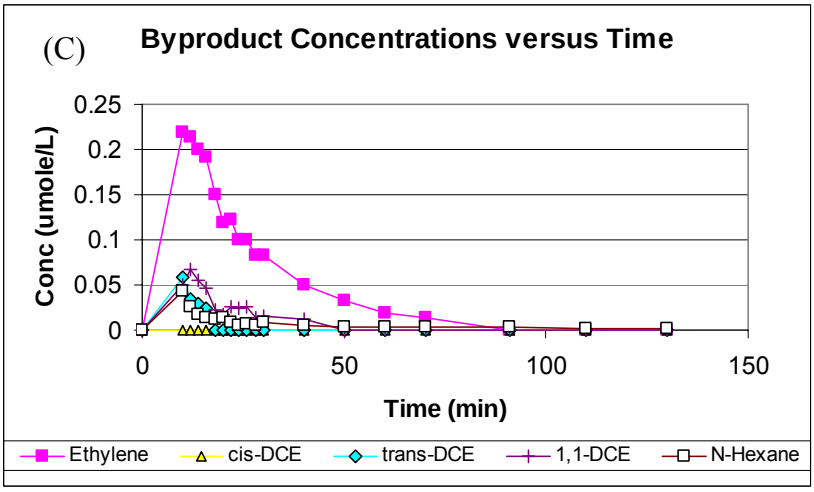

Figure B.12B Experiment #12 – pH = 5, [HCOOH*] = 4 mM, $[TCE]_0$ = 25 ppm cont.
(A) Molar Byproduct Distribution vs. Time [measured at the effluent]
(B) Ethane, Ethylene, VC Conc. vs. Time [measured at the effluent]
(C) Ethylene, DCE, Hexane Conc. vs. Time [measured at the effluent]

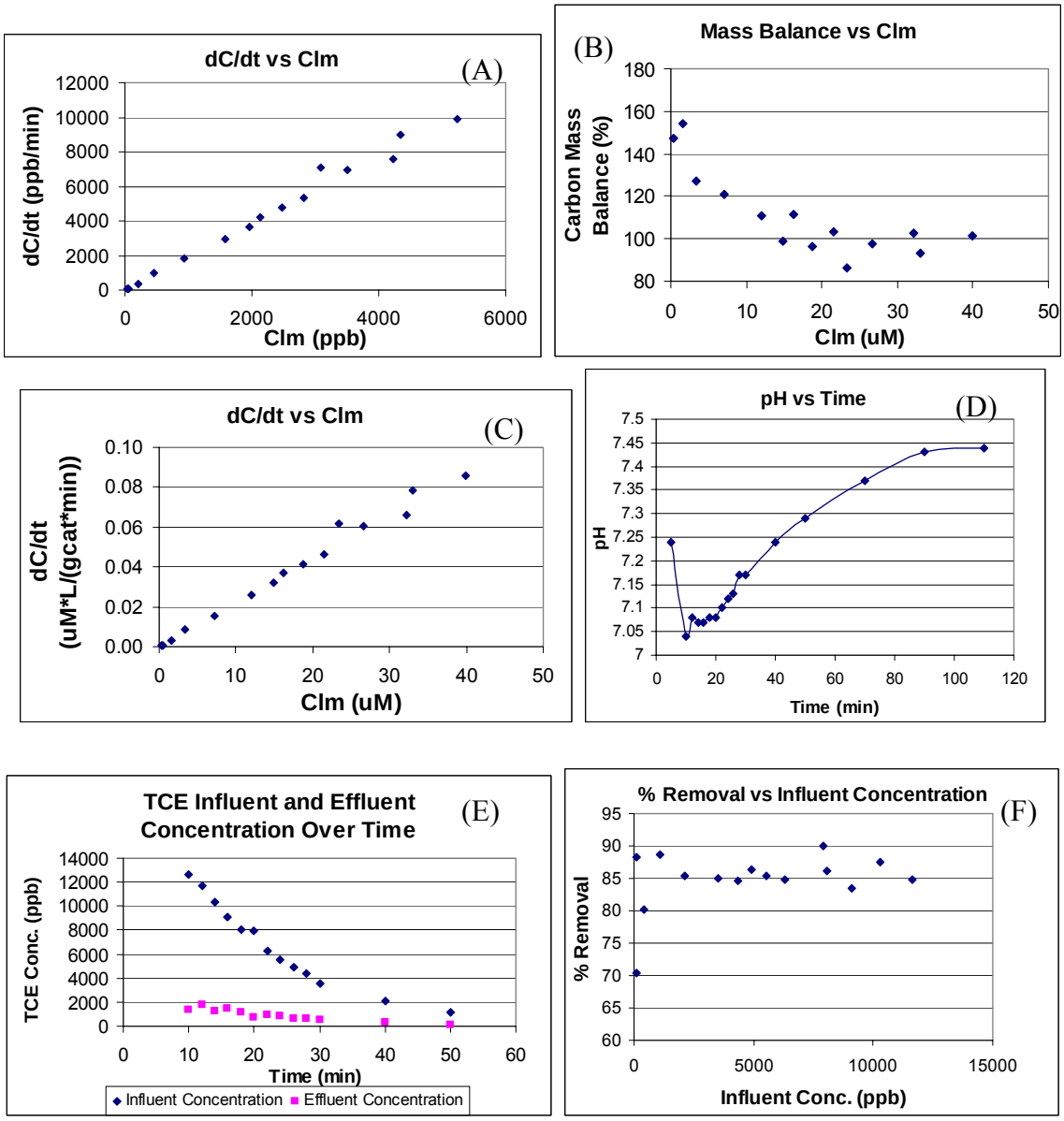

Figure B.13A Experiment #13 – pH = 6, [HCOOH*] = 4 mM, $[TCE]_0$ = 25 ppm
(A) Degradation Rate vs. Clm (B) Carbon Mass Balance vs. Clm
(C) Degradation Rate vs. Clm normalized (D) pH vs. Time [measured at the effluent]
(E) Influent and Effluent TCE conc. vs. Time
(F) % Removal vs. Influent conc.

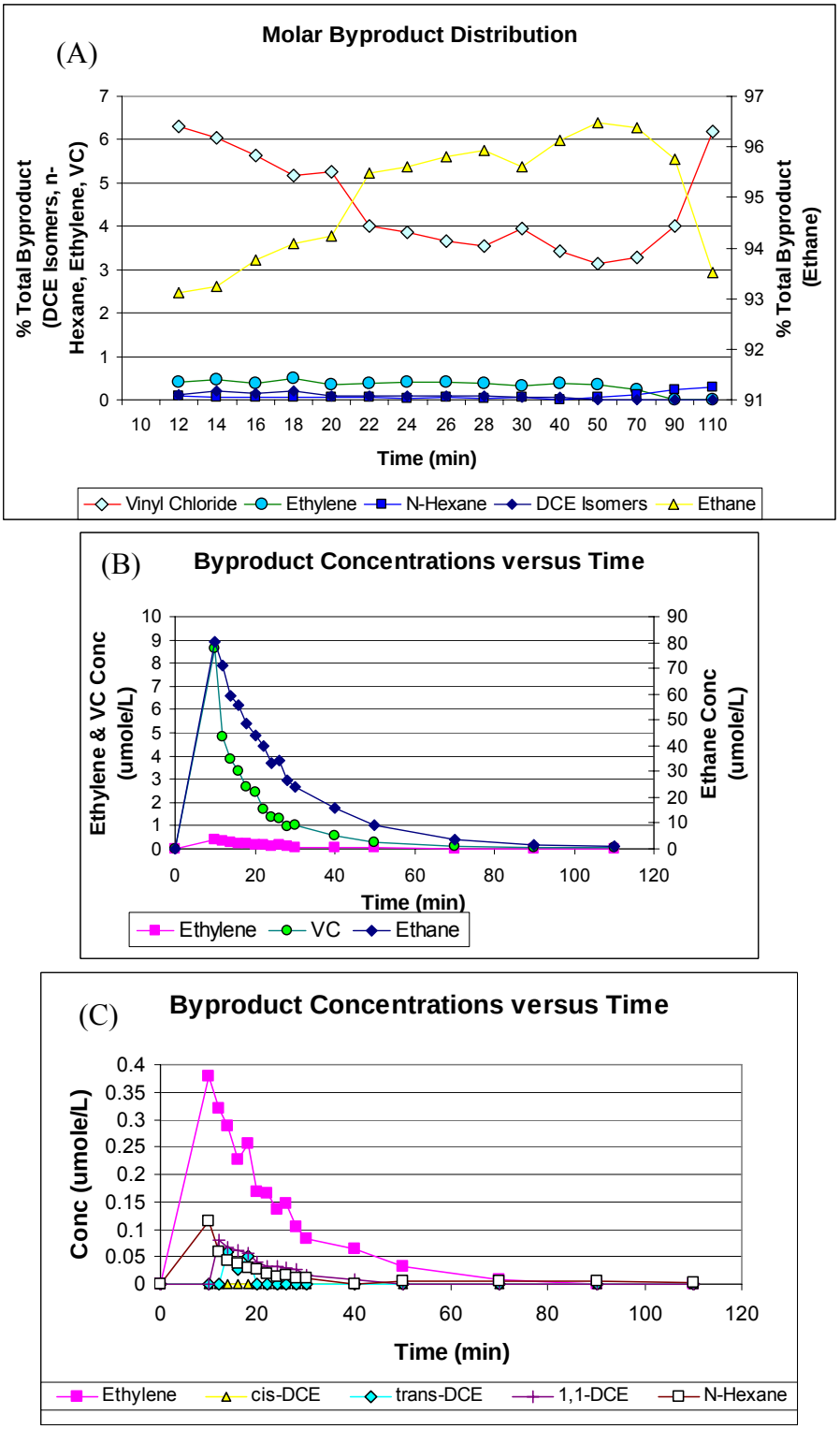

Figure B.13B Experiment #13 – pH = 6, [HCOOH*] = 4 mM, $[TCE]_0$ = 25 ppm cont.
(A) Molar Byproduct Distribution vs. Time [measured at the effluent]
(B) Ethane, Ethylene, VC Conc. vs. Time [measured at the effluent]
(C) Ethylene, DCE, Hexane Conc. vs. Time [measured at the effluent]

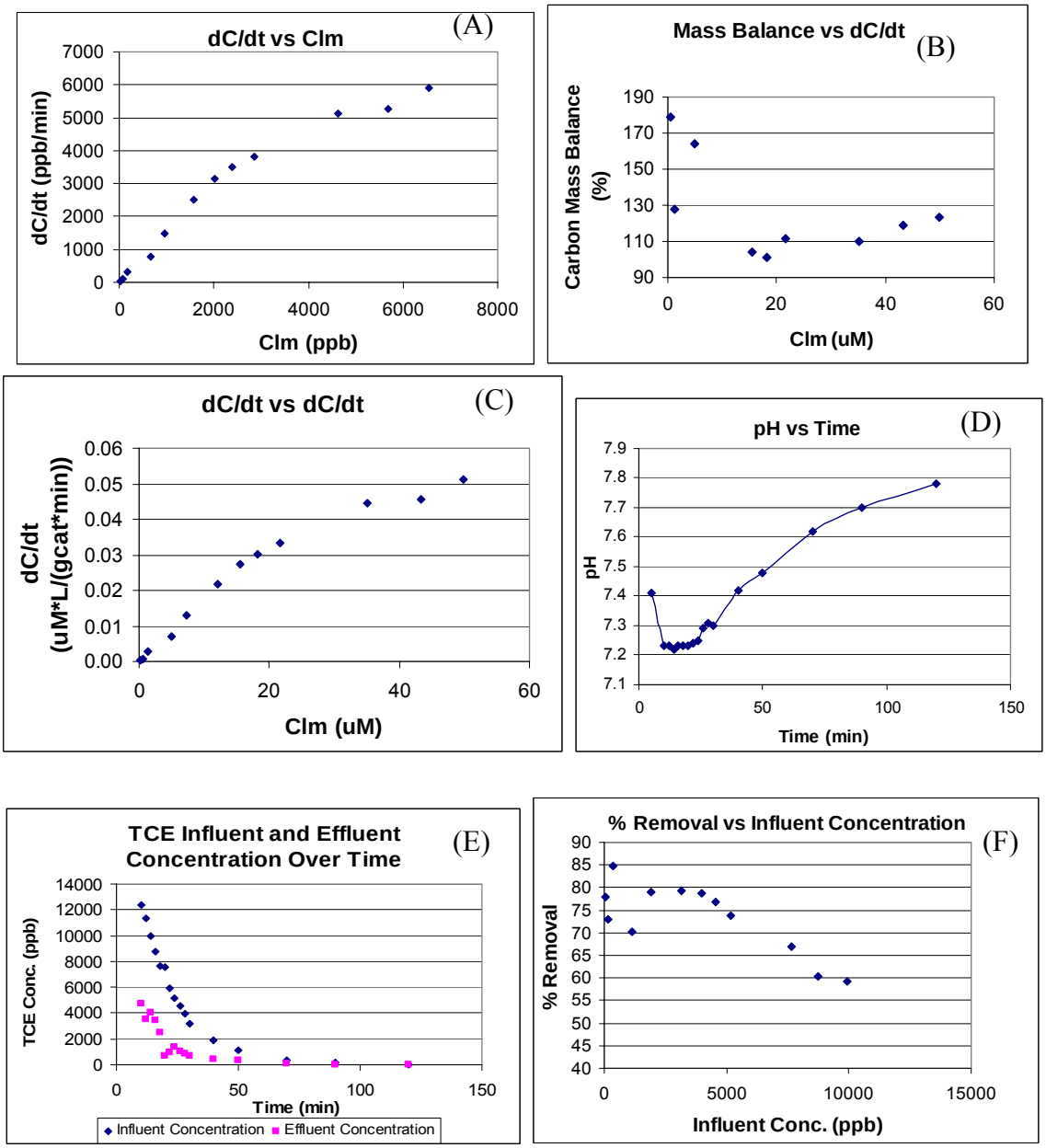

Figure B.14A Experiment #14 – pH = 7.5, [HCOOH*] = 4 mM, $[TCE]_0$ = 25 ppm
(A) Degradation Rate vs. Clm (B) Carbon Mass Balance vs. Clm
(C) Degradation Rate vs. Clm normalized (D) pH vs. Time [measured at the effluent]
(E) Influent and Effluent TCE conc. vs. Time
(F) % Removal vs. Influent conc.

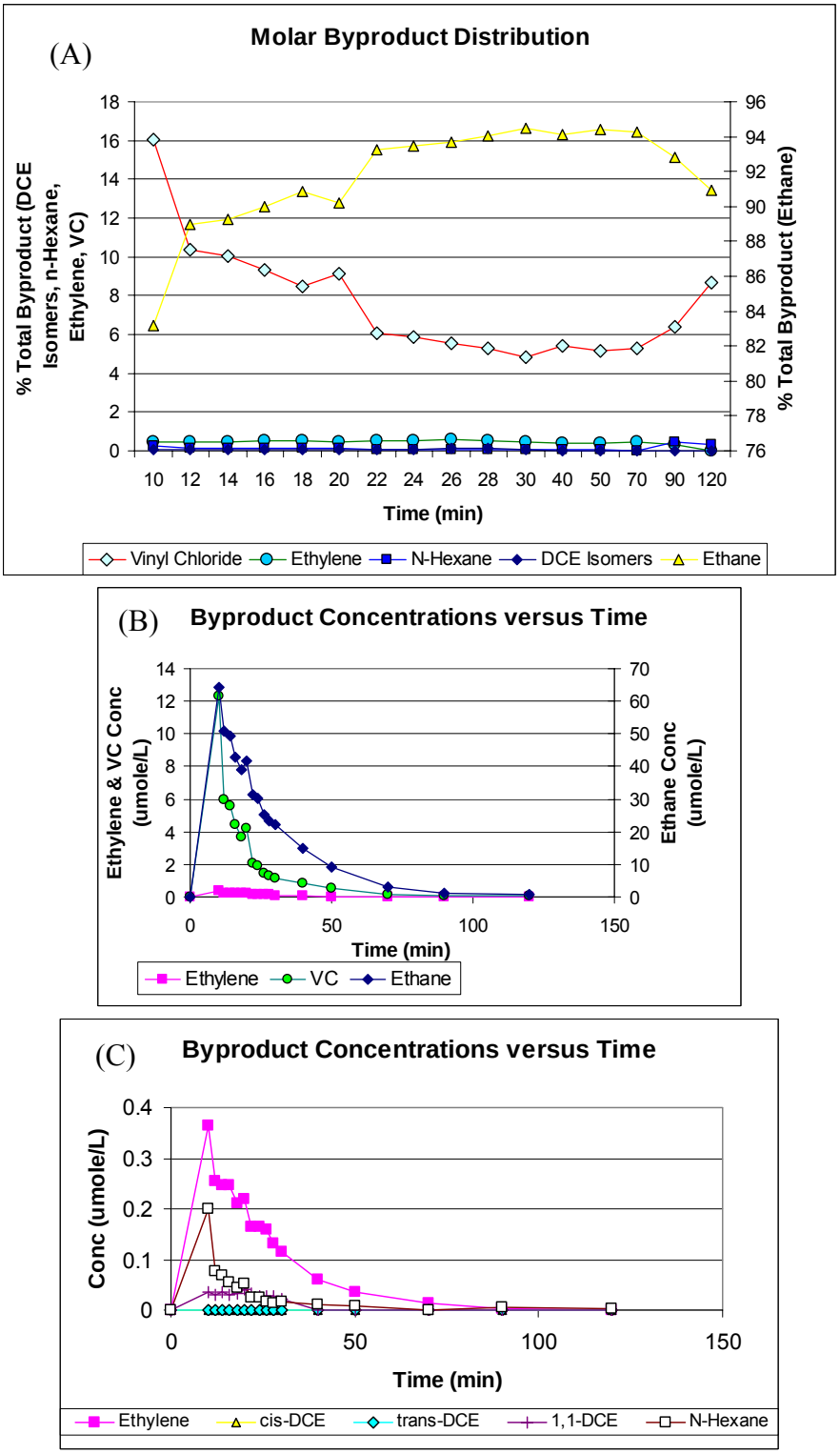

Figure B.14B Experiment #14 – pH = 7.5, [HCOOH*] = 4 mM, $[TCE]_0$ = 25 ppm cont.
(A) Molar Byproduct Distribution vs. Time [measured at the effluent]
(B) Ethane, Ethylene, VC Conc. vs. Time [measured at the effluent]
(C) Ethylene, DCE, Hexane Conc. vs. Time [measured at the effluent]

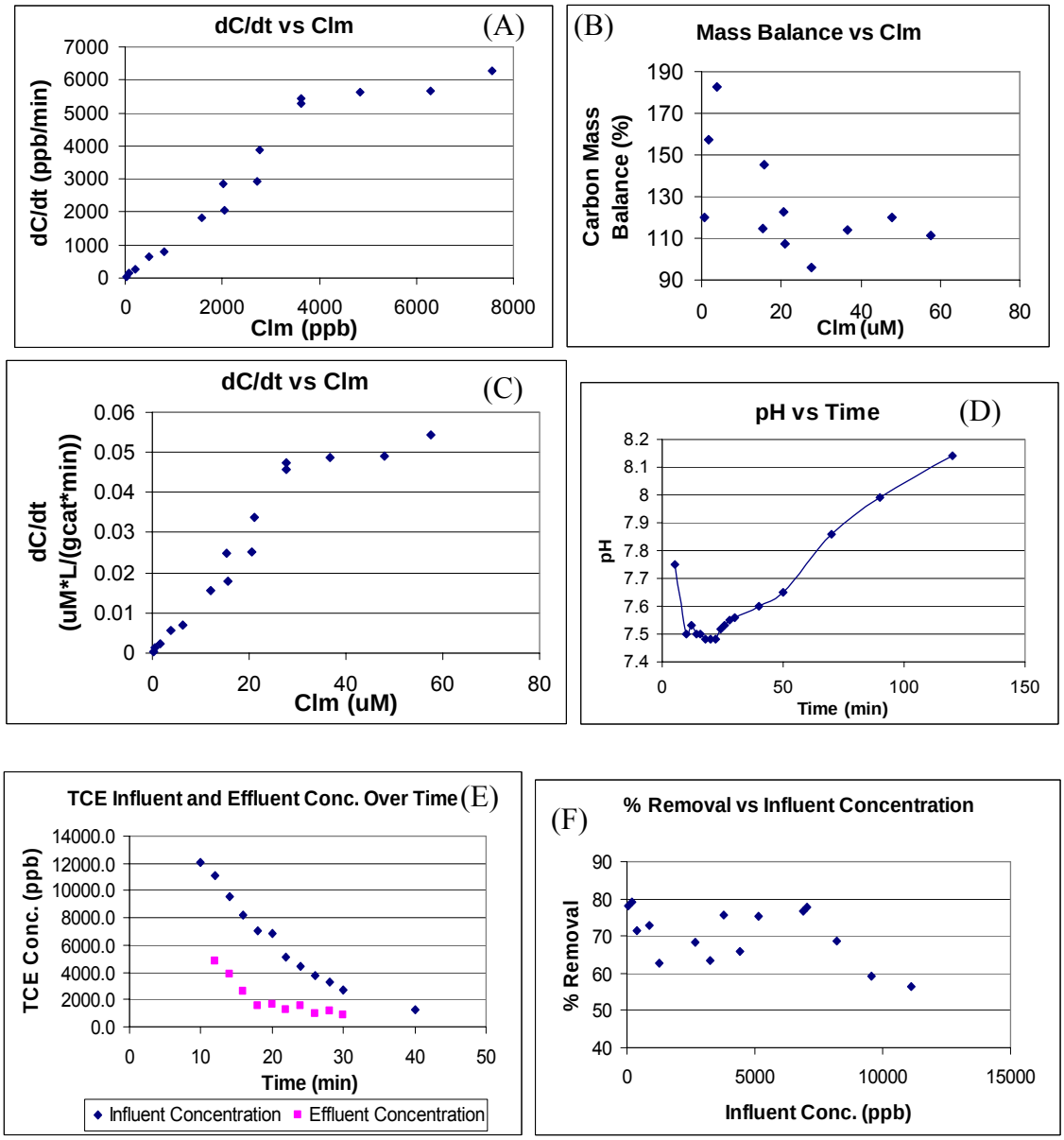

Figure B.15A Experiment #15 – pH = 8, [HCOOH*] = 4 mM, $[TCE]_0$ = 25 ppm
(A) Degradation Rate vs. Clm (B) Carbon Mass Balance vs. Clm
(C) Degradation Rate vs. Clm normalized (D) pH vs. Time [measured at the effluent]
(E) Influent and Effluent TCE conc. vs. Time
(F) % Removal vs. Influent conc.

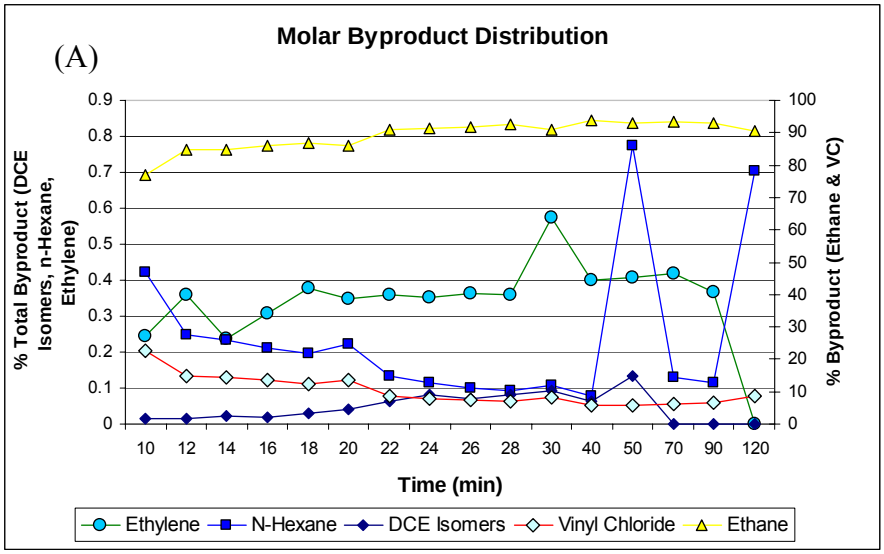

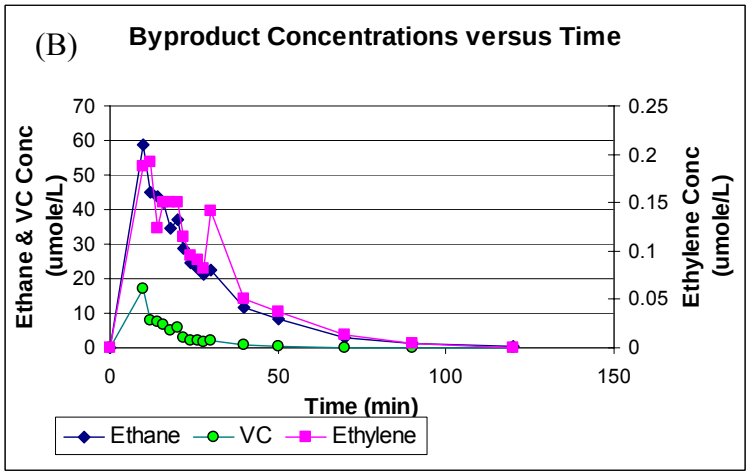

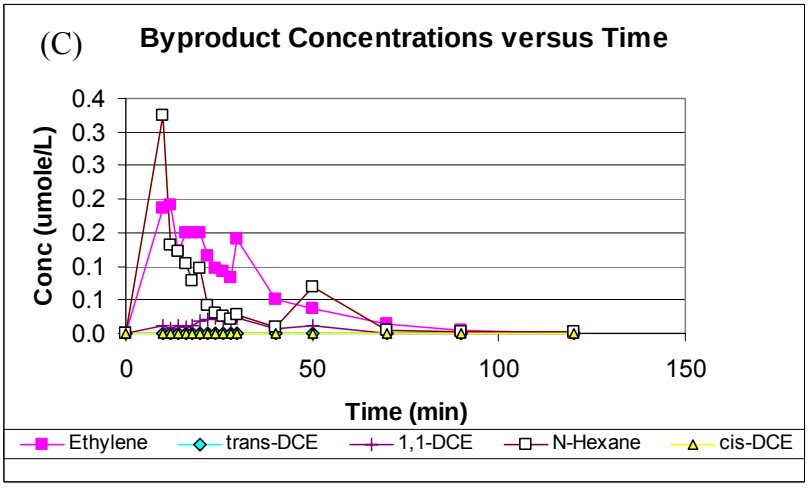

Figure B.15B Experiment #15 – pH = 8, [HCOOH*] = 4 mM, $[TCE]_0$ = 25 ppm cont.
(A) Molar Byproduct Distribution vs. Time [measured at the effluent]
(B) Ethane, Ethylene, VC Conc. vs. Time [measured at the effluent]
(C) Ethylene, DCE, Hexane Conc. vs. Time [measured at the effluent]

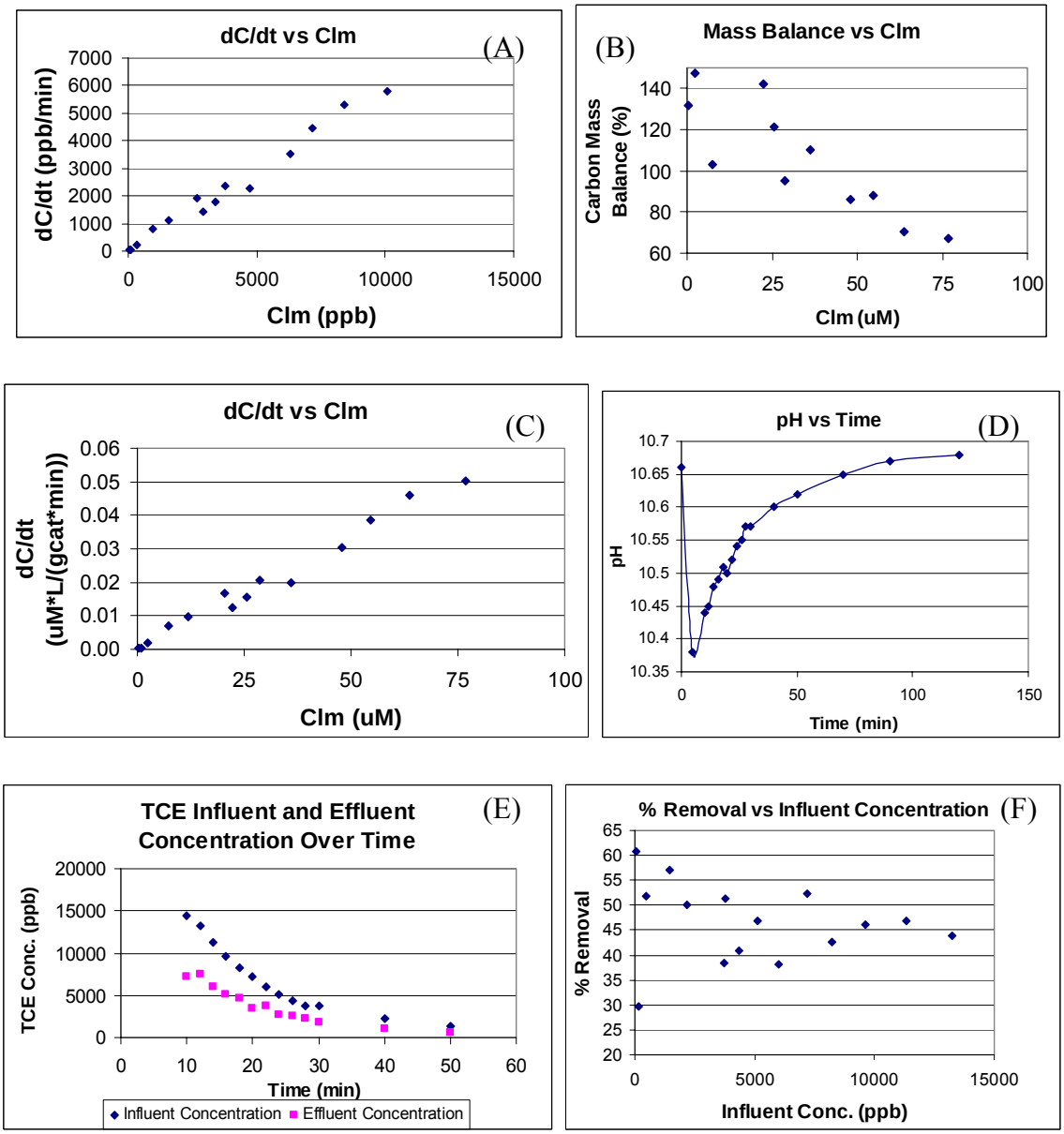

Figure B.16A Experiment #16 – pH = 11, [HCOOH*] = 4 mM, $[TCE]_0$ = 25 ppm
(A) Degradation Rate vs. Clm (B) Carbon Mass Balance vs. Clm
(C) Degradation Rate vs. Clm normalized (D) pH vs. Time [measured at the effluent]
(E) Influent and Effluent TCE conc. vs. Time
(F) % Removal vs. Influent conc.

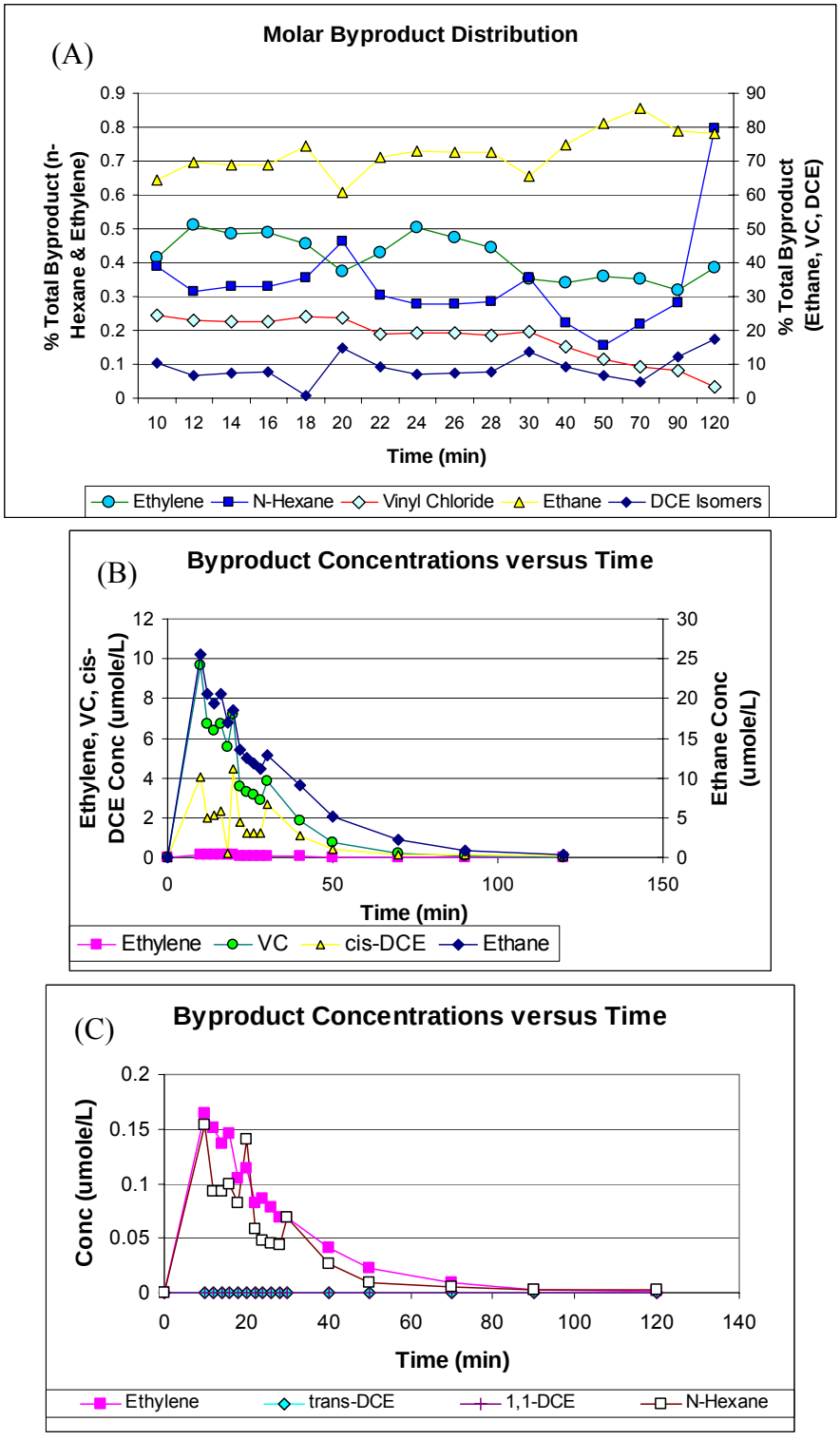

Figure B.16B Experiment #16 – pH = 11, [HCOOH*] = 4 mM, $[TCE]_0$ = 25 ppm cont.
(A) Molar Byproduct Distribution vs. Time [measured at the effluent]
(B) Ethane, Ethylene, VC Conc. vs. Time [measured at the effluent]
(C) Ethylene, DCE, Hexane Conc. vs. Time [measured at the effluent]

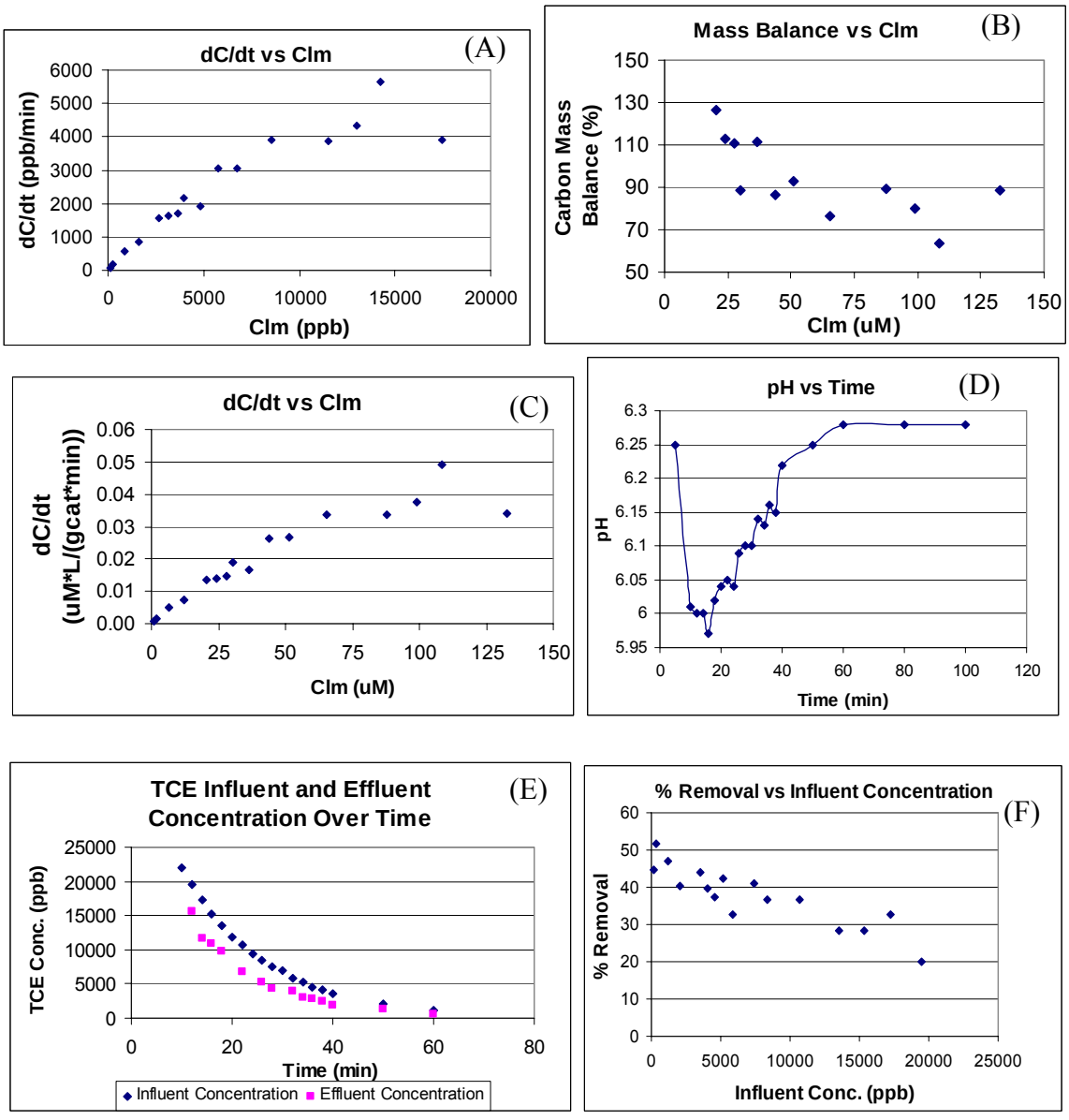

Figure B.17A Experiment #17 – pH = 4, [HCOOH*] = 0.5 mM, $[TCE]_0$ = 45 ppm
(A) Degradation Rate vs. Clm (B) Carbon Mass Balance vs. Clm
(C) Degradation Rate vs. Clm normalized (D) pH vs. Time [measured at the effluent]
(E) Influent and Effluent TCE conc. vs. Time
(F) % Removal vs. Influent conc.

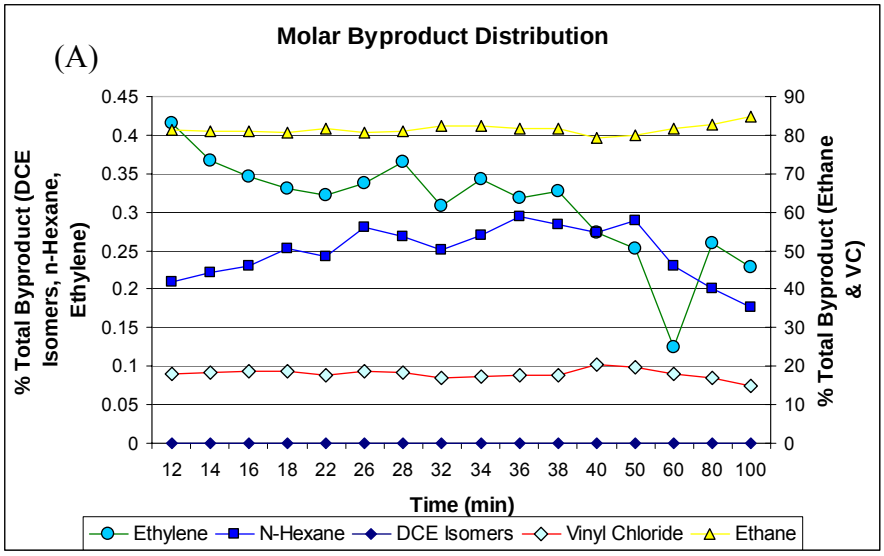

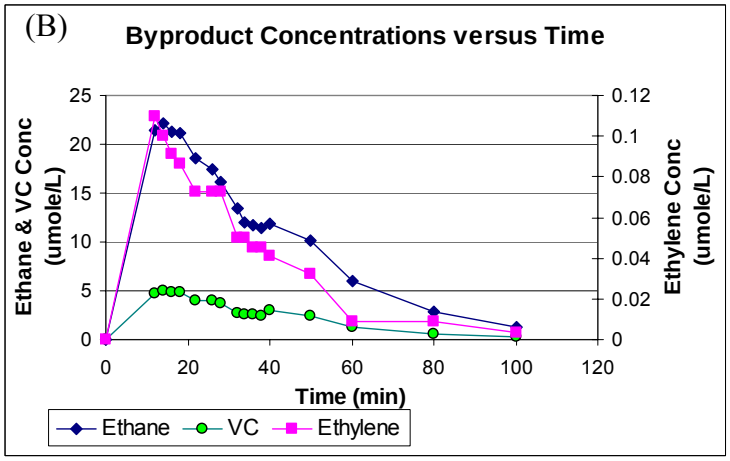

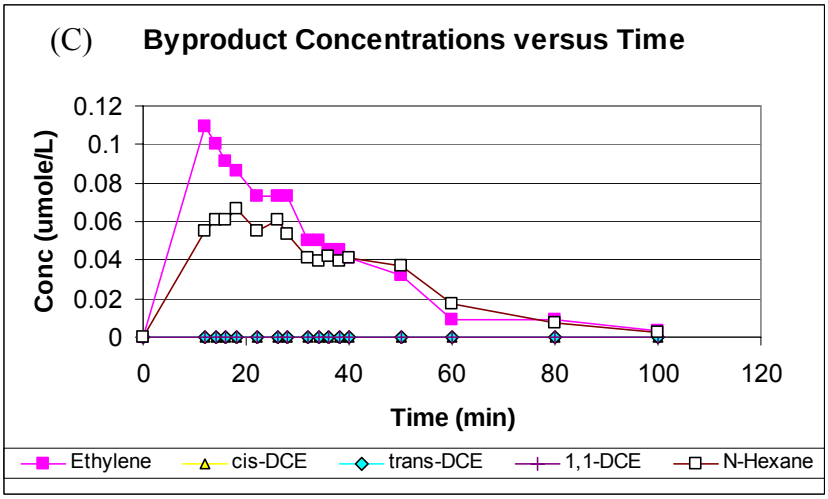

Figure B.17B Experiment #17 – pH = 4, [HCOOH*] = 0.5 mM, $[TCE]_0$ = 45 ppm cont.
(A) Molar Byproduct Distribution vs. Time [measured at the effluent]
(B) Ethane, Ethylene, VC Conc. vs. Time [measured at the effluent]
(C) Ethylene, DCE, Hexane Conc. vs. Time [measured at the effluent]

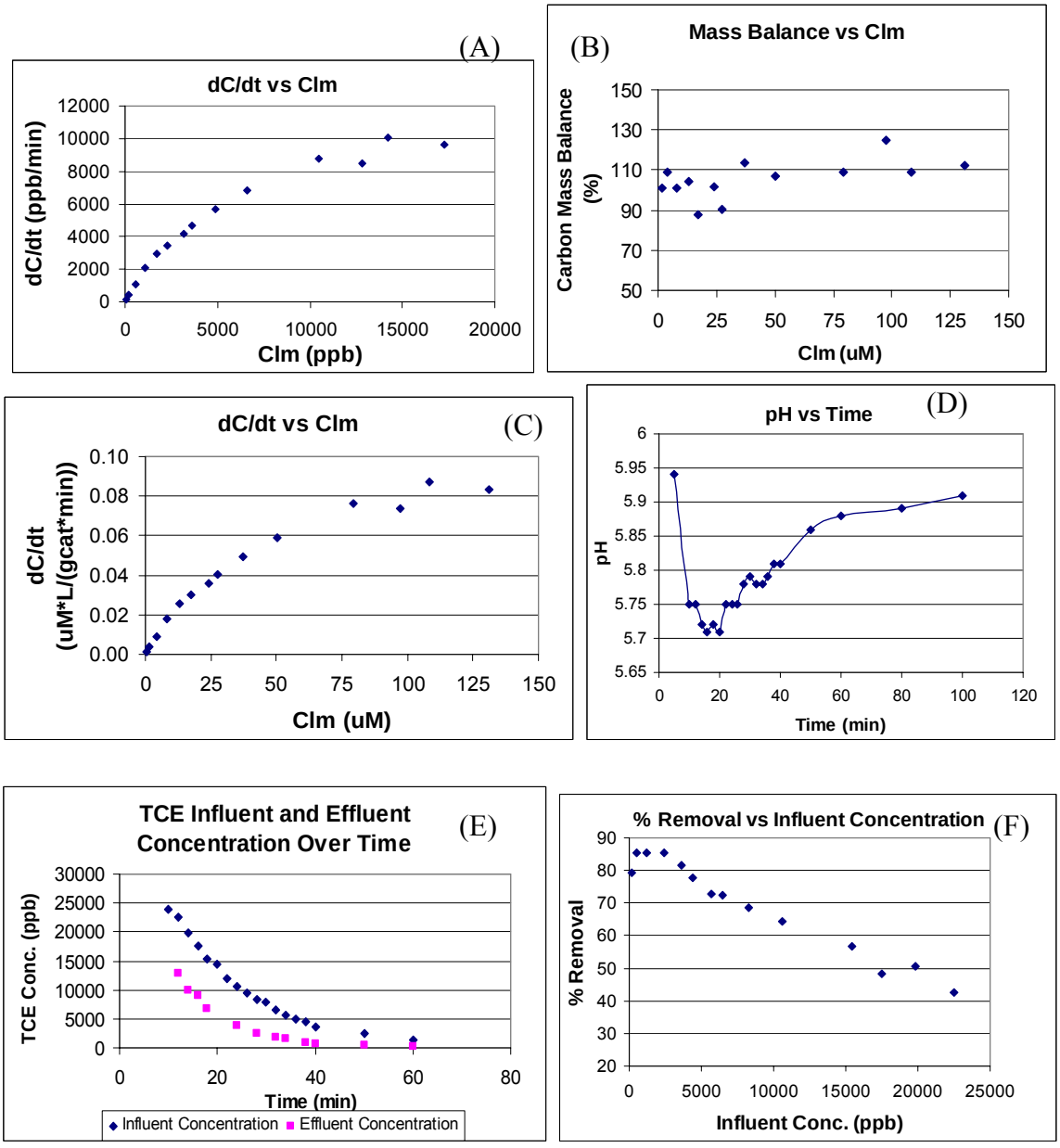

Figure B.18A Experiment #18 – pH = 4, [HCOOH*] = 1 mM, $[TCE]_0$ = 45 ppm
(A) Degradation Rate vs. Clm (B) Carbon Mass Balance vs. Clm
(C) Degradation Rate vs. Clm normalized (D) pH vs. Time [measured at the effluent]
(E) Influent and Effluent TCE conc. vs. Time
(F) % Removal vs. Influent conc.

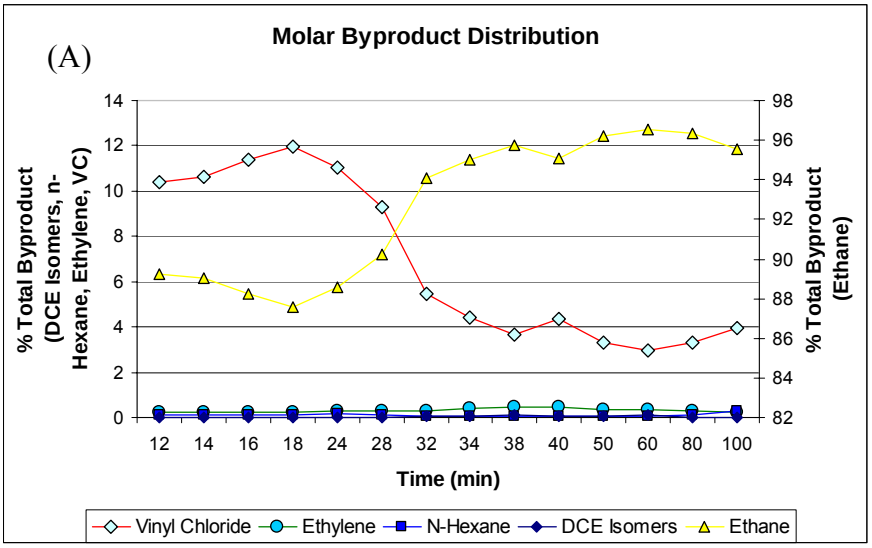

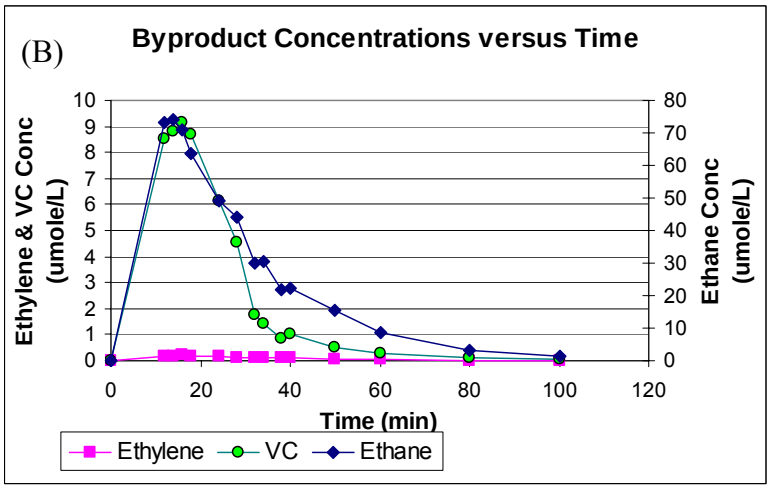

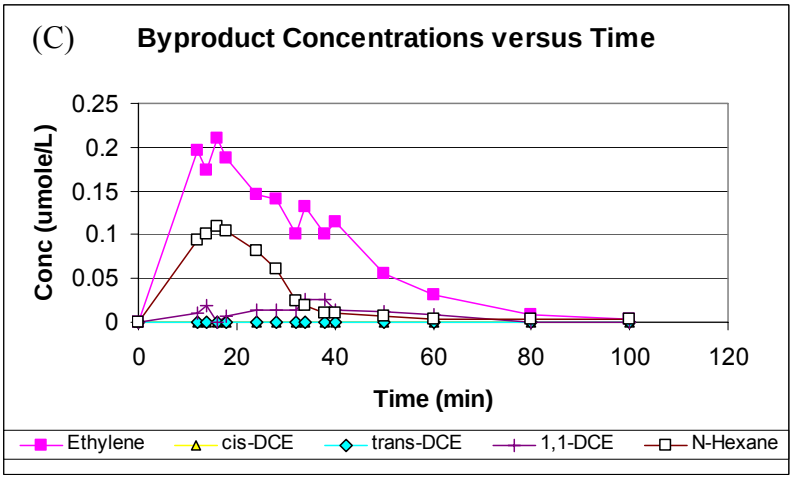

Figure B.18B Experiment #18 – pH = 4, [HCOOH*] = 1 mM, $[TCE]_0$ = 45 ppm cont.
(A) Molar Byproduct Distribution vs. Time [measured at the effluent]
(B) Ethane, Ethylene, VC Conc. vs. Time [measured at the effluent]
(C) Ethylene, DCE, Hexane Conc. vs. Time [measured at the effluent]

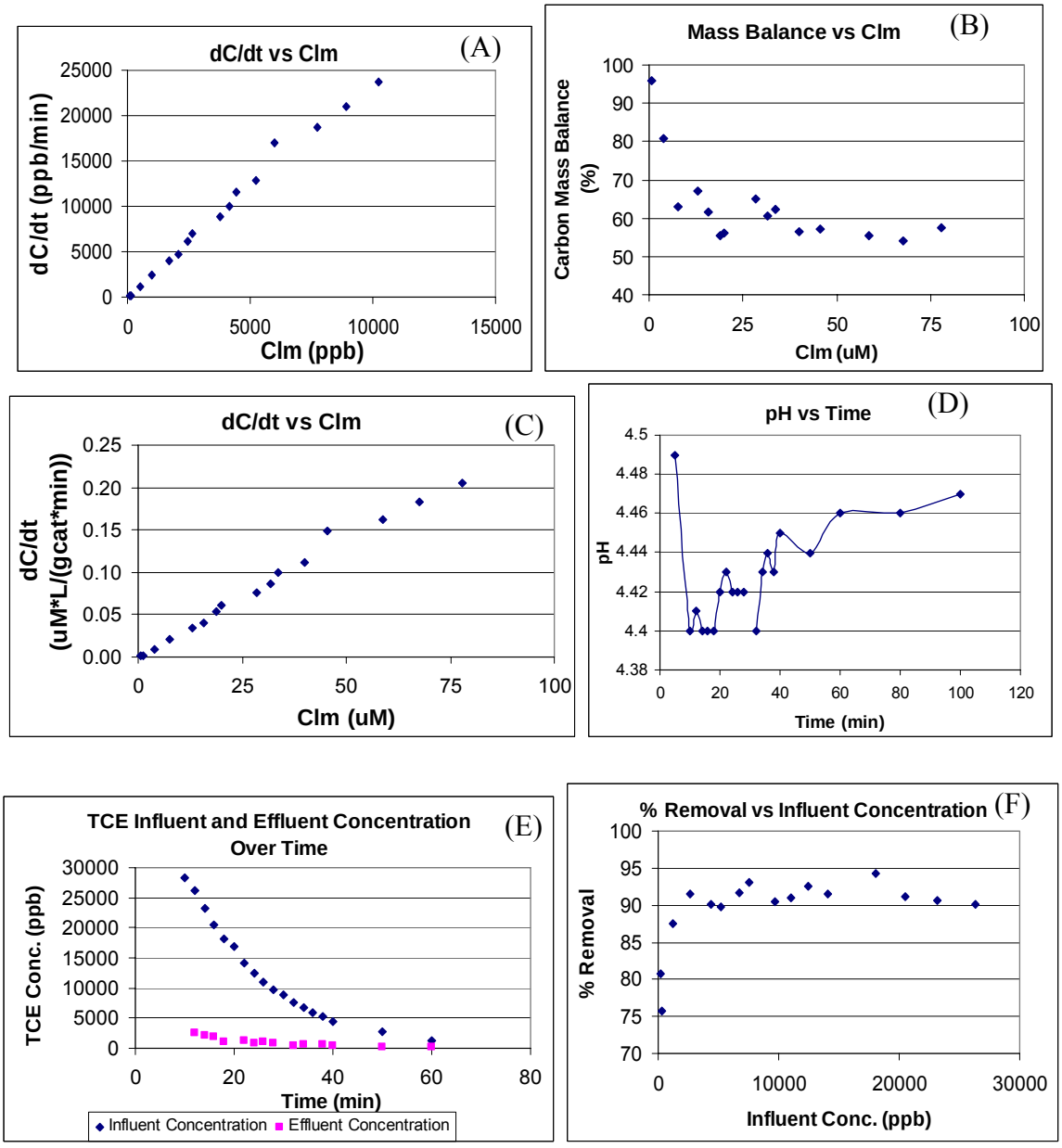

Figure B.19A Experiment #19 – pH = 4, [HCOOH*] = 10 mM, $[TCE]_0$ = 45 ppm
(A) Degradation Rate vs. Clm (B) Carbon Mass Balance vs. Clm
(C) Degradation Rate vs. Clm normalized (D) pH vs. Time [measured at the effluent]
(E) Influent and Effluent TCE conc. vs. Time
(F) % Removal vs. Influent conc.

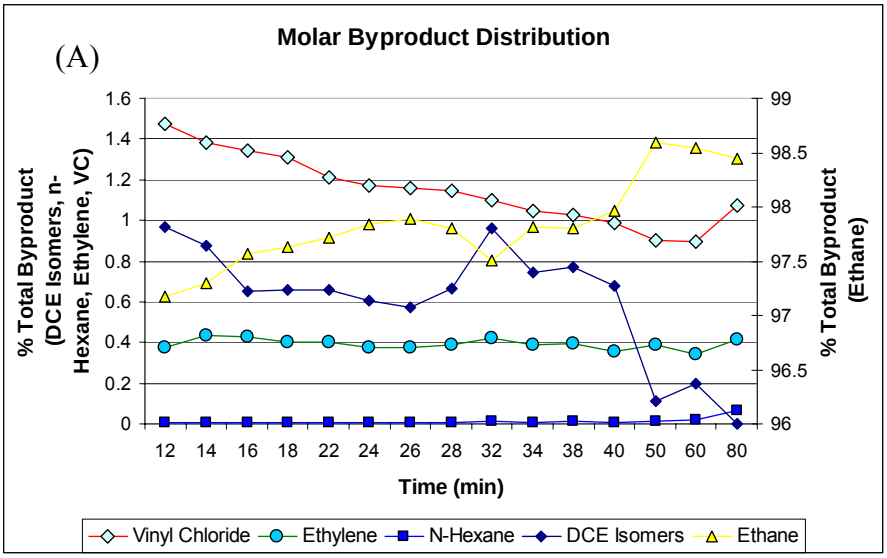

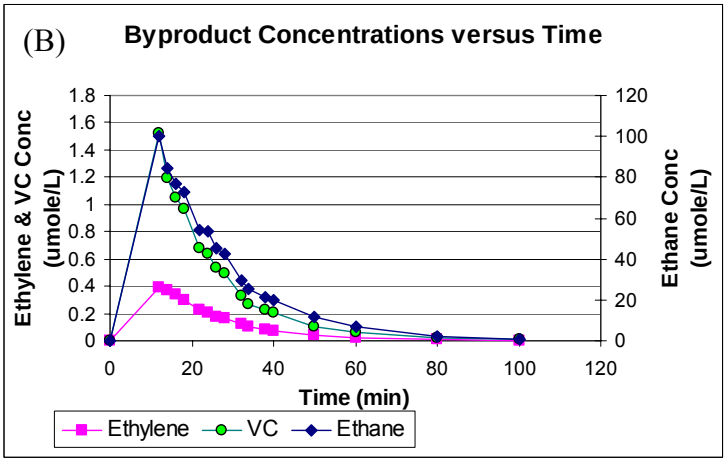

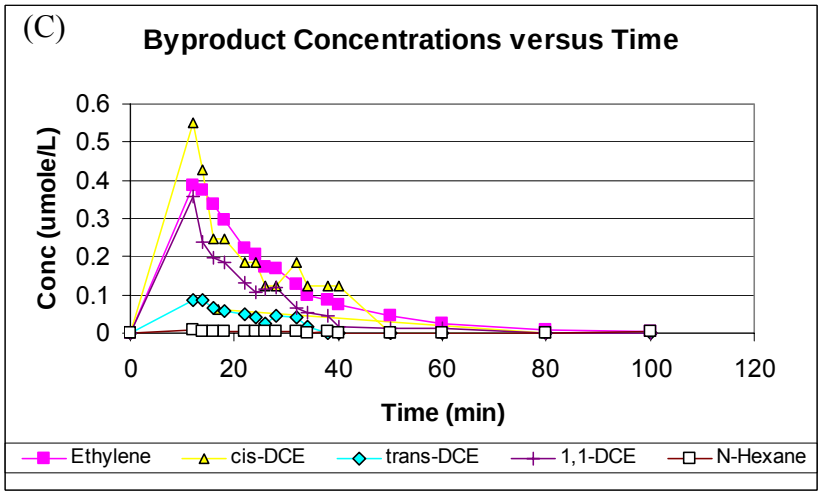

Figure B.19B Experiment #19 – pH = 4, [HCOOH*] = 10 mM, $[TCE]_0$ = 45 ppm cont.
(A) Molar Byproduct Distribution vs. Time [measured at the effluent]
(B) Ethane, Ethylene, VC Conc. vs. Time [measured at the effluent]
(C) Ethylene, DCE, Hexane Conc. vs. Time [measured at the effluent]

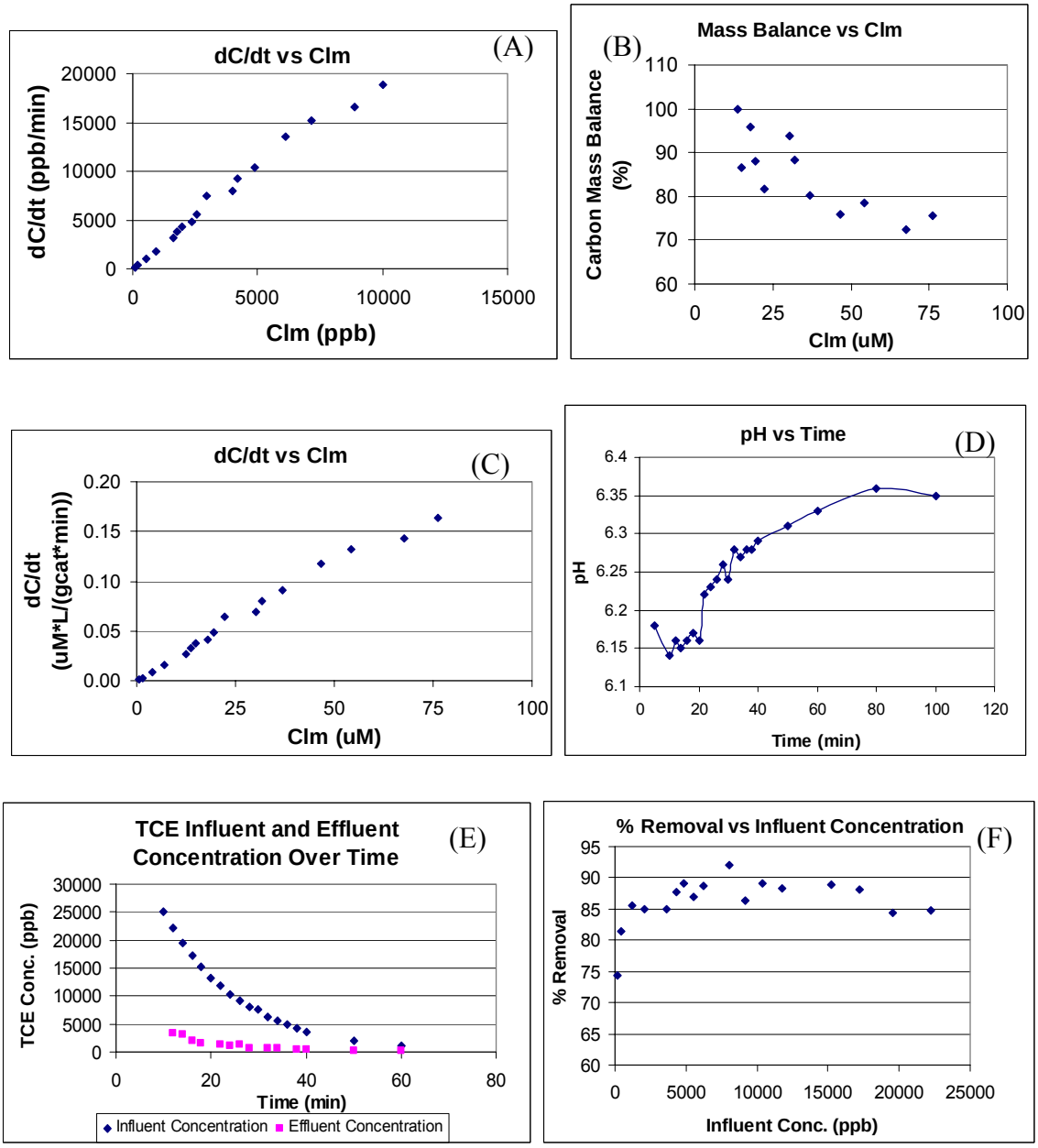

Figure B.20A Experiment #20 – pH = 5, [HCOOH*] = 10 mM, $[TCE]_0$ = 45 ppm
(A) Degradation Rate vs. Clm (B) Carbon Mass Balance vs. Clm
(C) Degradation Rate vs. Clm normalized (D) pH vs. Time [measured at the effluent]
(E) Influent and Effluent TCE conc. vs. Time
(F) % Removal vs. Influent conc.

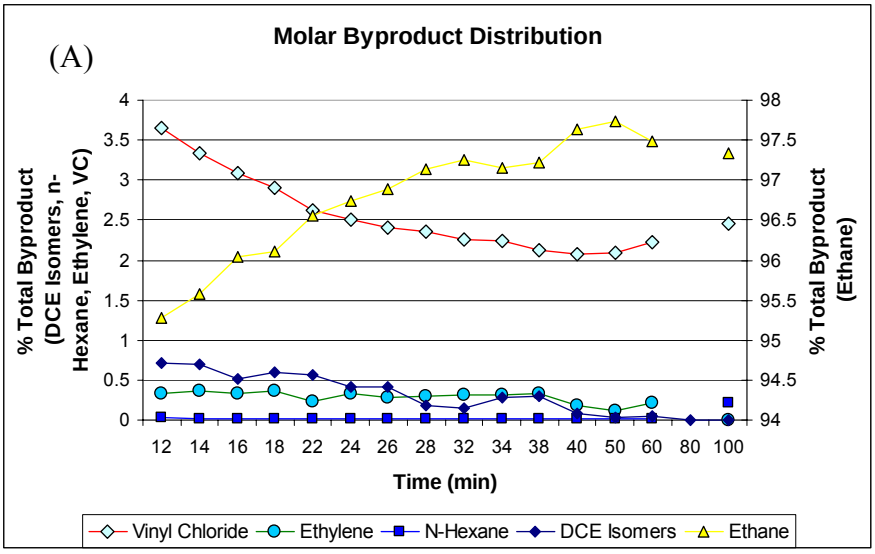

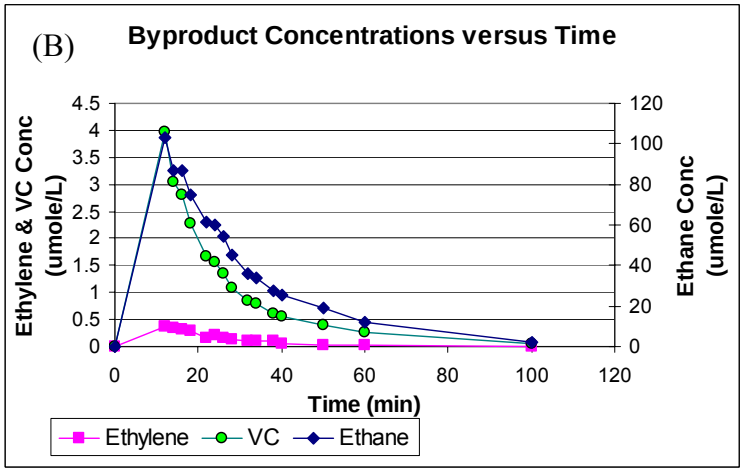

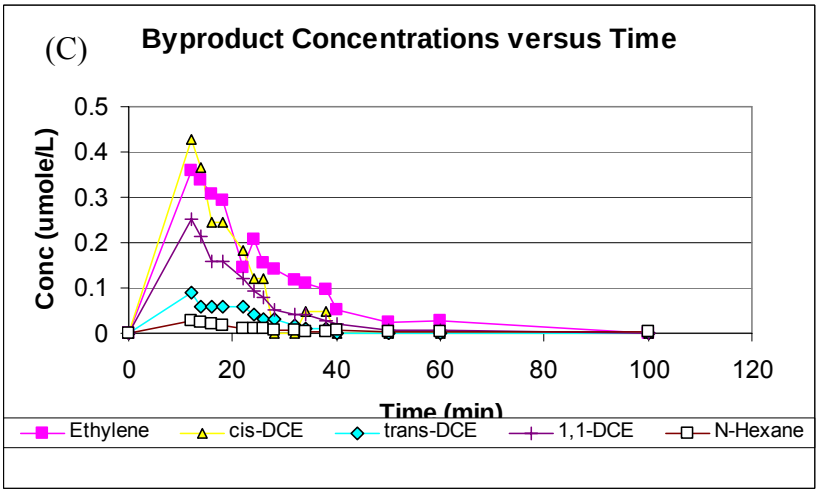

Figure B.20B Experiment #20 – pH = 5, [HCOOH*] = 10 mM, $[TCE]_0$ = 45 ppm cont.
(A) Molar Byproduct Distribution vs. Time [measured at the effluent]
(B) Ethane, Ethylene, VC Conc. vs. Time [measured at the effluent]
(C) Ethylene, DCE, Hexane Conc. vs. Time [measured at the effluent]

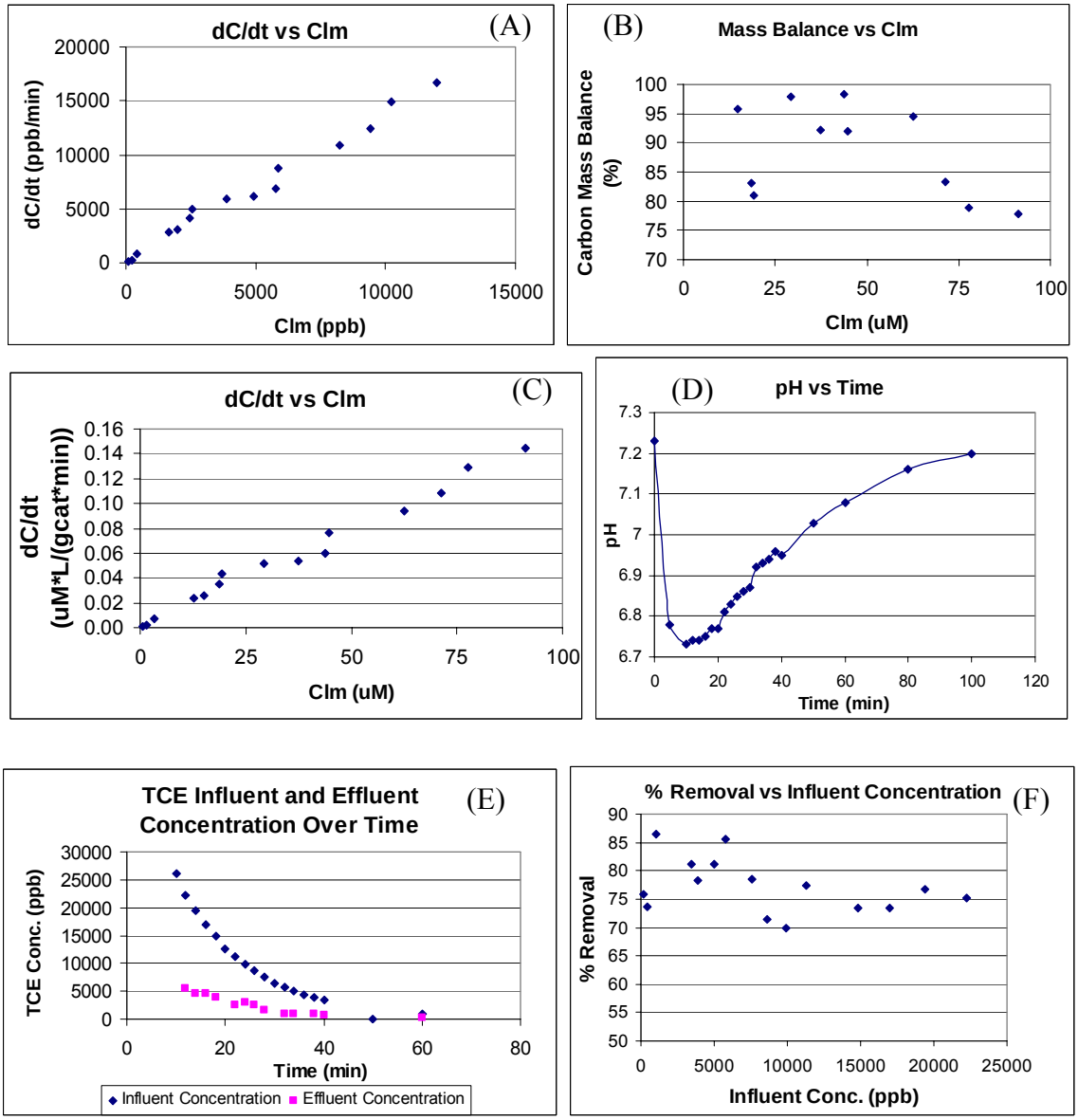

Figure B.21A Experiment #21 – pH = 6, [HCOOH*] = 10 mM, $[TCE]_0$ = 45 ppm
(A) Degradation Rate vs. Clm (B) Carbon Mass Balance vs. Clm
(C) Degradation Rate vs. Clm normalized (D) pH vs. Time [measured at the effluent]
(E) Influent and Effluent TCE conc. vs. Time
(F) % Removal vs. Influent conc.

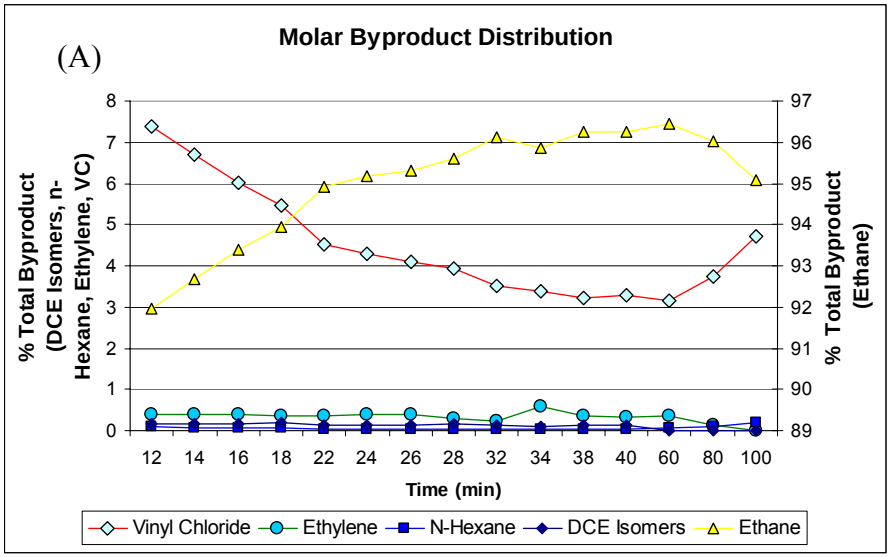

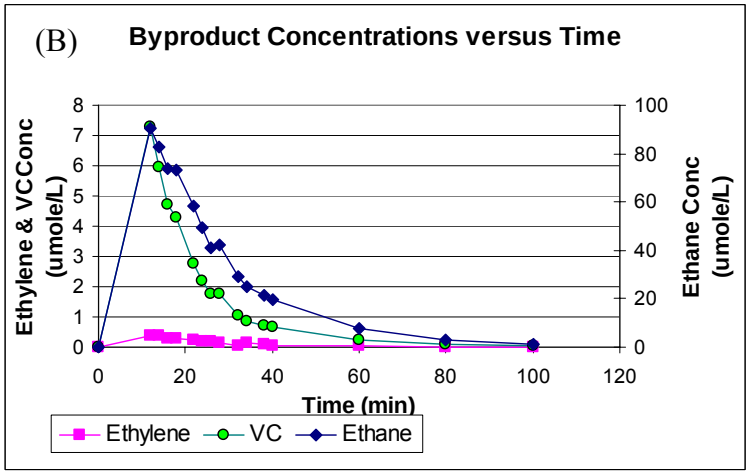

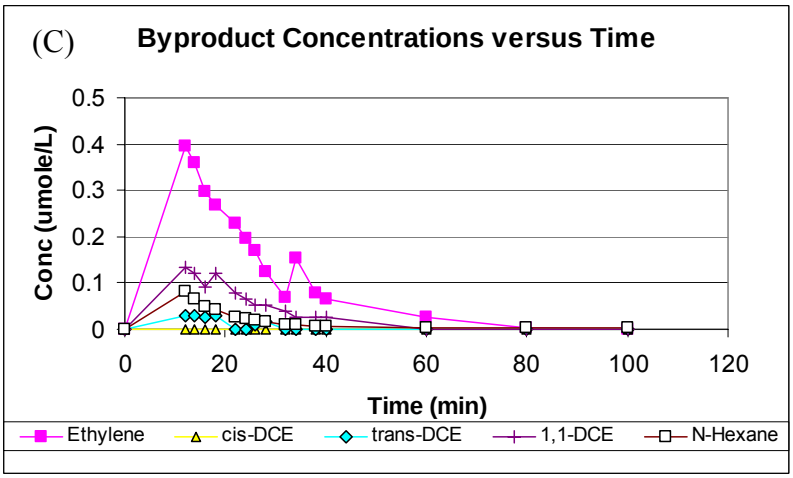

Figure B.21B Experiment #21 – pH = 6, [HCOOH*] = 10 mM, $[TCE]_0$ = 45 ppm cont.
(A) Molar Byproduct Distribution vs. Time [measured at the effluent]
(B) Ethane, Ethylene, VC Conc. vs. Time [measured at the effluent]
(C) Ethylene, DCE, Hexane Conc. vs. Time [measured at the effluent]

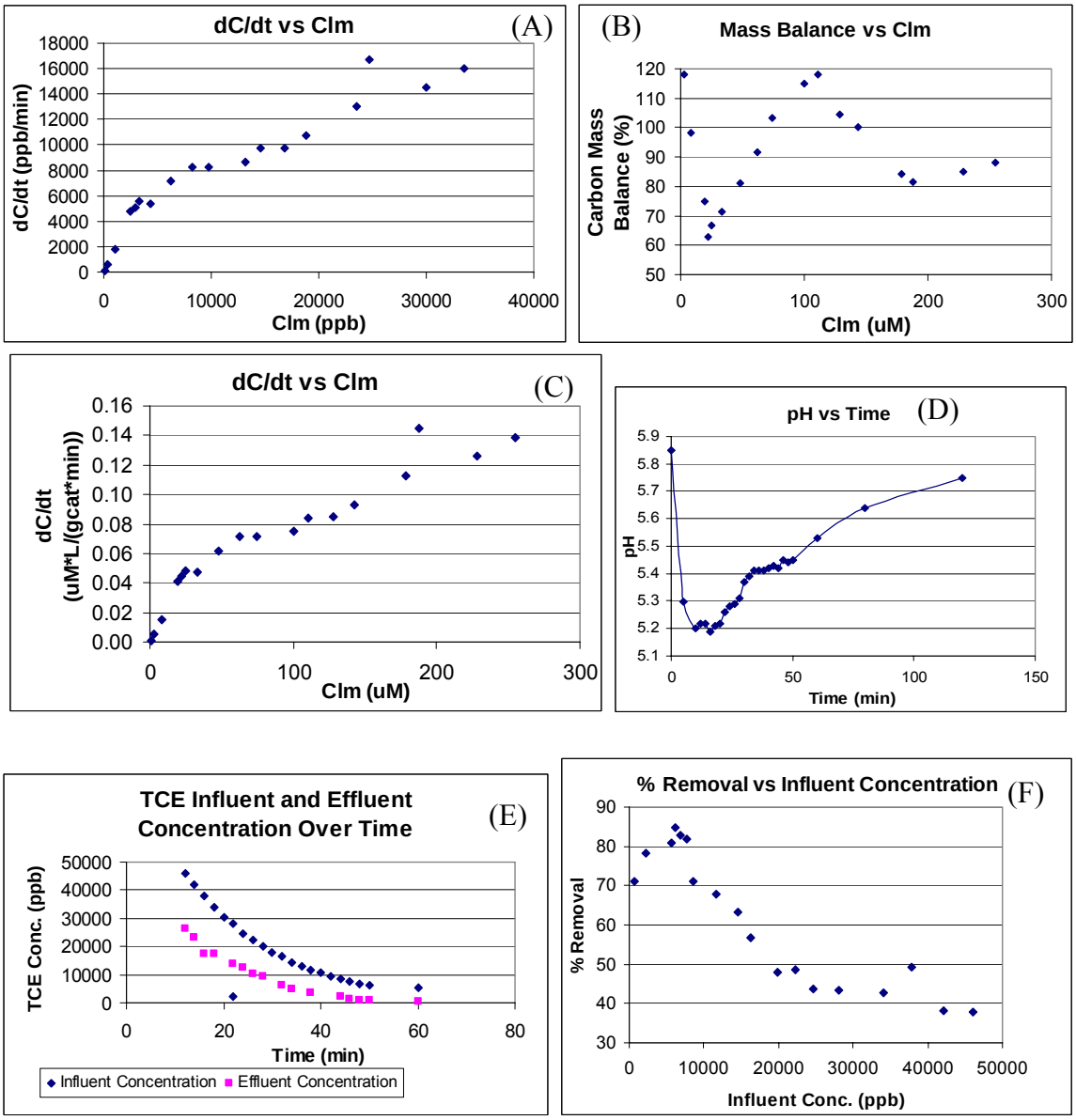

Figure B.22A Experiment #22 – pH = 4, [HCOOH*] = 1 mM, $[TCE]_0$ = 91.4 ppm
(A) Degradation Rate vs. Clm (B) Carbon Mass Balance vs. Clm
(C) Degradation Rate vs. Clm normalized (D) pH vs. Time [measured at the effluent]
(E) Influent and Effluent TCE conc. vs. Time
(F) % Removal vs. Influent conc.

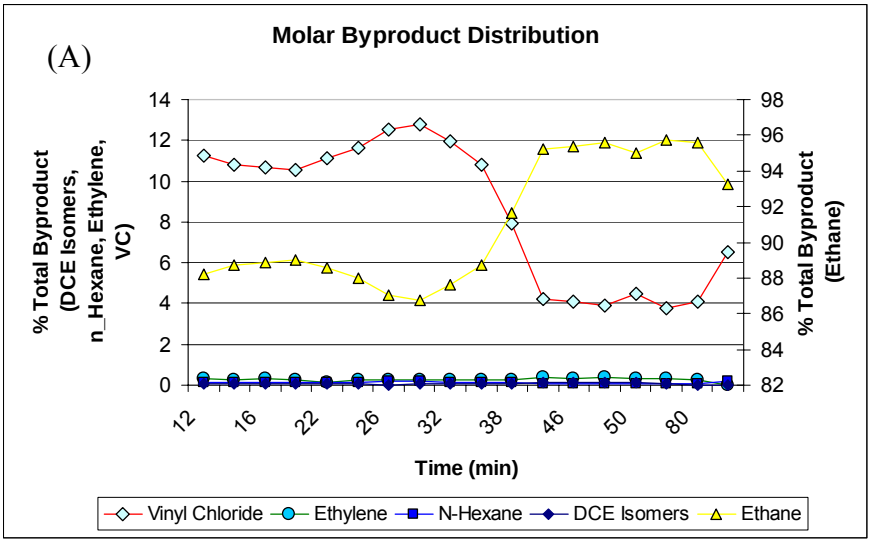

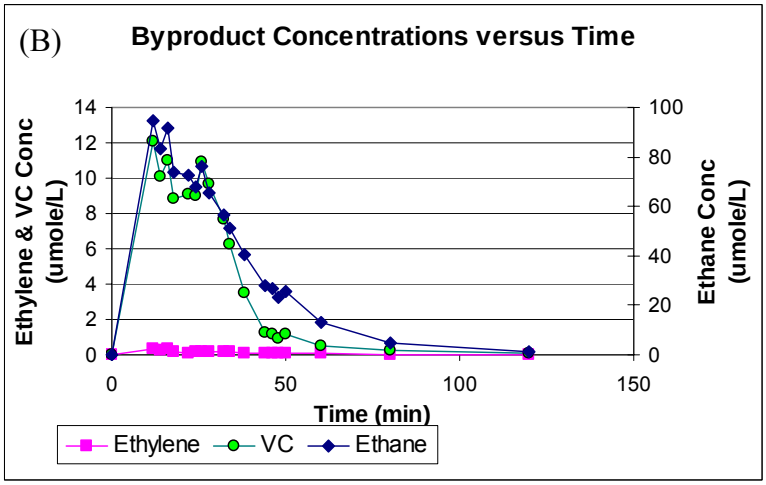

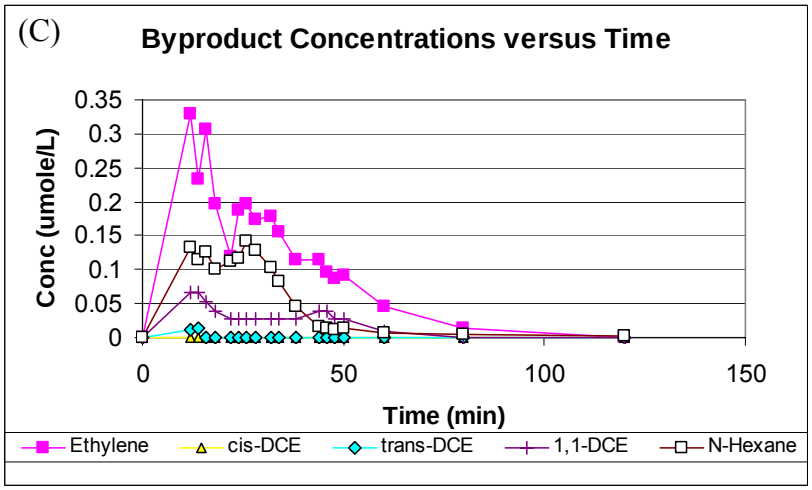

Figure B.22B Experiment #22 – pH = 4, [HCOOH*] = 1 mM, $[TCE]_0$ = 91.4 ppm cont.
(A) Molar Byproduct Distribution vs. Time [measured at the effluent]
(B) Ethane, Ethylene, VC Conc. vs. Time [measured at the effluent]
(C) Ethylene, DCE, Hexane Conc. vs. Time [measured at the effluent]

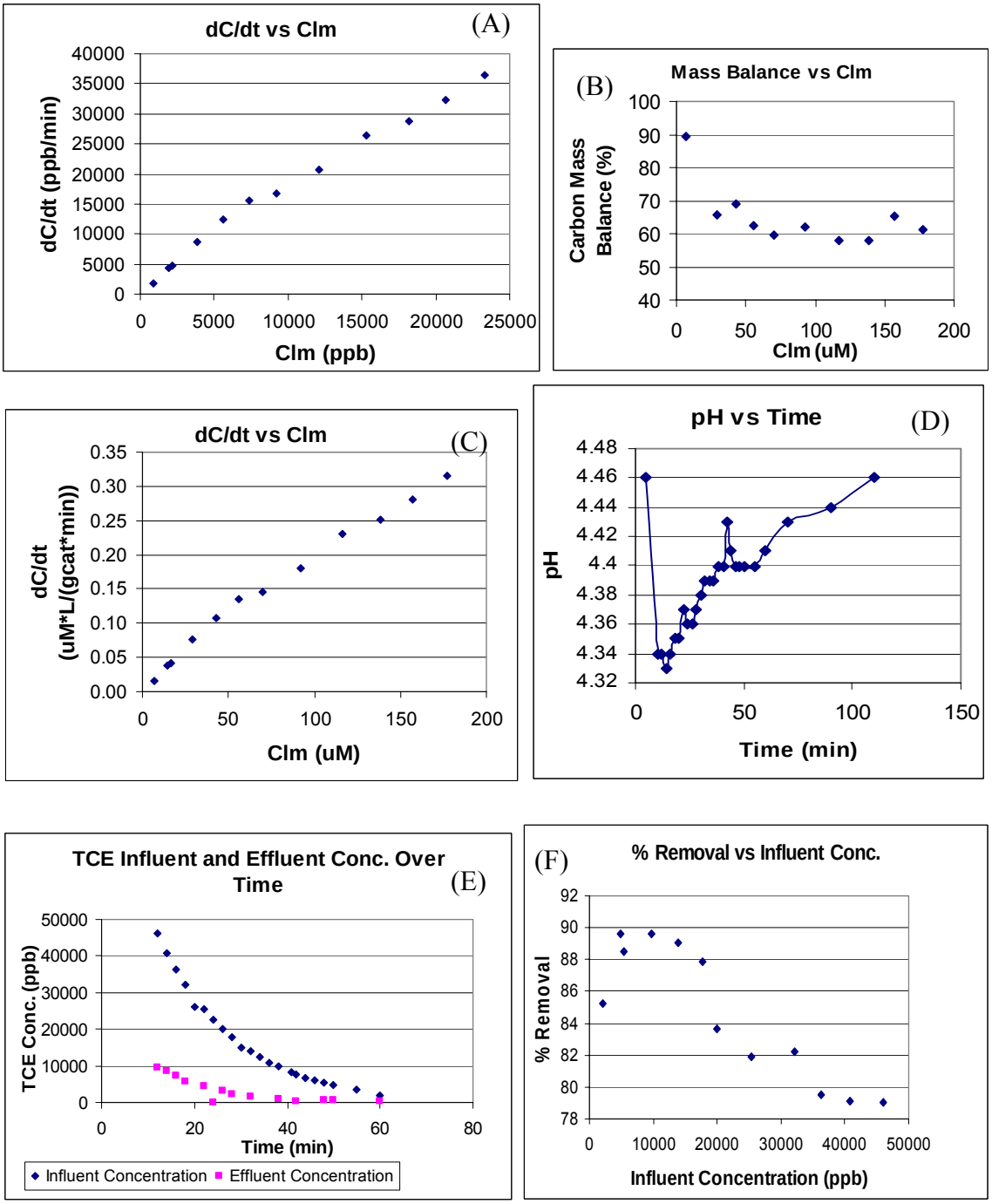

Figure B.23A Experiment #23 – pH = 4, [HCOOH*] = 10 mM, $[TCE]_0$ = 91.4 ppm
(A) Degradation Rate vs. Clm (B) Carbon Mass Balance vs. Clm
(C) Degradation Rate vs. Clm normalized (D) pH vs. Time [measured at the effluent]
(E) Influent and Effluent TCE conc. vs. Time
(F) % Removal vs. Influent conc.

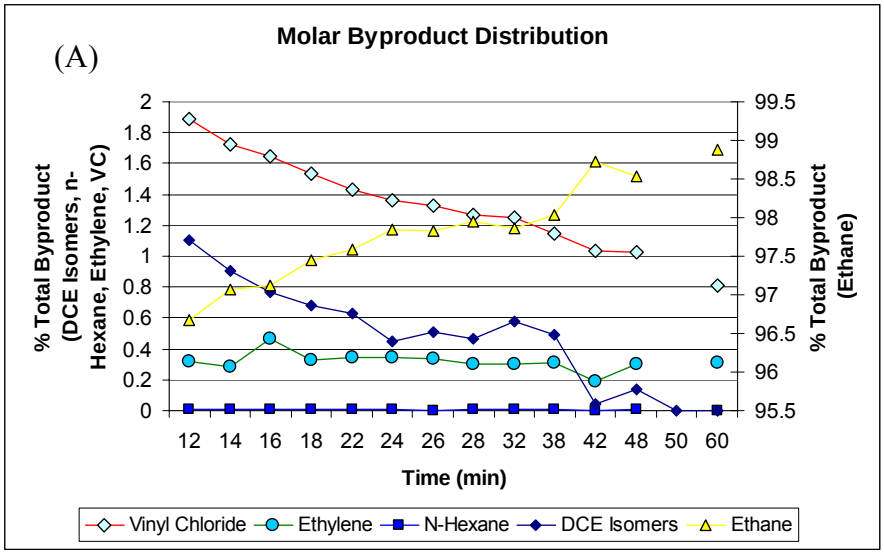

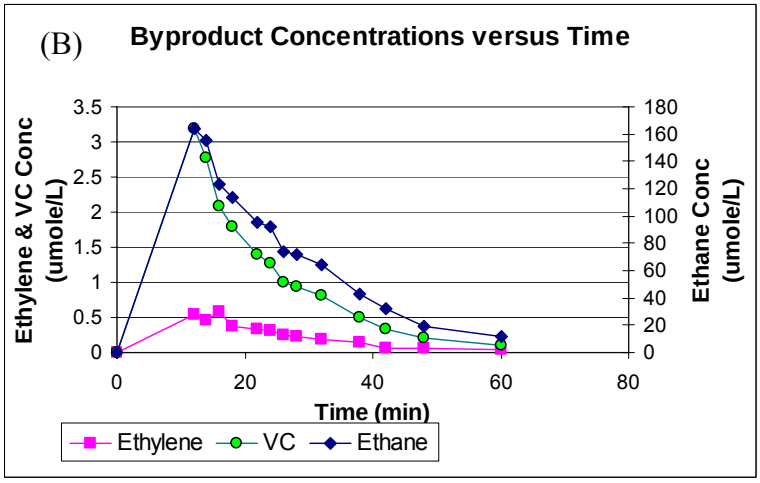

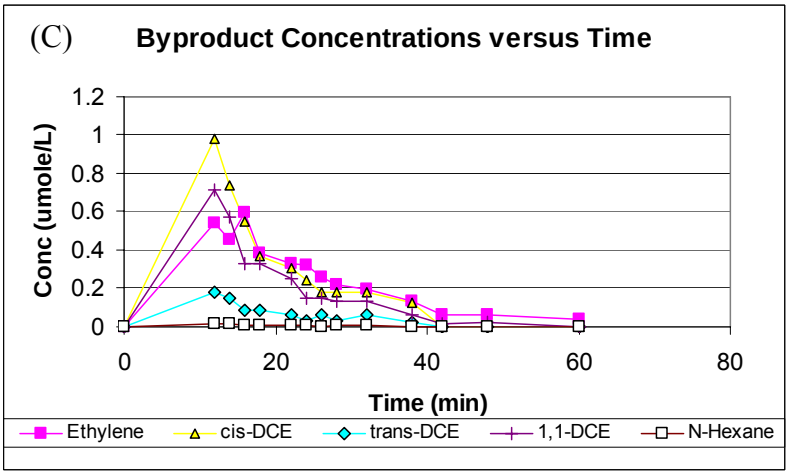

Figure B.23B Experiment #23 – pH = 4, [HCOOH*] = 10 mM, $[TCE]_0$ = 91.4 ppm cont.
(A) Molar Byproduct Distribution vs. Time [measured at the effluent]
(B) Ethane, Ethylene, VC Conc. vs. Time [measured at the effluent]
(C) Ethylene, DCE, Hexane Conc. vs. Time [measured at the effluent]

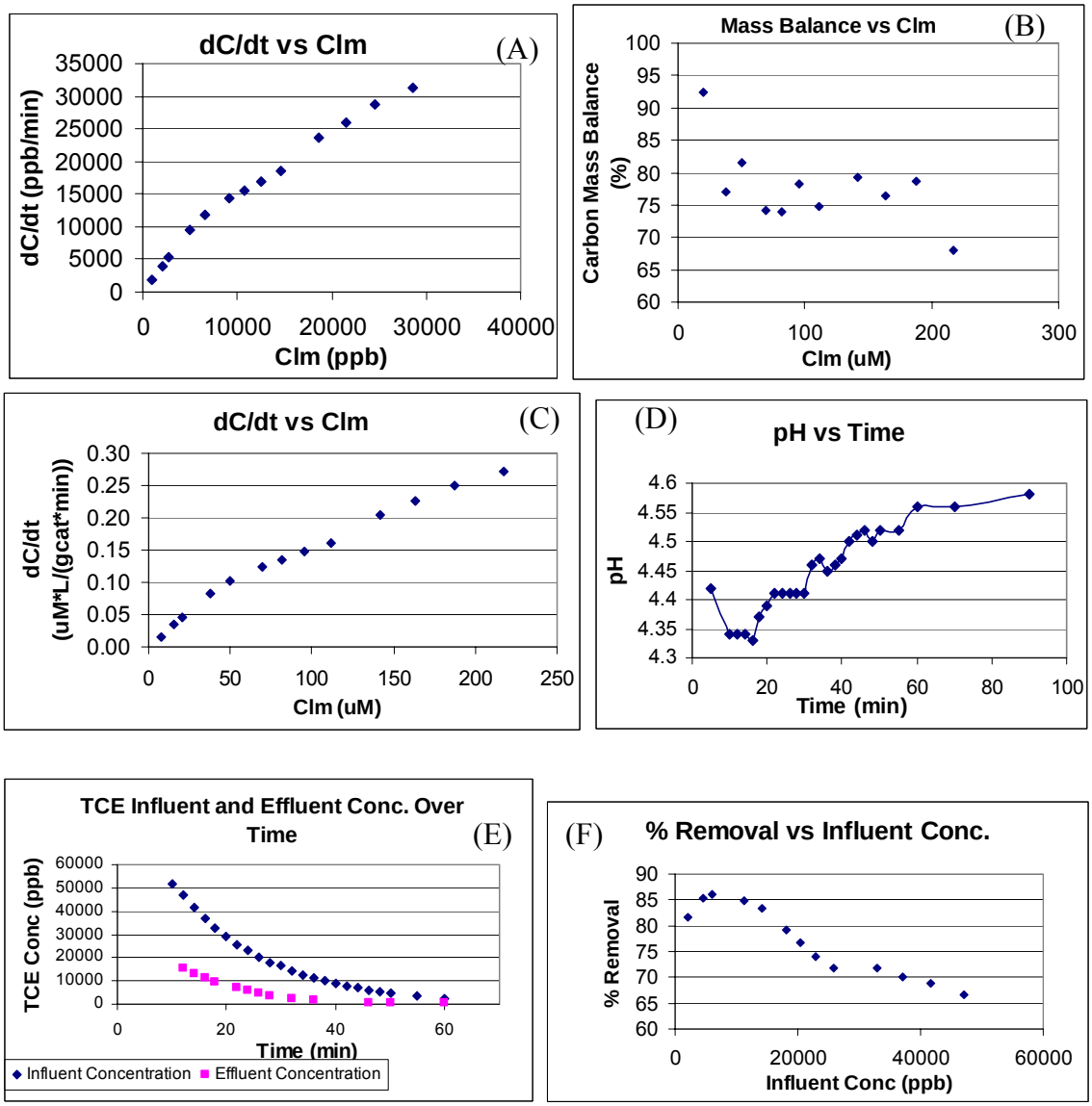

Figure B.24A Experiment #24 – pH = 4, [HCOOH*] = 4 mM, $[TCE]_0$ = 91.4 ppm
(A) Degradation Rate vs. Clm (B) Carbon Mass Balance vs. Clm
(C) Degradation Rate vs. Clm normalized (D) pH vs. Time [measured at the effluent]
(E) Influent and Effluent TCE conc. vs. Time
(F) % Removal vs. Influent conc.

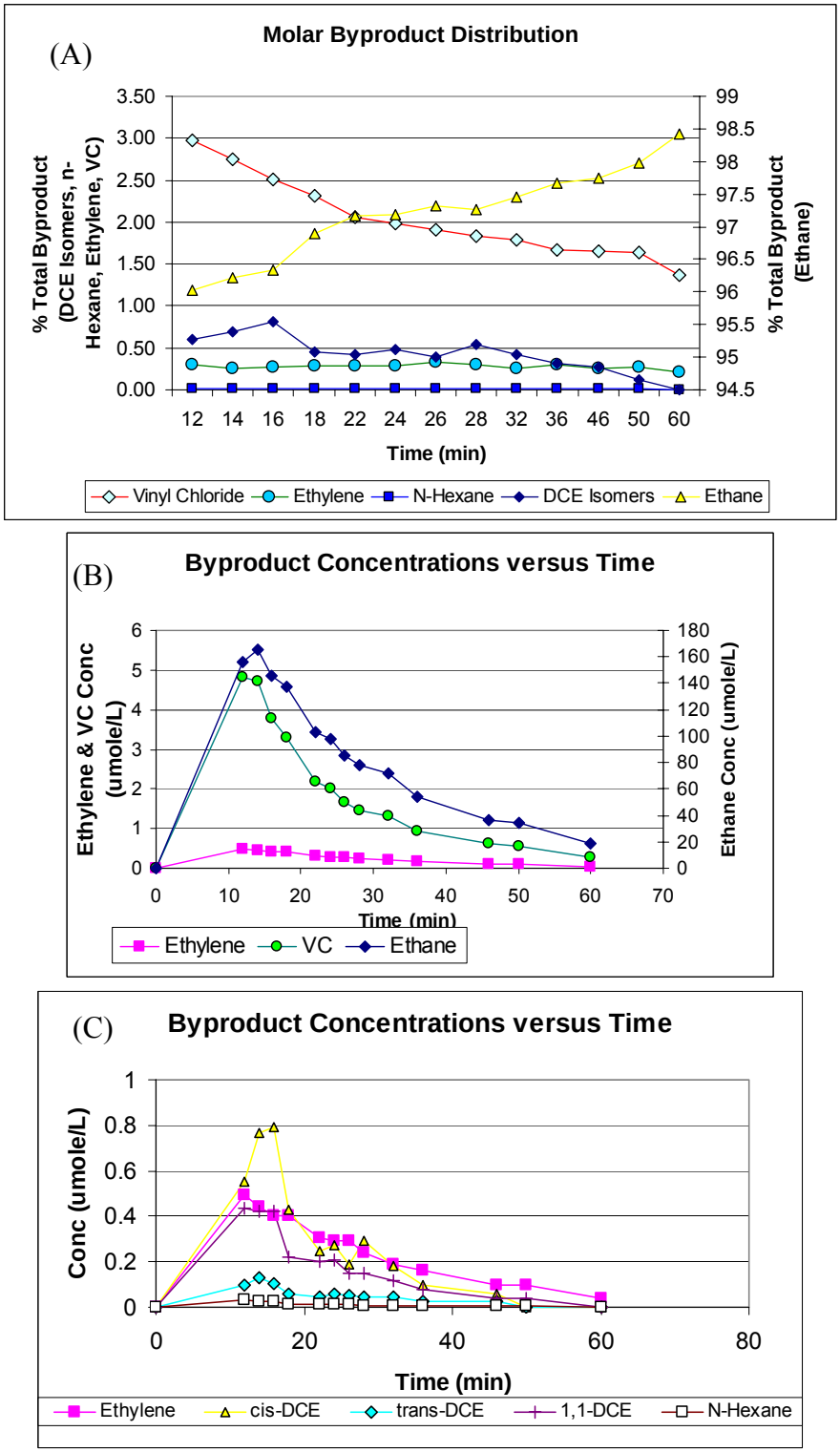

Figure B.24B Experiment #24 – pH = 4, [HCOOH*] = 4 mM, $[TCE]_0$ = 91.4 ppm cont.
(A) Molar Byproduct Distribution vs. Time [measured at the effluent]
(B) Ethane, Ethylene, VC Conc. vs. Time [measured at the effluent]
(C) Ethylene, DCE, Hexane Conc. vs. Time [measured at the effluent]

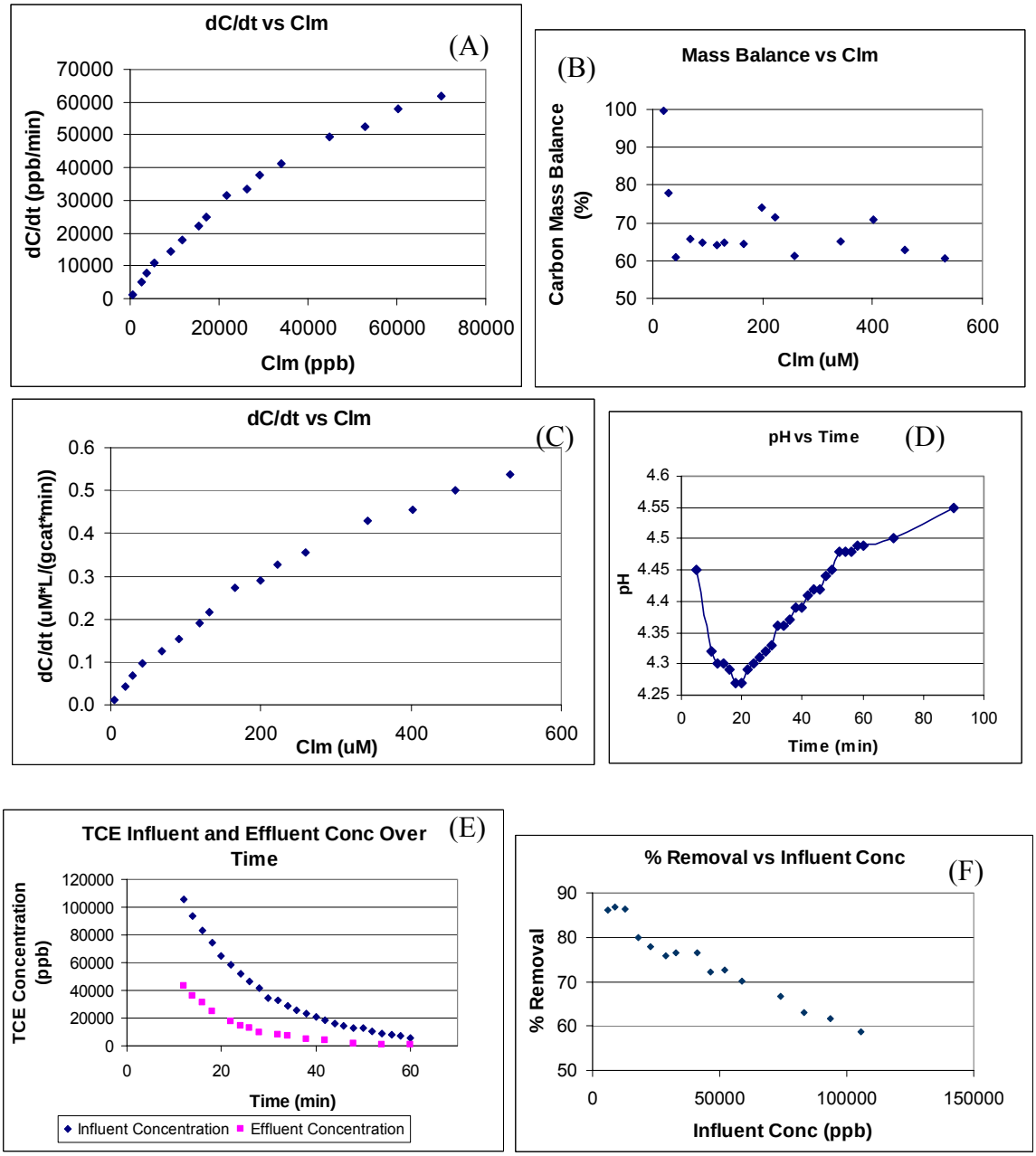

Figure B.25A Experiment #25 – pH = 4, [HCOOH*] = 4 mM, $[TCE]_0$ = 182.9 ppm
(A) Degradation Rate vs. Clm (B) Carbon Mass Balance vs. Clm
(C) Degradation Rate vs. Clm normalized (D) pH vs. Time [measured at the effluent]
(E) Influent and Effluent TCE conc. vs. Time
(F) % Removal vs. Influent conc.

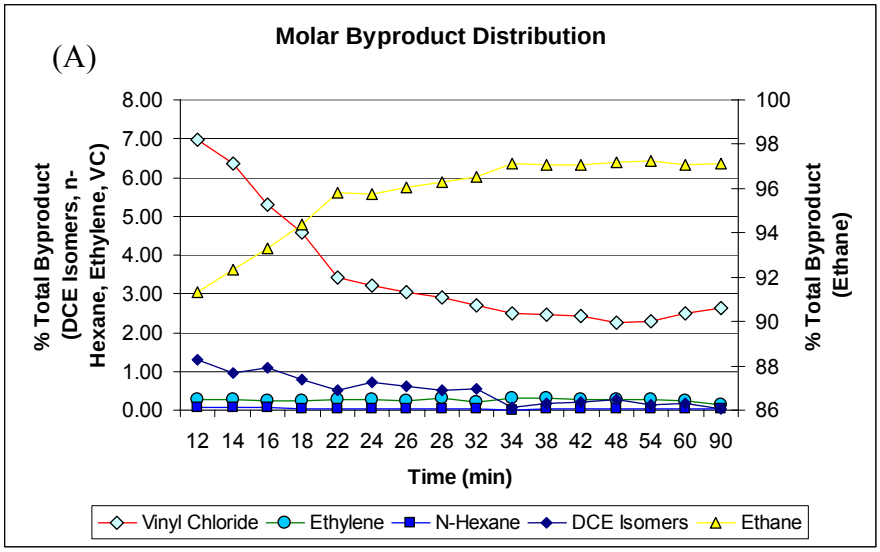

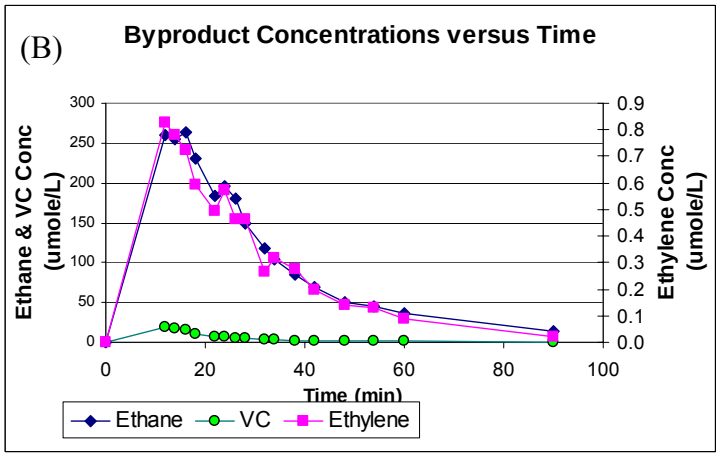

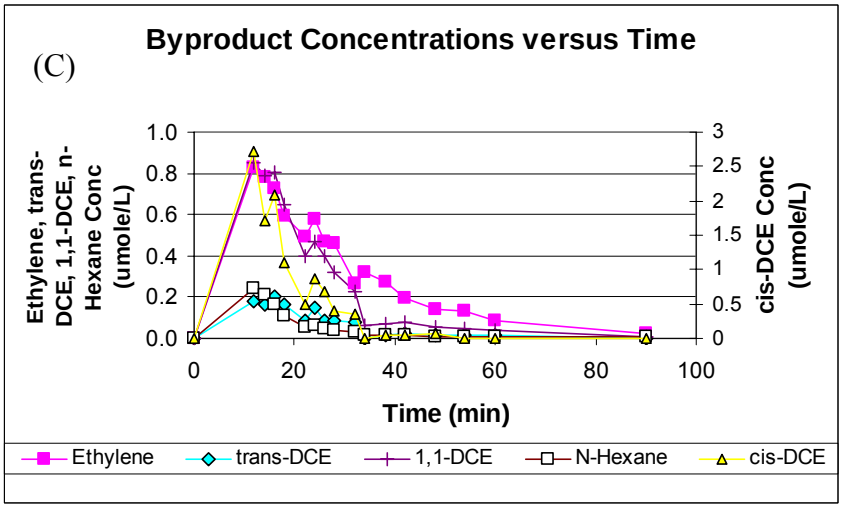

Figure B.25B Experiment #25 – pH = 4, [HCOOH*] = 4 mM, $[TCE]_0$ = 182.9 ppm cont.
(A) Molar Byproduct Distribution vs. Time [measured at the effluent]
(B) Ethane, Ethylene, VC Conc. vs. Time [measured at the effluent]
(C) Ethylene, DCE, Hexane Conc. vs. Time [measured at the effluent]

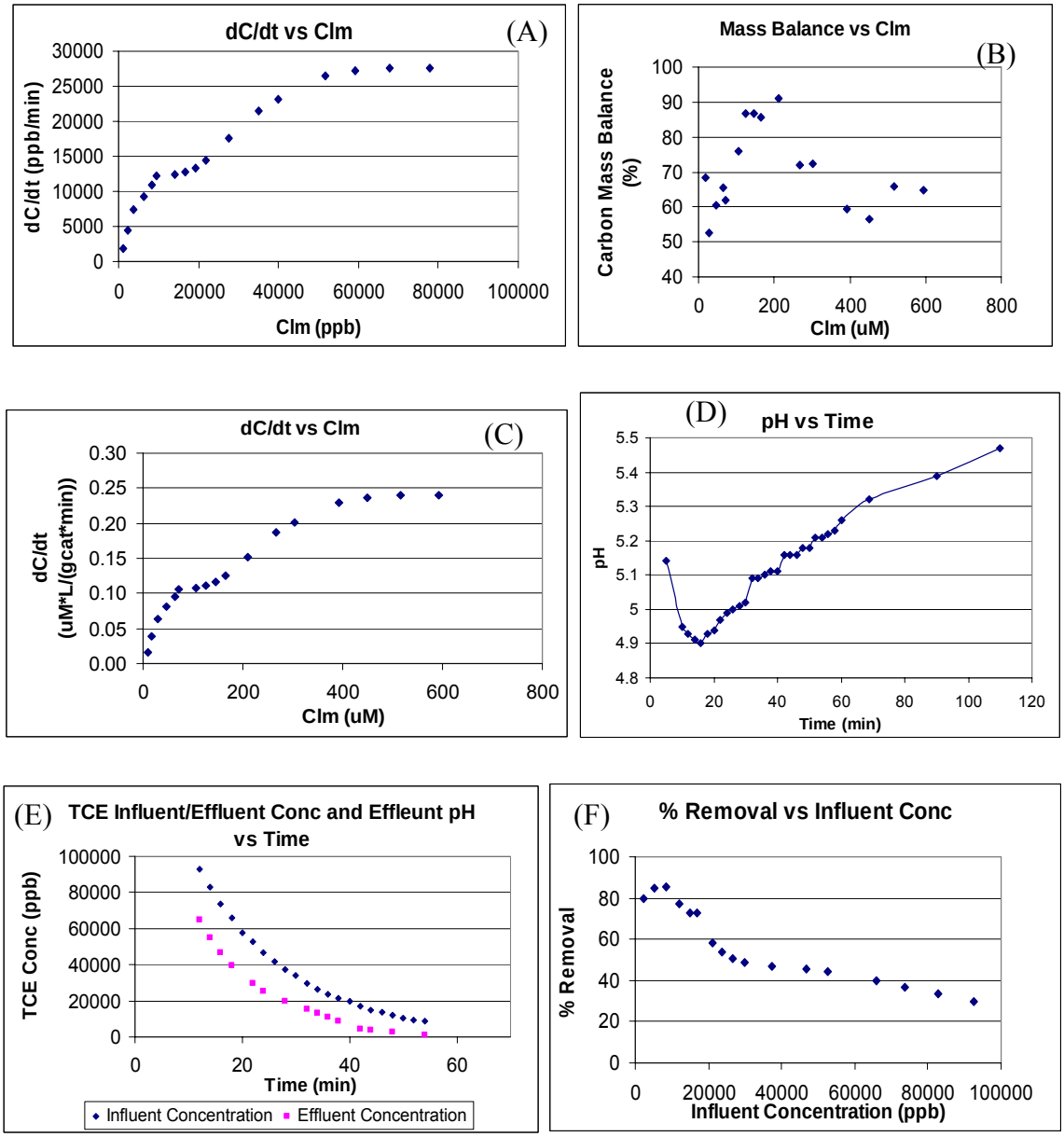

Figure B.26A Experiment #26 – pH = 4, [HCOOH*] = 1 mM, $[TCE]_0$ = 170 ppm
(A) Degradation Rate vs. Clm (B) Carbon Mass Balance vs. Clm
(C) Degradation Rate vs. Clm normalized (D) pH vs. Time [measured at the effluent]
(E) Influent and Effluent TCE conc. vs. Time
(F) % Removal vs. Influent conc.

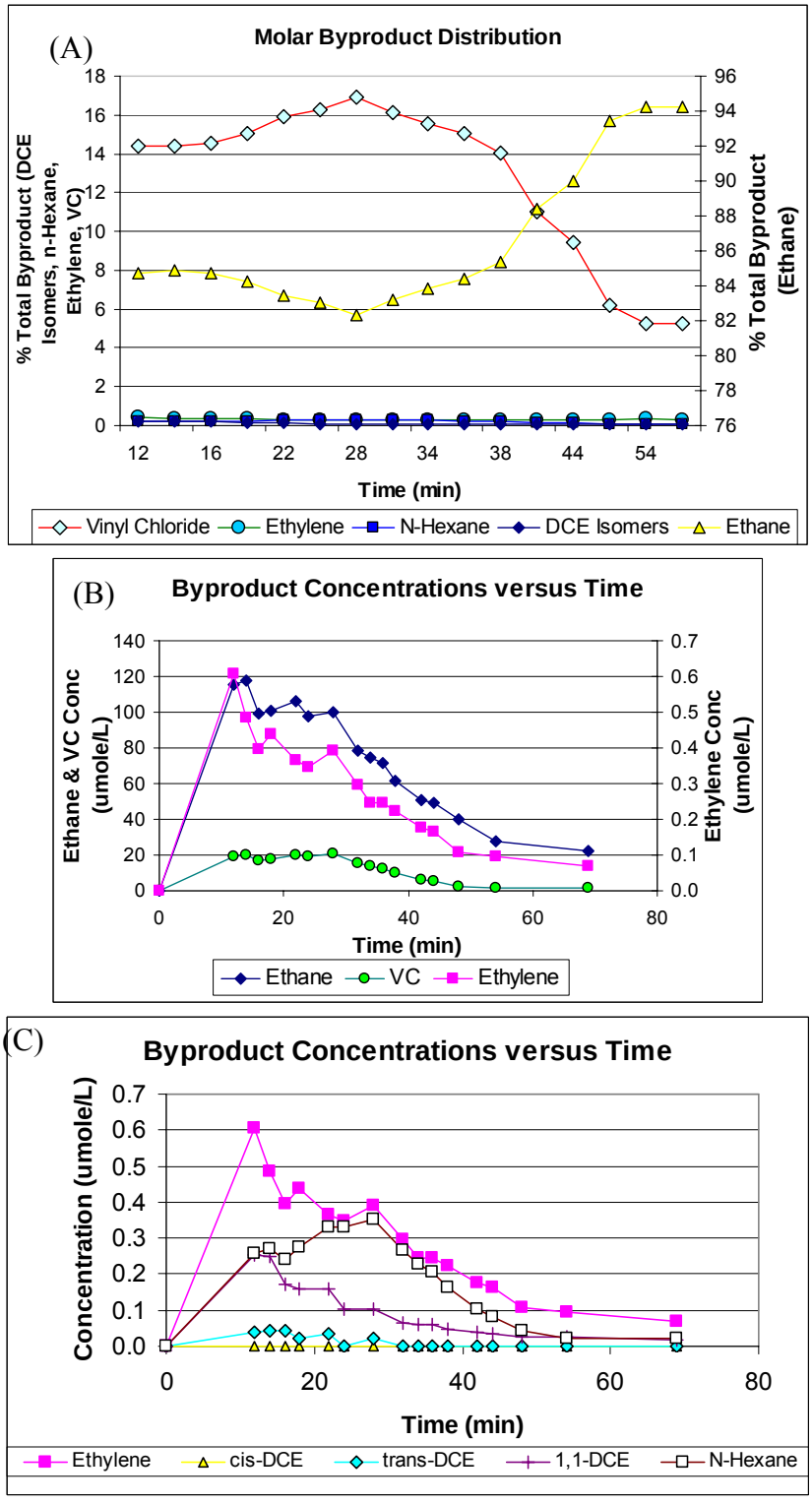

Figure B.26B Experiment #26 – pH = 4, [HCOOH*] = 1 mM, $[TCE]_0$ = 170 ppm cont.
(A) Molar Byproduct Distribution vs. Time [measured at the effluent]
(B) Ethane, Ethylene, VC Conc. vs. Time [measured at the effluent]
(C) Ethylene, DCE, Hexane Conc. vs. Time [measured at the effluent]

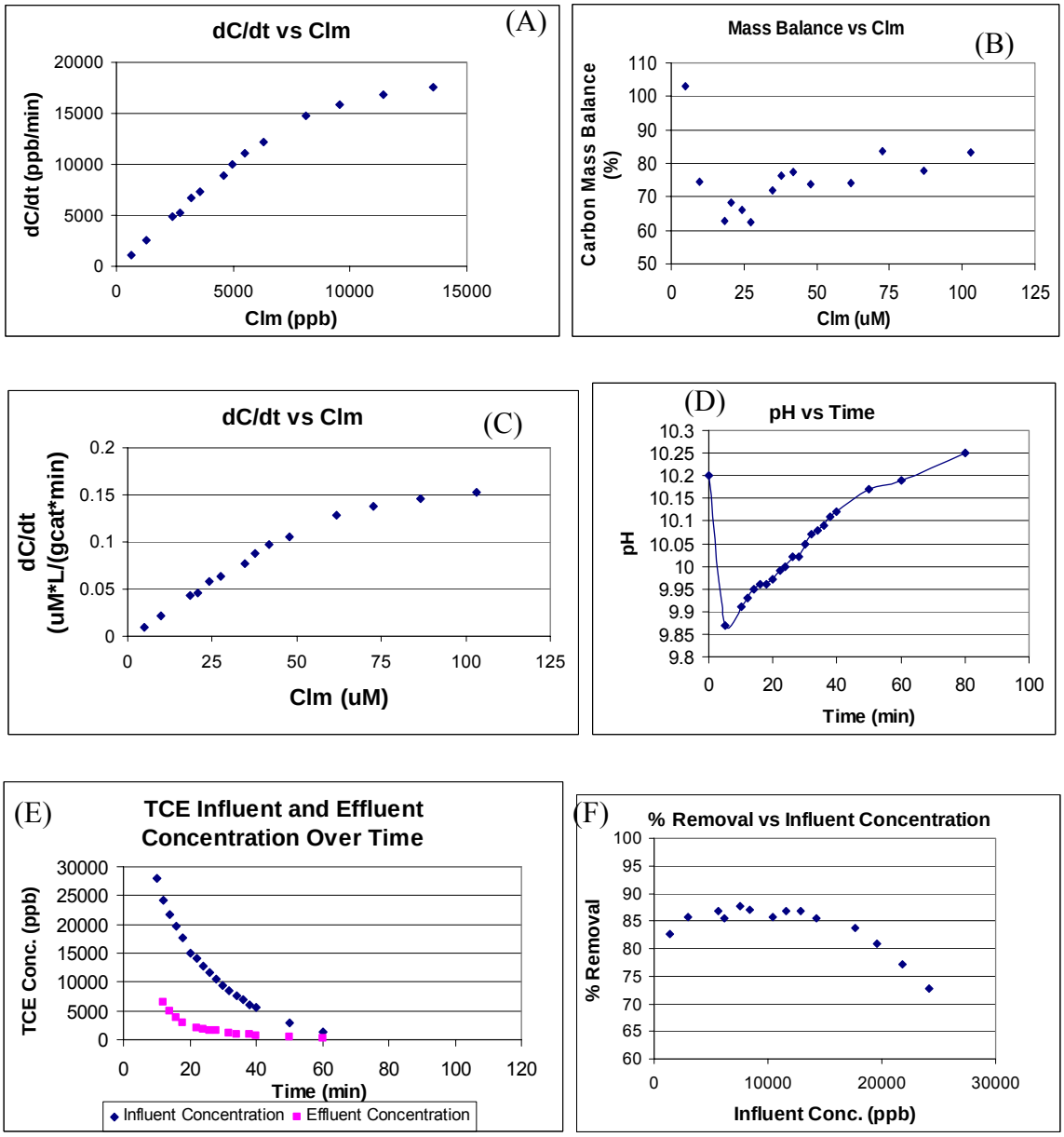

Figure B.27A Experiment #27 – pH = 10.5, 100% H_2, $[TCE]_0$=44.7ppm, [TAPS]=10mM
(A) Degradation Rate vs. Clm (B) Carbon Mass Balance vs. Clm
(C) Degradation Rate vs. Clm normalized (D) pH vs. Time [measured at the effluent]
(E) Influent and Effluent TCE conc. vs. Time
(F) % Removal vs. Influent conc.

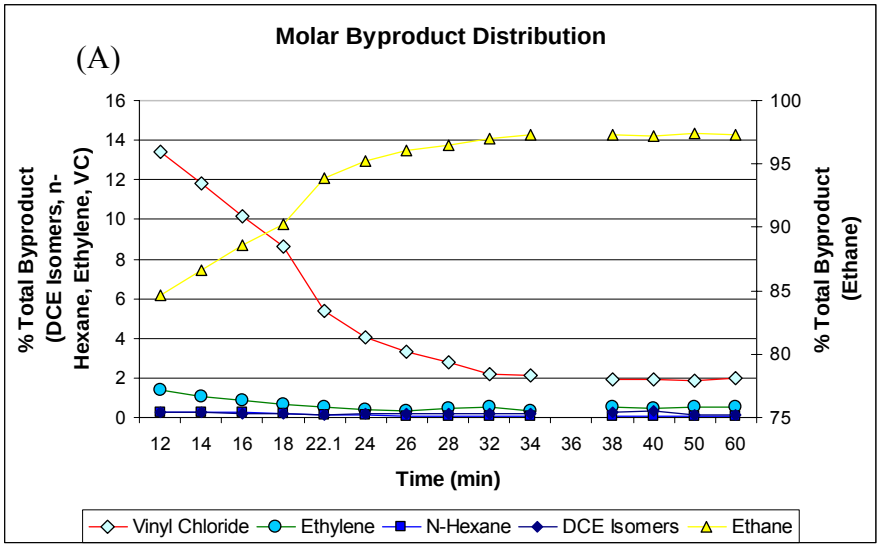

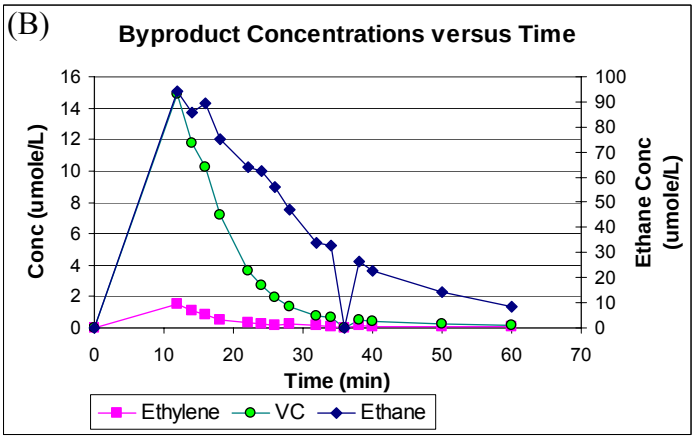

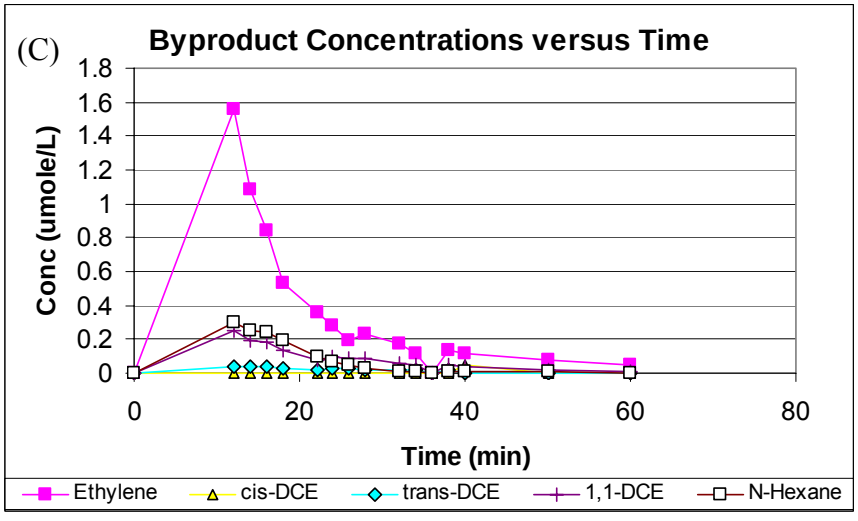

Figure B.27B Exp. #27 – pH = 10.5, 100% H_2, $[TCE]_0$=44.7ppm, [TAPS]=10mM cont.
(A) Molar Byproduct Distribution vs. Time [measured at the effluent]
(B) Ethane, Ethylene, VC Conc. vs. Time [measured at the effluent]
(C) Ethylene, DCE, Hexane Conc. vs. Time [measured at the effluent]

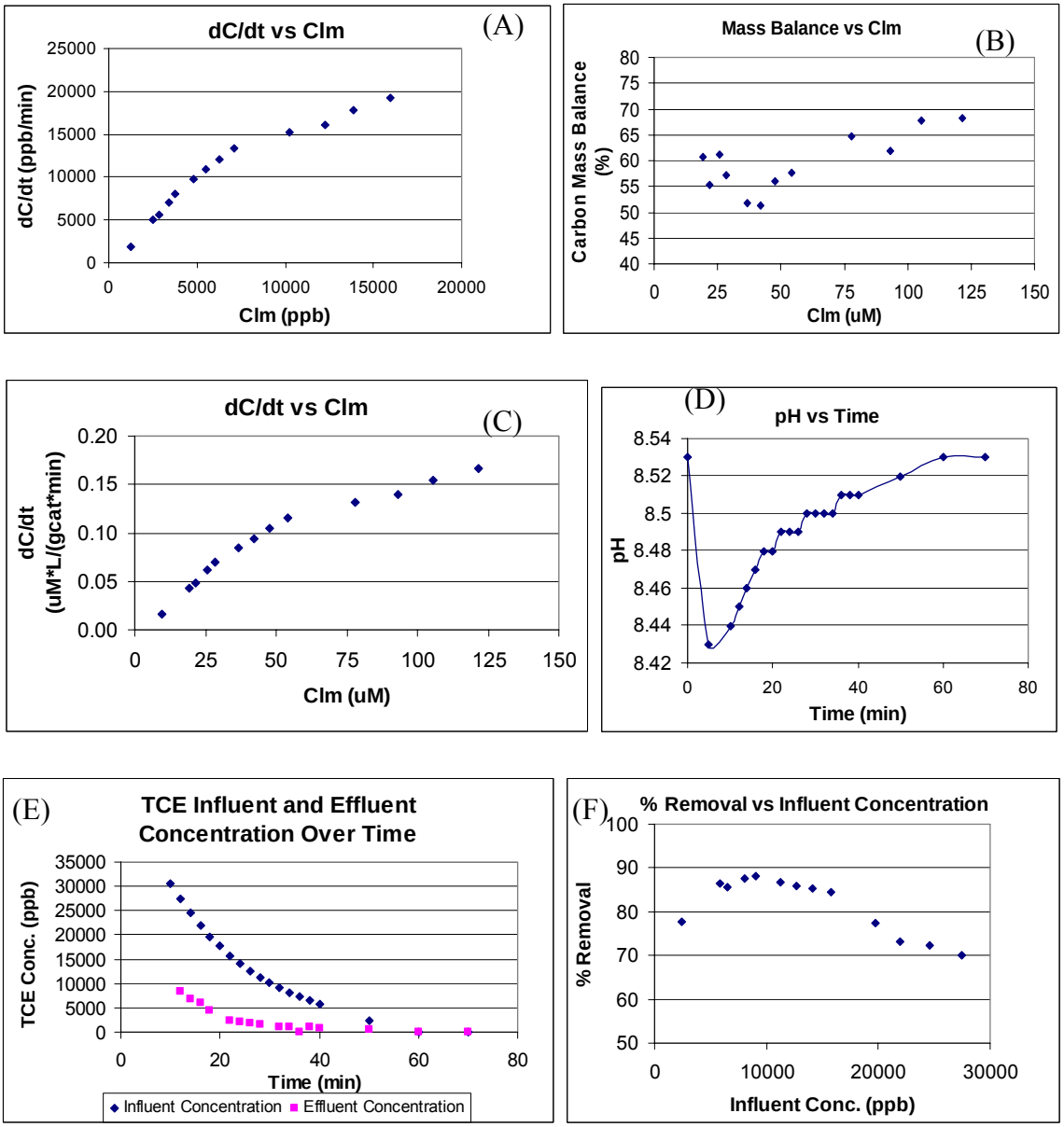

Figure B.28A Experiment #28 – pH = 8.53, 100% H_2, $[TCE]_0$=44.7ppm, [TAPS]=10mM
(A) Degradation Rate vs. Clm (B) Carbon Mass Balance vs. Clm
(C) Degradation Rate vs. Clm normalized (D) pH vs. Time [measured at the effluent]
(E) Influent and Effluent TCE conc. vs. Time
(F) % Removal vs. Influent conc.

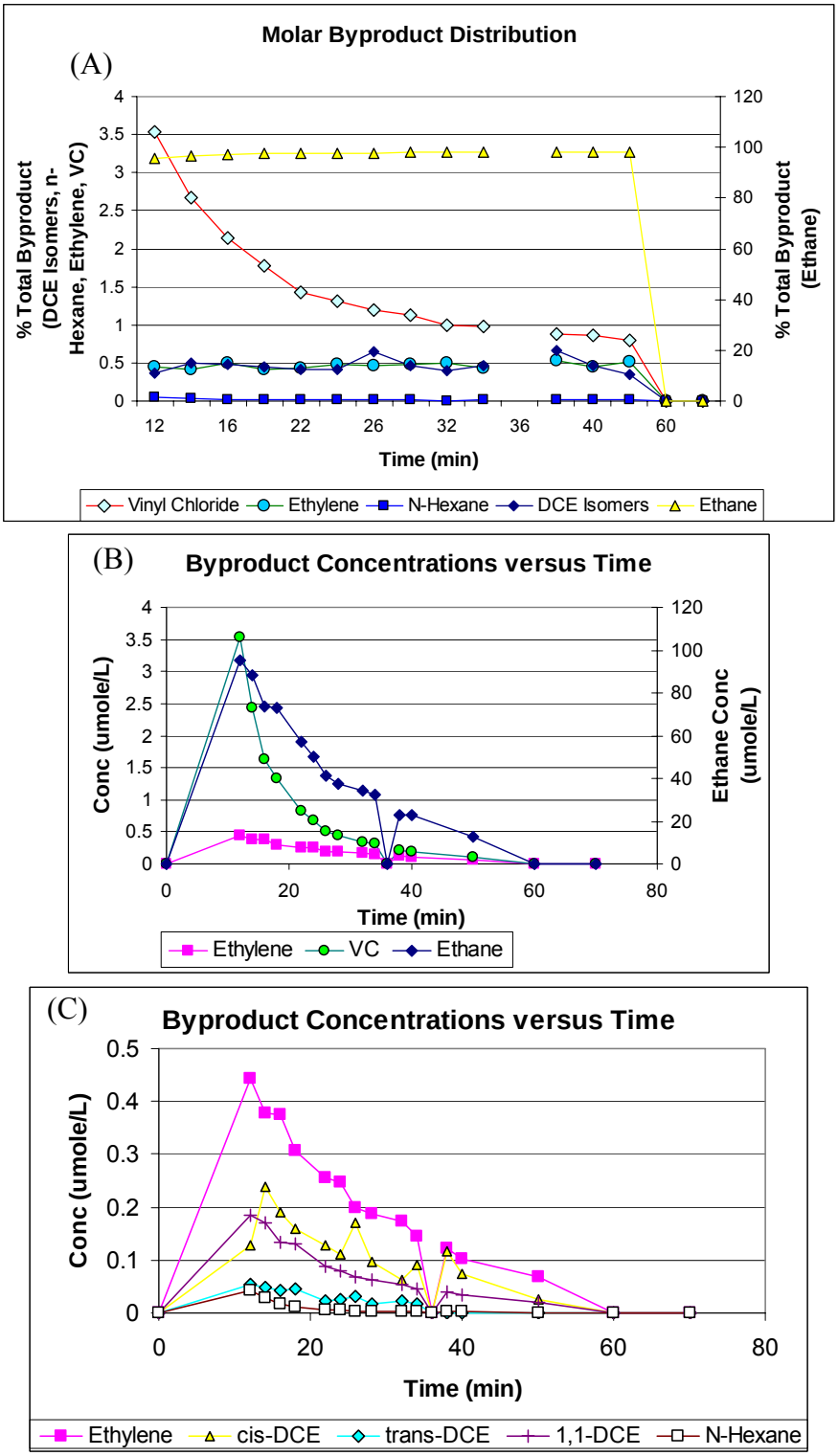

Figure B.28B Exp. #28 – pH = 8.53, 100% H_2, $[TCE]_0$=44.7ppm, [TAPS]=10mM cont.
(A) Molar Byproduct Distribution vs. Time [measured at the effluent]
(B) Ethane, Ethylene, VC Conc. vs. Time [measured at the effluent]
(C) Ethylene, DCE, Hexane Conc. vs. Time [measured at the effluent]

APPENDIX C: MICHAELIS-MENTEN MODEL FIT DATA

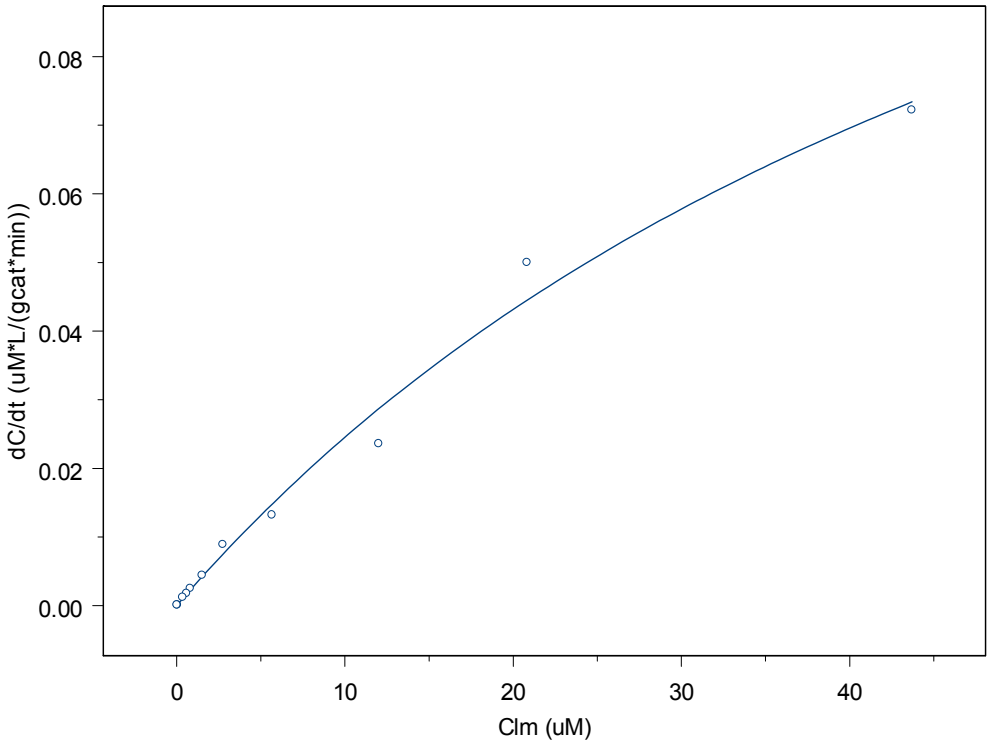

Figure C.1 Michaelis-Menten model fit to Experiment # 7 data: $[TCE]_0$ = 25 ppm, pH = 4, [HCOOH*] = 1 mM

V_{max} (μM*L/(g_{cat}*min))	0.179496
$K_{1/2}$ (μM)	63.187
V_{max} Standard Error	0.0315566
$K_{1/2}$ Standard Error	16.5099
Correlation of Parameters	0.988

Table C.1 Michaelis-Menten model parameters for Experiment # 7 data: $[TCE]_0$ = 25 ppm, pH = 4, [HCOOH*] = 1 mM

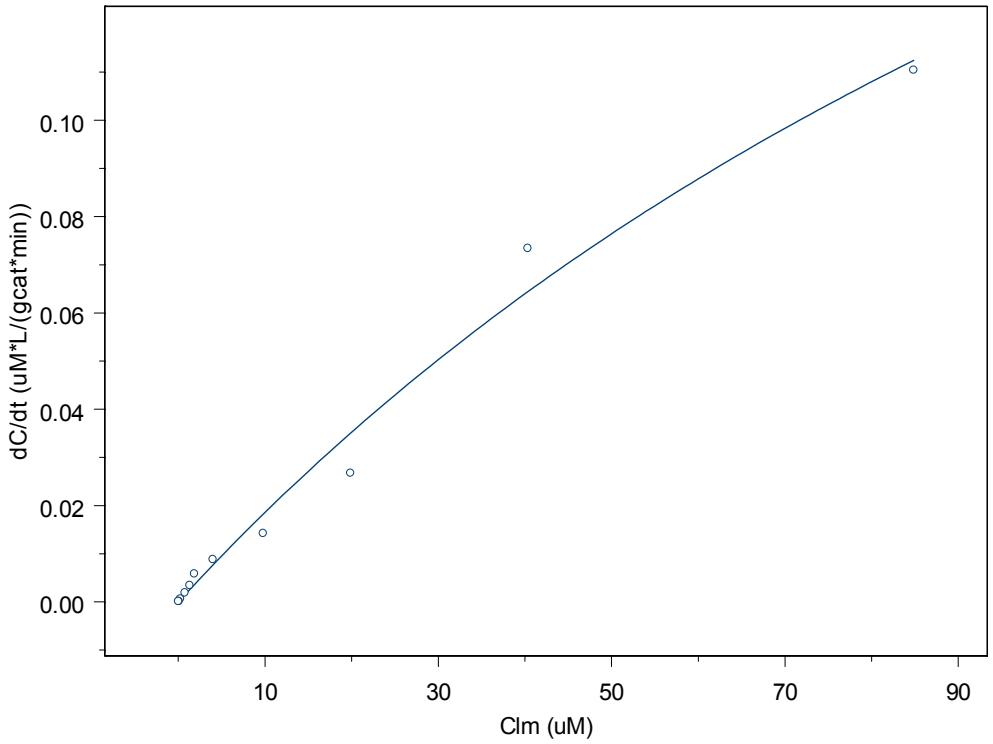

Figure C.2 Michaelis-Menten model fit to Experiment # 8 data: $[TCE]_0$ = 25 ppm, pH = 5, [HCOOH*] = 1 mM

V_{max} (μM*L/(g_{cat}*min))	0.346471
$K_{1/2}$ (μM)	176.642
V_{max} Standard Error	0.0964331
$K_{1/2}$ Standard Error	67.1242
Correlation of Parameters	0.994

Table C.2 Michaelis-Menten model parameters for Experiment # 8 data: $[TCE]_0$ = 25 ppm, pH = 5, [HCOOH*] = 1 mM

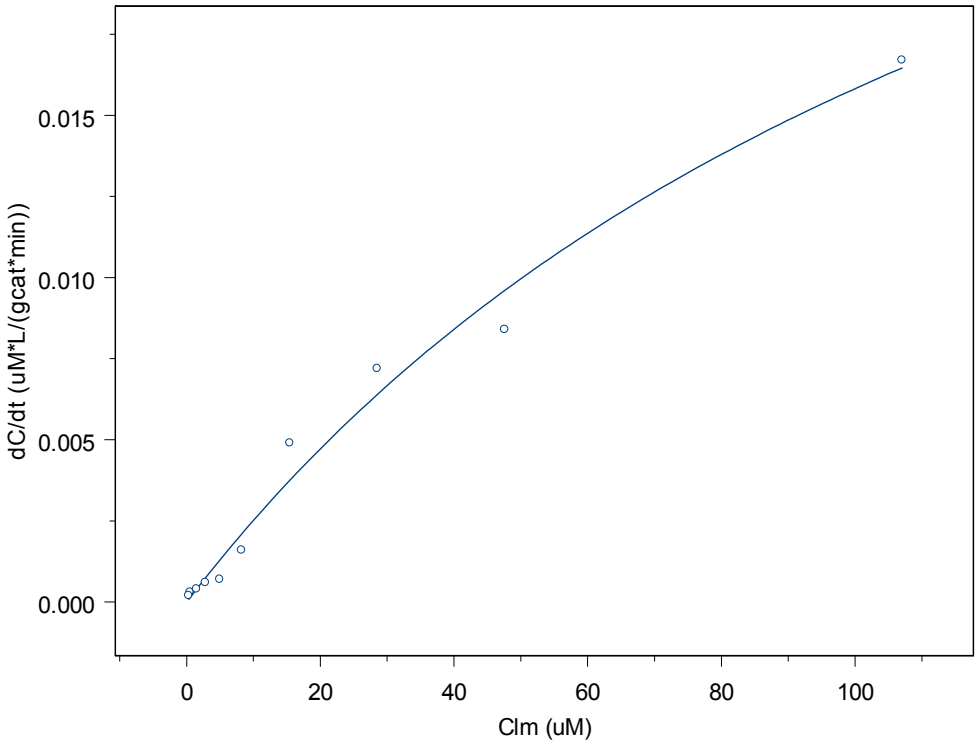

Figure C.3 Michaelis-Menten model fit to Experiment # 10 data: $[TCE]_0$ = 25 ppm, pH = 6, [HCOOH*] = 1 mM

V_{max} (μM*L/(g_{cat}*min))	0.0384412
$K_{1/2}$ (μM)	142.95
V_{max} Standard Error	0.00780254
$K_{1/2}$ Standard Error	43.7894
Correlation of Parameters	0.985

Table C.3 Michaelis-Menten model parameters for Experiment # 10 data: $[TCE]_0$ = 25 ppm, pH = 6, [HCOOH*] = 1 mM

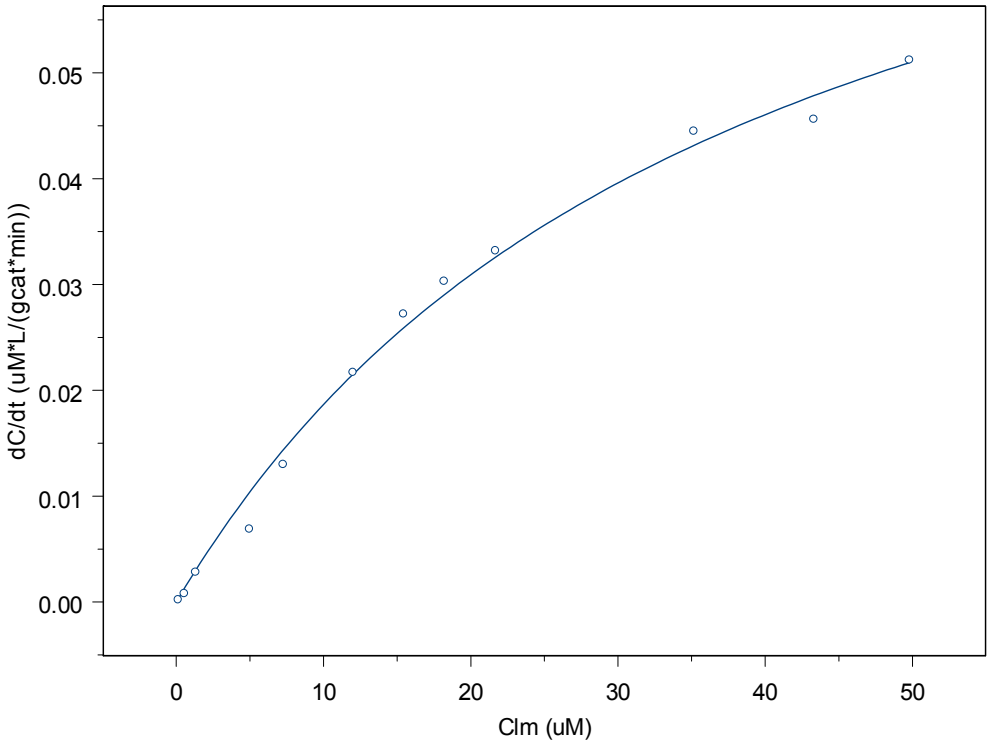

Figure C.4 Michaelis-Menten model fit to Experiment # 14 data: $[TCE]_0$ = 25 ppm, pH = 7.5, [HCOOH*] = 4 mM

V_{max} (μM*L/(g_{cat}*min))	0.0902102
$K_{1/2}$ (μM)	38.3459
V_{max} Standard Error	0.00668414
$K_{1/2}$ Standard Error	5.07135
Correlation of Parameters	0.977

Table C.4 Michaelis-Menten model parameters for Experiment # 14 data: $[TCE]_0$ = 25 ppm, pH = 7.5, [HCOOH*] = 4 mM

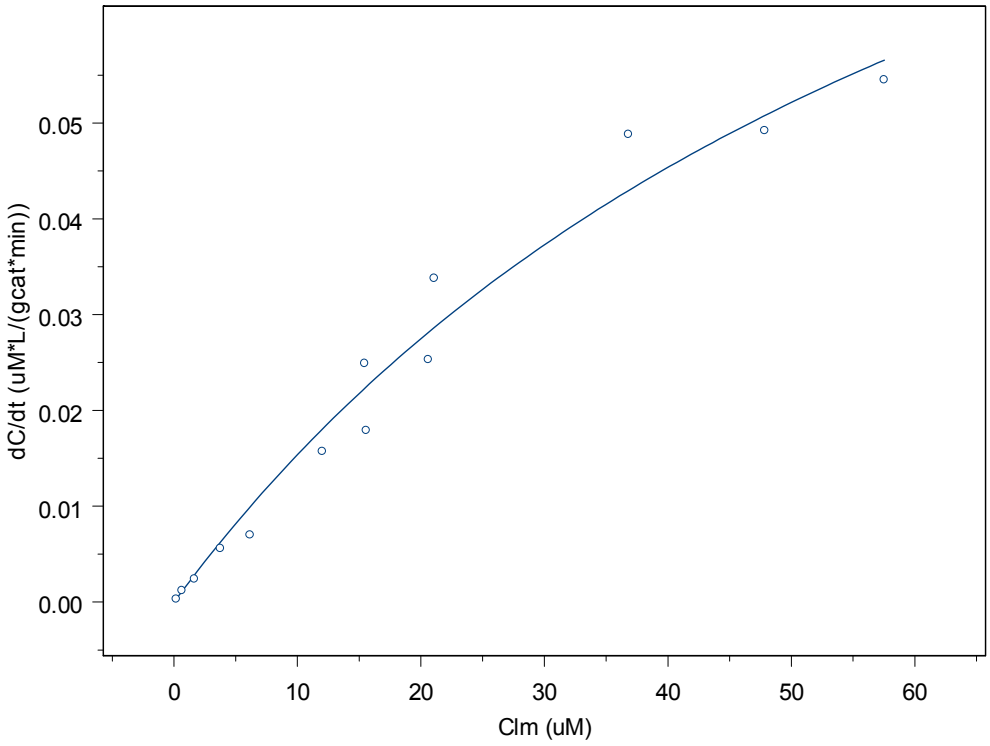

Figure C.5 Michaelis-Menten model fit to Experiment # 15 data: $[TCE]_0$ = 25 ppm, pH = 8, [HCOOH*] = 4 mM

V_{max} (μM*L/(g_{cat}*min))	0.129644
$K_{1/2}$ (μM)	74.3238
V_{max} Standard Error	0.0269163
$K_{1/2}$ Standard Error	22.9646
Correlation of Parameters	0.988

Table C.5 Michaelis-Menten model parameters for Experiment # 15 data: $[TCE]_0$ = 25 ppm, pH = 8, [HCOOH*] = 4 mM

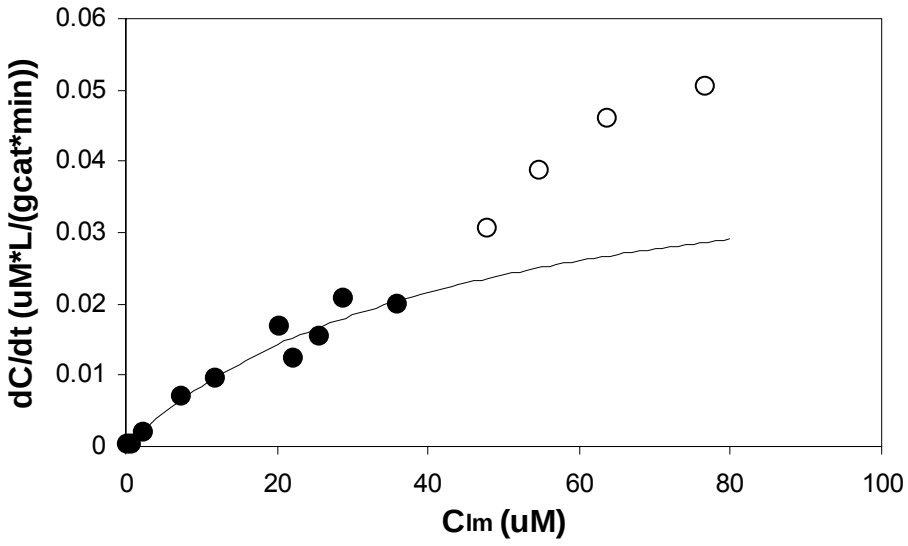

Figure C.6 Michaelis-Menten model fit to Experiment # 16 data: $[TCE]_0$ = 25 ppm, pH = 11, [HCOOH*] = 4 mM
(Modeled using solid symbols only)

V_{max} (μM*L/(g_{cat}*min))	0.0445012
$K_{1/2}$ (μM)	42.4871
V_{max} Standard Error	0.0162624
$K_{1/2}$ Standard Error	24.6761
Correlation of Parameters	0.993

Table C.6 Michaelis-Menten model parameters for Experiment # 16 data: $[TCE]_0$ = 25 ppm, pH = 11, [HCOOH*] = 4 mM

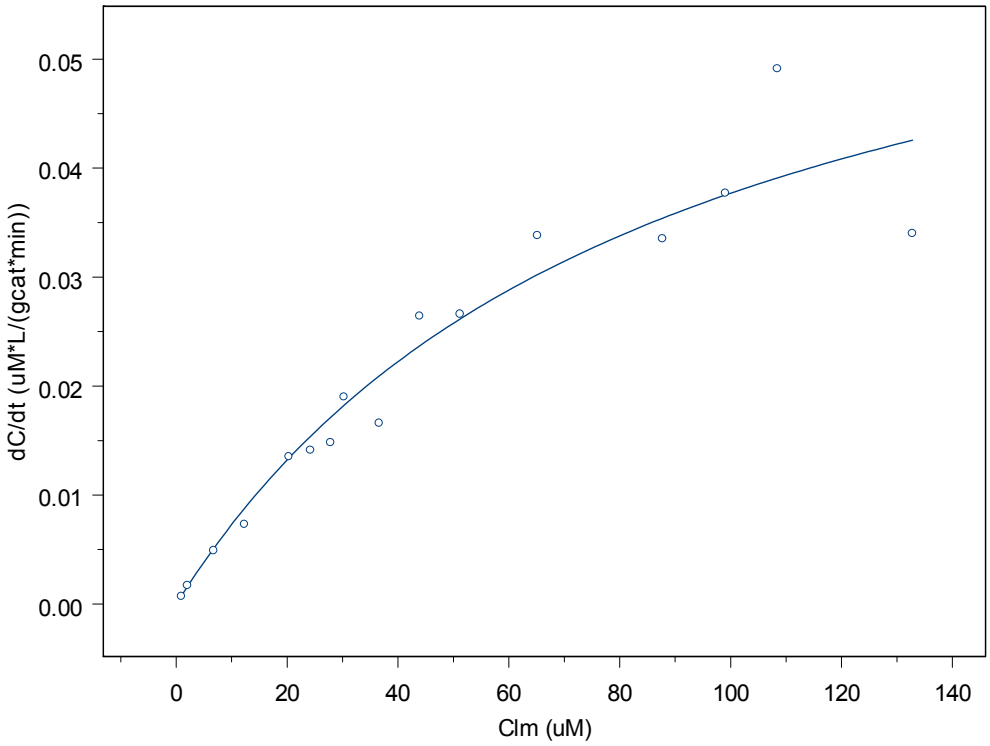

Figure C.7 Michaelis-Menten model fit to Experiment # 17 data: $[TCE]_0$ = 45 ppm, pH = 4, [HCOOH*] = 0.5 mM

V_{max} (μM*L/(g_{cat}*min))	0.0701607
$K_{1/2}$ (μM)	86.156
V_{max} Standard Error	0.0123477
$K_{1/2}$ Standard Error	27.7235
Correlation of Parameters	0.973

Table C.7 Michaelis-Menten model parameters for Experiment # 17 data: $[TCE]_0$ = 45 ppm, pH = 4, [HCOOH*] = 0.5 mM

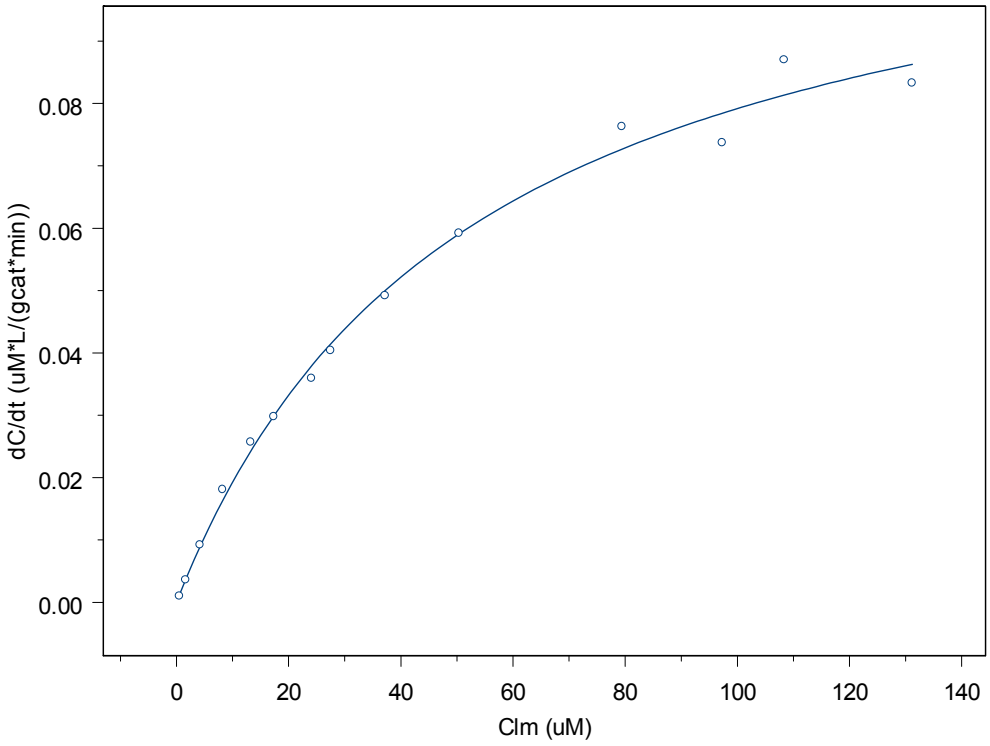

Figure C.8 Michaelis-Menten model fit to Experiment # 18 data: $[TCE]_0$ = 45 ppm, pH = 4, [HCOOH*] = 1 mM

V_{max} (μM*L/(g_{cat}*min))	0.121023
$K_{1/2}$ (μM)	52.8334
V_{max} Standard Error	0.00523025
$K_{1/2}$ Standard Error	5.10772
Correlation of Parameters	0.945

Table C.8 Michaelis-Menten model parameters for Experiment # 18 data: $[TCE]_0$ = 45 ppm, pH = 4, [HCOOH*] = 1 mM

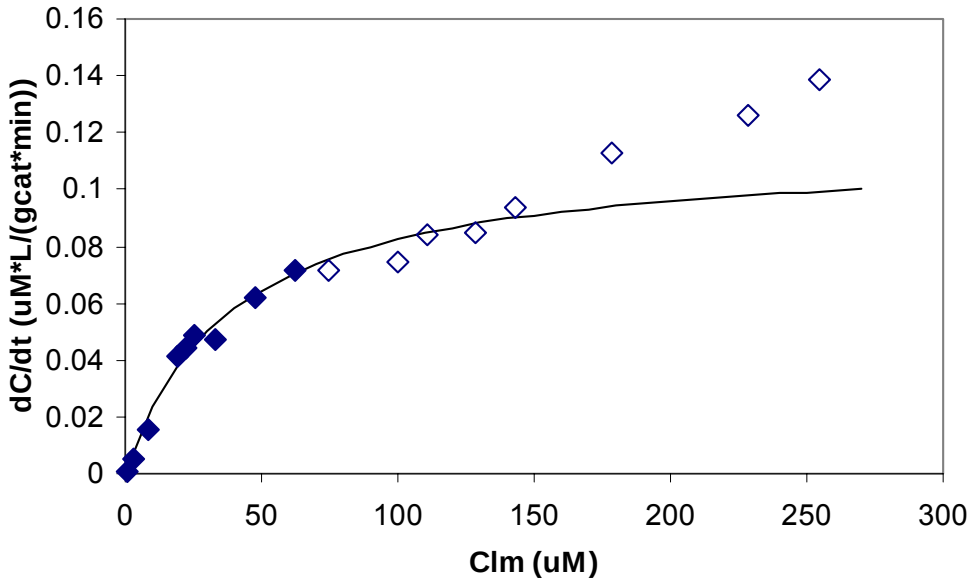

Figure C.9 Michaelis-Menten model fit to Experiment # 22 data: $[TCE]_0$ = 91.4 ppm, pH = 4, [HCOOH*] = 1 mM
(Modeled using solid symbols only)

V_{max} (μM*L/(g_{cat}*min))	0.114545
$K_{1/2}$ (μM)	38.8833
V_{max} Standard Error	0.0147911
$K_{1/2}$ Standard Error	9.58944
Correlation of Parameters	0.975

Table C.9 Michaelis-Menten model parameters for Experiment # 22 data: $[TCE]_0$ = 91.4 ppm, pH = 4, [HCOOH*] = 1 mM

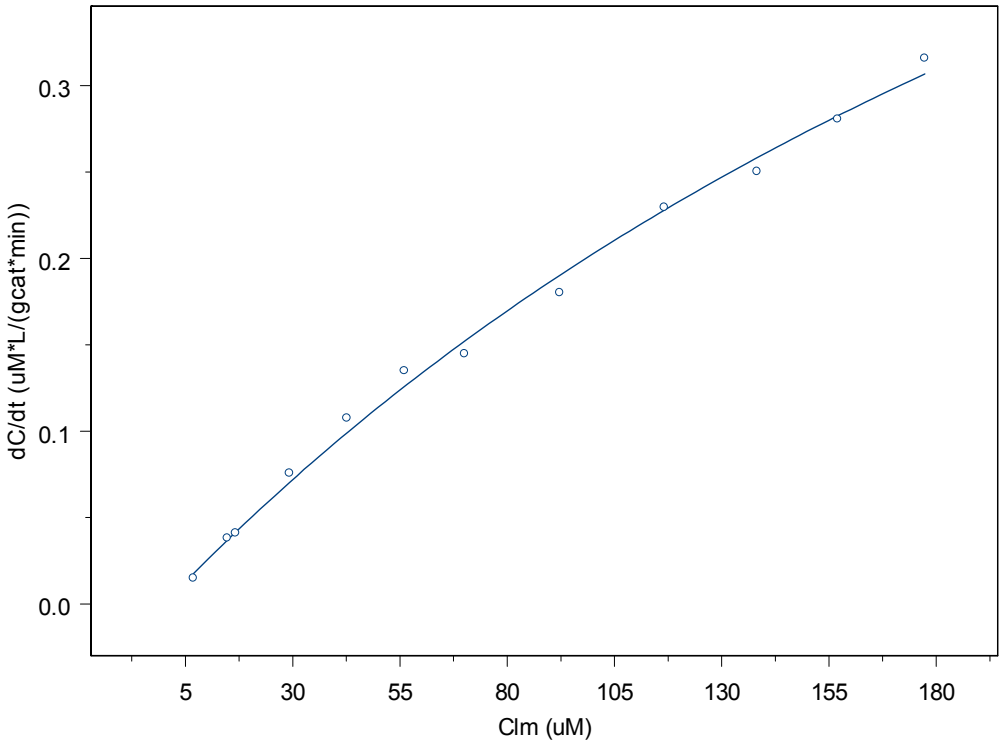

Figure C.10 Michaelis-Menten model fit to Experiment # 23 data: $[TCE]_0$ = 91.4 ppm, pH = 4, [HCOOH*] = 10 mM

V_{max} (μM*L/(g_{cat}*min))	0.913654
$K_{1/2}$ (μM)	350.813
V_{max} Standard Error	0.110762
$K_{1/2}$ Standard Error	57.8088
Correlation of Parameters	0.996

Table C.10 Michaelis-Menten model parameters for Experiment # 23 data: $[TCE]_0$ = 91.4 ppm, pH = 4, [HCOOH*] = 10 mM

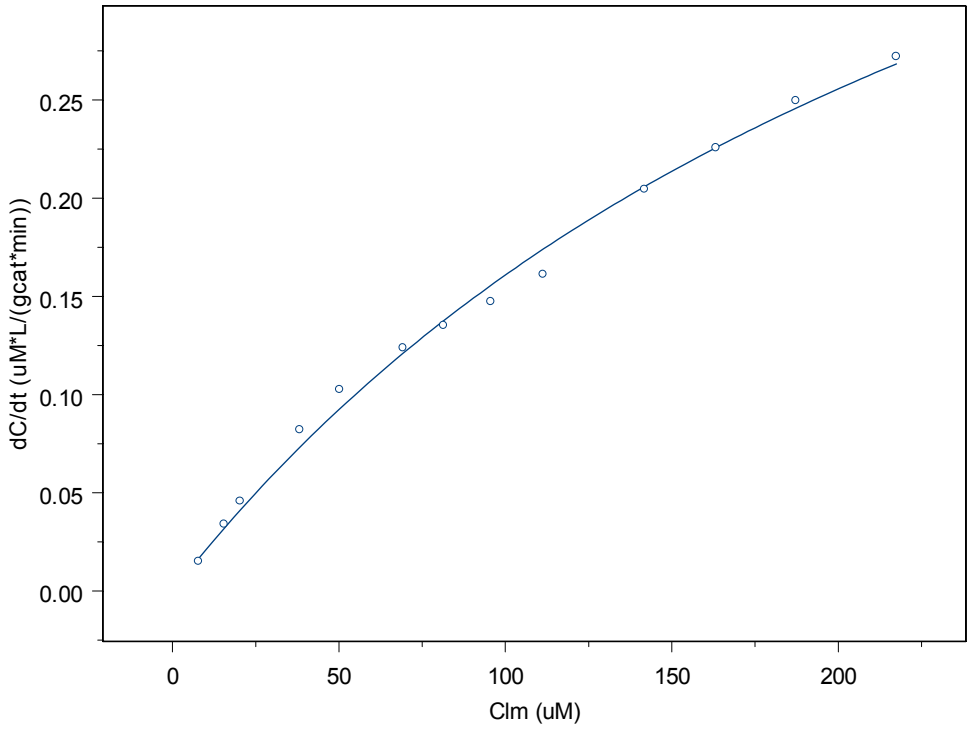

Figure C.11 Michaelis-Menten model fit to Experiment # 24 data: $[TCE]_0$ = 91.4 ppm, pH = 4, [HCOOH*] = 4 mM

V_{max} (μM*L/(g_{cat}*min))	0.621591
$K_{1/2}$ (μM)	286.337
V_{max} Standard Error	0.0551589
$K_{1/2}$ Standard Error	37.948
Correlation of Parameters	0.991

Table C.11 Michaelis-Menten model parameters for Experiment # 24 data: $[TCE]_0$ = 91.4 ppm, pH = 4, [HCOOH*] = 4 mM

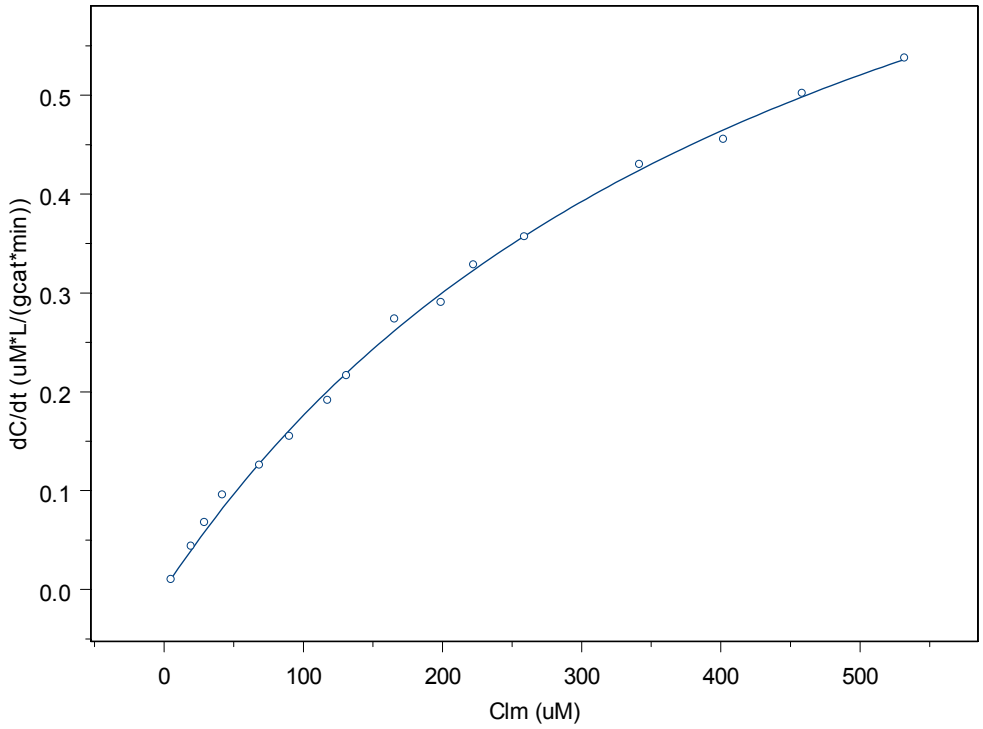

Figure C.12 Michaelis-Menten model fit to Experiment # 25 data: $[TCE]_0$ = 182.9 ppm, pH = 4, [HCOOH*] = 4 mM

V_{max} (μM*L/(g_{cat}*min))	1.01871
$K_{1/2}$ (μM)	478.686
V_{max} Standard Error	0.0349612
$K_{1/2}$ Standard Error	27.153
Correlation of Parameters	0.983

Table C.12 Michaelis-Menten model parameters for Experiment # 25 data: $[TCE]_0$ = 182.9 ppm, pH = 4, [HCOOH*] = 4 mM

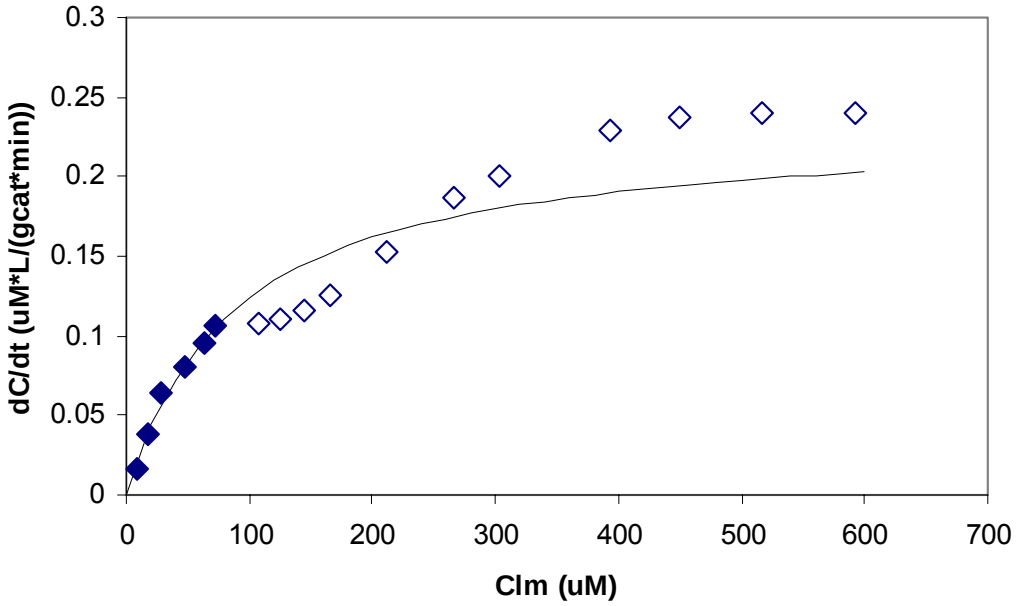

Figure C.13 Michaelis-Menten model fit to Experiment # 26 data: $[TCE]_0$ = 170 ppm, pH = 4, [HCOOH*] = 1 mM
(Modeled using solid symbols only)

V_{max} (μM*L/(g_{cat}*min))	0.23215
$K_{1/2}$ (μM)	87.2871
V_{max} Standard Error	0.0405767
$K_{1/2}$ Standard Error	24.5304
Correlation of Parameters	0.99

Table C.13 Michaelis-Menten model parameters for Experiment # 25 data: $[TCE]_0$ = 182.9 ppm, pH = 4, [HCOOH*] = 4 mM

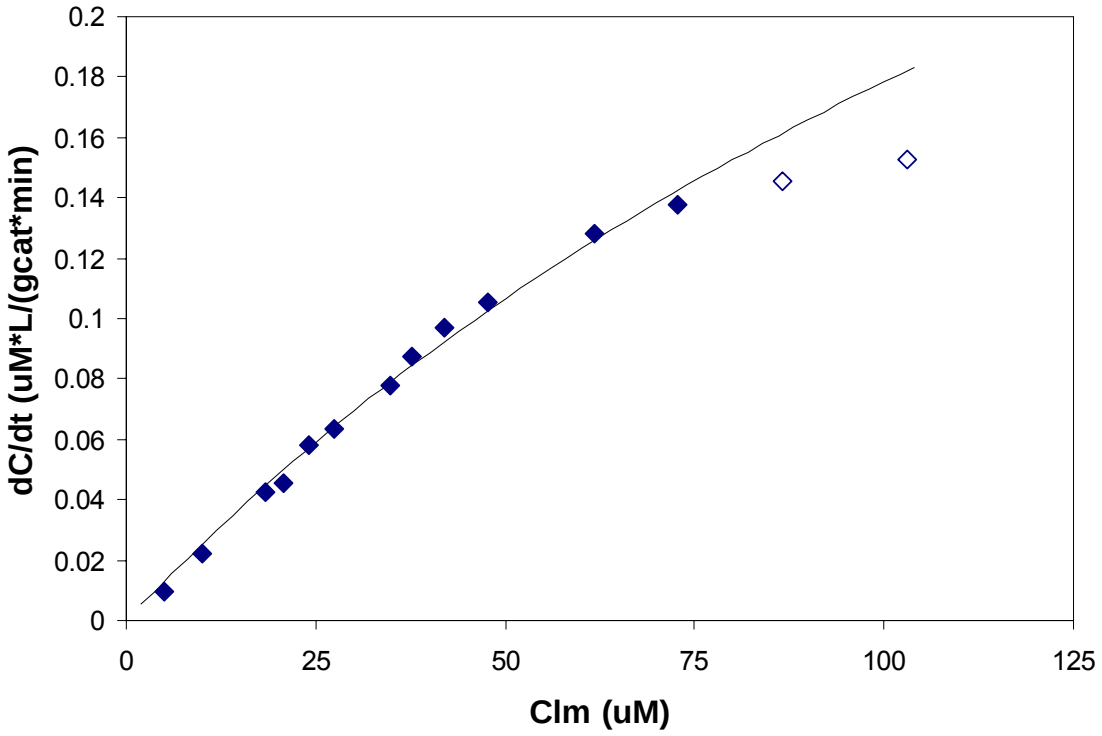

Figure C.14 Michaelis-Menten model fit to Experiment # 27 data: $[TCE]_0$ = 44.7 ppm, pH = 10.5, 100% H_2
(Modeled using solid symbols only)

V_{max} (μM*L/(g_{cat}*min))	0.54515
$K_{1/2}$ (μM)	205.689
V_{max} Standard Error	0.0864977
$K_{1/2}$ Standard Error	40.3285
Correlation of Parameters	0.998

Table C.14 Michaelis-Menten model parameters for Experiment # 27 data: $[TCE]_0$ = 44.7 ppm, pH = 10.5, 100% H_2

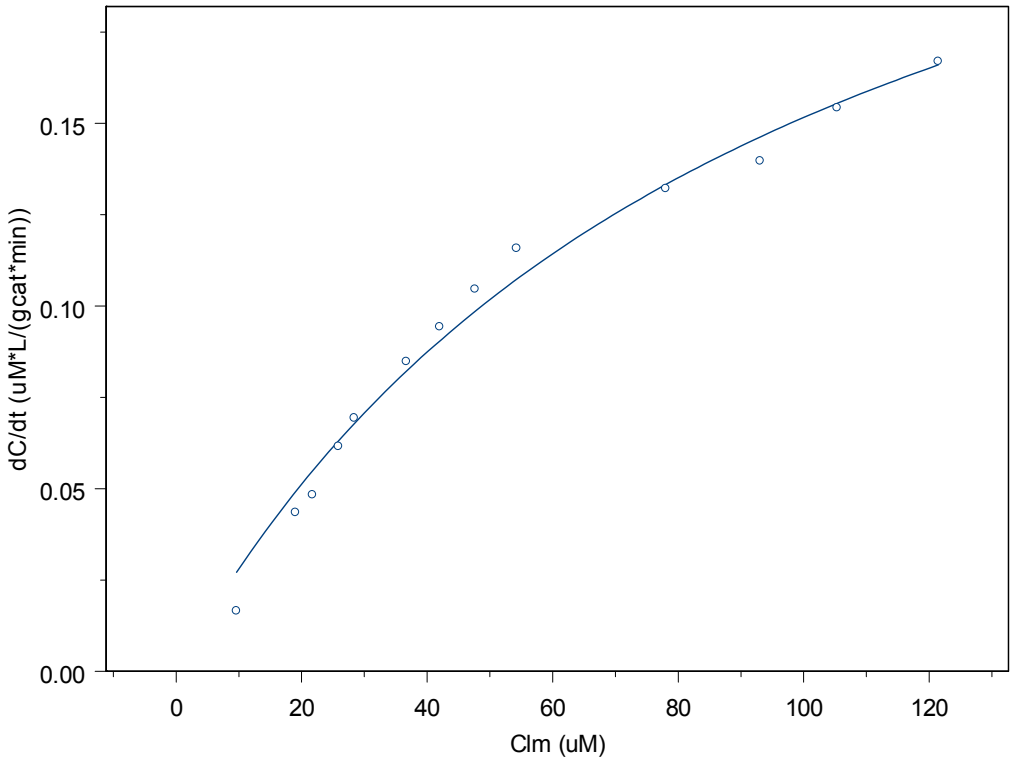

Figure C.15 Michaelis-Menten model fit to Experiment # 28 data: $[TCE]_0$ = 44.7 ppm, pH = 8.5, 100% H_2

V_{max} (μM*L/(g_{cat}*min))	0.297312
$K_{1/2}$ (μM)	96.0867
V_{max} Standard Error	0.0223986
$K_{1/2}$ Standard Error	12.46
Correlation of Parameters	0.979

Table C.15 Michaelis-Menten model parameters for Experiment # 28 data: $[TCE]_0$ = 44.7 ppm, pH = 8.5, 100% H_2

REFERENCES

AFCEE (2003) *Tri-Service Bioremediation Guidance Manual*. Retrieved 24 February 2003, from http://www.afcee.brooks.af.mil/eq/triservice/2003/bioremediationmanual03.ppt.

Arnold, W., Roberts, L. Pathways and kinetics of chlorinated ethylene and chlorinated acetylene reaction with Fe(0) particles. *Environmental Science and Technology, Vol 34*, No. 9. 1794-1805, 2000.

Boggs, K. G. *Bench-Scale Investigation of Catalytic Dehalogenation of Chlorinated Ethenes with Palladium Metal*. MS Thesis, Wright State University, Dayton OH, July 2000.

Chang, C. C., Reo, C. M., Lund, C. R. F. The effect of a membrane reactor upon catalyst deactivation during hydrodechlorination of dichloroethane. *Applied Catalysis B: Environmental, Vol 20*, No. 4. 309-317, 1999.

Daub, K., Wunder, V. K., Dittmeyer, R. Studies on the use of catalytic membranes for reduction of nitrate in drinking water. *Chemical Engineering Science, Vol.54*, No.1. 1577-1582, 1999.

Defense Environmental Restoration Program (DERP), Fiscal Year 2002 Annual Report to Congress, Washington: Government Printing Office, 2002.

DENIX (2003) *Trichloroethylene Risk Assessment*. Retrieved 1 March 2003, from http://www.denix.osd.mil/denix/DOD/Policy/Army/AERTA/Need_assessment/A15b/a15b_r3.html.

DENIX (2002) *States Praise Trichloroethylene Analysis; Industry, DoD Criticize EPA's Conclusions*. Retrieved 18 April 2003, from http://www.denix.osd.mil/denix/DOD/News/Pubs/DER/19Feb02/36.doc.html

Domenico, P. A., Schwartz, F. W. Physical and Chemical Hydrogeology, Second Edition. New York: John Wily and Sons, Inc., 1998.

Ellis, D. E., Lutz, E. J., Klecka, G. M., Pardieck, D. L., Salvo, J. J., Heitkamp, M. A., Gannon, D. J., Mikula, C. C., Vogel, C. M., Sayles, G. D., Kampbell, D. H., Wilson, J. T., Maiers, D. T. Remediation Technology Development Forum Intrinsic Remediation Project at Dover Air Force Base, Delaware. Symposium on Natural Attenuation of Chlorinated Organics in Groundwater. Dallas, TX. 11-13 September, 1996.

Furukawa, Y., Kim, J. W., Watkins, J., Wilkins, R. T. Formation of ferrihydrite and associated iron corrosion products in permeable reactive barriers of zero-valent iron. *Environmental Science and Technology, Vol 36*. 5469-5475, 2002.

Gavaskar, A. R. Design and construction techniques for permeable reactive barriers. *Journal of Hazardous Materials, Vol 68*. 41-71, 1999.

Hathaway, G., Proctor, N., Hughes, J. Proctor and Hughes' Chemical Hazards of the Workplace, Fourth Edition. New York: Van Nostrand Reinhold, 1996.

Horold, S., Vorlop, K. D., Tacke, T., Sell, M. Development of catalysts for a selective nitrate and nitrite removal from drinking water. *Catalysis Today, Vol. 17*, No. 1. 21-30, 1993.

Interstate Technology and Regulatory Cooperation (ITRC) Work Group: In Situ Bioremediation Work Team. "Natural Attenuation of Chlorinated Solvents in Groundwater: Principles and Practices." Unpublished Technical/Regulatory Guidelines. Washington D.C. September 1999.

Klaassen, C. Casarett and Doull's Toxicology: The Basic Science of Poisons, Sixth Edition. New York: McGraw-Hill Medical Publishing Division, 1996.

Kopinke, F., Mackenzie, K., Köhler, R. Catalytic hydrodechlorination of groundwater contaminants in water and in the gas phase using Pd/γ-Al_2O3. *Applied Catalysis G: Environmental, Vol 44*. 15-24, 2003.

Kovenklioglu, S., Cao, Z., Shah, D., Farrauto, R., Balko, E. Direct catalytic hydrodechlorination of toxic organics in wastewater. *AIChE Journal, Vol 38*, No. 7. 1003-1012, 1992.

Kramer, H., Levy, M., Warshawsky, A. Hydrogen storage by the bicarbonate/formate reaction. Studies on the activity of Pd Catalysts. *International Journal of Hydrogen Energy, Vol 20*, No. 3. 229, 1995.

Lowry, G. V., Reinhard, M. Pd-catalyzed TCE dechlorination in water: Effect of H_2(aq) and H_2-Utilizing competitive solutes on the TCE dechlorination rate and product distribution. *Environmental Science and Technology, Vol 35*, No. 4. 696-702, 2001.

Lowry, G. V., Reinhard, M. Pd catalyzed TCE dechlorination in ground water: Solute effects, biological control, and oxidative catalyst regeneration. *Environmental Science and Technology, Vol 34*, No. 15. 3217-3223, 2000.

Lowry, G. V., Reinhard, M. Hydrodehalogenation of 1- to 3-carbon halogenated organic compounds in water using a palladium catalyst and hydrogen gas. *Environmental Science and Technology, Vol 33*, No. 11. 1905-1910, 1999.

Mars, P., Scholten, J., Zwietering, P. The catalytic decomposition of formic acid. *Advances in Catalysis today and related subjects*, *Vol 14*. 35-113, 1963.

Masters, G. M. Introduction to Environmental Engineering and Science, Second Edition. Upper Saddle River: Prentice Hall, Inc., 1998.

McMahon, P. G., K. F. Dennehy, and M. W. Sandstrom. Hydraulic and Geochemical Performance of a Permeable Reactive Barrier Containing Zero-Valent Iron. *Ground Water, Vol 37(3)*: 396-404, 1999.

McNab, W., Reinhard, M., Ruiz, R. In-situ destruction of chlorinated hydrocarbons in groundwater using catalytic reductive dehalogenation in a reactive well: testing and operational experiences. *Environmental Science and Technology, Vol 34*, No. 1, 149-153, 2000.

McNab, W., Ruiz, R. Palladium-catalyzed reductive dehalogenation of dissolved chlorinated aliphatics using electrolytically-generated hydrogen. *Chemosphere, Vol 37*, No. 5. 925-936, 1998.

Munakata, N., Cunningham, J., Reinhard, M., Ruiz R., Lebron, C. "Palladium Catalysts in Horizontal Flow Treatment Wells: Field-Scale Design and Laboratory Study," *Proceedings of the Third International Conference on Remediation of Chlorinated and Recalcitrant Compounds*, Paper 2H-33. Columbus: Battelle Press, 2002.

Munakata, N., Roberts, P., Reinhard, M., McNab, W. Catalytic dechlorination of halogenated hydrocarbon compounds using supported palladium: a preliminary assessment of matrix effects. *Groundwater Quality, Vol 250*, 491-496, 1998.

Muftikian, R., Fernando, Q., Korte, N. A method for the rapid dechlorination of low molecular weight chlorinated hydrocarbons in water. *Water Research, Vol 29*, No. 10, 2434-2439, 1995.

National Research Council, Alternatives for Ground Water Cleanup. Washington: National Academy Press, 1994.

National Research Council, In Situ Bioremediation: When does it work? Washington: National Academy Press, 1993.

Niekamp, S.W. Palladium-Catalyzed Dehalogenation of Chlorinated Organic Pollutants in Natural and Synthetic Groundwater. MS Thesis, Wright State University, Dayton OH, June 2001.

Page, G. Comparison of groundwater and surface water for patterns and levels of contamination by toxic substances. *Environmental Science and Technology, Vol 15,* 1475-1480, 1981.

Pankow, J., Cherry, J. Dense Chlorinated Solvents and other DNAPLs in Groundwater. Portland: Waterloo Pres, 1996.

Perrone, L., Prati, L., Rossi, M. Removal of chlorinated organic compounds from water by catalytic dehydrohalogenation. *Applied Catalysis B: Environmental, Vol 15.* 241-246, 1998.

Phillips, D. L. *Palladium-catalyzed destruction of nitro aromatic contaminated groundwater*. MS Thesis, AFIT/GEE/ENV/03-21. School of Engineering and Environmental Management, Air Force Institute of Technology, (AU), Wright Patterson Air Force Base Ohio, February 2003.

Pintar, A., Batista, J., Levec, J., Kajiuchi, T. Kinetics of the catalytic liquid-phase hydrogenation of aqueous nitrate solutions. *Applied Catalysis B: Environmental, Vol 11*, No. 1. 81-98, 1996.

Prüsse, U., Vorlop, K. Supported bimetallic palladium catalysts for water-phase nitrate reduction. *Journal of Molecular Catalysis A: Chemical, Vol 173*, 313-328, 2001.

Prüsse, U., Hähnlein, M., Daum, J., Vorlop, K. Improving the catalytic nitrate reduction. *Catalysis Today, Vol 55*, 79-90, 2000.

Roberts, L., Totten, L., Arnold, W., Burris, D., Campbell, T. Reductive Elimination of chlorinated ethylenes by zero-valent metals. *Environmental Science and Technology, Vol 30,* No. 8. 2654-2659, 1996.

Rylander, P. N. Hydrogenation Methods. Orlando: Academic Press, 1985.

Schreier, C. G., Reinhard, M. Catalytic hydrodehalogenation of chlorinated ethylenes using palladium and hydrogen for the treatment of contaminated water. *Chemosphere, Vol 31*, No. 6. 3475-3487, 1995.

Schüth, C., Disser, S., Schüth, F., Reinhard, M. Tailoring catalysts for hydrodechlorinating chlorinated hydrocarbon contaminants in groundwater. *Applied Catalysis B: Envionmental, Vol 28*. 147-152, 2000.

Sellers, K. Fundamentals of Hazardous Waste Site Remediation. New York: Lewis Publishers, 1999.

Strategic Environmental Research and Development Program (SERDP). Information Bulletin. Hrndon, VA: SERDP Support Office, No. 17, Summer 2003.

Siantar, D. P., Schreier, C. G., Chou, C., Reinhard, M. Treatment of 1,2-Digromo3-Chlororopane and nitrate-contaminated water with zero-valent iron or hydrogen/palladium catalysts. *Water Resources, Vol 30*, No. 10. 2315-2322, 1996.

Snoeyink, V., Jenkins, D. Water Chemistry. New York: John Wiley & Sons, 1980.

Stoppel, C. M., Goltz, M. N. Modeling Pd-Catalyzed Destruction of Chlorinated Ethenes in Groundwater. *ASCE Journal of Environmental Engineering, Vol 129,* No. 2.147-154, 2003.

Stoppel, C. M. *A Model for Palladium Catalyzed Destruction of Chlorinated Ethene Contaminated Groundwater*. MS Thesis, AFIT/GEE/ENV/01M-21. School of Engineering and Environmental Management, Air Force Institute of Technology, (AU), Wright Patterson Air Force Base Ohio, March 2001.

Thomas, J. M., Thomas, W. J. Principles and Practices of Heterogeneous Catalysis. New York: VCH Publishers Inc., 1997.

United States Environmental Protection Agency (U.S. EPA). "Ground water and drinking water consumer fact sheet on: vinyl chloride." Excerpt from unpublished article. n. pag. http://www.epa.gov/OGWDW/dwh/c-voc/vinylchl.html. 13 December 2003.

U.S. EPA. "Use of Monitoring Natural Attenuation at Superfund, RCRA Corrective Action, and Underground Storage Tank Sites," Office of Solid Waste and Emergency Response Directive 9200.4-17, 1997.

Wiedemeier, T. H., Rifai, H. S., Newell, C. J., Wilson, J. T. Natural Attenuation of fuels and chlorinated solvents in the Subsurface. New York: John Wiley & Sons Inc., 1999.

Williams, P., Burson, J. Industrial Toxicology: Safety and Health Applications in the Workplace. New York: Van Nostrand Reinhold, 1985.

VITA

Captain Matthew D Welling graduated from Jackson High School, Ohio in 1995. He then entered the Ohio University in Athens to commence his undergraduate studies. He graduated with a Bachelor of Science degree in Civil Engineering and was commissioned as an Air Force officer and was recognized as a Distinguished Graduate from ROTC in June 1999.

His first assignment was at Dyess AFB, Texas where he was assigned to the 7th Civil Engineer Squadron and served as both the resources officer and chief of the Simplified Base Engineering Requirements (SABER) contract. In August 2002, he entered the Graduate Engineering and Environmental Management program of the Graduate School of Engineering and Management, Air Force Institute of Technology.

REPORT DOCUMENTATION PAGE

Form Approved OMB No. 074-0188

1. REPORT DATE *(DD-MM-YYYY)*	**2. REPORT TYPE**	**3. DATES COVERED** *(From – To)*
23-03-2004	**Master's Thesis**	Sep 2002 – Mar 2004

4. TITLE AND SUBTITLE

AN EVALUATION OF FORMATE AS AN ELECTRON DONOR TO FACILITATE PALLADIUM (PD) - CATALYZED DESTRUCTION OF CHLORINATED ALIPHATIC HYDROCARBONS

5a. CONTRACT NUMBER

5b. GRANT NUMBER

5c. PROGRAM ELEMENT NUMBER

6. AUTHOR(S)

Welling, Matthew, D., Captain, USAF

5d. PROJECT NUMBER
If funded, enter ENR #

5e. TASK NUMBER

5f. WORK UNIT NUMBER

7. PERFORMING ORGANIZATION NAMES(S) AND ADDRESS(S)
Air Force Institute of Technology
Graduate School of Engineering and Management (AFIT/EN)
2950 Hobson Way, Building 641
WPAFB OH 45433-7765

8. PERFORMING ORGANIZATION REPORT NUMBER

AFIT/GEM/ENV/04M-21

9. SPONSORING/MONITORING AGENCY NAME(S) AND ADDRESS(ES)
HQ AFCEE/ERS
Attn: Mrs. Erica S. K. Becvar, M.S.
3300 Sidney Brooks
Brooks City-Base TX 78235-5112 DSN: 240-4314

10. SPONSOR/MONITOR'S ACRONYM(S)

11. SPONSOR/MONITOR'S REPORT NUMBER(S)

12. DISTRIBUTION/AVAILABILITY STATEMENT
APPROVED FOR PUBLIC RELEASE; DISTRIBUTION UNLIMITED

13. SUPPLEMENTARY NOTES

14. ABSTRACT

The focus of this study was to determine the effectiveness of using a palladium (Pd) catalyst with formate as a reductant to treat CAH-contaminated groundwater. TCE was used as a model CAH. Other investigators have focused on hydrogen gas (H_2) as a reductant to treat CAH-contaminated groundwater. However, when using H_2 as a reductant, catalyst deactivation is observed due to the production of hydrochloric acid. In this study, formic acid was used as the reductant, resulting in no observed catalyst deactivation even at high contaminant concentrations. Reaction rates achieved when using 100% H_2 as a reductant could be matched by using 4 mM (184 mg/L) formic acid. At increased formic acid concentrations, system performance exceeded performance achievable when using H_2. It is also noted that while hydrogen is an explosive, low solubility gas, formic acid can easily and safely be added to contaminated water. The aforementioned work has shown that this method for treating CAH-contaminated groundwater by using formic acid and a Pd-catalyst is more efficient, safe, and less costly than using hydrogen gas as a reductant.

15. SUBJECT TERMS
Chlorinated Aliphatic Hydrocarbon (CAH), Palladium, Formic Acid, Formate, Reduction, Hydrodehalogenation, Trichloroethylene, TCE, Catalytic Reduction, Groundwater Contamination

16. SECURITY CLASSIFICATION OF:			**17. LIMITATION OF ABSTRACT**	**18. NUMBER OF PAGES**	**19a. NAME OF RESPONSIBLE PERSON**
REPORT	**ABSTRACT**	**c. THIS PAGE**			Dr. Mark N. Goltz (ENV)
U	**U**	**U**	**UU**	194	**19b. TELEPHONE NUMBER** *(Include area code)* (937) 255-3636, ext 4638; e-mail: Mark.Goltz@afit.edu

Standard Form 298 (Rev: 8-98)
Prescribed by ANSI Std. Z39-18